

**Doctoral Dissertation**

**DEVELOPMENT OF A METHOD OF  
REMAINING LIFE PREDICTION FOR AN AGED BRIDGE BASED ON  
CONCRETE CORES AND CROSS-SECTION  
CUTTING-OFF GIRDERS**

「コンクリートコア試験および切り出し主桁断面試験による老朽橋梁  
の余寿命推定手法の開発」



**RATNA WIDYAWATI**

**Department of Environmental Science and Engineering  
Graduate School of Science and Engineering  
Yamaguchi University, Japan  
March, 2015**

# ABSTRACT

---

The remaining life prediction is a crucial part of the systematization of maintenance planning whereby it can be used to estimate the life span of the bridge. A large number of reinforced concrete (RC) bridges in Japan have aged, requiring increased maintenance, decision making concerning whether to maintain or to demolish the aged bridges. The results of the remaining life prediction can be used to assist in the decision making of whether to carry out maintenance works such as repairs/strengthening or demolish works of the aged bridges.

The reinforced concrete (RC) structures, such as bridges which are exposed to the environment become highly influenced by environmental conditions, causing reduction in their remaining life. High level of carbon dioxide in the environment resulting from high traffic volume leads to carbonation of concrete, which causes deterioration of concrete. Chloride attack should be considered as another factor of deterioration if the location of the bridge is near the sea. Either carbonation or chloride attack or both can lead to corrosion of the reinforcing bars.

This thesis introduces the details of how to predict the remaining life of an aged RC-T girder bridge based on carbonation test. Carbonation test is one of the field tests required to determine the performance of concrete from material point of view which is affected by an environmental condition. Moreover, to establish a method to predict the remaining life based on the chloride ion and carbonation tests results of the concrete cores and the cross-section cutting-off girders. A flowchart is presented for the proposed method to predict the remaining life of an RC bridge based on the extent of deterioration due to carbonation and chloride attack. The demolition of the SK Bridge provided a good opportunity to obtain many types of useful information from an existing bridge.

The concrete cores were tested for carbonation and chloride ions whereas the cross-section cutting-off girders were tested for carbonation only. The results of the concrete cores investigation show that the main factor in the deterioration of the bridge is carbonation and that chloride ion attack has also contributed to the deterioration of the bridge. The end of the service life was defined as the point at which the cumulative amount of steel corrosion reached a critical value of  $Q = 75 \text{ mg/cm}^2$  which is obtained by BREX system.

# 学位論文の要旨

---

橋梁の余寿命予測には、橋梁の寿命を推定する維持管理計画のシステム化が重要である。日本における多くの鉄筋コンクリート（RC）橋梁が老朽化しており、老朽橋梁の維持管理要否判定や架け替え要否の判定が必要になっている。老朽橋梁の余寿命推定による結果が、老朽橋梁の維持管理要否判定や架け替え要否の判定に利用されている。

自然環境に露出されている橋梁を含むRC構造物は、環境条件による影響を多く受けるため余寿命が減少する。また、高交通量による環境中の二酸化炭素の高濃度化は、RC構造物の中性化を引き起こし、劣化を進行させる。さらに、海に近い鉄筋コンクリート構造物は、塩化物イオンによる塩害も起こり、劣化を進行させる場合もある。中性化または塩害どちらにおいても、RC構造物中の鋼材の腐食が促進される。

本論文は、中性化試験に基づく、老朽化した RC-T 桁橋梁の余寿命を推定する際の詳細な手法について述べる。中性化試験は実地試験の一種で、コンクリートの環境因子の影響を含む材料的観点における性能を知ることができる。塩化物イオンと中性化に基づく余寿命推定方法を確立するために、具体的にコンクリート・コアと横断方向に切断した桁での結果を用いる。フローチャートは、RC 橋の余寿命を推定するための、中性化と塩害による劣化の程度に基づく手法を示している。撤去中の橋梁である SK 橋を用いることで、既存の橋梁から有意な様々な情報得ることができる。

採取したコンクリート・コアにおいては中性化試験及び塩化物イオン試験を行う。一方で、対象橋梁よる横断方向に切断した桁においては、中性化試験のみ行う。コンクリート・コアにおける試験結果においては、対象橋梁における主たる劣化因子が中性化によるものであることが示された。また、塩化物イオンによる劣化因子もある程度含んでいることも示された。余寿命は BREX システムから得られる鉄筋累積腐食量  $Q = 75 \text{ mg/cm}^2$  となる位置である。

# ACKNOWLEDGEMENT

---

Firstly, I would like to express my deepest gratitude to my supervisor, Professor Ayaho Miyamoto, for his intellectual guidance, advice and encouragement. He continuously and persuasively conveyed a spirit of adventure in regard to research. Without his continuous technical and constructive guidance this dissertation would not have been possible.

Secondly, I would like to deeply thank Assistant Professor Hisao Emoto for his continuous technical support guidance during my research.

Thirdly, I would like to deeply thank Dr. Jun Takahashi, for his continuously expert advice and guiding my research work.

I would also like to thank the dissertation committees; Professor Miyamoto, Professor Sekine, Professor Kita, Professor Nakamura, and Assistant Professor Emoto, for their advice and suggestion in regard to the improvement of my dissertation.

I would like to express my special appreciation to Associate Professor Eiji Matsuo, for grating me the opportunity of joining Yamaguchi University, Graduate School of Science and Engineering.

Special gratitude goes to The Directorate General for Higher Education (DGHE), Ministry of Research and Technology of Republic Indonesia for granting me a scholarship, also my employers Lampung University, for granting me the opportunity to pursue my further studies.

Special thank Mr. Suzuki and Miss Kochi, and my laboratory colleagues; Mr. Hugo, Mr. Tanaka, Nabende, Tweli, Hirano, Yamamoto, Mr. Asano, Mr. Nakano, Mr. Nagata, Mr. Yamamura, Mr. Katsushima, Mr. Nishida, Mr. Murata, Mr. Furukawa, Mr. Kawamoto, Mr. Nagasaki, and Mr. Iwai for sharing ideas and knowledge, warm acceptance and colorful life in our laboratory.

My friends, Gatot Eko Susilo, Ratna Sulistyanti, Evi, Riri, Mella, Devia, Rina, Didik, Djadjis, Sita, Haidar, Kardi, Ovi, Abu, Rivai, Dhita, Ridwan, Corina, Bob, Isao Haraguchi and Parvis Moradipour, for their warm friendship, help and the good times together.

My beloved late parents, for their encouraging and inspiring words, also my Mommy Ita Abioso, my aunties, and BTP, for their never ending support and love.

Finally, special thank Tanyo AP. Soedarmono and my beloved son Priagung Satria Wicaksana, for their patience, understanding, support and love.

# TABLE OF CONTENTS

---

ABSTRACT .....	iii
学位論文の要旨 .....	iv
ACKNOWLEDGEMENTS .....	v
TABLE OF CONTENTS .....	vi
LIST OF FIGURES .....	xii
LIST OF TABLES .....	xvi
NOTATIONS .....	xviii

## CHAPTER 1: INTRODUCTION

1.1 Background .....	1
1.2 Significance .....	2
1.3 Objectives .....	3
1.4 Organization .....	4
1.5 References .....	5

## CHAPTER 2: LITERATURE REVIEW

2.1 Introduction .....	7
2.2 Remaining life and service life prediction .....	7
2.3 Carbonation .....	11
2.4 Chloride attack .....	15
2.5 Corrosion .....	17

## CHAPTER 3: REMAINING LIFE PREDICTION OF AN AGED BRIDGE BASED ON CONCRETE CORES TEST

3.1 Introduction .....	31
3.2 Target bridge and research purpose .....	32
3.3 Core examination .....	34
3.3.1 Extract of concrete cores .....	34
3.3.2 Chloride ion test .....	34
3.3.3 Carbonation test .....	36
3.4 Result of concrete core test .....	37
3.4.1 Analysis of chloride ion content .....	37
3.4.2 Results of carbonation depth measurement .....	41
3.4.3 Identification of main deterioration factors .....	42
3.5 Remaining life prediction method through concrete core test .....	44
3.5.1 Concept of remaining life prediction method based on carbonation test.....	44
3.5.2 Remaining life prediction results .....	48

3.5.3 Discussion .....	53
3.5.3.1 Influence of the amount of reinforcement corrosion on evaluation result .....	53
3.5.3.2 Influence of the moisture content on evaluation result .....	55
3.5.3.3 Simple method of the remaining life prediction .....	59
3.6 Proposal of evaluation of entire span based on local evaluation .....	60
3.7 Conclusions .....	63
3.8 References .....	64

**CHAPTER 4: REMAINING LIFE PREDICTION OF AN AGED BRIDGE  
BASED ON CARBONATION TEST FOR CROSS-SECTION  
CUTTING-OFF GIRDERS**

4.1 Introduction .....	66
4.2 Target bridge and research purpose .....	68
4.3 Method of cross-section cutting-off girders tests .....	68
4.3.1. Cross-section cutting-off girders .....	68
4.3.2. Examination of cross-section cutting-off girders .....	72
4.3.3. Thickness of concrete cover measurement .....	72
4.3.4. Carbonation test .....	73
4.3.5. Carbonation depth measurement .....	73
4.4 Results of cross-section cutting-off girders tests .....	74
4.4.1 Concrete cover thickness measurement results .....	74
4.4.2 Carbonation depth measurement results .....	79
4.4.3 Remaining concrete cover results .....	84
4.4.4 Carbonation rate coefficient .....	85
4.4.5 Chloride ion content .....	86
4.5 Remaining life prediction method through cross-section cutting-off girders .....	88
4.5.1 Cross-section cutting-off girders .....	88
4.5.2 Remaining life prediction for the case in which the deterioration is caused by carbonation and also affected by chloride ion .....	88
4.5.3 Remaining life prediction for the case in which the deterioration is caused only by carbonation .....	98
4.5.4 Discussion .....	102
4.6 Conclusion .....	104
4.7 Conclusion .....	106

**5.1 CHAPTER 5: COMPARISON OF REMAINING LIFE PREDICTION OF  
CONCRETE CORES USING CROSS-SECTION  
CUTTING-OFF GIRDERS**

5.1 Introduction .....	108
5.2 Comparison between the results of remaining life prediction of concrete cores and cross-section cutting-off girders in averages.....	109
5.3 Comparison between the results of remaining life prediction of concrete cores and cross-section cutting-off girders based on the location of extracting concrete core .....	113
5.4 Comparison between the results of remaining life prediction of concrete cores and cross-section cutting-off girders based on the location of girders of each span .....	117
5.5 Comparison between the results of remaining life prediction of concrete cores and cross-section cutting-off girders based on the location of girders.....	126
5.6 Conclusions .....	130
5.7 References .....	130

**CHAPTER 6: CONCLUSIONS**

6.1 Conclusions.....	131
6.2 Future works .....	133

APPENDIX .....	A-1
----------------	-----

# LIST OF FIGURES

---

Fig. 1.1	Flow of study of remaining life prediction .....	5
Fig. 2.1	Service life model by Tutti (1982) .....	8
Fig. 2.2	Service life model by Verma (2013) .....	9
Fig. 2.3	Stage of reinforcing bar corrosion model by Ahmad (2002) .....	10
Fig. 2.4	Schematic description of life service model .....	11
Fig. 2.5	Conceptual view of deterioration progress due to carbonation .....	12
Fig. 2.6	Conceptual view of deterioration progress due to chloride ion .....	16
Fig. 2.7	Corrosion process .....	18
Fig. 2.8	Remaining concrete cover .....	20
Fig. 3.1	Geographical location of SK Bridge .....	32
Fig. 3.2	General view of SK Bridge .....	33
Fig. 3.3	Spans 1 and 3 of SK Bridge .....	35
Fig. 3.4	Concrete cores locations .....	35
Fig. 3.5	Extracting concrete cores .....	36
Fig. 3.6	Concrete cores specimens .....	36
Fig. 3.7	Chloride ion test .....	37
Fig. 3.8	Carbonation test .....	37
Fig. 3.9	Types of chloride ion content in Span 3 .....	39
Fig. 3.10	Chloride ion content distributions in Span 1 .....	41
Fig. 3.11	Flowchart of remaining life .....	45
Fig. 3.12	Illustration of the basic equation to calculate Q .....	46
Fig. 3.13	Plotted of remaining life prediction based on the location of extracted concrete cores in Span 3 (1 <sup>st</sup> case).....	49
Fig. 3.14	Plotted of remaining life prediction based on the location of extracted concrete cores in Span 1 (2 <sup>nd</sup> case).....	52
Fig. 3.15	Plotted of remaining life prediction based on the location of extracted concrete cores in Span 3 (2 <sup>nd</sup> case).....	52
Fig. 3.16	Comparison of predicted life of extracted concrete cores between 1 <sup>st</sup> case and 2 <sup>nd</sup> case .....	53
Fig. 3.17	Relationship between assumed cumulative amount of steel corrosion (Q) and life expectancy .....	56
Fig. 3.18	Influence of moisture content (W) on life expectancy .....	56
Fig. 3.19	Relationship between assumed cumulative amount of steel corrosion (Q) and life expectancy of Span 1 .....	59

Fig. 3.20 Relationship between assumed cumulative amount of steel corrosion (Q) and life expectancy of Span 3 .....	59
Fig. 3.21 Influence of moisture content (W) on life expectancy of Span 1 .....	59
Fig. 3.22 Influence of moisture content (W) on life expectancy of Span 3 .....	59
Fig. 3.23 In-span distribution of remaining life of main girder in case where only Type (c) distribution in Fig. 9 is involved .....	62
Fig. 3.24 In-span distribution of remaining life of main girder in case where both Type (a) and Type (b) distribution in Fig. 9 are included .....	63
Fig. 4.1 Schematic illustration of service life prediction .....	67
Fig. 4.2 General view and locations of SK Bridge .....	69
Fig. 4.3 Spans 1 and 3 of SK Bridge .....	69
Fig. 4.4 Cross section cutting-off girders of SK Bridge .....	70
Fig. 4.5 Sketch of cross-section cutting-off girder of SK Bridge .....	70
Fig. 4.6 Cross-section cutting-off girders locations .....	71
Fig. 4.7 Removal girder .....	73
Fig. 4.8 Wire saw machine .....	73
Fig. 4.9 Measurement of thickness of concrete cover .....	74
Fig. 4.10 Carbonation test .....	74
Fig. 4.11 Spraying phenolphthalein solution.....	74
Fig. 4.12 Carbonation depth measurement .....	74
Fig. 4.13 The thickness of concrete cover in Span 1 .....	76
Fig. 4.14 The thickness of concrete cover in Span 3 .....	76
Fig. 4.15 Normal distribution of the concrete cover in Span 1 sea side .....	77
Fig. 4.16 Normal distribution of the concrete cover in Span 1 bottom side .....	77
Fig. 4.17 Normal distribution of the concrete cover in Span 1 mountain side .....	77
Fig. 4.18 Normal distribution of the concrete cover in Span 3 sea side .....	78
Fig. 4.19 Normal distribution of the concrete cover in Span 3 bottom side .....	78
Fig. 4.20 Normal distribution of the concrete cover in Span 3 mountain side .....	78
Fig. 4.21 Carbonation depth in Span 1 .....	80
Fig. 4.22 Carbonation depth in Span 3 .....	80
Fig. 4.23 Normal distribution of the carbonation in Span 1 sea side .....	81
Fig. 4.24 Normal distribution of the carbonation in Span 1 bottom side .....	81
Fig. 4.25 Normal distribution of the carbonation in Span 1 mountain side .....	81
Fig. 4.26 Normal distribution of the carbonation in Span 3 sea side .....	82
Fig. 4.27 Normal distribution of the carbonation in Span 3 mountain side .....	82
Fig. 4.28 Normal distribution of the carbonation in Span 3 bottom side (repaired) ....	83
Fig. 4.29 Normal distribution of the carbonation in Span 3 bottom side (no repaired) .....	83
Fig. 4.30 Remaining concrete cover of Span 1 .....	84
Fig. 4.31 Remaining concrete cover of Span 3 .....	84

Fig. 4.32	Flowchart of remaining life prediction in this study .....	90
Fig. 4.33	Service life prediction due to carbonation and chloride ion of Span 1 .....	93
Fig. 4.34	Service life prediction due to carbonation and chloride ion of Span 3 .....	94
Fig. 4.35	Remaining life prediction due to carbonation and chloride ion of Span 1 and 3 .....	96
Fig. 4.36	Service life prediction due to carbonation and chloride ion of Span 1 and 3 .....	96
Fig. 4.37	Normal distribution of service life due to carbonation and chloride ion in Span 1 and Span 3 .....	98
Fig. 4.38	Normal distribution of service life due to carbonation only in Spans 1 and 3 .....	100
Fig. 4.39	Normal distribution of service life due to carbonation only in Spans 1 and 3 calculated using the Root t rule .....	102
Fig. 4.40	Comparison of remaining life due to carbonation and chloride ion and carbonation only of Span 1 and Span 3 .....	103
Fig. 5.1	Diagram of the verification of remaining life prediction results .....	109
Fig. 5.2	Service life prediction of concrete cores of Span 1 .....	111
Fig. 5.3	Service life prediction of concrete cores of Span 3 .....	111
Fig. 5.4	Comparison of remaining life prediction results between concrete cores and cross-section cutting-off girders in both Spans 1 and 3 on average .....	113
Fig. 5.5	Comparison of service life prediction results between concrete cores and cross-section cutting-off girders in both Spans 1 and 3 on average .....	113
Fig. 5.6	Relationship between remaining life prediction of concrete cores and cross-section cutting-off girders in Spans 1 and 3 based on the location of extracted cores .....	117
Fig. 5.7	Cross-section cutting-off girders based on the location of girders of each spans .....	118
Fig. 5.8	Relationship between remaining life prediction of concrete cores and cross-section cutting-off girders in Spans 1 and 3 based on the location of girders of each span .....	120
Fig. 5.9	Comparison between distribution of service life prediction of cross-section cutting-off girders in Span 1 and Span 3 based on the location of girders of each span .....	121
Fig. 5.10	Normal distribution of service life prediction in span 1 sea side .....	122
Fig. 5.11	Normal distribution of service life prediction in span 3 sea side .....	122
Fig. 5.12	Normal distribution of service life prediction in span 1 bottom side .....	123
Fig. 5.13	Normal distribution of service life prediction in span 3 bottom side .....	123
Fig. 5.14	Normal distribution of service life prediction in span 1 mountain side .....	124
Fig. 5.15	Normal distribution of service life prediction in span 3 mountain side .....	124

Fig. 5.16 Comparison of remaining life prediction of cross-section cutting-off girders in Span 1 and Span 3 based on the location of girders of each span	125
Fig. 5.17 Merged girders of spans 1 and 3 based on the location of girders	126
Fig. 5.18 Service life distribution of merged girders of spans 1 and 3	127
Fig. 5.19 Normal distribution of service life prediction in spans 1 and 3 sea side	127
Fig. 5.20 Normal distribution of service life prediction in spans 1 and 3 bottom side	128
Fig. 5.21 Normal distribution of service life prediction in spans 1 and 3 mountain side	128
Fig. 5.22 Comparison of remaining life prediction of merged girders of Span 1 and Span 3 based on the location of girders	129

# LIST OF TABLES

---

Table 2.1	Definition of deterioration stages due to carbonation .....	12
Table 2.2	Definition of deterioration stages due to chloride ion .....	16
Table 2.3	Grade of corrosion and state of steel .....	18
Table 2.4	Grade of structural appearance corrosion and stage of deterioration .....	19
Table 2.5	Summary and comparison of literature review .....	22
Table 3.1	Number of the collected concrete cores .....	36
Table 3.2	Results of chloride ion content analysis (1 <sup>st</sup> case) .....	38
Table 3.3	Results of chloride ion content analysis (2 <sup>nd</sup> case) .....	40
Table 3.4	Results of carbonation depth measurement .....	42
Table 3.5	Results of remaining life prediction (1 <sup>st</sup> case) .....	49
Table 3.6	Results of remaining life prediction (2 <sup>nd</sup> case) .....	50
Table 3.7	Results of assumed cumulative amount of steel corrosion ( $Q$ ) and life expectancy( $X$ ) (1 <sup>st</sup> case) .....	56
Table 3.8	Results of influence of moisture content ( $W$ ) on life expectancy( $X$ ) (1 <sup>st</sup> case).....	56
Table 3.9	Results of assumed cumulative amount of steel corrosion ( $Q$ ) and life expectancy( $X$ ) (2 <sup>nd</sup> case) .....	57
Table 3.10	Results of influence of moisture content ( $W$ ) on life expectancy( $X$ ) (2 <sup>nd</sup> case).....	58
Table 4.1	Number of cross-section cutting-off girders.....	69
Table 4.2	Thicknesses of concrete cover of Spans 1 and 3 .....	75
Table 4.3	Carbonation depths of Spans 1 and 3 .....	79
Table 4.4	Carbonation rate coefficient of Spans 1 and 3 .....	85
Table 4.5	Chloride ion content results of Spans 1 and 3 .....	87
Table 4.6	Remaining life prediction due to carbonation and chloride ion of Span 1 ..	92
Table 4.7	Remaining life prediction due to carbonation and chloride ion of Span 3 ..	92
Table 4.8	Remaining life prediction of Spans 1 and 3 .....	97
Table 4.9	Remaining life prediction carbonation only of Spans 1 and 3 .....	99
Table 4.10	Remaining life prediction carbonation only of Spans 1 and 3 calculated using Root t rule .....	101
Table 5.1	Remaining life prediction due to the carbonation and chloride ion of the concrete cores in Spans 1 and 3 .....	110
Table 5.2	Remaining life prediction of concrete cores and cross-section cutting-off girders based on the location of extracted cores .....	115

Table 5.3	Correlation coefficient calculation of the remaining life prediction in Span 1 based on the location of extracted cores .....	116
Table 5.4	Correlation coefficient calculation of the remaining life prediction in Span 3 based on the location of extracted cores .....	116
Table 5.5	Remaining life prediction of concrete cores and cross-section cutting-off based on the location of girders of each span .....	118
Table 5.6	Correlation coefficient calculation of the remaining life prediction in Span 1 based on the location of girders of each span .....	119
Table 5.7	Correlation coefficient calculation of the remaining life prediction in Span 3 based on the location of girders of each span .....	119
Table 5.8	Remaining life prediction of the merged girders of spans 1 and 3 based on the location of girders .....	126

# NOTATIONS

---

- $A$  = carbonation rate, mm/s<sup>0.5</sup> (Eq. 3.3, Eq. 4.1)
- $d(t)$  = carbonation depth time  $t$ , mm (Eq. 3.3, Eq. 4.1)
- $t$  = period of carbonation, years (Eq. 3.3, Eq. 4.1)
- $C(x,t)$  = chloride ion content in depth  $x$  at time  $t$ , kg/m<sup>3</sup>  
(Eq. 3.1, Eq. 4.3)
- $C_0$  = chloride ion content at the concrete surface, kg/m<sup>3</sup>  
(Eq. 3.1, Eq. 4.3)
- $D_{ap}$  = apparent diffusion coefficient of the chloride ion, cm<sup>2</sup>/years  
(Eq. 3.1, Eq. 4.3)
- $C_i(x,0)$  = initial chloride ion content in concrete, kg/m<sup>3</sup> (Eq. 3.1, Eq. 4.3)
- $V$  = steel corrosion rate, mg/cm<sup>2</sup>/years  
(Eq. 3.4, Eq. 3.5, Eq. 4.4, Eq. 4.5)
- $Cl$  = chloride ion content at the reinforcement location, kg/m<sup>3</sup>  
(Eq. 3.4, Eq. 3.5, Eq. 4.4, Eq. 4.5)
- $k$  = correction at temperature tmp, °C using Eq. 2.17  
(Eq. 3.4, Eq. 3.5, Eq. 4.4, Eq. 4.5, Eq. 4.6)
- tmp = temperature, °C  
(Eq. 3.6, Eq. 4.6)
- $C$  = remaining concrete cover, mm  
(Eq. 3.5, Eq. 4.5)
- $W$  = surface moisture content of concrete, percent  
(Eq. 3.5, Eq. 3.12, Eq. 3.13 Eq. 3.14, Eq. 4.5)
- $Q_{CR}$  = cumulative amount of corrosion were obtained by BREX system equal  
75 mg/cm<sup>2</sup>
- $R$  = remaining life, years (Eq. 3.2, Eq. 3.9, Eq. 3.10, Eq. 3.11,  
Eq. 3.12, Eq. 3.13, Eq. 3.14, Eq. 3.16, Eq. 4.2)
- $X$  = life expectancy, years (Eq. 3.2)
- $N$  = period of service life, years (Eq. 3.2)
- $Q(t)$  = cumulative amount of steel corrosion  $Q$  at time  $t$ , mg/cm<sup>2</sup> (Eq. 3.7, Eq. 4.7)
- $\Delta t$  = time step, years (Eq. 3.7, Eq. 4.7)
- $V(t)$  = steel corrosion rate  $V$  at time  $t$ , mg/cm<sup>2</sup>/years (Eq. 3.7, Eq. 3.8, Eq. 4.7)
- $Q(0)$  = cumulative amount of steel corrosion  $Q$  at  $t = 0$ , mg/cm<sup>2</sup>  
(Eq. 3.7, Eq. 3.8, Eq. 4.7, Eq. 4.8)
- $V(0)$  = steel corrosion rate  $V$  at  $t = 0$ , mg/cm<sup>2</sup>/years (Eq. 3.8, Eq. 4.8)

- $Q$  = cumulative amount of corrosion,  $\text{mg}/\text{cm}^2$  (Eq. 3.9, Eq. 3.10, Eq. 3.11)  
 $X_0$  = service life in case where  $Q$  is assumed to be  $10 \text{ mg}/\text{cm}^2$  (Eq. 3.15)  
 $X_1$  = service life in case where  $Q$  is assumed to be  $75 \text{ mg}/\text{cm}^2$  (Eq. 3.15)
- $SL$  = service life, years (Eq. 4.2)  
 $EL$  = elapsed time, years (Eq. 4.2)

# Chapter 1: INTRODUCTION

---

## 1.1 Background

Lifetime management for civil infrastructure is becoming the most important issue in sustainable development of societies around world. In advanced countries the benefits of long-term management of civil infrastructure has been recognized by the experts of the discipline. Integrated lifetime management and maintenance planning includes continuous condition assessment, predictive modeling of performance, maintenance planning and decision-making procedures regarding maintenance action [1].

Remaining life prediction is a crucial part of the systematization for maintenance planning because it can be used to estimate the end of bridge's life. The reinforced concrete (RC) structures such as bridges are exposed to the environment are strongly influenced by environmental conditions during their service life resulting in reducing of the remaining life. High level of carbon dioxide as a result of the high traffic volume leads to carbonation process. Chloride attack should be considered as another factor of deterioration if the location of the bridge is near the sea. Either carbonation or chloride attack or both can lead to corrosion of the reinforcing bar. The most serious deterioration mechanisms that occur in RC bridges are associated with corrosion [2].

An integrated lifetime management system for civil infrastructure in Japan, particularly bridges, becomes crucial based on the large number of aged bridges that need to gain attention. If the remaining life of an aged bridge is to be maximized, it is necessary to regularly assess the structural performance of the bridge. It is important to make appropriate safety evaluations and remaining life predictions [3~5].

The Bridge Management System (J-BMS), which integrated with a Bridge Rating EXpert system (BREX), is one of the useful methods to evaluate the remaining life prediction of an existing concrete bridge [6,7]. However, the BREX system result needs to be verified. To verify this system, concrete cores were extracted from some parts of the target bridge to conduct the carbonation and chloride ion tests. The results of carbonation and chloride ion tests will be used to assume the remaining life prediction [8,9].

In this thesis, remaining life prediction is obtained from the results of chloride ion and carbonation test of concrete cores and cross-section cutting-off girders of SK Bridge. Remaining life prediction estimates are from concrete cores which represent the local evaluation results of the girders. In contrast, remaining life prediction based on cross-sections cutting-off girders represents the entire girders.

## **1.2 Significance**

The remaining life prediction is important as a part of the bridge maintenance system. An aged bridge requires increased maintenance and requires that decisions be made concerning whether to maintain or to demolish these aged bridges. Remaining life prediction is one of the methods to estimate the end of life of the bridge and moreover to determine how best to make these decisions.

This thesis establish the new method to predict the remaining life of an aged bridge using the limited number of concrete cores, and verify the remaining life prediction results using cross-section cutting-off girders.

The performance of the concrete based on concrete cores represents performance of the locations from which the cores are extracted. Carbonation and chloride ion tests were conducted on concrete cores. Remaining life prediction results from concrete cores represent the local evaluation results of the girders. In contrast, remaining life prediction based on cross-sections cutting-off girders represent the entire girders. This thesis describes the first known application of carbonation testing to cross-section cutting-off girders of the bridge.

Remaining life of both concrete cores and cross-section cutting-off girders was calculated using some equations according to the method to predict the remaining life, with the requirement that the cumulative amount of steel corrosion ( $Q_{CR}$ ) equal  $75 \text{ mg/cm}^2$ . This value is similar with the remaining life as indicated by the BREX system in the evaluation of deterioration of the bridge due to chloride ion attack [4,5].

Therefore the possibilities will be open to identifying the relationships between local evaluation results (were obtained by examining concrete cores), overall structural evaluation results (were obtained from the BREX system), and the entire evaluation results (were obtained by examining cross-section cutting-off girders). By expanding the scope of an evaluation from local to the entire structure of the bridge, it may also be possible to enhance testing efficiency by reducing the total number of the concrete cores which are necessary for testing.

### **1.3 Objectives**

The main objectives of this study are:

1. Develop a method for estimating the remaining life prediction of an aged bridge through the chloride ion and carbonation tests on concrete cores and cross-section cutting-off girders.
2. Determine the main deterioration factor of an aged bridge, whether due to chloride attack or carbonation, through the chloride ion and carbonation tests on concrete cores and cross-section cutting-off girders.
3. Estimate the remaining life and service life prediction from concrete cores and cross-section cutting-off girder. The service life prediction is restricted by a criterion value i.e. cumulative amount of steel corrosion  $Q = 75 \text{ mg/cm}^2$ , which is obtain by the BREX system.
4. Verify the remaining life prediction results of the concrete cores with cross-section cutting-off girders.

## 1.4 Organization

The flow of this study is developing of a method for assuming the remaining life prediction as shown in Fig. 1.1. The organization of this thesis is based on and presented by the flow analyses. This thesis consists of six chapters. The outline of the thesis can be summarized as follow:

Chapter 1 deals with the introduction of this thesis. The background of this study, significance, objectives and organization of the thesis are discussed.

Chapter 2 reviews the literature related to remaining life, service life, and the influencing factors, i.e., carbonation, chloride ion and corrosion.

Chapter 3 discusses the implementation of chloride ion and carbonation tests on concrete cores to define the main deterioration factor of an aged bridge. Moreover it explains a method for estimating the remaining life prediction of an aged bridge through the chloride ion and carbonation tests on concrete cores.

Chapter 4 deals with the chloride ion and carbonation tests which have been applied to cross-section cutting-off girders. This study describes the first known application of carbonation testing to cross-sections cutting-off girders from a bridge. The main deterioration factors, whether due to chloride attack or carbonation were also discussed. Finally, estimate the remaining life prediction using the method that is developed in Chapter 3.

Chapter 5 studies the verification of remaining life prediction results of concrete cores using cross-section cutting-off girders of an aged bridge. According to the results of investigation on concrete cores (in Chapter 3) and cross-section cutting-off girders (in Chapter 4), the remaining life predictions were compared. Furthermore, it will verify how local evaluation results based on concrete cores tests can be used for the evaluation of the entire span based on cross-section cutting-off girders.

Chapter 6 concludes the objectives of the thesis have been achieved. A few suggestions concerning further studies necessary in this field are provided.

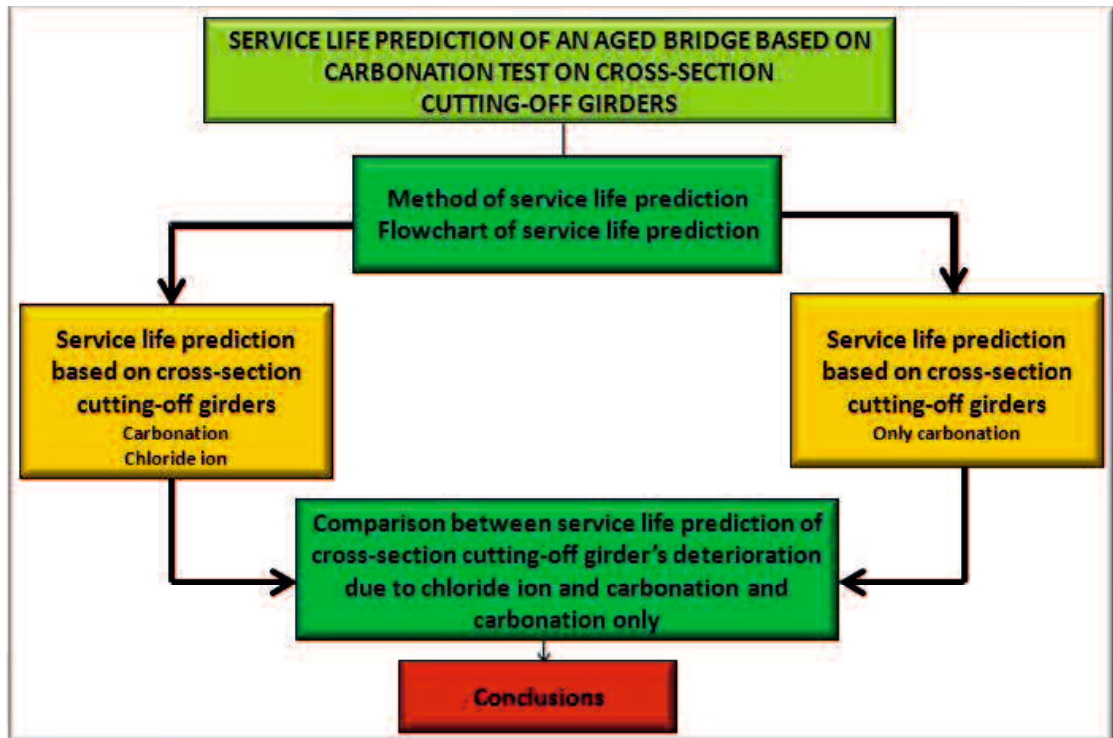


Fig. 1.1 The flow of the study of remaining life prediction

## 1.5 References

- [1] A. Sarja, Predictive and optimized life cycle management, Building and Infrastructure, Taylor & Francis, 2006.
- [2] R. Widyawati, A. Miyamoto, H. Emoto, J. Takahashi, Service life prediction of an aged bridge based on carbonation test of cross-section cutting-off girders, Journal of The Society of Materials Science, Japan, Vol., No. 5, 2015.
- [3] A. Miyamoto, H. Emoto, J. Takahashi, K. Hiraoka, Remaining life evaluation and its verification of aged bridge based on field inspections, (in Japanese), Concrete Research and Technology, Vol. 23, No. 3, pp. 119–132, 2012.
- [4] J. Takahashi, H. Emoto, A. Miyamoto, A proposal on bridge soundness evaluation system's verification method based on concrete core testing, (in Japanese), Proceedings of the Japan Concrete Institute, Vol. 34, No. 2, pp. 1399–1404, 2012.
- [5] H. Emoto, J. Takahashi, A. Miyamoto, Learning effect in diagnosis and remaining life estimation of concrete bridges by J-BMS using visual inspection results, (in Japanese), Proceedings of the Japan Concrete Institute, Vol. 34, No. 2, pp. 1393–1398, 2012.

- [6] A. Miyamoto, M. Kushida, H. Morikawa, K. Kinoshita, Development and reliability enhancement of neuro-fuzzy expert system for concrete bridge diagnosis, (in Japanese), Proceedings of the Japan Society of Civil Engineers, 510-VI-26, pp. 91–101, 1995.
- [7] A. Miyamoto, K. Kawamura, H. Nakamura, Optimal maintenance planning for existing bridges using bridge management system (BMS), (in Japanese), Proceedings of the Japan Society of Civil Engineers, 588-VI-38, pp. 191–208, 1998.
- [8] J. Takahashi, H. Emoto, R. Widyawati and A. Miyamoto, Remaining life prediction of an aged bridge based on concrete core test, (in Japanese), Proceedings of the Japan Concrete Institute, Vol. 36, No. 2, pp. 1339-1344, 2014.
- [9] R. Widyawati, J. Takahashi, H. Emoto, and A. Miyamoto, Remaining life prediction of an aged bridge based on concrete core test, 2<sup>nd</sup> International Conference on Sustainable Civil Engineering Structures and Construction Materials, SCESCM, Yogyakarta, Sept 23-25, pp. 1-10, 2014.

# Chapter 2: LITERATURE REVIEW

---

## 2.1 Introduction

This chapter deals with a literature review according to remaining life prediction method of reinforced concrete (RC) structure based on carbonation test. First, this chapter explains the definition of remaining life and service life predictions then defines how this is used to estimate the remaining life prediction, i.e. carbonation, chloride ion content and corrosion.

## 2.2 Remaining life prediction

Remaining life prediction is a period between the time of investigation (elapsed time) and the end of service life. The remaining life prediction for a concrete structure in cases where section loss is due to steel corrosion is expressed as the number of years of life expected if the section loss is left uncorrected [1].

The Bridge Management System (J-BMS), which integrated with a Bridge Rating EXpert system (BREX), is one of the useful methods to assume the remaining life prediction of an existing concrete bridge [2,3]. BREX is a system that is designed for evaluating the present performance of the target bridge. The outputs are load-carrying capability and durability of each structure member. The input data for rating the concrete bridge are the technical specification of the target bridge, environmental conditions, traffic volume, and other subjective information that can be obtained through detailed visual inspection results. Evaluation results were thus obtained as the soundness level of the remaining life. This information processing approach makes it possible to deal with cases involving a large number of influencing factors.

In the remaining life prediction by the BREX system, deterioration curves are applied to structural soundness scores obtained on the basis of visual inspection results. It has also been reported that in the prediction method by the BREX system, the cumulative amount of steel corrosion in the last year of the predicted remaining life was  $Q = 75 \text{ mg/cm}^2$  [4,5].

There are few opinions regarding the definition of service life. Ref. [6] defined the service life of RC structures as a period of a structure that can meet the performance requirement based on defined repair and maintenance. According to Ref. [7] service life of the RC or PC structures at the initial time of steel corrosion was started when the carbonation occurred in a concrete surface until protection's steel disappeared. Ref. [8] considered that the service life is a period during initial use until the depassivation of the reinforcing bar occurred. Ref. [9] defined the end of service life was reached when depassivation of the reinforcement had occurred due to carbonation. Ref. [10] considers that the service life only corresponds to corrosion initiation stages, it is assumed when the chloride content at the level of reinforcement has reached a critical value of  $1.2 \text{ kg/m}^3$ . Ref. [11] defined the residual service life is time remaining for the crack to increase on the surface of concrete caused by expansion of corrosion.

Service life of RC structures has been divided into several stages by previous researchers. Fig. 2.1 shows the Tutti's model for predicting deterioration. This model divided the service life of RC structures into two stages, i.e., initiation and propagation stages [12]. Initiation stage is the time required for carbon dioxide or chloride ion to reach the reinforcing bar and start the initiation corrosion. Propagation stage is the time between the initiation corrosion and the initiation cracking has occurred.

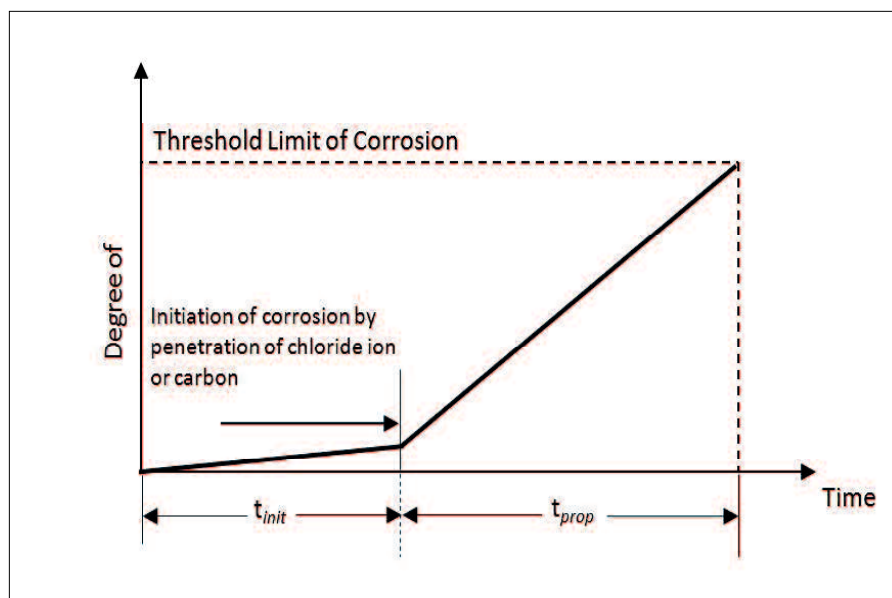


Fig. 2.1 Service life model by Tutti (1982)

Fig. 2.2 shows the model of service life prediction by Verma. In this model, service life prediction of RC structures is also divided into two stages, initiation and propagation stages, similar to Tutti's model. Initiation stage is the time period required for the initiation corrosion either when the carbonation depth is reached in the concrete cover or the chloride ion has reached the threshold value. Propagation stage is the time period between initiation and failure of the structures [13].

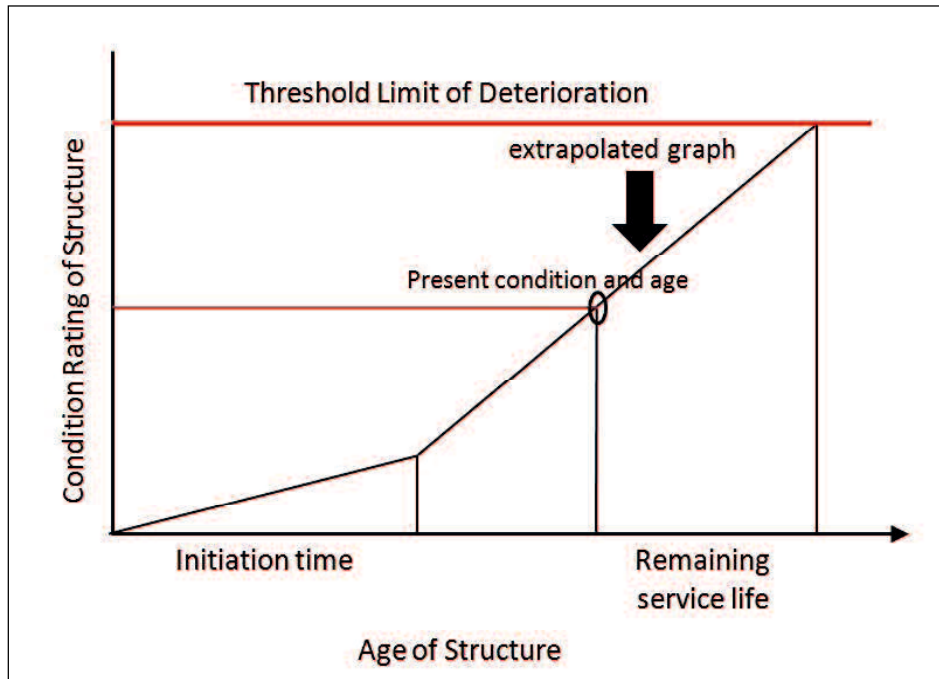


Fig. 2.2 Service life model by Verma (2013)

According to Ahmad's model, the state of corrosion process has three stages, depassivation, propagation and final state, as shown in Fig. 2.3. Depassivation is the loss of oxide (passive layer) on the reinforcing bar which protects the reinforcing bar from corrosion. Depassivation was initially formed when the concrete became acidic due to the carbon dioxide or chloride penetration. The process of depassivation takes an initiation period, which is the time from initial condition (construction) to the time due to initiation of corrosion (depassivation). The propagation phase starts from the time of depassivation to the final stage. During the final stage, the corrosion will lead to cracking and spalling of concrete cover [11]. The critical time,  $t_{cr}$ , can be define as follows:

$$t_{cr} = t_p + t_{cor} \quad (2.1)$$

Where  $t_{cr}$  is critical time in years,  $t_p$  is time from construction to the time of initial corrosion (depassivation) in years and  $t_{cor}$  is time from the depassivation to the final stage in years, when it has reached the critical time. Therefore, the service life can be estimated to the critical time as given by Eq. 2.1.

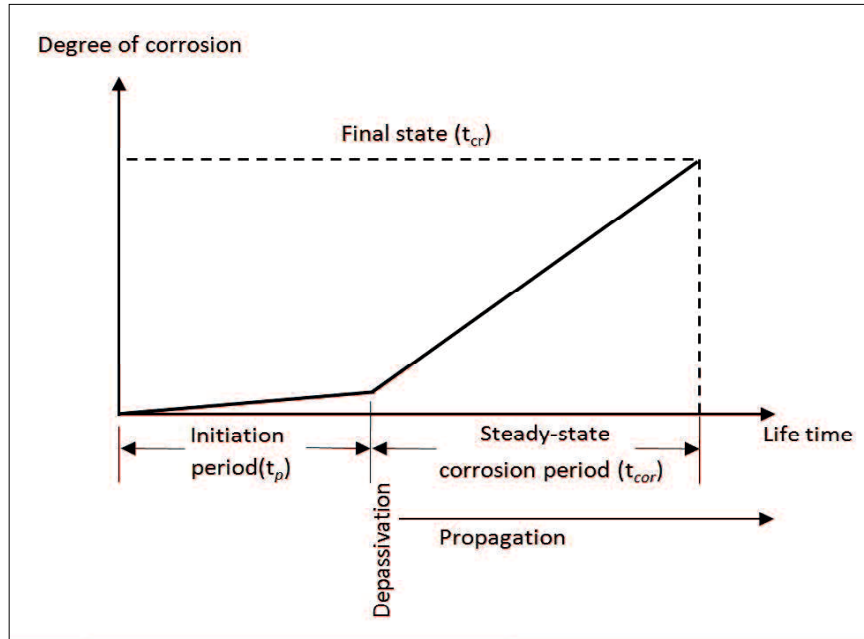


Fig. 2.3 Stages of reinforcing bar corrosion model by Ahmad (2002)

Based a conceptual model illustrated in Fig. 2.4 which shows a two-stage service life model. The service life ( $t_s$ ) can be defined as the total time to reach a given corrosion induced damage level, which is the sum of the corrosion-initiation time ( $t_i$ ) and the propagation time ( $t_p$ ) corresponding to a given level of damage, as follows:

$$t_s = t_i + t_p \quad (2.2)$$

Several different estimates of service life can be obtained using this conceptual model. In Ref. [14] the end of service life is defined as the time to onset of spalling.

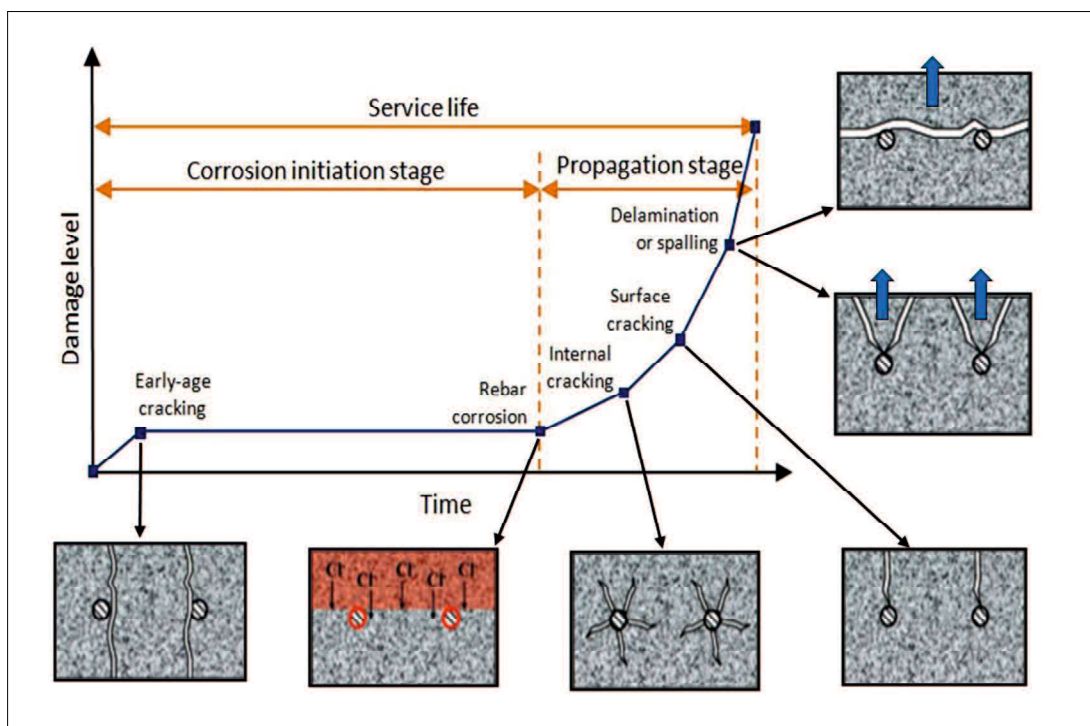


Fig. 2.4 Schematic description of the service life model

### 2.3 Carbonation

Deterioration of concrete in service may be the result of physical and chemical process such as attack by chloride and carbon dioxide. In reinforced concrete (RC) the most deterioration mechanisms are due to corrosion of the reinforcing bar [15]. Reinforcing bar in the RC structures are protected from corrosion by a thin oxide layer that form in reinforcing bar's surface due to the high alkalinity of concrete. The water void in the concrete has the pH value in the range of 12.5-13.5. The high pH level makes the steel reinforcement passive and protects it from corrosion. Corrosion may start when this passivation layer is destroyed, either by chloride penetration or due to a reduction in the pH value of concrete below a value of 9. Such a reduction in alkalinity is the result of carbonation of the  $\text{Ca}(\text{OH})_2$  in the concrete mass, i.e., its reaction with the atmospheric  $\text{CO}_2$  that diffuses through the pores of concrete. The corrosion of steel reinforcement induces cracking and then peeling of concrete cover [16].

Carbonation in structures means the carbonation reaction of carbon dioxide and cement hydrate as result of the penetration of the carbon dioxide of the air into concrete [17]. It is generally recognized that the environment is an important factor in the

carbonation process [18,19]. The reaction of carbon dioxide and cement hydrate as follows:



Deterioration due to carbonation and steel corrosion during the incubation stage, propagation stage, acceleration stage and deterioration stage is shown in Fig. 2.5 and Table 2.1 as follow:

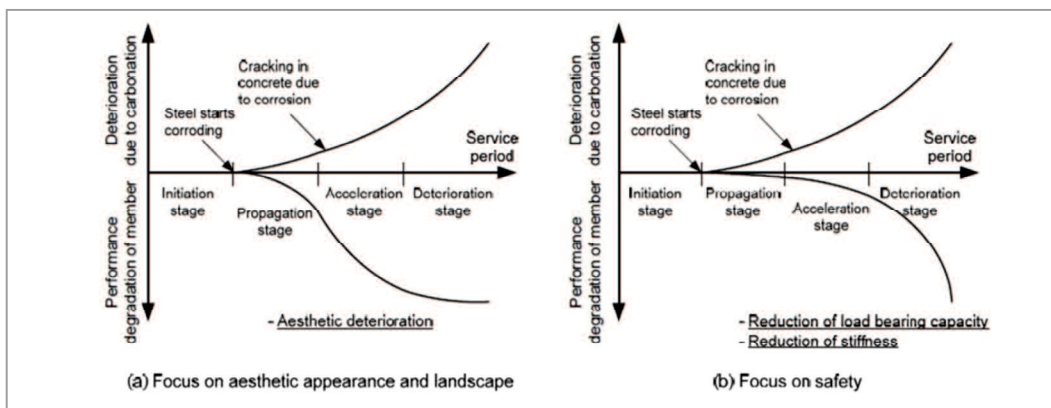


Figure 2.5 Conceptual view of deterioration progress due to carbonation

Table 2.1 Definition of deterioration stages due to carbonation

Stage of deterioration	Definition	Factor determining the stage
Initiation stage	Until the depth of carbonation reaches the limit state for the occurrence of corrosion	Rate of carbonation
Propagation stage	From the initiation of corrosion steel until cracking due to corrosion	Rate of steel corrosion
Acceleration stage	Stage in which steel corrodes at a high rate due to cracking due to corrosion	Rate of corrosion of steel with cracks
Deterioration stage	Stage in which load bearing capacity is reduced considerably due to increased steel corrosion	

The performance of degradation of an RC structure due to carbonation is examined when the carbonation depth reaches the limit of the initial steel corrosion as the initiation stage. The propagation stage is restricted by the initiation of corrosion to cracking due to carbonation. In the acceleration stage and the deterioration stage, factors determining these stages are the rates of corrosion of the steel due to cracking [20].

The model of carbonation of concrete is mostly based on Fick's first law of diffusion. The amount of carbon dioxide (CO<sub>2</sub>) which penetrates the concrete due the CO<sub>2</sub> gradient between the outer air of environment and the content in the concrete can be balanced:

$$dm = D.A.\frac{c_1 - c_2}{x}.dt \quad (2.4)$$

where  $dm$  is mass increment of CO<sub>2</sub> transported by diffusion during the time interval  $dt$  in kgCO<sub>2</sub>,  $D$  is CO<sub>2</sub> diffusion coefficient of carbonated concrete in m<sup>2</sup>/s,  $A$  is surface area considered in m<sup>2</sup>,  $c_1$  is CO<sub>2</sub> concentration of environment in kgCO<sub>2</sub>/m<sup>3</sup>,  $c_2$  is CO<sub>2</sub> concentration at the carbonation front in the concrete in kgCO<sub>2</sub>/m<sup>3</sup>,  $dt$  is time interval in second, and  $x$  is depth of carbonation in meter.

At the carbonation front, CO<sub>2</sub> reacts with alkalis of the pore water solution to form various types of carbonates phases, which can be balanced:

$$dm = a.A.dx \quad (2.5)$$

where  $dm$  is mass of CO<sub>2</sub> transported required for the complete carbonation of the depth increment  $dx$  in kgCO<sub>2</sub>,  $a$  is CO<sub>2</sub> binding capacity of non-carbonated concrete in kgCO<sub>2</sub>/m<sup>3</sup>,  $A$  is surface area considered in m<sup>2</sup>, and  $dx$  is depth increment in meter.

The balances of the diffusion and the reaction process can be combined:

$$x.dx = -\frac{D}{a}(c_1 - c_2).dt \quad (2.6)$$

Assuming  $D$ ,  $a$  and  $(c_1 - c_2)$  to be neither time-dependent nor depth-dependent, integration leads to:

$$x^2 = \frac{2.D}{a} (c_1 - c_2).t^* \quad (2.7)$$

Where  $t^*$  is the exposure time.

Combining the single concentrations  $c_1$  and  $c_2$  into the concentration gradient  $\Delta C_s$  and solving for penetration depth gives:

$$x_c(t) = \sqrt{\frac{2.D.\Delta C_s}{a}}.\sqrt{t} \quad (2.8)$$

Combining the material parameters  $D$  and  $a$  with the environmental parameter  $\Delta C_s$  and expressing the exposure time  $t^*$  as the different in age  $t$  and the moment once the surface is exposed to  $\text{CO}_2$  finally equates to a simple square root of time (root  $t$ ) approach including only the carbonation rate  $K$ , which can be determined by structure investigations without further knowledge of the environmental condition or material properties.

$$x_c(t) = K\sqrt{(t - t_{\text{exp}})} \quad (2.9)$$

$t_{\text{exp}} = 0$ , then:

$$x_c(t) = K\sqrt{t} \quad (2.10)$$

Where  $K$  is the carbonation rate in  $\text{mm/s}^{0.5}$ ,  $t$  is the age of concrete at time of inspection in second,  $t_{\text{exp}}$  is the time until surface is exposed to  $\text{CO}_2$  in second.

Usually the time until exposure  $t_{\text{exp}}$  equal with zero as it is negligibly short compared to the service life. With the data of the age of structure and the exposure time (elapsed time), the equation can be solved for  $K$  [21].

The previous model is similar to the predicting the rate of carbonation progress according to Ref. [20]. The predicting of the carbonation rate is important to estimate the time length of initiation stage. In the case where the carbonation depth has been measured on the period of carbonation, the rate of carbonation can be obtained by the root  $t$  law.

It confirmed that the carbonation depth is in proportion of the square root of the period of carbonation, as follows:

$$A = \frac{d(t)}{\sqrt{t}} \quad (2.11)$$

Where  $d(t)$  is carbonation depth in mm at time  $t$  in year,  $A$  is carbonation rate in mm/year<sup>0.5</sup>, and  $t$  is the period of carbonation in year.

## 2.4 Chloride attack

Performance degradation of RC structure due to corrosion initiated by chloride attack is a severe problem, particularly on RC structure which is located near the sea. The chloride ion ingresses in the concrete cover and lead to the initiation of corrosion [22]. Corrosion can be initiated by changes to the passivating alkaline to the acidic environment with the presence of aggressive compound such as chloride [23]. Chloride attack in RC structure due to corrosion leads cracking and spalling in the concrete cover.

Deterioration due to chloride attack and steel corrosion progresses during the initiation stage, propagation stage, acceleration stage and deterioration stage as shown in Table 2.2 and Fig. 2.6 Initiation stage was reached when the chloride ion concentration on the surface of steel reaches the marginal concentration for the occurrence of corrosion is 1.2 kg/cm<sup>3</sup> in accordance with Ref. [24].

In order to evaluate the accurate estimation of the length of initiation stage, the predicting of chloride ion diffusion should be conducted. Fick's second law in of diffusion equation Eq. (2.12) is one of the methods to obtain the predicting of chloride ion distribution. Eq. (2.13) is a solution of Eq. (2.12) which is obtained on the basis of assumption that the surface chloride ion content is constant. Eq. (2.13) has been generally used for analyzing the rate of chloride penetration.

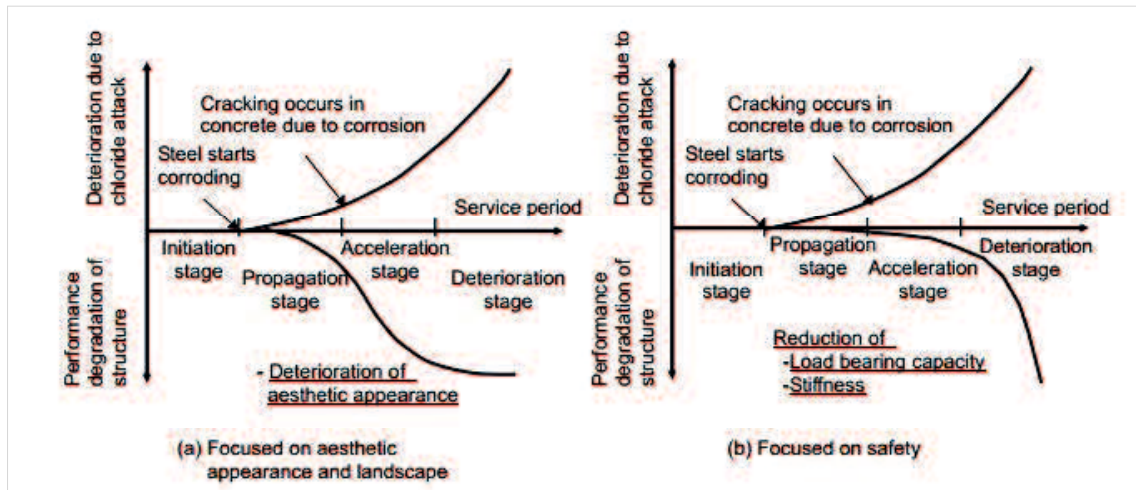


Fig. 2.6 Conceptual view of deterioration progress due to chloride ion

Table 2.2 Definition of deterioration stages due to chloride ion

Stage of deterioration	Definition	Factor determining the stage
Initiation stage	Until the chloride ion concentration on the surface of steel reaches the marginal concentration for the occurrence of corrosion	Diffusion of chloride ion Initially contained chloride ion concentration
Propagation stage	From the initiation of corrosion steel until cracking due to corrosion	Rate of steel corrosion
Acceleration stage	Stage in which steel corrodes at a high rate due to cracking due to corrosion	Rate of corrosion of steel with cracks
Deterioration stage	Stage in which load bearing capacity is reduced considerably due to increased steel corrosion	

The chloride ion content in Eq. (2.13) is the total chloride amount per unit volume of concrete. The chloride ion diffusion coefficient in Eq. (2.13) is referred as an apparent diffusion coefficient.

$$\frac{\partial C}{\partial t} = D_c \left( \frac{\partial^2 C}{\partial x^2} \right) \quad (2.12)$$

Where  $C$  is chloride ion concentration in the liquid phase in  $\text{kg/m}^3$ ,  $D_c$  is chloride diffusion coefficient in  $\text{cm}^2/\text{year}$ ,  $x$  is depth from concrete surface in meter, and  $t$  is time in year.

$$C(x, t) = C_0 \cdot \left(1 - \operatorname{erf} \left[ \frac{x}{2\sqrt{(D_{ap} \cdot t)}} \right] \right) + C_i(x, 0) \quad (2.13)$$

Where  $C(x, t)$  is the chloride ion content in depth  $x$  at time  $t$  in  $\text{kg/m}^3$ ,  $C_0$  is the chloride ion content at the concrete surface in  $\text{kg/m}^3$ ,  $D_{ap}$  is the apparent diffusion coefficient of the chloride ion in  $\text{cm}^2/\text{year}$ , and  $C_i(x, 0)$  is the initial chloride ion content in concrete in  $\text{kg/m}^3$ .

The surface chloride ion content and apparent chloride ion diffusion coefficient were predicted by fitting curve of data of the distribution of chloride ion content using Eq. (2.13). The apparent diffusion coefficient of chloride ion can be obtained from the distribution of chloride ion content in accordance with JSCE-G 573 "Measurement method for distribution of total chloride ion in concrete structure [25].

## 2.5 Corrosion

The most serious deterioration mechanisms that occur in RC bridges are associated with corrosion. The direct effects of corrosion are loss of reinforcing bar cross-section, increase in reinforcing bar diameter as the result of corrosion product, also change in the mechanical characteristics of the reinforcing bar. Effects of corrosion in reinforcing bar in RC are divided into two aspects, on the reinforcing bar itself and on the concrete [26].

The effect of corrosion in structural behavior of RC mainly is reduced strength as the result of loss of section of reinforcing bar. General corrosion is caused by ingress of chloride ion or carbonation of concrete [21]. It is generally associated with forming of rust steel oxides, which make an expansion of reinforcing bar as it corrodes, leads to cracking and eventually spalling of the concrete cover. The residual cross-sectional area  $A_{res}$  can be evaluated by Eq. (2.14):

$$A_{res} = A_0 - A_{corr} = \frac{\pi \cdot (d_b - 2p(t))^2}{4} \quad (2.14)$$

Where  $A_0$  is original cross-sectional area in  $\text{mm}^2$ ,  $A_{corr}$  is loss in cross-sectional area in  $\text{mm}^2$ ,  $b_d$  is original reinforcing bar diameter in  $\text{mm}$  and  $p(t)$  is corrosion penetration depth in  $\text{mm}^2$ .

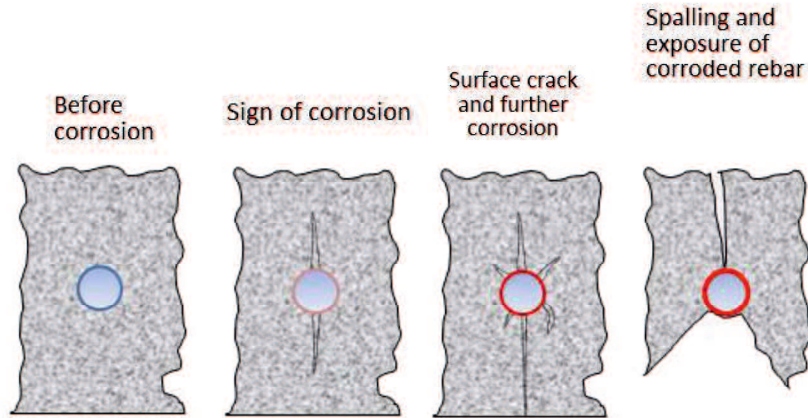


Fig. 2.7 Corrosion process

Fig. 2.7 shows the corrosion process due to chloride ion or carbonation in concrete. The corrosion process of reinforcing bar begins with the rust expanding on the surface of the reinforcing bar and causing cracks near the steel. Over time, the corrosion formed and causes more severe cracking until the concrete cover breaks away from the reinforcing bar, eventually causing spalling.

Based on Ref. [20] to simplify the method of measurement of reinforcing bar corrosion, the state of reinforcing bar corrosion is graded for evaluation it was shown in Table 2.3.

Table 2.3 Grade of corrosion and state of steel

Grade of corrosion	State of steel
I	Mild scale. Thin and compact rust layer all over the steel. No rust adhesion on concrete surface.
II	Swelling rust exist at some locations but it spotty in small area
III	No lack of section can be visually recognized. Swelling rust exists all around the reinforcing bar or throughout the length of reinforcing bar
IV	Lack of section of reinforcing bar

Table 2.4 can be used as a guideline of condition steel corrosion when the monitoring of steel corrosion is conducted by using a non-destructive test and electrochemical methods which were applied to corrosion caused by carbonation (in fewer cases) and chloride ion attack. In cases where the performance of structure could not be evaluated directly from the state of concrete and steel, the defect of the concrete structure appearance provides data for performance evaluation. Table 2.4 shows the grade of structural appearance and stage of deterioration due to carbonation and chloride ion attack.

Table 2.4 Grade of structural appearance corrosion and stage of deterioration

Grade of structural appearance	State of deterioration	
	Due to carbonation	Due to chloride ion attack
I-1 (initiation stage)	No defect found in appearance. Remaining concrete cover is at or more than the limit of rust development	No defect found in appearance. The marginal chloride ion concentration for the occurrence of corrosion has not been exceeded.
I-2 (propagation stage)	No defect found in appearance. Remaining concrete cover is below more than the limit of rust development	No defect found in appearance. The marginal chloride ion concentration for the occurrence of corrosion has been exceeded. Corrosion initiates.
II-1 (first half of acceleration stage)	Cracking occurs due to corrosion	Cracking occurs due to corrosion. Leaching of rust is observed.
II-2 (second half of acceleration stage)	With the progress of cracking due to corrosion, peeling or spalling is found. No lack of section of steel.	Numerous cracks occur due to corrosion. Leaching of rust is observed. Partial peeling or spalling is found. The corrosion amount of steel increases.
III (deterioration stage)	Peeling or spalling are found with cracking due to corrosion. Lack of section of steel.	Numerous cracks occur due to corrosion. Crack width is large. Leaching of rust is observed. Peeling or spalling are found. Great displacement and deflection are observed.

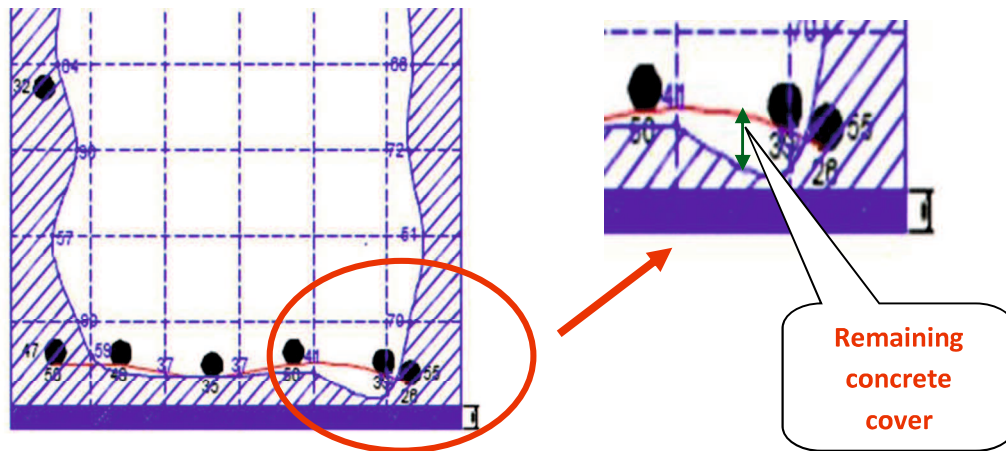


Fig. 2.8 Remaining concrete cover

Corrosion is generally caused by penetration of chloride ion or carbonation of concrete. Steel corrosion due to carbonation accelerates the degradation of RC structures performance. Corrosion will occur as the pH values drop around the steel. It is difficult to define an indicator for determining the initiation of corrosion, so previous researches identified that the initiation of corrosion using the thickness of remaining concrete cover. The thickness of remaining concrete cover is the difference between the thickness of concrete cover and the carbonation depth. It can be seen in Fig. 2.8.

As the limit of corrosion, previous researches concluded that corrosion occurs as the thickness of remaining concrete cover falls below 10 mm. The thickness of concrete cover can be obtained using the carbonation depth and the thickness of concrete cover measurements as the results of carbonation test.

In order to determine the volume of corroded steel which cause cracks due to corrosion caused by carbonation, electrolytic test should be conducted. The result of electrolytic testing can be used for reference because the corrosion progresses uniformly around the reinforcing bar during the test were conducted. The volume of corroded steel as the reference of the initiation of crack due to corrosion is approximately  $10 \text{ mg/cm}^2$ .

Corrosion due to chloride attack was also occurred as pH values drop around the steel. If the chloride ion exists and exceeded the value of chloride ion content in the reinforcing bar, the passivated layer will be destroyed and the reinforcing bar will start corroding. The initiation corrosion due to chloride ion attack can be determined as the marginal chloride ion concentration. The value of marginal chloride is  $1.2 \text{ kg/cm}^3$  in accordance with Ref. [24].

Corrosion rate is the speed at which any steel deteriorates in a specific environment. The speed or rate of deterioration depends on the environmental conditions and the type and condition of steel under reference. Environmental condition in this case is chloride and carbon dioxide. Ref. [27,28] introduced the equation to estimate steel corrosion rate which involving several factors that affect the corrosion rate as (1) chloride ion content at reinforcing bar location, (2) remaining concrete cover which is obtained by the thickness of concrete cover minus carbonation depth, (3) moisture content in the surface of concrete cover, and (4) temperature. Steel corrosion rate  $V$  is calculated using Eq. (2.15) if the remaining concrete cover at time  $t$  is greater than 10 mm, or using Eq. (2.16) if the remaining concrete cover is not greater than 10 mm.

$$V = 1.32(Cl - 1.2) \cdot k \quad (2.15)$$

$$V = (0.840W - 0.145C + 1.32Cl + 0.0293W \cdot C - 0.0917C \cdot Cl + 0.658Cl \cdot W - 2.52) \cdot k \quad (2.16)$$

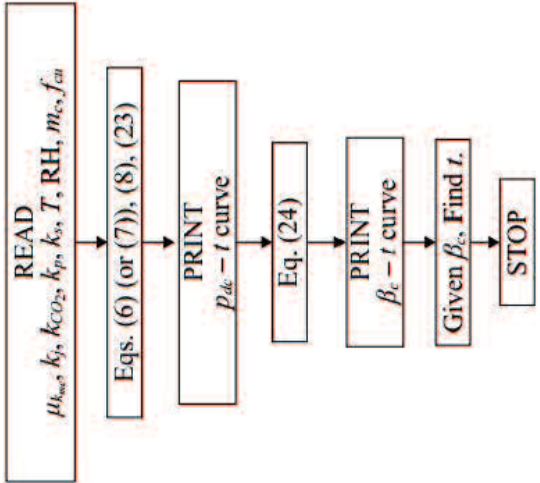
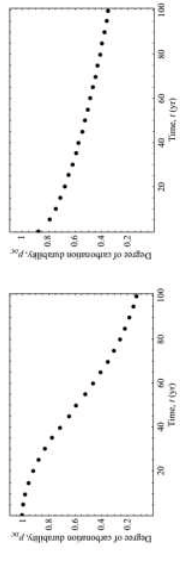
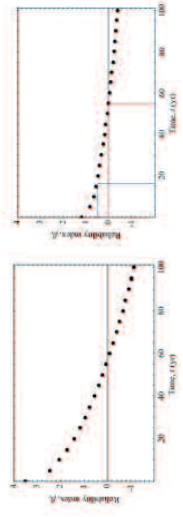
Where  $V$  is the steel corrosion rate in  $\text{mg/cm}^2/\text{year}$ ,  $Cl$  is the chloride ion content at the reinforcement location in  $\text{kg/m}^3$ ,  $C$  is the remaining concrete cover in mm,  $W$  is the surface moisture content of concrete in percent, and  $k$  is the correction at temperature  $tmp$  in  $^\circ\text{C}$ , which can be calculated by Eq. (2.17) as follows:

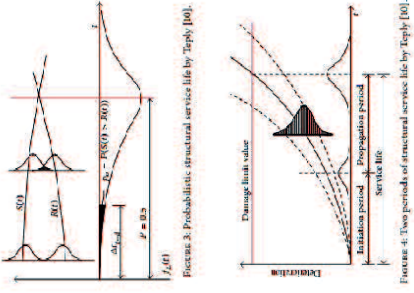
$$k = 1 + 0.0381x(tmp - 20) \quad (2.17)$$

The results of Steel corrosion rate  $V$  will be used to estimate the remaining life or the service life which is restricted by the cumulative amount of steel corrosion  $Q$  as the end of service life. Table 2.5 shows the review of several literatures relating to this study.

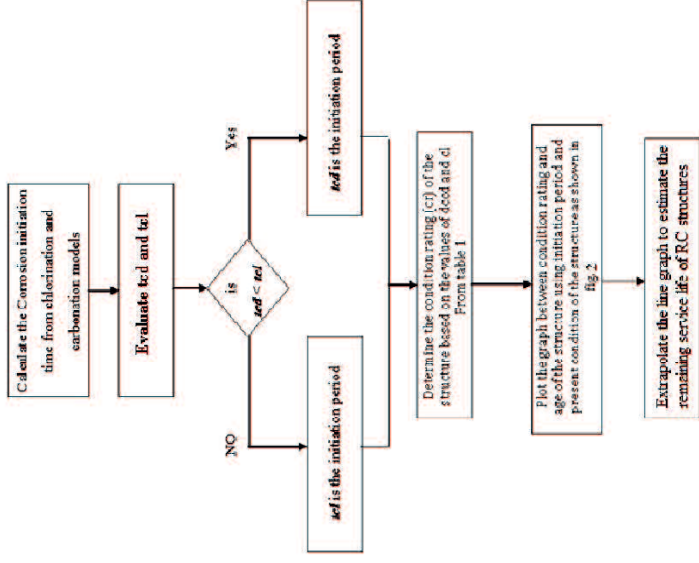
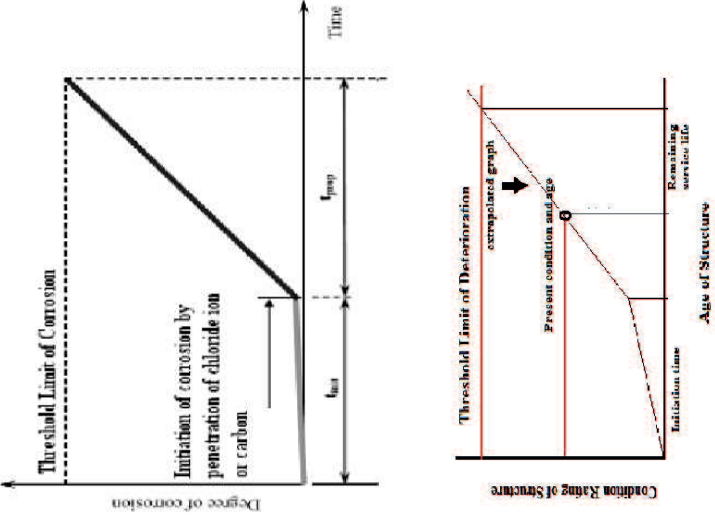
Table 2.5 Summary and comparison of the literatures review

No.	TITLE AUTHOR	RESEARCH PURPOSES	METHODS
1.	<p>Service life prediction of a concrete bridge structure subjected to carbonation</p> <p>Ref. [29]</p> <p>Ann et al. <i>Construction and Building Materials</i> 24, 2010, pp. 1494-1501</p>	<p>To evaluated the risk of carbonation of a concrete bridge in an urban area by measuring the carbonation rate and concrete cover depth in three different parts: the sound, the cracked and construction joint parts of cover concrete.</p> <p>To calculate the carbonation-free service life at the depth of the steel by safety factor method and the Monte Carlo simulation.</p>	<p>Limit state function for carbonation : The resistance to carbonation is expressed in Eq. (1):</p> $g(t) = R(t) - S(t) \quad (1)$ <p>Where <math>R(t)</math> denote the carbonation resistance (concrete cover depth) and <math>S(t)</math> denote the carbonation risk with time.</p> <p>The limit state of carbonation is expressed in Eq. (2):</p> $g(\phi R, \gamma S) = \phi R - \gamma S \quad (2)$ <p>Where <math>\phi</math> is for carbonation resistance factor, <math>\gamma</math> for carbonation risk factor, <math>R</math> for the concrete cover depth, and <math>S</math> for the carbonation depth.</p> <p>For the safety factor method, the SF can be determined as shown in Eq. (3):</p> $SF = \frac{\gamma_c}{\phi_c} \quad (3)$ <p>Where <math>\gamma_c</math> is the carbonation risk factor and <math>\phi_c</math> is the carbonation resistance factor.</p> <p>The probabilistic method was simultaneously adopted to predict the risk of carbonation at the depth of the steel in concrete. The ratio of number of the number of carbonation, calculated by Eq. (1), at the depth of the steel to the number of total trials, as given in Eq. (4):</p> $P_t = \frac{n(g(t)<0)}{N} \quad (4)$ <p>Where <math>P_t</math> is the probability of carbonation at the depth of the steel, and <math>n(g(t) &lt; 0)</math> denotes the number of carbonation depth of the steel out of <math>N</math> trials (100,000 trials in this study).</p> <p>The risk of carbonation at the depth of the steel was calculated both the SF method and a probabilistic method utilizing the Monte Carlo simulation.</p>

<p>2. Carbonation service life prediction of existing concrete viaduct/bridge using time-dependent reliability analysis</p> <p>Ref. [7]</p> <p style="text-align: right;">Liang et al. <i>Journal of Marine Science and Technology</i>, Vol. 21, No. 1, 2013, pp. 94-104</p>	<p>The objective of this study is to determine the carbonation life of existing concrete bridge. The carbonation life is predicted using the probability and reliability index analytical method.</p> <p>Service life of the RC or PC structure at the beginning of time of steel corrosion when concrete surface surfers from carbonation and loses the protection function to steel.</p> <p>The flow chart for carbonation service life prediction:</p> 	<p>The one-dimensional time-dependent probability density function for the concrete carbonation depth can be expressed in terms of</p> $f_x(x, t) = \frac{1}{\sqrt{2\pi}\sigma_x(t)} \exp \left[ -\frac{1}{2} \left( \frac{x - \mu_x(t)}{\sigma_x(t)} \right)^2 \right]$ <p>Where <math>t</math> is the carbonation time (year) estimated using Root <math>t</math> Law. <math>\mu_x(t)</math> and <math>\sigma_x(t)</math> are the mean and the standard deviation functions of carbonation depth of concrete.</p> <p>The carbonation remainder calculation model:</p> $x_o(t) = \frac{166(-RH^2 + 1.4RH - 0.4)(c-5)}{f_{cu}} \sqrt{\frac{t}{t_o}}, t \leq t_o$ $x_o(t) = \frac{166(-RH^2 + 1.4RH - 0.4)(c-5)}{f_{cu}}, t \leq t_o$ $x_o(t) = 4.86k_{mo}(-RH^2 + 1.5RH - 0.45)(c-5)(\ln f_{cu} - 2.30), c > 5mm$  <p>The time-dependent probability that corrosion may not occur:</p> $P_{DC}(t) = p\{k\sqrt{t} + x_o - c > 0\}$ <p>The corresponding time-dependent reliability index:</p> $\beta_c = -\phi^{-1}(P_{DC}(t))$ 
--	--	---

<p>3. Probabilistic evaluation of service life for reinforced concrete structures</p> <p>Ref. [6]</p>	<p>This paper present several probability based service life models developed by researchers for evaluating the probability of failure and estimating the residual life of RC structures.</p> <p>Service life of a RC structure is defined as time period during which structure will fulfill the required performance under defined repair and maintenance.</p>	<p><b>Orcesi and Frangopol</b> developed a model using lifetime function to evaluate a probability of survival of bridge components. The expression of the survival function (S) is shown:</p> $S(t) = 1 - F(t) = P(T > t) = \int_t^{\infty} f(u)du$
		<p><b>Li et al</b> presented a performance based on methodology for serviceability assessment of corrosion affected concretes structures. Methods of time-dependent reliability are employed to quantify the probability of serviceability failure.</p> $G(L, S, t) = L(t) - S(t)$ $ps(t) = P[G(L, S, t) \leq 0] = P(S(t) \geq L(t)]$
<p>Verma et al. <i>Chinese Journal of Engineering</i>, Vol.2014, 2014, pp. 201-208</p>		<p><b>Tejly</b> applied a probabilistic approach to predict the service life of concrete structure for modeling the deterioration effects.</p> <p>(i) Prediction of service life for structure during the design process. Assessment of existing structure, estimating residual service life</p>  <p>Figure 3: Probabilistic structural service life by Tejly [6].</p> <p>Figure 4: Two periods of structural service life by Tejly [6].</p>

4.	<p>Reinforcement corrosion in concrete structures, its monitoring and service life prediction-review</p> <p>Ref. [11]</p>	<p>This paper reviewed the remaining service life of a corroding structure carried out with the help of various available prediction models or experimental techniques, using data obtained through monitoring.</p>	<p><b>Bazant's Model</b>          Consider the volume expansion due to the formation of hydrated red rust (<math>\text{Fe}_2\text{O}_3</math>) over the residual bar core.          The duration of steady-state corrosion:  <math display="block">t_{cor} = \rho_{cor} \frac{DAD}{pJ_r}</math> <math display="block">J_r = \left(\frac{W}{F}\right) I_{corr}</math></p>
			<p><b>Wang and Zhao's Model</b>          A method using finite element analysis to determine the thickness of corrosion product, <math>\Delta</math>, corresponding to the time duration when the surface concrete cracks.  <math display="block">\frac{\Delta}{H} = \gamma = 0.33 \left(\frac{D}{C_p}\right)^{0.565} \cdot f_{cti}^{1.436}</math>         The value of H can be used to determine the time necessary for longitudinal cracking of concrete cover <math>t_{cor}</math> as :  <math display="block">t_{cor} = \frac{H}{P_r}</math></p>
<p>S. Ahmad  <b>Cement &amp; Concrete Composites</b> 25, 2003, pp. 459-471</p>			<p><b>Ahmad's Model</b>          An experimental model for service life prediction based on cumulative damage theory.          The final expression for total life of specimen <math>L_t</math>  <math display="block">L_t = \frac{L_c}{\left[1 - \left(\frac{K_2}{K_1}\right) \left\{\frac{F_0 \left(\frac{C_p}{D}\right)}{EI_a}\right\}\right]}</math></p>

<p>5. Estimating Residual Service Life of Deteriorated Reinforced Concrete Structures</p> <p>Ref. [13]</p>	<p>This study proposed a method for estimating residual service life of RC structures based on present condition evaluated by a proposed condition rating system.</p> <p>The present condition of RC structures based on the measured values of concrete cover, carbonation depth and chloride concentration at rebar depth through in-situ tests.</p> 	<p>Based on service life model by Tutti (1982) :</p>  <p>Developed a model to predict the residual service life of RC structures.</p> <p>Corrosion initiation period can be defined as time required for carbonation to reach the rebar level depth (carbonation depth equal to concrete cover).</p> <p>Carbonation models usually use Root t law. Chloride concentration induced corrosion process are modeled by Fick's 2<sup>nd</sup> Law, as follows:</p> $\frac{\partial c}{\partial t} = \frac{\partial}{\partial x} \left[ D \frac{\partial c}{\partial x} \right]$ <p>Where c is the chloride content at depth x and time t. D is the diffusion coefficient.</p>
--	---	--

	<p>Verma et al.  <i>American Journal of  Civil Engineering and  Architecture, Vol. 1,  No. 5, 2013, pp. 92-96</i></p>		<p>Corrosion initiation time can be evaluated using following equation:</p> $t_{\text{init}} = \frac{c^2}{4D} \left[ \text{erf}^{-1} \left( 1 - \frac{c_{\text{th}}}{c_s} \right) \right]^{-2}$ <p>Where c is concrete cover, cs is surface chloride content, cth is threshold chloride content, and erf is error function.</p> $\text{erf}(u) = \frac{2}{\sqrt{\pi}} \int_0^u e^{-t^2} dt$ <p>The variables are required to calculate initiation period and estimating residual service life :</p> <p>cc = concrete cover (mm)  cd = carbonation depth evaluated (mm)  dccc = difference between concrete cover and carbonation depth (mm)  = cc-cd  tcd = time period for carbonation to reach rebar depth after construction (from Root t Law).</p>
--	---	--	--

## 2.6 References

- [1] Japan Society of Civil Engineers, Structural performance of concrete structures undergoing material deterioration, (in Japanese), Concrete technology series no. 71, JSCE, 2006.
- [2] A. Miyamoto, M. Kushida, H. Morikawa, and K. Kinoshita, Development and reliability enhancement of neuro-fuzzy expert system for concrete bridge diagnosis, (in Japanese), Proceedings of the Japan Society of Civil Engineers, 510-VI-26, pp. 91–101, 1995.
- [3] A. Miyamoto, K. Kawamura, and H. Nakamura, Optimal maintenance planning for existing bridges using bridge management system (BMS), (in Japanese), Proceedings of the Japan Society of Civil Engineers, 588-VI-38, pp. 191–208, 1998.
- [4] A. Miyamoto, H. Emoto, J. Takahashi, and K. Hiraoka, Remaining life evaluation and its verification of aged bridge based on field inspections, (in Japanese), Concrete Research and Technology, Vol. 23, No. 3, pp. 119-132, 2012.
- [5] J. Takahashi, A. Miyamoto, and H. Emoto, Verification of estimation through concrete core testing of remaining life of bridge during its demolition, (in Japanese), Proceedings of the JSCE Annual Conference, VI226, 2011.
- [6] S.K. Verma, S.S. Bhadauria, and S. Akhtar, Probabilistic evaluation of service life for reinforced concrete structures, Chinese Journal of Engineering, Vol. 2014, pp. 201-208, 2014.
- [7] M.-T. Liang, T.R. Huang, and S.-A. Fang, Carbonation service life prediction of existing concrete viaduct/bridge using time-dependent reliability analysis, Journal of Marine Science and Technology, Vol. 21, No. 1, pp. 94-104, 2013.
- [8] W. Chai, W. Li, and H. Ba, Experimental study on predicting service life of concrete in marine environment, Civil Engineering Journal, Vol. 5, No. 1, pp. 93-99, 2011.
- [9] D. Vorechovska, B. Tepy, and M. Chroma, Probabilistic assessment of concrete structure durability under reinforcement corrosion, Journal of Performance of Constructed Facilities, Vol. 24, No. 6, 2010, pp. 571-579, 2010.
- [10] S.J. Kwon, U.J. Na, S.S. Park, and S.H. Jung, Service life prediction of concrete wharves with early-aged crack: Probabilistic approach for chloride diffusion, Structural Safety, 31, pp. 75-83, 2009.
- [11] S. Ahmad, Reinforcement corrosion in concrete structures, its monitoring and service life prediction – a review, Cement & Concrete Composite, 25, 459-471, 2003.
- [12] K. Tutti, Corrosion of steel in concrete, Swed. Cem. Con. Res. Ins., pp. 17-21, 1982.
- [13] S.K. Verma, S.S. Bhadauria, and S. Akhtar, Estimating Residual Service Life of Deteriorated Reinforced Concrete Structures, American Journal of Civil Engineering and Architecture, Vol. 1, No. 5, pp. 92-96, 2013.
- [14] D. Cusson, Z Lounis, and L. Daigle, Durability monitoring for improved service life predictions of concrete bridge decks in corrosive environments, Computer-Aided Civil and Infrastructure Engineering, 26, 524-541, 2011.

- [15] V.G. Papadakis, C.G. Vayenas, and M.N. Fardis, Physical and chemical characteristics affecting the durability of concrete, *ACI Materials Journal*, Title no. 88-M24, March-April, pp. 186-196, 1991.
- [16] V.G. Papadakis, C.G. Vayenas, and M.N. Fardis, Fundamental modeling and experimental investigation of concrete carbonation, *ACI Materials Journal*, Title no. 88-M43, July-August, pp. 363-373, 1991.
- [17] J.L. Parrott, Measurement and modeling of porosity in drying cement paste, *Materials Research Symposium Proceedings*, 85, pp. 91-104, 1987.
- [18] J.L. Parrott, A review of carbonation in reinforced concrete, *Cement and Concrete Association*, UK, 1987.
- [19] G. Villain, and G. Platret, Two experimental methods to determine carbonation profiles in concrete, *ACI Materials Journal*, 103, 4, pp. 265-271, 2014.
- [20] Japan Society of Civil Engineers, Standard specifications for concrete structures: maintenance, JSCE, 2007.
- [21] A. Sarja, Predictive and optimized life cycle management, *Building and Infrastructure*, Taylor & Francis, 2006.
- [22] S.K. Verma, S.S. Bhadauria, and S. Akhtar, Evaluating effect of chloride attack and concrete cover on the probability of corrosion, *Front. Struc. Civ. Eng.*, 7(4), pp. 379-390, 2013.
- [23] J.P. Broomfield, *Corrosion of steel in concrete*, E and FN Spon. London, 1997.
- [24] Japan Society of Civil Engineers, Standard specifications for concrete structures: design, JSCE, 2007.
- [25] Japan Society of Civil Engineers, Measurement method for distribution of total chloride ion in concrete structure, JSCE-G 573, 2007.
- [26] J. Cairns and Z. Zhao, Structural behavior of concrete beams with reinforcement exposed, *Proceedings of Institution of Civil Engineers: Structural and Buildings* 99, pp. 141-145, 1993.
- [27] R. Iijima, T. Sasaki, M. Yokota, and M. Matsushima, A study on corrosion of reinforcement in concrete subjected to combined effect of chloride attack and carbonation, (in Japanese), *Proceedings of the Concrete Structure Scenarios*, JSMS, Vol. 4, pp. 11-16, 2004.
- [28] R. Iijima, T. Kudo, and Y. Tamai, Effect of atmospheric temperature on corrosion rate of reinforcement in concrete, (in Japanese), *Proceedings of the Concrete Structure Scenarios*, JSMS, Vol. 8, pp. 299-304, 2008.
- [29] K.Y. Ann, S.-W. Pack, J.-P. Hwang, H.-W. Song, and S.-H. Kim, Service life prediction of a concrete bridge structure subjected to carbonation, *Construction and Building Materials*, 24, pp. 1494-1501, 2010.

# **Chapter 3: REMAINING LIFE PREDICTION OF AN AGED BRIDGE BASED ON CONCRETE CORES TESTS**

---

## **3.1 Introduction**

In recent years, the lifetime management of civil infrastructure has become one of the important issues in sustainable development in world societies. Civil infrastructure such as a bridge needs to be regularly assessed to make sure the continuity of the life of the bridge. Many efforts are now under way to ensure the longevity of the existing bridge through the improvement of the structural performance such as structural safety, remaining life, and so on, and management activities based on effective maintenance plans. An integrated lifetime management system for civil infrastructure in Japan, particularly bridges, becomes crucial based on the large number of aged bridges that need to gain attention. If the remaining life of an aged bridge is to be maximized, it is necessary to assess the structural performance of the bridge regularly. On the other hand, making a decision to remove an aged bridge is also an option. In order to make such a decision, it is important to make appropriate safety evaluation and remaining life prediction [1,2,3].

The Bridge Management System (J-BMS), which integrated with a Bridge Rating EXpert system (BREX), is one of the useful methods to assume the remaining life prediction of an existing concrete bridge [4,5]. BREX is a system that is designed for evaluating the present performance of the target bridge. The outputs are load-carrying capability and durability of each structure member. The input data for rating the concrete bridge are the technical specification of the target bridge, environmental conditions, traffic volume, and other subjective information that can be obtained through detailed visual inspection results. Evaluation results were thus obtained as the soundness level of the remaining life. This information processing approach makes it possible to deal with cases involving a large number of influencing factors. However, the BREX system result needs to be verified. To verify this system, concrete cores were extracted from some parts of the target bridge to conduct the carbonation and chloride ion tests. The result of carbonation and chloride ion tests will be used to assume the remaining life prediction.

This study aimed to evaluate the deterioration process of concrete cores extracted from an aged bridge (approximately 72 years old in service). Considering the most dominant factor affecting the deterioration of the bridge, between carbonation and chloride attack, based on the location of the bridge. In particular, propose a method of remaining life prediction in a case where the deterioration factor is caused mainly by chloride ion and the deterioration factor is caused mainly by carbonation. Furthermore, considering how local evaluation results based on concrete cores tests can be used for the evaluation of the entire span.

### 3.2 Target bridge and research purpose

The investigation was conducted by extracting concrete cores from an aged bridge (SK Bridge). SK Bridge had been constructed on the main route of the National Highway No. 2. Carbonation is considered to be the main deterioration factor because of the heavy traffic volume. There is also concern about the possibility of chloride attack because SK Bridge is located within 1 km upstream from the mouth of the river pouring into the Seto Inland Sea; it can be seen in Fig. 3.1.

SK Bridge is a T-girder concrete bridge. It has eight spans, and each span consists of five girders. Table 3.1 shows the geographical location of SK-Bridge. The bridge has a total length of 168 m and a width of 11 m. SK Bridge had been completed in 1942. After approximately 70 years in service, the bridge had been demolished in 2013. The general view of SK Bridge can be seen in Fig. 3.2.

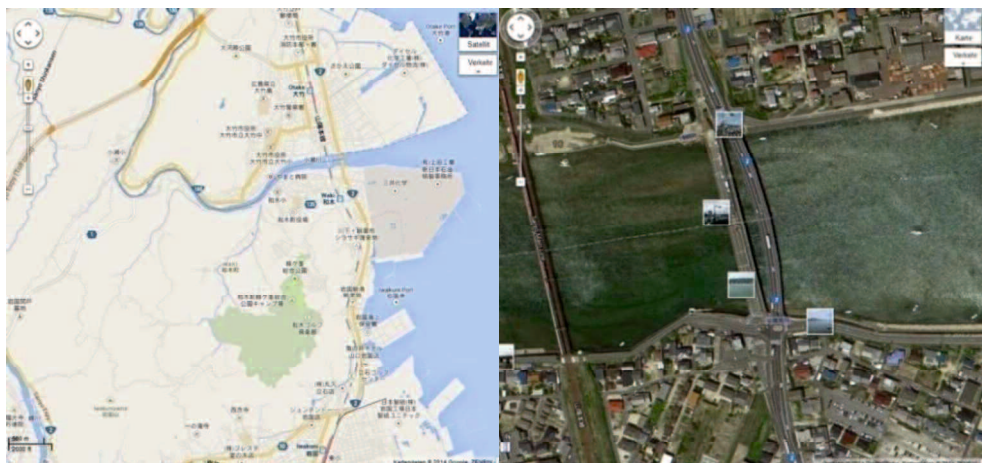


Fig. 3.1 Geographical location of SK-Bridge



Fig. 3.2 General view of SK Bridge

The research purpose is to evaluate the deterioration factor of concrete cores extracted from SK Bridge. Also to develop a method for predicting the remaining life of the bridge in case where the deterioration factor is caused mainly by chloride ion and deterioration factor is caused mainly by carbonation.

This study was started by extracting concrete cores from SK Bridge. Then concrete cores were analyzed to consider the main deterioration factors, either carbonation or chloride attack. The results of concrete cores analysis will be used to decide which the most dominant factor affected the deterioration of the bridge, between carbonation and chloride attack. Finally, the remaining life can be predicted by choosing the prediction flow related to the main factor of deterioration.

The steps in the flow is possible to make clear the relationship between the concrete core test results and the evaluation results obtained from the BREX system based on visual inspection results. Based on visual inspection, the reinforcing bars have been found corroded. The thickness of concrete cover is approximately 40~45 mm. In the flow, the remaining life prediction on the end of service life was calculated using equations with the requirement that the cumulative amount of steel corrosion ( $Q_{CR}$ ) equal with 75 mg/cm<sup>2</sup>. This value is similar with the remaining life as indicated by the BREX system in the evaluation of deterioration of the bridge due to chloride ion attack [1,6].

Moreover it will open the possibilities to identifying the relationship between local evaluation results were obtained by examining concrete cores extracted from the bridge and overall structural evaluation results were obtained from the BREX system or making effective use of different evaluation methods for assessment. By expanding the scope of an evaluation from local to the entire structure of the bridge, it may also be possible to enhance testing efficiency by reducing the total number of concrete cores which are necessary for testing.

### **3.3 Core examination**

#### **3.3.1 Extract of concrete cores**

In this study, concrete cores were extracted from Girder 1 to Girder 5 of Spans 1 and 3 (Fig. 3.3), which are the inspected girder spans. The coring locations are shown in Fig. 3.4 for Spans 1 and 3 with black dots (●) and white dots (○). The concrete cores were extracted from four regions roughly demarcated according to cross beam locations in each span. It was assumed, for purpose of this study that each core shows the average state of internal deterioration in each region [7]. The extracted concrete cores were examined for chloride ion content test called C-series that is identified as ● and “C”. The numbers of C-series are 11 specimens for Span 1 and 12 specimens for Span 3. M-series were examined for carbonation test that is identified as ○ and “M”. The numbers of M-series are 15 specimens for Span 1 and 20 specimens for Span 3 as shown in Table 3.1. Fig. 3.5 shows extraction of the concrete cores and concrete cores specimen is shown in Fig. 3.6.

#### **3.3.2 Chloride ion test**

The concrete cores of C-series were analyzed for chloride ion content. The concrete cores at depth between 0 and 105 mm in depth direction were divided into seven pieces (at interval of 15 mm) and, thus, prepared for analyzing the chloride ion content. The measurement was conducted in accordance with JIS A 1154: 2003; “Methods of test for chloride ion content in hardened concrete,” and the specimens were examined down to the depth at which the initial chloride ion content could be determined. In the test method, the total amount of chloride ion contained in the powder sample which is extracted with nitric acid, and its mass rate to the sample was measured. The chloride ion content test equipment can be seen in Fig. 3.7.

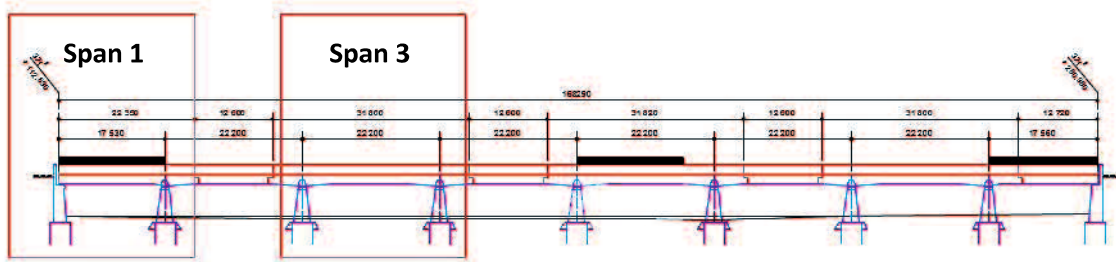


Fig. 3.3 Spans 1 and 3 of SK Bridge

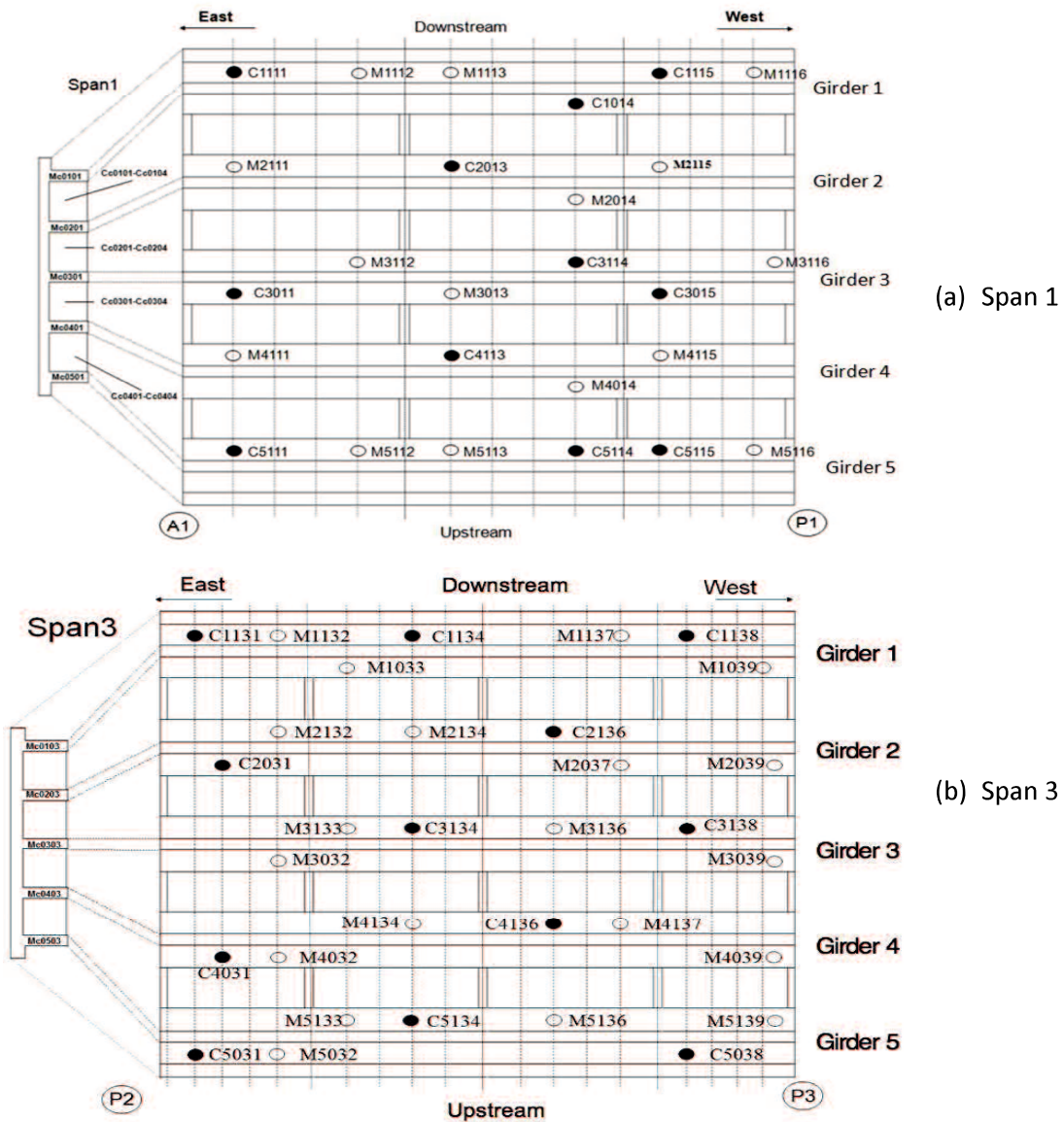


Fig. 3.4 Concrete cores locations

- : concrete coring location for chloride ion investigation
- : concrete coring location for carbonation depth investigation

Table 3.1 Number of concrete cores

No	Girder	Number of specimen			
		C-series		M-series	
		Span 1	Span 3	Span 1	Span 3
1	G1	3	3	3	4
2	G2	1	2	3	4
3	G3	3	3	3	4
4	G4	1	2	3	4
5	G5	3	3	2	4

### 3.3.3 Carbonation test

The concrete cores of the M-series were analyzed for carbonation test. The measurement of carbonation depth was conducted in accordance with JIS A 1152: 2011; “Method for Measuring Carbonation Depth of Concrete.” The carbonation test is most commonly carried out by spraying 1% phenolphthalein solution on the surface of the concrete cores (see Fig. 3.8). The carbonation depth was assessed using 1% phenolphthalein solution, the indicator that appears pink (or purple) in contact with alkaline concrete. Colored area is detected alkaline area, defined as the healthy concrete area (un-carbonated). Colorless area is defined as the carbonation area. To avoid further carbonation on the cutting-off surface, the carbonation test was carried out immediately within 30 minutes after cleaning. Carbonation depth is the distance between the concrete cover surface and the boundary between colored and uncolored areas.



Fig. 3.5 Extraction concrete cores



Fig. 3.6 Concrete cores specimen



Fig. 3.7 Chloride ion test



Fig. 3.8 Carbonation test

### 3.4 Results of concrete cores test

#### 3.4.1 Analysis of chloride ion content

The initial chloride ion and surface chloride ion contents were predicted by fitting curve of data. Based on the analysis results obtained previously, the apparent diffusion coefficient of chloride ion was calculated from the following equation:

$$C(x,t) = C_0 \cdot (1 - \operatorname{erf} \left[ \frac{x}{2\sqrt{(D_{ap} \cdot t)}} \right]) + C_i(x,0) \quad (3.1)$$

Where  $C(x,t)$  is the chloride ion content in depth  $x$  at time  $t$ ,  $C_0$  is the chloride ion content at the concrete surface,  $D_{ap}$  is the apparent diffusion coefficient of the chloride ions, and  $C_i(x,0)$  is the initial chloride ion content in concrete.

The results related to the chloride ion test of concrete cores (C-series) divided into two cases, in order to get the values of the chloride ion content. The 1<sup>st</sup> case, the chloride ion content distribution of concrete cores can be classified into three types as shown in Fig. 3.9 [8,9]. Table 3.2 shows the chloride ion content distribution types of different cores corresponding to Fig. 3.9. Type (a) is affected by small chloride ion content and carbonation, type (b) is affected by large chloride ion content and carbonation, and type (c) is affected by only chloride ion content. In this case, as it can be seen from the chloride ion content, distributions are shown in Fig. 3.9. Eq. (3.1) is difficult to apply to the type (a)

and type (b) distributions are shown in Table 3.2. Therefore, Table 3.2 shows the calculated values of  $C_0$ ,  $D_{ap}$ , and  $C_i(x, 0)$  for only type (c) distribution.

The unknown parameters corresponding to Eq. (3.1) were determined by using the respective analysis results obtained from the divided concrete cores specimens. The thickness concrete cover was approximately 40 mm on average from cross-sectional observation. The analysis results, therefore, obtained from corresponding depth (30–45 mm) in concrete cores were used as chloride ion contents at the reinforcement locations.

Table 3.2 shows the calculated values regarding the chloride ion content analysis only in Span 3. The number of concrete cores is 12 specimens. The number of type (c) specimens is 8 specimens. Therefore, the calculation of remaining life prediction in 1<sup>st</sup> case is only performed on concrete cores C-series type (c).

Table 3.2 Results of chloride ion content analysis (1<sup>st</sup> case)

Girder No.	Core specimen No.	Surface chloride ion content $C_0$ (kg/m <sup>3</sup> )	Apparent diffusion coefficient $\times 10^{-8}$ $D_{ap}$ (cm <sup>2</sup> /s)	Initial chloride ion content $C_i(x, 0)$ (kg/m <sup>3</sup> )	Chloride ion content at reinforcement location $C(x, t)$ (kg/m <sup>3</sup> )	Types shown in Figure 3.9
1	C1131	-	-	-	0.58	(a)
	C1134	1.00	0.08	0.30	0.32	(c)
	C1138	-	-	-	0.53	(a)
2	C2031	-	-	-	0.90	(a)
	C2136	-	-	-	1.36	(b)
3	C3134	1.10	0.45	0.10	0.46	(c)
	C3138	0.85	0.10	0.15	0.21	(c)
4	C4031	0.85	0.50	0.15	0.48	(c)
	C4136	1.32	0.05	0.12	0.14	(c)
5	C5031	1.27	0.04	0.22	0.21	(c)
	C5134	1.32	0.04	0.12	0.16	(c)
	C5038	1.30	0.03	0.30	0.30	(c)

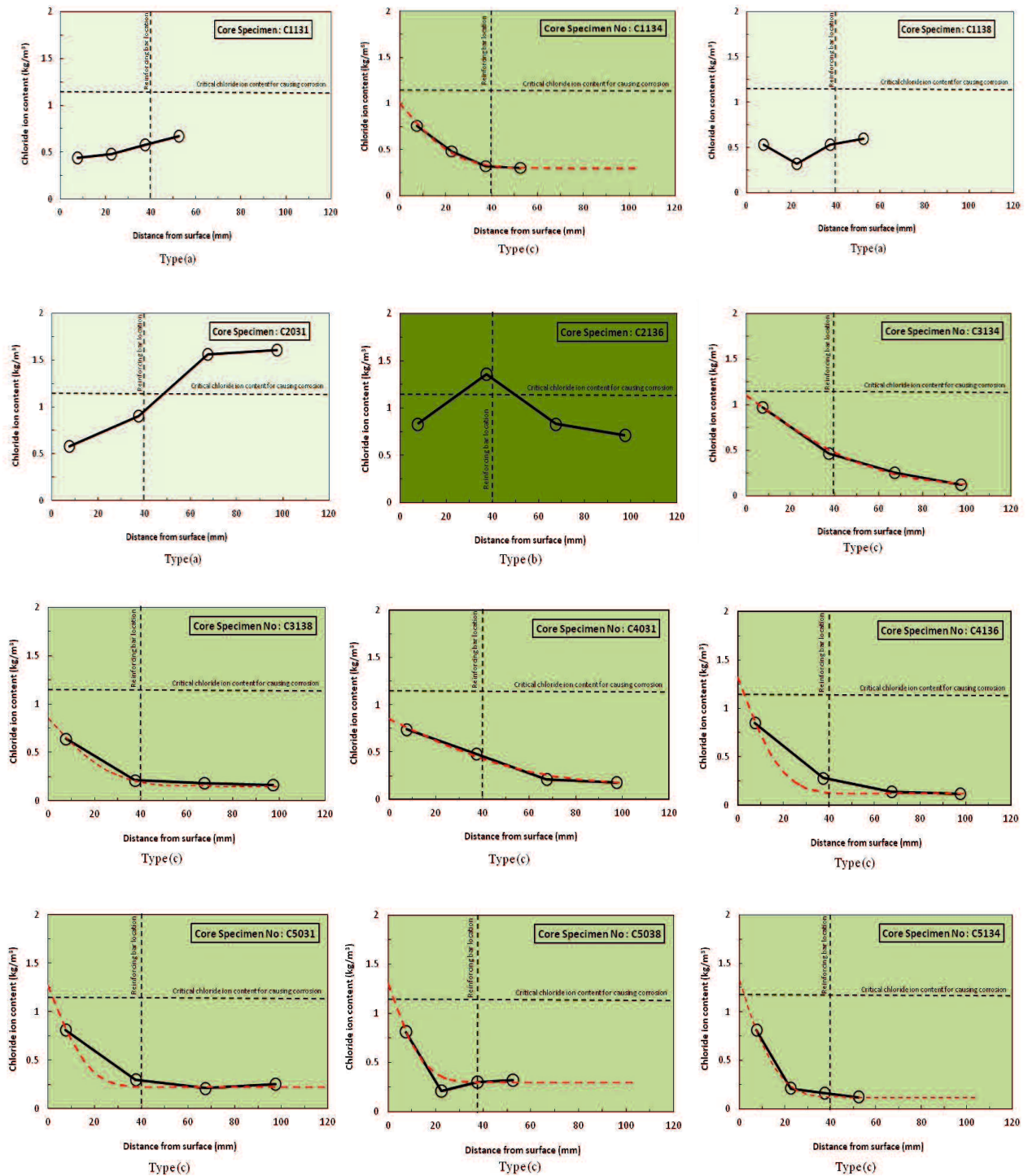


Fig. 3.9 Types of chloride ion content distribution in Span 3

The 2<sup>nd</sup> case, the influence of carbonation is considered on the calculation of the chloride ion contents results. The Table 3.3 shows the calculated values of  $C_0$ ,  $D_{ap}$ , and  $C_i(x, 0)$ . The thickness concrete cover was approximately 45 mm on average from cross-sectional observation. The analysis results also obtained from corresponding depth (30–45 mm) in concrete cores were used as chloride ion contents at the reinforcement locations.

Table 3.3 shows the calculated values regarding the chloride ion content analysis both in Spans 1 and 3. The number of concrete cores is 23 specimens. Therefore, the calculation of remaining life prediction in 2<sup>nd</sup> case is performed on all of concrete cores C-series. Fig. 3.10 shows the chloride ion content distribution of Span 1.

Table 3.3 Results of chloride ion content analysis (2<sup>nd</sup> case)

Span No.	Girder No.	Core specimen No.	Surface chloride ion content $C_0$ (kg/m <sup>3</sup> )	Apparent diffusion coefficient $\times 10^{-8}$ $D_{ap}$ (cm <sup>2</sup> /s)	Initial chloride ion content $C_i(x, 0)$ (kg/m <sup>3</sup> )	Chloride ion content at reinforcement location $C(x, t)$ (kg/m <sup>3</sup> )
Span 1	1	C1014	1.10	0.60	0.60	1.00
		C1111	0.60	0.50	0.40	0.60
		C1115	0.80	0.60	0.60	0.90
	2	C2113	2.30	0.90	0.65	1.80
	3	C3011	2.50	1.80	0.90	2.50
		C3015	2.60	1.80	0.50	2.10
		C3114	3.80	1.50	0.80	3.00
	4	C4113	3.10	0.40	0.40	1.30
	5	C5111	3.90	1.80	0.80	3.20
		C5114	1.80	1.80	0.60	1.70
C5115		1.40	1.80	0.30	1.20	
Span 3	1	C1131	0.70	0.40	0.40	0.60
		C1134	0.70	0.08	0.30	0.30
		C1138	0.90	0.40	0.30	0.55
	2	C2031	2.50	0.40	0.50	1.20
		C2136	1.90	0.40	0.65	1.20
	3	C3134	1.00	0.40	0.10	0.40
		C3138	0.70	0.10	0.15	0.18
	4	C4031	0.90	0.08	0.18	0.20
		C4136	1.20	0.05	0.12	0.12
	5	C5031	1.30	0.05	0.20	0.20
C5134		1.10	0.05	0.12	0.12	
C5038		0.80	0.05	0.30	0.30	

The results of the chloride ion content analysis in the investigated main girders (2<sup>nd</sup> case) almost half of the number is relatively higher than the requirement of the critical chloride ion content for steel corrosion is assigned by 1.2 kg/m<sup>3</sup>. The chloride ion test results reveal some specimens which are affected by large chloride ion content and also carbonation.

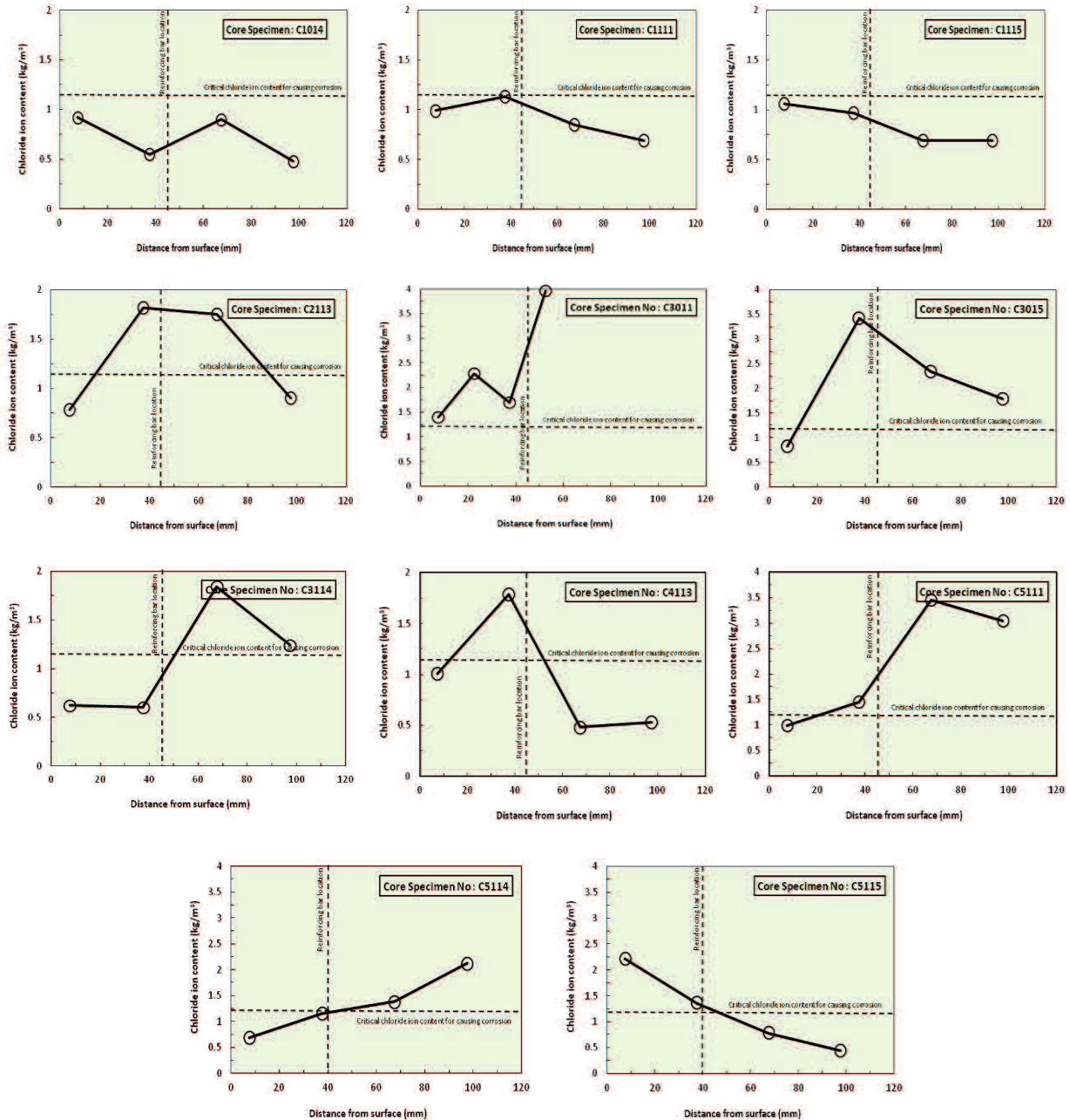


Fig. 3.10 Chloride ion content distributions in Span 1

### 3.4.2 Results of carbonation depth measurement

Table 3.4 shows the results of carbonation depth measurement for concrete cores (M-series). The carbonation depth results shown in Table 3.4 are the average of the values obtained from 10-point measurements, maximum values, standard deviations, and carbonation rate values corresponding to the average.

Table 3.4 Results of carbonation depth measurement

Span No.	Girder No.	Core specimen No.	Carbonation depth (mm)			Carbonation rate (mm/year <sup>0.5</sup> )
			Average value	Maximum value	Standard deviation	
Span 1	1	M1112	65.6	72	5.3	7.84
		M1113	39.6	48	8.7	4.73
		M1116	59.4	65	4.6	7.10
	2	M2014	46.8	52	3.3	5.59
		M2111	51.2	60	7.5	6.12
		M2115	41.6	50	5.3	4.97
	3	M3013	74.4	77	2.4	8.89
		M3112	45.6	54	6.1	5.45
		M3116	55.0	62	3.7	6.57
	4	M4014	68.0	85	12.9	8.13
		M4111	125.4	135	6.8	14.99
		M4115	76.8	82	4.6	9.18
	5	M5112	45.0	52	8.0	5.38
		M5113	52.2	70	16.0	6.24
		M5116	56.0	62	4.6	6.69
Span 3	1	M1132	54.0	60	5.7	6.45
		M1033	52.6	55	2.1	6.29
		M1137	40.2	47	5.9	4.80
		M1039	52.4	56	1.9	6.26
	2	M2132	43.6	48	4.3	5.21
		M2134	58.2	56	4.2	6.96
		M2037	53.8	57	3.1	6.43
		M2039	79.8	90	8.5	9.54
	3	M3032	11.2	15	4.5	1.34
		M3133	44.6	80	27.0	5.33
		M3136	46.0	55	5.3	5.50
		M3039	40.8	58	14.5	4.88
	4	M4032	58.4	77	9.6	6.98
		M4134	51.4	55	2.9	6.14
		M4137	42.2	47	3.7	5.04
		M4039	51.6	70	12.1	6.17
	5	M5032	56.8	62	2.8	6.79
		M5133	37.4	48	7.0	4.47
M5136		60.6	90	19.9	7.24	
M5139		43.8	55	9.5	5.24	

### 3.4.3 Identification of main deterioration factors

Based on Ref [10], the critical chloride ion content for steel corrosion is assigned by  $1.2 \text{ kg/m}^3$ . As shown in Table 3.2, the average chloride ion content in the investigated main girders (1<sup>st</sup> case) of  $0.47 \text{ kg/m}^3$  which is lower than the critical chloride ion content for steel corrosion ( $1.2 \text{ kg/m}^3$ ). It can be seen in Table 3.2 that only 1 of the 12 points on the bridge older than 70 years at which measurements were taken showed a value slightly higher than the critical chloride ion content for steel corrosion. Table 3.3 shows the average chloride ion content in the investigated main girders (2<sup>nd</sup> case) of  $1.07 \text{ kg/m}^3$  which is also lower than the requirement. However, the average chloride ion content in 2<sup>nd</sup> case is relatively higher than the 1<sup>st</sup> case. The chloride ion test results reveal some specimens which are affected by large chloride ion content and carbonation.

Table 3.4 shows the result of carbonation depth measurements. As shown in Table 3.4, the average value of the carbonation depth in the main girder is 49 mm, which is greater than the thickness of concrete cover. This means that the requirement of the remaining (un-carbonated) concrete cover (10 mm) [10], which is an indicator of the degree of influence of carbonation, was considerably exceeded. In nearly half of the concrete cores investigated, the maximum value of carbonation depth was reaching 60 mm or greater, which is considerably greater than the concrete cover.

To take the concrete coring environment into consideration, the water samples taken near the SK Bridge (the target bridge) and the estuary were analyzed. This water analysis revealed that the  $\text{Cl}^-$  and the  $\text{Na}^+$  contents of the water near the SK Bridge were lower than those of the seawater in the estuary, and that they were also lower than half the  $\text{Cl}^-$  and  $\text{Na}^+$  contents of the water near KT Bridge [11], which was deemed to have deteriorated because of chloride attack.

From these results, it was concluded that the deterioration of the SK Bridge was caused mainly by carbonation in view of the fact that the chloride ion contents at the reinforcement locations had not reached the critical chloride ion content for steel corrosion and that the carbonation depth was considerably greater than the thickness concrete cover.

### 3.5 Remaining life prediction method through concrete cores tests

#### 3.5.1 Concept of remaining life prediction method based on carbonation depth

The remaining life prediction for a concrete structure in a case where section loss due to steel corrosion is expressed as the number of years of life expected if the section loss is left uncorrected [12]. Therefore, the remaining life  $R$  can be expressed using the life expectancy  $X$  (years) and the period of service  $N$  (years) as Eq. (3.2).

$$\text{Remaining life } (R) = \text{Life expectancy } (X) - \text{Period of service } (N) \quad (3.2)$$

The method for predicting the service life is available for calculation based on allowable stress, remaining reinforcing bar cross-sectional percentage, and limited state design method. In this paper, however, the remaining life was assessed in terms of the progress of deterioration over time due to carbonation, which is a deterioration factor identified in Section 3.5.3. It is assumed that the deterioration due to carbonation provides an environment that affects factors contributing to corrosion of the reinforcing bar, such as chloride ion and moisture content. Attention is paid on the cumulative amount of steel corrosion due to the spread of carbonation, and the service life of a bridge is deemed to exceed when the cumulative amount of steel corrosion reaches the critical value. The remaining life then was predicted by using Eq. (3.2).

Figure 3.11 shows the flowchart of the remaining life prediction methods in the case where deterioration is caused by chloride attack and the case where it is caused by carbonation (area shown by a dotted line). Based on Fig. 3.11, it can be seen that when the remaining concrete cover is 10 mm or less, it can be recognized that the main deterioration factor is carbonation. In order to predict the life expectancy  $X$  in year, it is necessary to have three types of information: carbonation depth, cumulative amount of steel corrosion, and steel corrosion limit as the criterion for determining service life.

The carbonation depth  $d(t)$  in mm at time  $t$  in year is calculated by using the carbonation rate coefficient  $A$  by Eq. (3.3). The changes in the carbonation depth over time are predicted in accordance with the  $\sqrt{t}$  law and the carbonation rate coefficient  $A$  is calculated from the carbonation depth  $d(t)$  at time  $t$  by using the following equation:

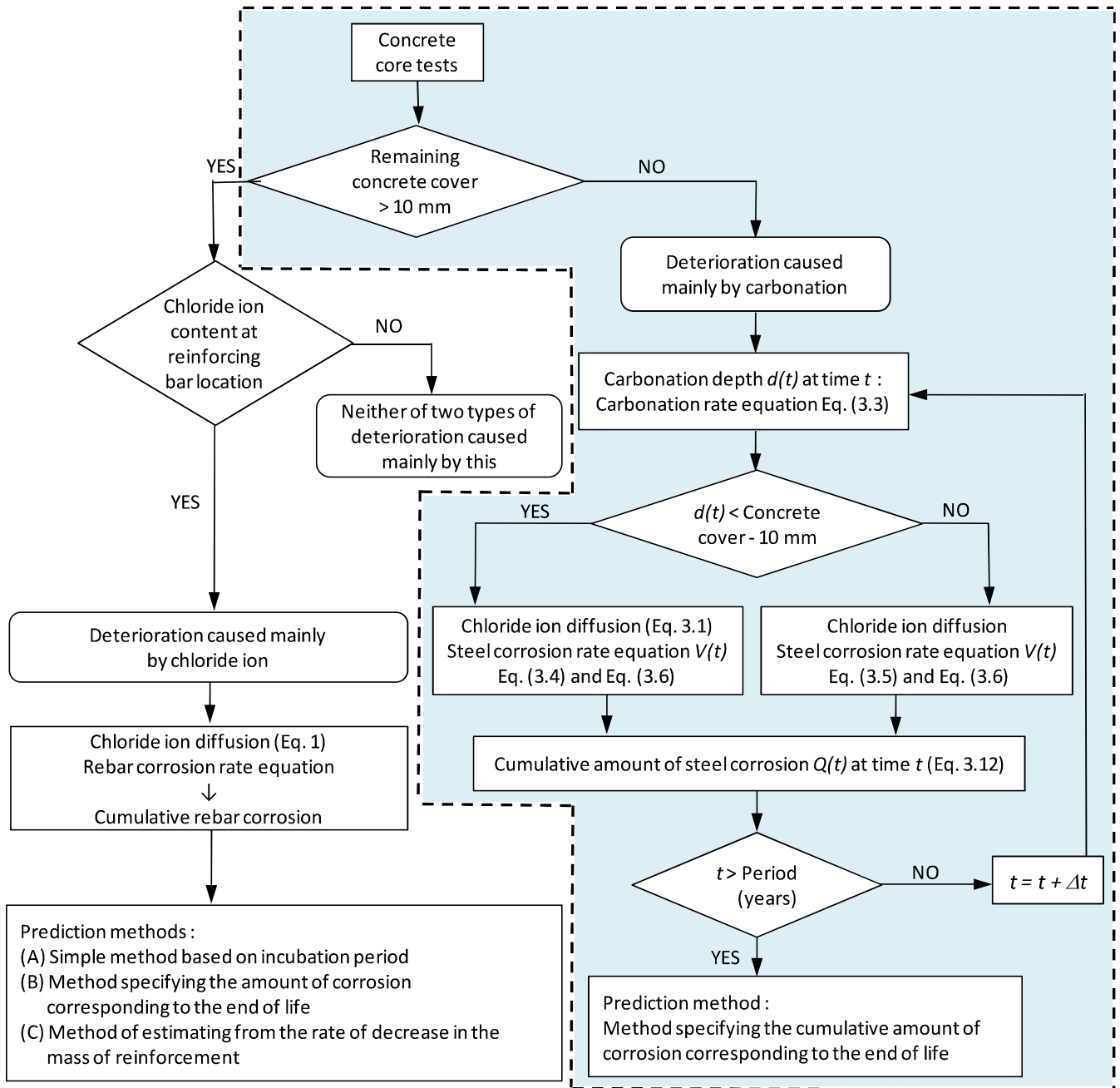


Fig. 3.11 Flowchart of remaining life prediction

$$A = \frac{d(t)}{\sqrt{t}} \quad (3.3)$$

To estimate steel corrosion, the steel corrosion rate  $V$  is calculated as follows: the steel corrosion rate  $V$  is calculated by using Eq. (3.4) if the remaining concrete cover (concrete cover – carbonation depth) at time  $t$  is greater than 10 mm, or using Eq. (3.5) if the remaining concrete cover is not greater than 10 mm [13,14].

$$V = 1.32(Cl - 1.2)k \quad (3.4)$$

$$V = (0.840W - 0.145C + 1.32Cl + 0.0293W \cdot C - 0.0917C \cdot Cl + 0.658Cl \cdot W - 2.52)k \quad (3.5)$$

Where  $V$  (mg/cm<sup>2</sup>/year) is the steel corrosion rate,  $Cl$  (kg/m<sup>3</sup>) is the chloride ion content at the reinforcement location,  $C$  (mm) is the remaining concrete cover,  $W$  (%) is the surface moisture content of concrete, and  $k$  is the correction at temperature  $t_{mp}$  (°C), which can be calculated by Eq. (3.6) as follows:

$$k = 1 + 0.0381(t_{mp} - 20) \quad (3.6)$$

The cumulative amount of corrosion  $Q(t)$  in Eq. (3.12) was obtained from the basic equation using Riemann Integral for the discrete data. The illustration is shown in Fig. 3.12. The basic equation of Riemann Integral as the sum of the areas of the rectangles is shown in Eq. (3.7) as follows:

$$\sum_{i=1}^N f(x_i) \Delta x \quad (3.7)$$

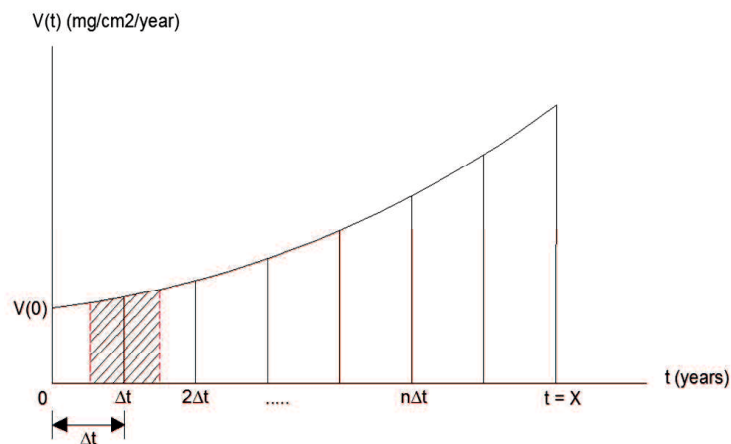


Fig. 3.12 Illustration of the basic equation to calculate  $Q$

Figure 3.12 shows that the steel corrosion rate  $V$  at time  $t$  equal with time step  $\Delta t$ , can be expressed using Eq. (3.8) for the midpoint value, as follows:

$$V(t) = \frac{V\left(t - \frac{\Delta t}{2}\right) + V\left(t + \frac{\Delta t}{2}\right)}{2} \Delta t \quad (3.8)$$

The Eq. (3.8) was substituted into Eq. (3.7) and the equation can be formed as Eq. (3.9) as follows:

$$\sum_{t=\Delta t}^{t=X} V(t) \Delta t = \sum_{t=\Delta t}^{t=X} \frac{V\left(t - \frac{\Delta t}{2}\right) + V\left(t + \frac{\Delta t}{2}\right)}{2} \Delta t \quad (3.9)$$

The summation of Riemann integral over  $t=\Delta t, \dots, x$  should be equal to  $Q(t) - Q(0)$  as shown in Eqs. (3.10) and (3.11) as follows:

$$\sum_{t=\Delta t}^{t=X} V(t) = Q(t) - Q(0) \quad (3.10)$$

$$\sum_{t=\Delta t}^{t=X} \left( \left( V\left(t - \frac{\Delta t}{2}\right) + V\left(t + \frac{\Delta t}{2}\right) \right) \frac{\Delta t}{2} \right) = Q(t) - Q(0) \quad (3.11)$$

Hence, based on Ref. [14,15] the cumulative amount of steel corrosion  $Q(t)$  at time  $t$  can be calculated by Eq. (3.12) as follows:

$$Q(t) = Q(0) + \sum_{t=\Delta t}^{t=X} \left( \frac{\Delta t}{2} \left( V\left(t - \frac{\Delta t}{2}\right) + V\left(t + \frac{\Delta t}{2}\right) \right) \right) \quad (3.12)$$

Where  $Q(0)$  can be calculated by Eq. (3.13) as

$$Q(0) = \frac{\Delta t}{4} \left( V(0) + V\left(\frac{\Delta t}{2}\right) \right) \quad (3.13)$$

Past studies [1,11] reported a simple calculation method using the incubation period and a method that defines the cumulative amount of steel corrosion as methods that can be used in the case where the main deterioration factor is chloride ions. In this paper, the remaining life  $R$  was calculated from Eq. (3.2) on the basis of the time  $t = t_1$  elapsed before the cumulative amount of steel corrosion calculated by using Eq. (3.12) reaches the cumulative amount of steel corrosion  $Q(t_1)$  at which the service life is assumed to the end.

### 3.5.2 Remaining life prediction results

It has been reported [17] that the criterion value  $Q$  of steel corrosion assumed for the purpose of the remaining life prediction ranges widely from 1 to 576 mg/cm<sup>2</sup>. In the remaining life prediction by the BREX system, deterioration curves are applied to structural soundness scores obtained on the basis of visual inspection results. It has also been reported [1,6] that in the prediction method by the BREX system, the cumulative amount of steel corrosion in the last year of the predicted remaining life was  $Q = 75$  mg/cm<sup>2</sup>.

In this paper, therefore, the remaining life prediction was made both in the case where the criterion value  $Q$  is defined as the cumulative amount of steel corrosion of  $Q = 10$  mg/cm<sup>2</sup>, which is said to be the critical amount of corrosion for initial cracking due to carbonation [10], and the case where  $Q$  is defined as the cumulative amount of steel corrosion of  $Q = 75$  mg/cm<sup>2</sup>, which is the same as the remaining life indicated by the BREX system in the evaluation of deterioration due to chloride ions shown in Fig. 3.12. For 1<sup>st</sup> case, this prediction was made for the eight concrete cores (C-series) shown in Table 3.2 for which the apparent diffusion coefficient of chloride ions was determined. For the carbonation rate, the results for M-series concrete cores extracted from the nearest locations shown in Fig. 3.4 were used. The values used for concrete cover,  $t_{mp}$  in Eq. (3.6) and  $W$  in Eq. (3.5), were 40 mm, 16°C (mean temperature), and 4% [18,19], respectively.

Table 3.5 shows the results of the remaining life prediction in 1<sup>st</sup> case where the calculation of remaining life only in the concrete cores C-series type (c) in Span 3. As shown in Table 3.5, the time before reaching the critical amount of corrosion for initial cracking due to carbonation [17] is 37.5 years on average, and approximately 40 years later, the cumulative amount of steel corrosion specified as the criterion value indicating the end of the remaining life is reached. Furthermore, the average value of the remaining life prediction is 7.9 years on average, and it can be seen that the remaining life prediction varies between -13 years and 40 years, depending on the coring locations.

Figure 3.13 show the plotted of remaining life prediction based on the location of extracted concrete cores on Span 3 (1<sup>st</sup> case). In this figure, the result of remaining life prediction in the actual bridge were varies significantly, however, the average value of the

remaining life prediction was used to estimate the remaining life prediction of the entire span 3. Based on the remaining life prediction method that have been established in this thesis, the remaining life prediction of SK Bridge is 7.9 years, means the end the life of the SK Bridge is 77.9 years.

Table 3.5 Results of remaining life prediction (1<sup>st</sup> case)

Girder No.	Core Specimen No.	Q=10mg/cm <sup>2</sup>	Q=75 mg/cm <sup>2</sup>		
		Cracking limit (years)	Predicted life X (years)	Remaining life R (years)	Result of Eq. (12) (years)
1	C1134	27	62	-8	-9
3	C3134	38	69	-1	3
	C3138	46	92	22	21
4	C4031	24	57	-13	-15
	C4136	44	95	25	21
5	C5031	28	62	-8	-6
	C5134	54	110	40	38
	C5038	39	76	6	9
Average (years)		37.5	77.9	7.9	7.8

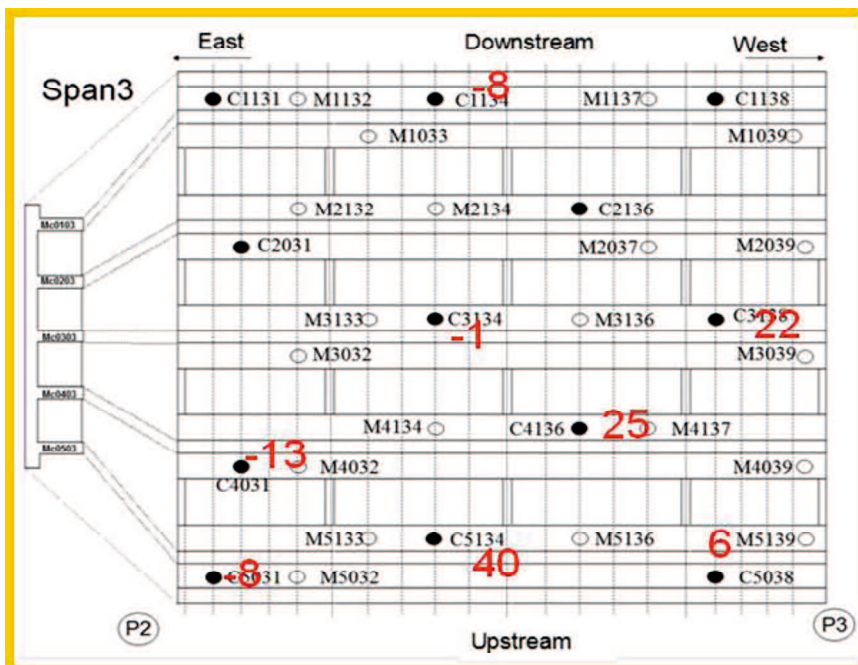


Fig. 3.13 Plotted of remaining life prediction based on the location of extracted concrete cores in Span 3 (1<sup>st</sup> case)

The results of the remaining life prediction of Spans 1 and 3 are shown in Table 3.6. The time before reaching the critical amount of corrosion for initial cracking is 33.0 years and 49.8 years in average, respectively.

Table 3.6 Results of remaining life prediction (2<sup>nd</sup> case)

Girder No.	Core Specimen No.	Q = 10 mg/cm <sup>2</sup>	Q = 75 mg/cm <sup>2</sup>		
		Cracking limit (years)	Predicted life X (years)	Remaining life R (years)	Result of Eq. (12) (years)
<b>SPAN 1</b>					
1	C1014	24	42	-30	-29
	C1111	60	87	15	16
	C1115	29	49	-23	-23
2	C2113	42	55	-17	-16
3	C3011	38	50	-22	-21
	C3015	19	30	-42	-41
	C3114	29	38	-34	-33
4	C4113	24	41	-31	-30
5	C5111	32	49	-23	-22
	C5114	34	48	-24	-25
	C5115	32	49	-23	-23
Average (years)		33.0	48.9	-23.1	-22.5
<b>SPAN 3</b>					
1	C1131	36	61	-11	-11
	C1134	38	73	1	1
	C1138	61	89	17	18
2	C2031	51	69	-3	-3
	C2136	34	52	-20	-20
3	C3134	52	85	13	13
	C3138	63	110	38	39
4	C4031	35	74	2	2
	C4136	62	114	42	41
5	C5031	36	75	3	3
	C5134	76	132	60	60
	C5038	53	91	19	19
Average (years)		49.8	85.4	13.4	13.5

There is relatively significant difference in the calculation of the life expectancy. In Span 1, the cumulative amount of steel corrosion indicating the end of the remaining life is reached on 48.9 years in average. That means the age of the bridge is shorter than the period of service (72 years) when the investigation was conducted. On the other hand, the life expectancy of Span 3 reached 85.4 years in average. There are about 23 years left until the end of the remaining life is reached. The average value of the remaining life prediction is -23.1 years in Span 1 which means the end of life of the bridge has been exceeded. In the Span 3, the average value of the remaining life prediction is 13.4 years on average. From Table 3.6, it can be seen that the remaining life prediction varies between -42 years and 60 years, depending on the location of extracting the concrete cores.

Figure 3.14 show the plotted of remaining life prediction based on the location of extracted concrete cores on Span 1 (2<sup>nd</sup> case). In this figure, the result of remaining life prediction in the actual bridge were varies significantly, The remaining life prediction of SK Bridge is -23.1 years, means the end the life of the SK Bridge is 48.9 years.

The plotted of remaining life prediction based on the location of extracted concrete cores on Span 3 (2<sup>nd</sup> case) is shown in Fig. 3.15. The result of remaining life prediction in the actual bridge were also varies significantly. The remaining life prediction of SK Bridge is 13.4 years, means the end the life of the SK Bridge is 85.4 years.

The comparison of the results of predicted life of concrete cores between 1<sup>st</sup> case and 2<sup>nd</sup> case can be seen in Fig. 3.16. According to the time of investigation equal with 72 years, the aged of Span 3 (1<sup>st</sup> case) and Span 3 (2<sup>nd</sup> case) both are more than 72 years, so the remaining life prediction of both are positive value. On the other hand the remaining prediction of Span 1 (2<sup>nd</sup> case) is negative value, meaning the Span 1 have already reached the end of life before the time of investigation.

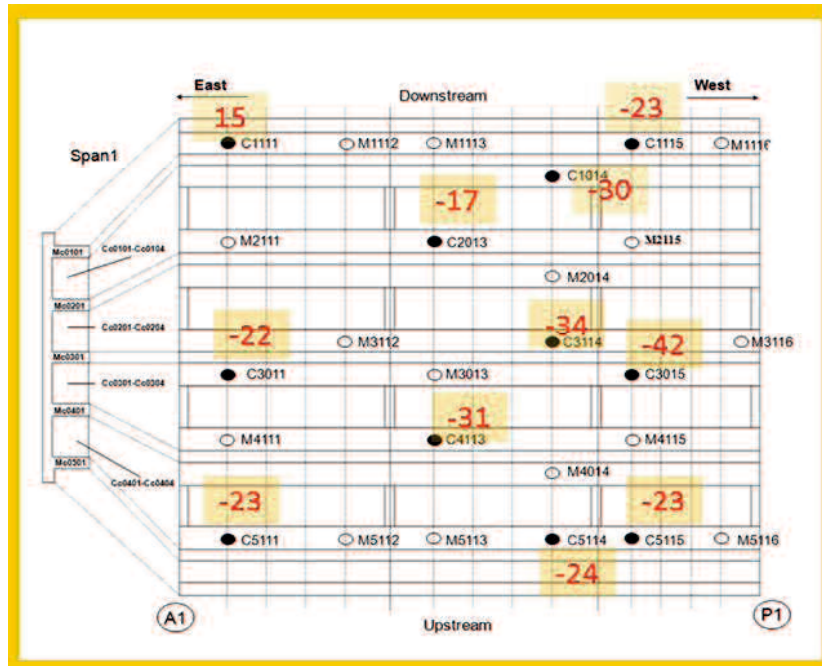


Fig. 3.14 Plotted of remaining life prediction based on the location of extracted concrete cores in Span 1 (2<sup>nd</sup> case)

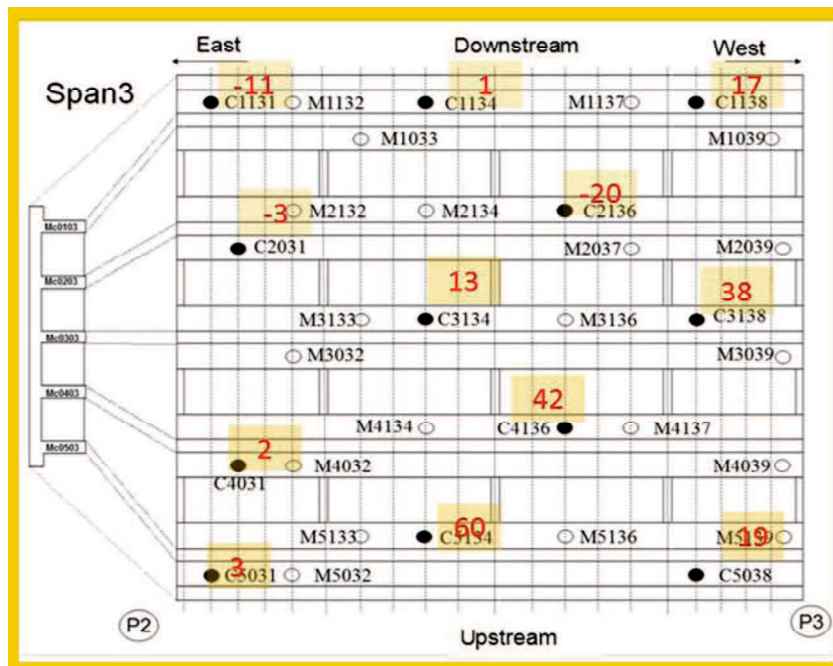


Fig. 3.15 Plotted of remaining life prediction based on the location of extracted concrete cores in Span 3 (2<sup>nd</sup> case)

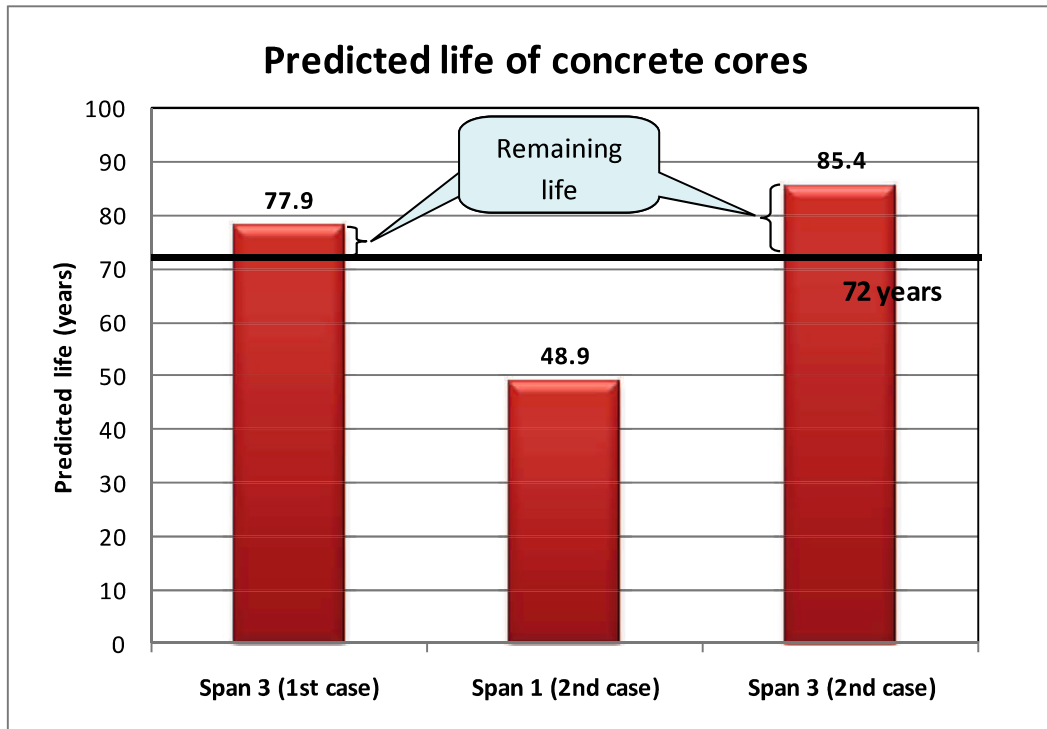


Fig. 3.16 Comparison of predicted life of extracted concrete cores between 1<sup>st</sup> case and 2<sup>nd</sup> cases.

### 3.5.3 Discussion

#### 3.5.3.1 Influence of the amount of reinforcement corrosion on evaluation results

In the remaining life prediction shown in Table 3.5, the cumulative amount of steel corrosion of 75 mg/cm<sup>2</sup>, which is similar with prediction obtained from the BREX system, was used in the case where the main deterioration factor is chloride attack [1,6]. However, because the setting value is thought to be important in the remaining life prediction, the degree of influence of assumed values of the cumulative amount of steel corrosion on the remaining life prediction results for each core was investigated. Table 3.7 shows the relationship between the assumed values of the cumulative amount of steel corrosion  $Q$  and life expectancy  $X$ . Hence, the relationship between the remaining life  $R$  and the cumulative amount of steel corrosion  $Q$  in 1<sup>st</sup> case can be represented by Eq. (3.14) as follows:

$$R = 13.7 \cdot Q^{0.403} - 70 \quad (3.14)$$

It can be seen from Fig. 3.17, if the criterion value  $Q$  is assumed to be  $100 \text{ mg/cm}^2$  (10 times the critical amount of corrosion for initial cracking due to carbonation), the averages service life is 89 years from Eq. (3.14); therefore, the remaining life is 19 years. In this case, the remaining life is longer than the results shown in Table 3.5 by 10 years or more years.

If the criterion value  $Q$  is assumed to be  $50 \text{ mg/cm}^2$  (five times the critical amount of corrosion for initial cracking due to carbonation), the remaining life is  $-6$  years (i.e., a negative value). It is found, therefore, that although the criterion value  $Q$  was assumed to be  $75 \text{ mg/cm}^2$  in Table 3.5, it is necessary to consider the value of parameter  $Q$  through comparison with the results of the remaining life prediction by the BREX system, taking into consideration the fact that main deterioration factors may be different.

The relationship between the assumed values of the cumulative amount of steel corrosion  $Q$  and life expectancy  $X$  in 2<sup>nd</sup> case for both Spans 1 and 3 is shown in Table 3.9. The results are shown in Figs. 3.19 and 3.20. The relationship between the remaining life  $R$  and the cumulative amount of steel corrosion  $Q$  in 2<sup>nd</sup> case for each Spans 1 and 3 can be represented by Eq. (3.15) and Eq. (3.16) as follows:

$$R = 17.36 \cdot Q^{0.241} - 72 \quad (3.15)$$

$$R = 23.05 \cdot Q^{0.303} - 72 \quad (3.16)$$

There is the difference between 1<sup>st</sup> case and 2<sup>nd</sup> case in the period of service. In 1<sup>st</sup> case, the period of service was assumed by 70 years and in 2<sup>nd</sup> case was assumed by 72 years.

Equations (3.15) and (3.16) show the remaining life prediction in Spans 1 and 3. From the equations it can be seen that the remaining life prediction of Span 1 (Eq. (3.15)) is lower than the remaining life prediction of Span 3 (Eq. (3.16)). The results are similar with the result of remaining life prediction that shown in Table 3.6.

### 3.5.3.2 Influence of the moisture content on evaluation results

The remaining life prediction shown in Table 3.5 is based on measured values obtained by using concrete cores. The moisture content in Eq. (3.5), however, was assumed to be 4% in view of data such as exposure test results [18,19]. In the case of a bridge exposed to an environment with tidal action, the moisture content may be greater than 4%. The influence of the moisture content, therefore, on the remaining life was evaluated.

Life expectancy  $X$  at moisture contents  $W$  of 4%, 6%, 8%, and 10% was calculated for the concrete cores shown in Table 3.8. The results are shown in Fig. 3.18. The relationship between the remaining life  $R$  and the moisture content  $W$  in 1<sup>st</sup> case was given by Eq. (3.17) as follows:

$$R = 205 \cdot W^{-0.746} - 70 \quad (3.17)$$

Figure 3.18 shows that the replacement moisture content  $W$  tends to affect the remaining life prediction. It can be seen from Fig. 3.18 that when the moisture content  $W$  is low (approximately 5% or lower), it tends to greatly affect the remaining life. On the other hand, when the moisture content  $W$  is high (higher than approximately 5%), its influence on the remaining life is small. It can be concluded, therefore, that it is good practice to measure the moisture content of the concrete surface in advance if the remaining life is to be predicted with higher accuracy than can be achieved through concrete cores testing.

The relationship between the assumed values of the replacement moisture content  $W$  and life expectancy  $X$  in 2<sup>nd</sup> case for both Spans 1 and 3 is shown in Table 3.10. The results are shown in Figs. 3.21 and 3.22. The relationship between the replacement moisture content  $W$  and the remaining life in 2<sup>nd</sup> case for each Spans 1 and 3 can be represented by Eq. (3.18) and Eq. (3.19) as follows:

$$R = 74.654 \cdot W^{-0.333} - 72 \quad (3.18)$$

$$R = 125.46 \cdot W^{-0.403} - 72 \quad (3.19)$$

Table 3.7 Results of assumed cumulative amount of steel corrosion ( $Q$ ) and life expectancy( $X$ ) (1<sup>st</sup> case)

Girder No.	Core Specimen No.	Q = 10 mg/cm <sup>2</sup>	Q = 50 mg/cm <sup>2</sup>	Q = 75 mg/cm <sup>2</sup>	Q = 100 mg/cm <sup>2</sup>	Q = 200 mg/cm <sup>2</sup>
		Cracking limit (years)	Predicted life X (years)	Predicted life X (years)	Predicted life X (years)	Predicted life X (years)
1	C1134	29	52	62	71	96
3	C3134	39	60	69	77	102
	C3138	48	78	92	103	103
4	C4031	26	45	53	60	81
	C4136	47	80	95	107	139
5	C5031	27	52	64	74	97
	C5134	57	93	110	124	163
	C5038	39	63	76	88	123
Average (years)		39.0	65.4	77.6	88.0	113.0

Table 3.8 Results of Influence of moisture content ( $W$ ) on life expectancy( $X$ ) (1<sup>st</sup> case)

Girder No.	Core Specimen No.	Moisture content ( $W$ )			
		4%	6%	8%	10%
1	C1134	62	43	36	32
3	C3134	69	52	45	41
	C3138	92	63	52	48
4	C4031	53	39	32	28
	C4136	95	62	51	46
5	C5031	64	43	34	30
	C5134	110	72	61	56
	C5038	76	53	44	41
Average (years)		77.6	53.4	44.4	40.3

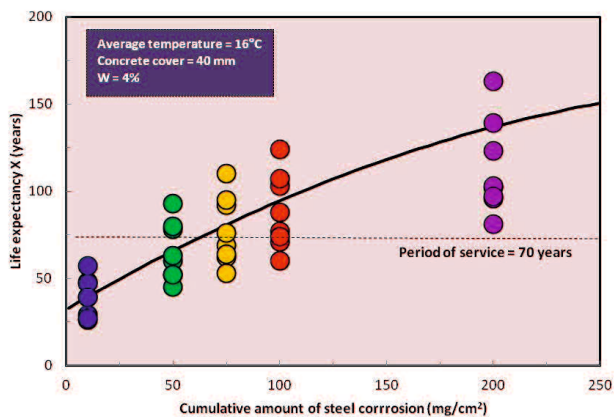


Fig. 3.17 Relationship between assumed cumulative amount of steel corrosion ( $Q$ ) and life expectancy ( $X$ )

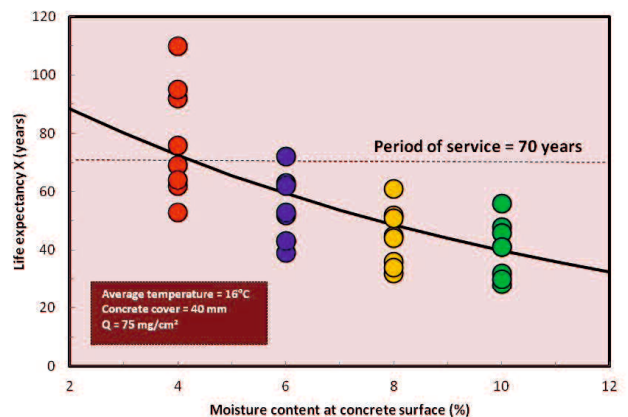


Fig. 3.18 Influence of moisture content ( $W$ ) on life expectancy( $X$ )

Table 3.9 Results of assumed cumulative amount of steel corrosion ( $Q$ ) and life expectancy( $X$ ) (2<sup>st</sup> case)

Girder No.	Core Specimen No.	$Q = 10 \text{ mg/cm}^2$	$Q = 50 \text{ mg/cm}^2$	$Q = 75 \text{ mg/cm}^2$	$Q = 100 \text{ mg/cm}^2$	$Q = 200 \text{ mg/cm}^2$
		Cracking limit (years)	Predicted life X (years)	Predicted life X (years)	Predicted life X (years)	Predicted life X (years)
<b>SPAN 1</b>						
1	C1014	24	36	42	47	47
	C1111	60	78	87	96	125
	C1115	29	42	49	55	75
2	C2113	42	51	55	60	75
3	C3011	38	47	50	54	66
	C3015	19	26	30	33	44
	C3114	29	35	38	41	52
4	C4113	24	36	41	45	58
5	C5111	32	46	49	52	63
	C5114	34	43	48	52	67
	C5115	32	43	49	54	71
Average (years)		33.0	43.9	48.9	53.5	67.5
<b>SPAN 3</b>						
1	C1131	36	53	61	69	93
	C1134	38	62	73	83	114
	C1138	61	80	89	98	126
2	C2031	51	63	69	75	93
	C2136	34	46	52	57	73
3	C3134	52	75	85	94	122
	C3138	63	95	110	123	162
4	C4031	35	62	74	84	111
	C4136	62	97	114	127	166
5	C5031	36	63	75	85	113
	C5134	76	113	132	147	191
	C5038	53	78	91	103	140
Average (years)		49.8	73.9	85.4	95.4	125.3

Table 3.10 Results of Influence of moisture content ( $W$ ) on life expectancy( $X$ ) (2<sup>st</sup> case)

Girder No.	Core Specimen No.	Moisture content ( $W$ )			
		4%	6%	8%	10%
<b>SPAN 1</b>					
1	C1014	42	34	30	21
	C1111	87	72	66	63
	C1115	49	39	35	32
2	C2113	55	49	46	44
3	C3011	50	46	45	44
	C3015	30	25	23	22
	C3114	38	35	33	32
4	C4113	41	34	30	27
5	C5111	49	46	45	44
	C5114	48	42	39	37
	C5115	49	41	37	35
Average (years)		49	42.1	39.0	36.5
<b>SPAN 3</b>					
1	C1131	53	48	42	39
	C1134	62	53	45	41
	C1138	80	73	67	64
2	C2031	63	60	56	54
	C2136	46	43	39	37
3	C3134	75	65	57	53
	C3138	95	78	67	63
4	C4031	62	51	42	37
	C4136	97	76	65	60
5	C5031	63	52	42	38
	C5134	113	91	80	75
	C5038	78	67	58	55
Average (years)		73.9	63.1	55.0	51.3

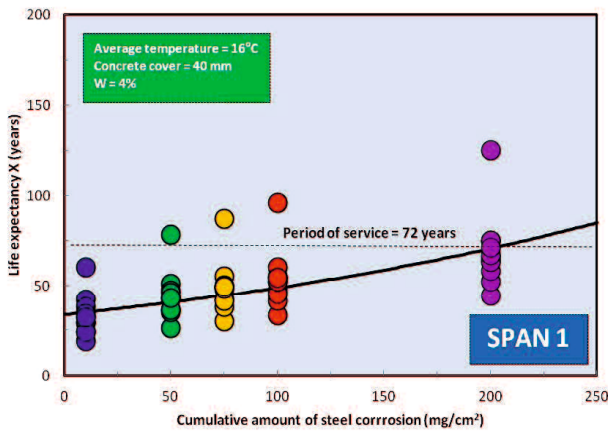


Fig. 3.19 Relationship between assumed cumulative amount of steel corrosion ( $Q$ ) and life expectancy ( $X$ )

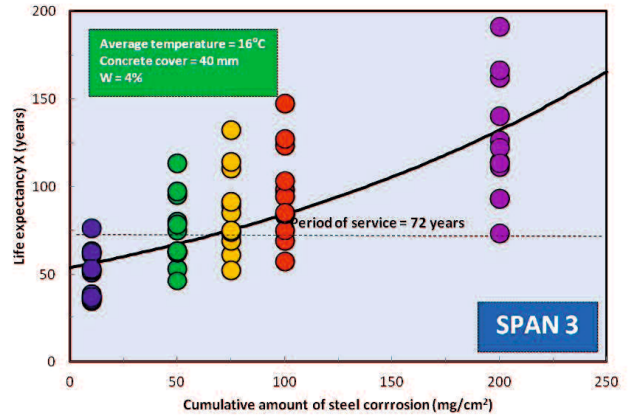


Fig. 3.20 Relationship between assumed cumulative amount of steel corrosion ( $Q$ ) and life expectancy ( $X$ )

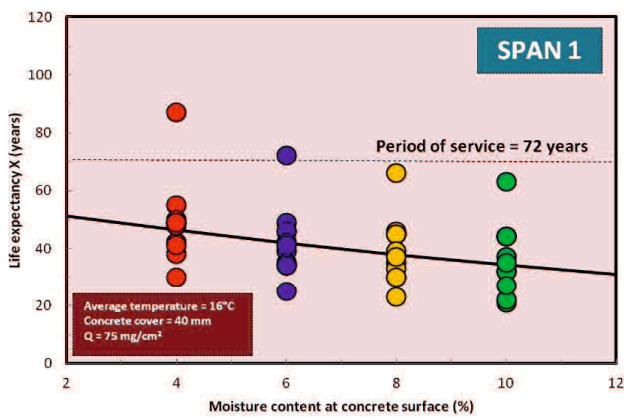


Fig. 3.21 Influence of moisture content ( $W$ ) on life expectancy ( $X$ )

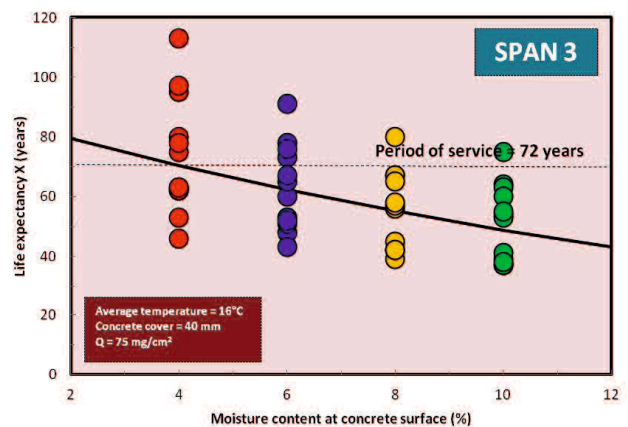


Fig. 3.22 Influence of moisture content ( $W$ ) on life expectancy ( $X$ )

### 3.5.3.3 Simple method of the remaining life prediction

In Table 3.5,  $X_0$  represent the service life in case where  $Q$  is assumed to be  $10 \text{ mg/cm}^2$  and let  $X_1$  represent the service life in case where  $Q$  is assumed to be  $75 \text{ mg/cm}^2$ . The relationship between  $X_0$  and  $X_1$  can be found in Eq. (3.20) as follows:

$$X_1 = 2.1 \cdot X_0 \quad (3.20)$$

From Eq. (3.20), it can be seen that the service life at  $Q = 75 \text{ mg/cm}^2$  is 2.1 times the time before the amount of steel corrosion reaches the critical amount of corrosion for initial cracking due to carbonation. The proportionality coefficient in Eq. (3.20), which varies depending on the cumulative amount of steel corrosion, determined for the remaining life prediction, was 1.7 when  $Q$  was  $50 \text{ mg/cm}^2$  and 2.4 when  $Q$  was  $100 \text{ mg/cm}^2$ . This indicates that the method of multiplying the time before the critical amount of corrosion for initial cracking due to carbonation by a coefficient can be used as a simple method of the remaining life prediction.

### 3.6 Proposal of evaluation of entire span based on local evaluation

The remaining life prediction shown in Table 3.5 is estimated based on local evaluation because it is based on a small number of the concrete cores evaluations. In this chapter, we consider how local evaluation results can be used for the evaluation of the entire span [1].

The remaining life  $R$  predicted from Table 3.5 is expressed as a cubic function of  $x$  and  $y$  as shown in Eq. (3.21) for the concrete coring location  $(x,y)$  shown in Fig. 3.4:

$$R = a + bx + cx^2 + dy + ey^2 + fx^3 + gy^3 + hx^2y + icy^2 \quad (3.21)$$

Because there are a total of nine unknown coefficients, a-i, these can be obtained by the least-square method. Then this is the numerical expression between the concrete coring locations and the remaining life prediction results. In the equation,  $x$  ranges from 0.5 to 4.5 ( $x=0.5\sim 4.5$ ) from left to right in the longitudinal direction of the bridge, and  $y$  is the direction from Girder 1 to Girder 5 ( $y=1\sim 5$ ).

The remaining life prediction results shown in Table 3.5 were substituted in Eq. (3.21), and the values of the coefficients were determined so that the differences were minimized. The coefficients thus determined were as follows:  $a = -136$ ,  $b = -115$ ,  $c = -29.7$ ,  $d = -19.7$ ,  $e = -11.75$ ,  $f = -5.15$ ,  $g = -1.52$ ,  $h = -5.20$ , and  $i = 2.41$ . From the obtained cubic function, the predicted remaining life distribution contours were drawn as shown in Fig. 3.23. In Fig. 3.23, a remaining life of  $-5$  years or less is shown in red color region, and a remaining life of 15 years or more is shown in blue color region. As shown in Fig. 3.23, in all main girders, there are regions with a negative value of the remaining life on the east side. In

Girder 1 and Girder 2 located on downstream side, there are regions extending to the middle section of the girder where a negative value of the remaining life is shown. Thus, it has been found that the condition of the entire span of each girder can be visualized.

Table 3.5 shows the predicted (calculated) remaining lives obtained from the approximation formula and the average values that take into account the remaining life distribution obtained by using the approximation formula. These indicate that the approximation results are close to the original prediction results and that the average value (7.8 years) that takes into account the remaining life distribution obtained by use of the approximation formula is close to the simply calculated averages of the concrete cores test results shown in Table 3.

Figure 3.20 shows the results in the case where the main deterioration factor is carbonation. It can be seen from Table 3.2 that in the cases shown in Figs. 3.9(a) and 3.9(b), the chloride ion content tends to be high at the reinforcement locations under the influence of carbonation. It can be inferred, therefore, that the remaining lives of both Girders 1 and 2, in which there are Type (a) and Type (b) distributions, are shorter than the predicted remaining lives given by the approximation formula shown in Fig. 3.9.

Hence, it is thought likely that there will be large expenses of red color regions indicating a remaining life of  $-5$  years or shorter. For a distribution of the type shown in Fig. 3.9(a), therefore, the chloride ion contents at the reinforcement locations, where there are no changes over time, were used for  $Cl$  in Eq.(3.5). For a distribution of the type shown in Fig. 3.9(b), the coefficients in Eq. (3.1) were determined from the chloride ion contents at deeper levels. The remaining life prediction results thus obtained were used in conjunction with the results shown in Table 3.5 to derive an approximation function. The coefficients determined were as follows:  $a = -42.6$ ,  $b = 84.3$ ,  $c = -27.8$ ,  $d = -75.1$ ,  $e = 33.8$ ,  $f = 3.68$ ,  $g = -4.24$ ,  $h = -2.52$  and  $i = 1.83$ . On the basis of the equation with the coefficients, the remaining life distribution contours shown in Fig. 3.23 were obtained. The contours thus obtained show remaining lives of both Girders 1 and 2 that are shorter than the results shown in Fig. 3.23. In this case, the average of the remaining lives taking into account the distributions obtained by using the approximation formula was 7.8 years.

From this fact, it can be concluded that if the concrete cores test results that make it possible to derive an approximation formula, such as Eq. (3.21), for simulating the

predicted remaining life with a certain level of accuracy are available, those results including distribution visualizations such as Figs. 3.23 and 3.24 can be used for evaluation of the entire spans.

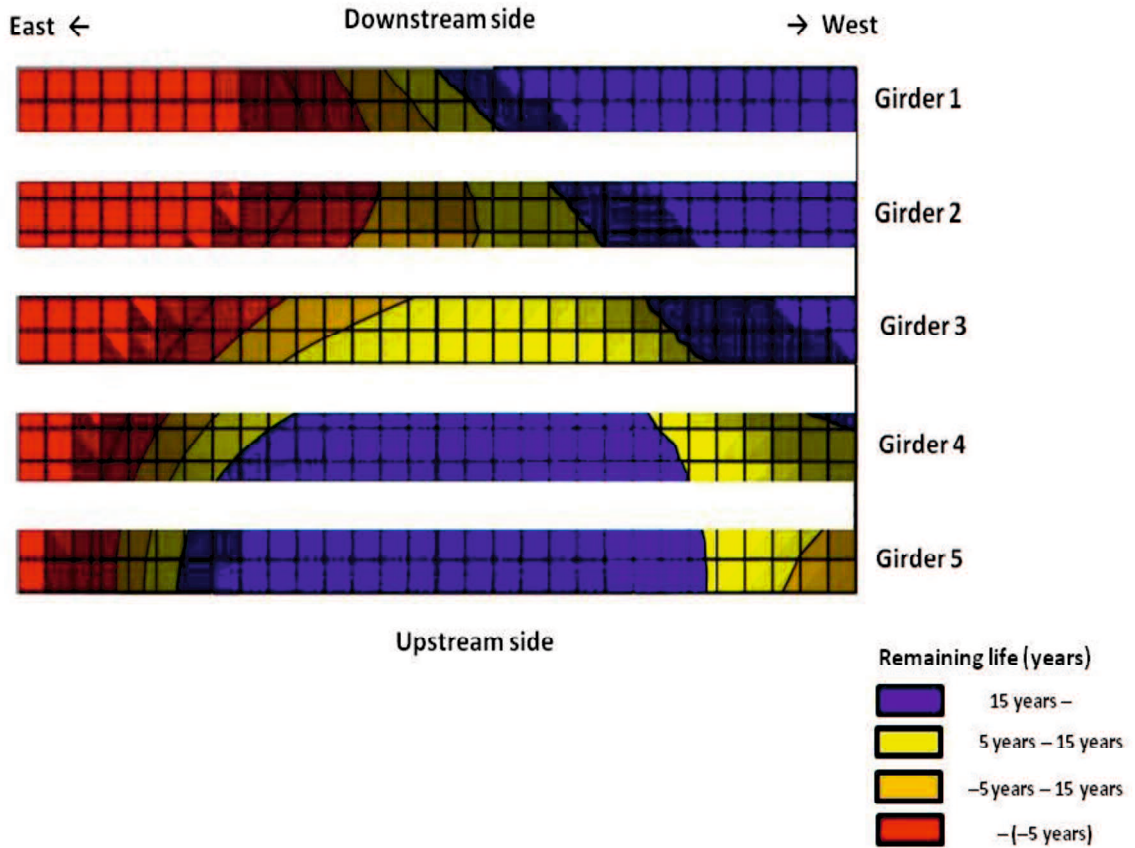


Fig. 3.23 In-span distribution of remaining life of main girder in case where only Type (c) distribution in Fig. 3.9 is involved



4. It has been found that the localized concrete cores test results can be used for entire span evaluation by visualized distribution results by use of an approximating function.

### 3.8 References

- [1] A. Miyamoto, H. Emoto, J. Takahashi, and K. Hiraoka, Remaining life evaluation and its verification of aged bridge based on field inspections, in Japanese, Concrete Research and Technology, Vol. 23, No. 3, pp.119–132, 2012.
- [2] J. Takahashi, H. Emoto, and A. Miyamoto, A proposal on bridge soundness evaluation system's verification method based on concrete core testing, in Japanese, Proceedings of the Japan Concrete Institute, Vol. 34, No. 2, pp. 1399–1404, 2012.
- [3] H. Emoto, J. Takahashi, and A. Miyamoto, Learning effect in diagnosis and remaining life estimation of concrete bridges by J-BMS using visual inspection results, in Japanese, Proceedings of the Japan Concrete Institute, Vol. 34, No. 2, pp. 1393–1398, 2012.
- [4] A. Miyamoto, M. Kushida, H. Morikawa, and K. Kinoshita, Development and reliability enhancement of neuro-fuzzy expert system for concrete bridge diagnosis, in Japanese, Proceedings of the Japan Society of Civil Engineers, 510-VI-26, 1995, pp. 91–101, 1995.
- [5] A. Miyamoto, K. Kawamura, and H. Nakamura, Optimal maintenance planning for existing bridges using bridge management system (BMS), in Japanese, Proceedings of the Japan Society of Civil Engineers, 588-VI-38, pp. 191–208, 1998.
- [6] J. Takahashi, A. Miyamoto, and H. Emoto, Verification of estimation through concrete core testing of remaining life of bridge during its demolition, in Japanese, Proceedings of the JSCE Annual Conference, VI226, 2011.
- [7] H. Nakamura, J. Takahashi, H. Emoto, and A. Miyamoto, A study on variability of measured chloride contents of concrete in marine environment, in Japanese, Proceedings of the Japan Concrete Institute, Vol. 31, No. 2, pp. 1549–1554, 2009.
- [8] K. Sakai, M. Omori, and M. Boulfiza, A study on evaluation of combined effect of chloride ion intrusion and carbonation on concrete, in Japanese, Concrete Research and Technology, Vol. 17, No. 2, 2006.
- [9] H. Kuroda, M. Yokota, T. Sasaki, and M. Matsushima, Corrosion rate of reinforcement in concrete subjected to combined effect of chloride attack and carbonation, in Japanese, Abstracts of papers presented at the 60<sup>th</sup> Annual Conference of Japan Society of Civil Engineers, Part 5, pp. 763–764, 2005.

- [10] Japan Society of Civil Engineers, Standard specifications for concrete structures: maintenance, JSCE, 2007. (17)
- [11] A. Miyamoto, H. Emoto, and J. Takahashi, Role of old Kotogawa Bridge and soundness evaluation during demolition, in Japanese, Infrastructure management series no. 15, Research Center for Environmental Safety, Yamaguchi University, 2011.
- [12] Japan Society of Civil Engineers, Structural performance of concrete structures undergoing material deterioration, in Japanese, Concrete technology series no. 71, JSCE, 2006.
- [13] R. Iijima, T. Sasaki, M. Yokota, and M. Matsushima, A study on corrosion of reinforcement in concrete subjected to combined effect of chloride attack and carbonation, in Japanese, Proceedings of the Concrete Structure Scenarios, JSMS, Vol. 4, pp. 11–16, 2004.
- [14] R. Iijima, T. Kudo, and Y. Tamai, Effect of atmospheric temperature on corrosion rate of reinforcement in concrete, in Japanese, Proceedings of the Concrete Structure Scenarios, JSMS, Vol. 8, pp. 299–304, 2008.
- [15] J. Takahashi, R. Widyawati, H. Emoto, and A. Miyamoto, Remaining life prediction of an aged bridge based on concrete core test, in Japanese, Proceedings of the Japan Concrete Institute, Vol. 36, No. 2, pp. 1339-1344, 2014.
- [16] Widyawati, R., Takahashi, J., Emoto, H., and Miyamoto, A., "Remaining life prediction of an aged bridge based on concrete core test", 2<sup>nd</sup> International Conference on Sustainable Civil Engineering Structures and Construction Materials, 2014.
- [17] Japan Society of Civil Engineers, Report from JSCE Subcommittee on Corrosion Evaluation and Protection for Reinforcing Steel in Concrete, (Subcommittee 338), in Japanese, JSCE, 2007.
- [18] H. Koga, H. Aoyama, H. Watanabe, and Y. Kimura, Outdoor exposure test on concrete moisture content reducing effect of surface impregnation materials, in Japanese, Proceedings of the Japan Concrete Institute, Vol. 31, No. 1, pp. 1939–1944, 2009.
- [19] H. Koga, and H. Watanabe, Results of moisture content monitoring of concrete exposed outdoors, in Japanese, Proceedings of the Japan Concrete Institute, Vol. 28, No. 1, pp. 641–646, 2006.

# Chapter 4: REMAINING LIFE PREDICTION OF AN AGED BRIDGE BASED ON CARBONATION TEST FOR CROSS-SECTION CUTTING-OFF GIRDER

---

## 4.1 Introduction

A large number of reinforced concrete (RC) bridges in Japan have become aged, requiring increased maintenance and requiring decisions be made concerning whether to maintain or to demolish these aged bridges. Remaining life prediction is a crucial part of the systematization of bridge maintenance.

The remaining life of a bridge is highly influenced by environmental conditions. Bridges are typically exposed to a range of environmental conditions during their service lives. High levels of carbon dioxide as a result of high traffic volumes contribute to carbonation, which can result in significant deterioration and can have a significant effect on the service life of an RC bridge. Chloride ion attack should be considered as another factor in RC bridge deterioration if the bridge is located near the sea. Both carbonation and chloride ion attack can lead to corrosion of the reinforcing bars. The most serious deterioration mechanisms that occur in RC bridges are associated with corrosion.

Various definitions of service life and remaining life have been proposed [1~6]. In this study, the end of the service life was defined as the point at which the total amount of steel corrosion due to carbonation and/or chloride ion attack reached a critical value. The remaining life was calculated as the elapsed time  $EL$  (in this case, 72 years) minus the service life  $SL$  in years [7]. The service life was divided into four stages: initiation, propagation, acceleration, and deterioration. The initiation stage is identified on the basis of the measured carbonation depth and the thickness of remaining concrete cover. The initiation of corrosion occurs when the thickness of remaining concrete cover falls below 10 mm. The propagation stage can be defined as the stage in which cracking occurs due to corrosion. Cracking will be occurred if the cumulative amount of steel corrosion approximately  $10 \text{ mg/cm}^2$ . [8] The acceleration and the deterioration stages are defined with respect to the critical value of the total amount of steel corrosion, which in this study was taken to be  $75 \text{ mg/cm}^2$  [9][10]. Fig. 4.1 shows a schematic illustration of service life prediction.

Under ordinary circumstances, concrete cores are extracted from some parts of a bridge to evaluate the performance of the concrete. Many studies of carbonation in RC bridges have been conducted. However, this paper describes the first known application of carbonation testing to girder cross sections cut from a bridge. In addition, many studies have proposed methods to predict the service life of RC bridges. However, such methods are typically based on the deterioration due only to carbonation or only to chloride ion attack.

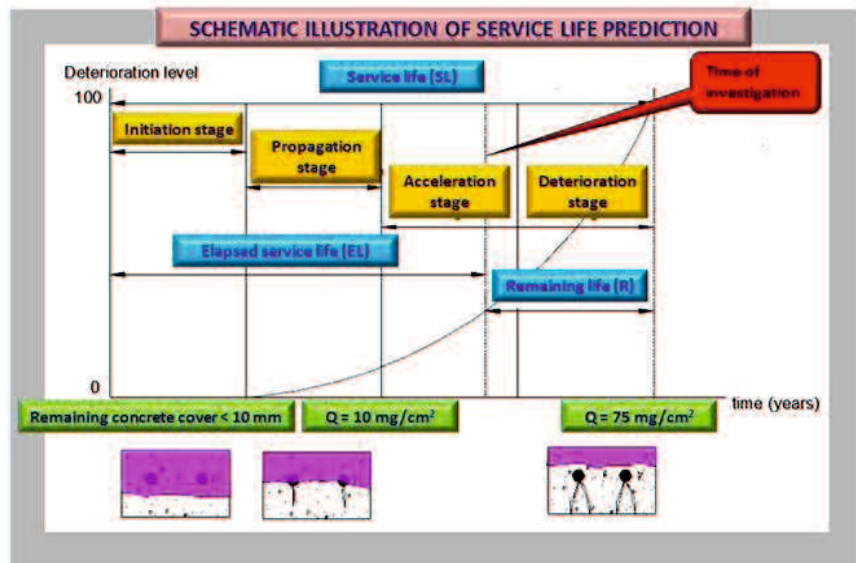


Fig. 4.1 Schematic illustration of service life prediction

This chapter proposes a method to predict the remaining life of an aged RC bridge based on the extent of deterioration due to carbonation and chloride ion attack. In addition, a flowchart for this remaining life prediction method is presented. The bridge considered in this study was demolished, and girders were removed from it. Cross-section cutting-off were cut from these girders, and these cross-sections cutting-off were examined to determine the thickness of the concrete cover and the carbonation depth of the sea sides, bottom sides, and mountain sides of the girders. The remaining prediction method makes use of the following types of information: (1) the thickness of the concrete cover, (2) the carbonation depth, (3) the carbonation rate, (4) the chloride ion content, (5) the average temperature, and (6) the surface moisture content. Information on items (4)–(6) were obtained from tests on concrete cores. The service life predicted by the proposed method represents the predicted remaining life for the entire span of the bridge.

## **4.2 Target bridge and research purpose**

In this study, carbonation tests were conducted on cross-sections cutting-off girders of an aged bridge, SK Bridge, which is a T-girder RC bridge (Fig. 4.2). The bridge had eight spans, and each span consisted of five girders. The bridge had a total length of 168 m and a width of 11 m. Construction of SK Bridge was completed in 1942. After 72 years of service, the bridge was demolished in 2013. SK Bridge was constructed on the main route of National Highway No. 2, which connects Waki-shi in Yamaguchi Prefecture and Otake-shi in Hiroshima Prefecture. SK Bridge was exposed to high levels of carbon dioxide during its service life because of the high traffic volume on the main route. The main deterioration factor was suspected to have been carbonation. However, chloride ion attack may also have contributed to the deterioration of the bridge because the bridge was located less than 1 km upstream from the estuary of the Sagawa River, which flows into the Seto Inland Sea.

The research purpose are considering which is the more dominant factor affect the deterioration of the bridge, between carbonation and chloride ion, based on the location of the bridge. Assuming the remaining life prediction used the cross-section cutting-off girders of an aged bridge, which is affected by carbonation with the presence of chloride attack based on the location of the bridge and comparing the remaining life prediction in which the deterioration caused by carbonation and chloride ion and caused only by carbonation.

## **4.3 Method of cross-section cutting-off girder tests**

### **4.3.1 Cross-section cutting-off girders**

The demolition of the bridge provided a good opportunity to obtain many types of useful information. Two spans, Span 1 and Span 3, shown in Fig. 4.3, were inspected. Each span consisted of five girders, Girder 1 (G1) through Girder 5 (G5). Table 4.1 shows the total number of cross-sections cutting-off girders of Spans 1 and 3. The figure and the sketch of cross-section cutting-off girders are shown in Figs. 4.4 and 4.5, respectively.

The girders had been cut into pieces with the maximum weight approximately 10 tons, in order to move from the bridge location to the demolishing place. The total number of cross-section cutting-off girders of Span 1 and Span 3 were 49 and 67, respectively. Table 4.1 shows the number of cross-section cutting-off girders based on its location.

Table 4.1 Number of cross-section cutting-off girders

No	Girder symbol	Number of cutting-off cross section	
		Span 1	Span 3
1.	G1	8	11
2.	G2	11	15
3.	G3	11	15
4.	G4	11	15
5.	G5	8	11
	<b>Total</b>	49	67

Each cross-section cutting-off girders has an identification symbol. It was given the identity as: **H-number-Y**, where "H" is Hiroshima side and "Y" is Yamaguchi side. "Number" is the number of cross-section cutting-off girders, 1 to 116 pieces. The cross-section cutting-off girders locations with the identification symbol for each cross-section cutting-off girders are shown in Fig. 4.5(a) for Span 1 and Fig. 4.5(b) for Span 3.



Fig. 4.2 General view of SK Bridge

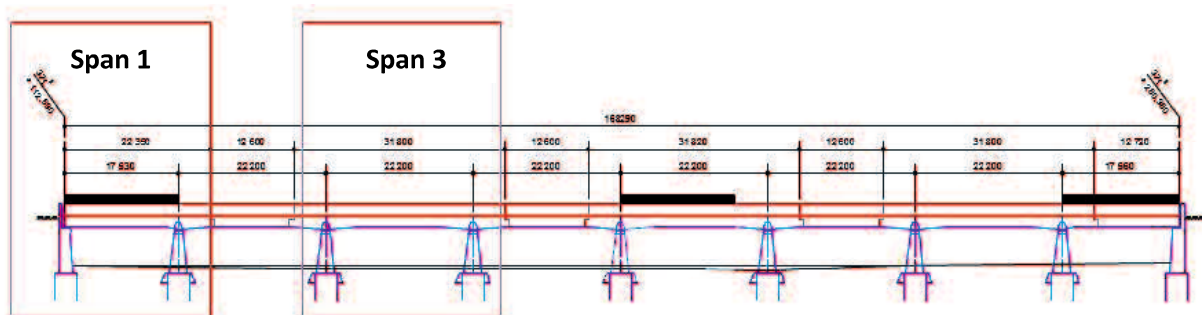


Fig. 4.3 Spans 1 and 3 of SK-Bridge



Fig. 4.4 Cross-section cutting-off girder of SK-Bridge

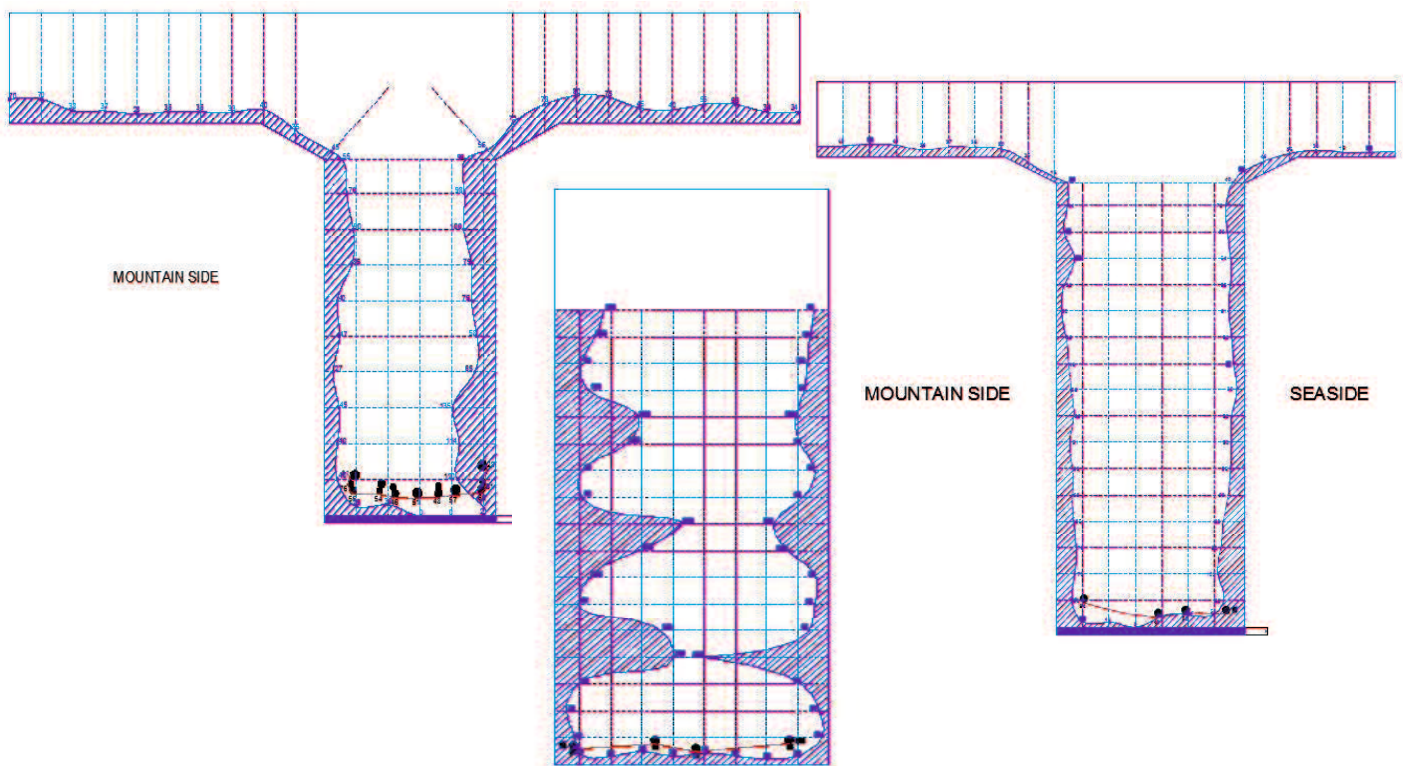
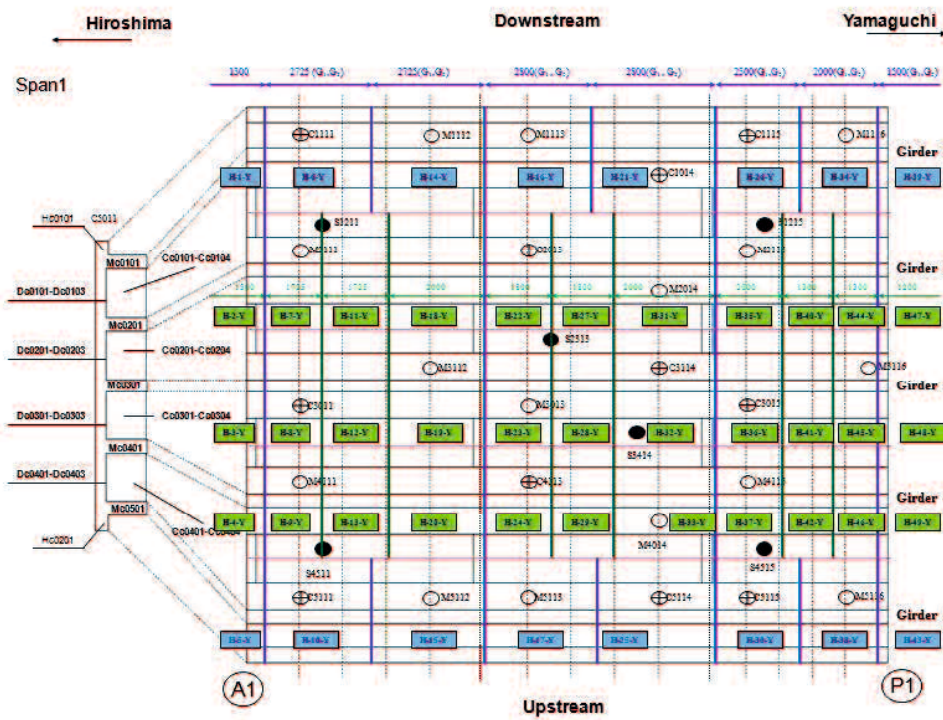
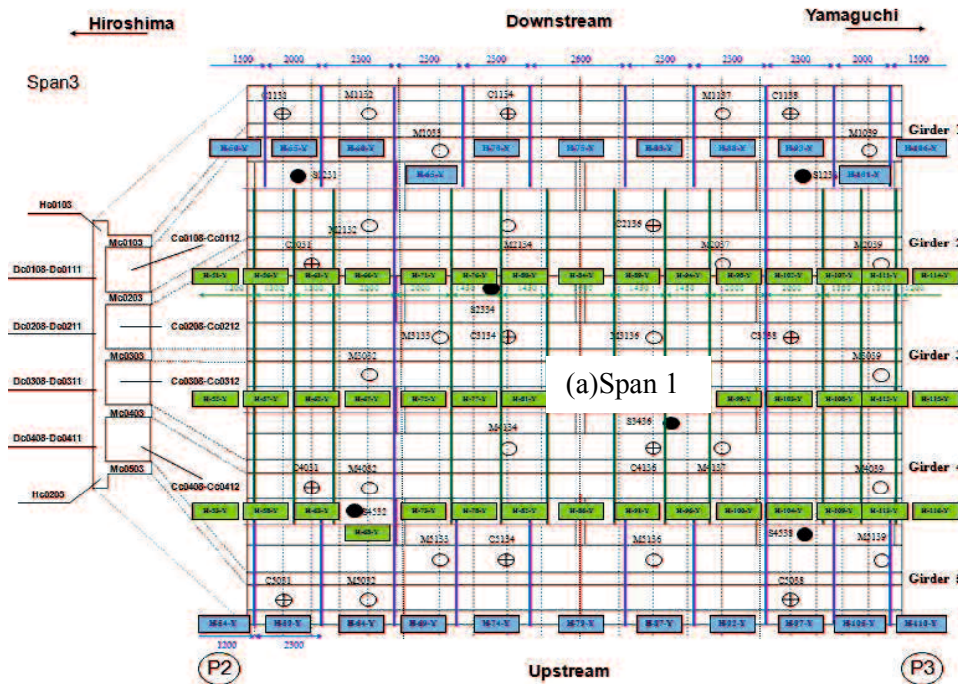


Fig. 4.5 Sketch of cross-section cutting-off girder of SK-Bridge



(a) Span 1



(b)Span 3

Fig. 4.6 Cross-section cutting-off girders locations

### **2.6.1 Examination of cross-section cutting-off girder**

The demolition of SK Bridge began with the removal of each span of the main girders of the bridge. The first girder removed was the outer girder on the mountain side, G5. The outer girder on the sea side, G1, was removed next, and then the inner girders, G4, G2, and G3 were removed. After the girders were removed from the bridge, they were placed on a temporary bridge as seen in Fig. 4.7.

On the temporary bridge the removed full girders were cut into parts as shown in Table 4.2. The cutting process used the special equipment for cutting concrete called a wire saw machine with the diamond wire. Fig. 4.8 shows a wire saw machine and the cutting process. The cross-section cutting-off girder was cut with a maximum weight approximately 10 tons, it is the maximum weight that could be moved by a truck to a particular place to be demolished.

### **2.6.2 The thickness of concrete cover measurement**

The cross-sections cutting-off girders were examined to measure the thickness of the concrete cover on the reinforcement. The thickness of the concrete cover is very important because the concrete cover serves to protect the reinforcing bars from damage due to environmental exposure. Among the environmental effects that may cause corrosion in reinforcing bars are attacks by carbon dioxide, acid, and salt [11]. As we know, corrosion in the reinforcing bar affected the deterioration of the reinforced concrete structures. Therefore, the thickness of concrete cover should be controlled to meet the minimum requirements needed.

The thickness of concrete cover is the thickness of concrete between the concrete cover surface and the outer reinforcing bar. In this investigation, the location of embedded reinforcing bars is quite varied. Then, the value of thickness of concrete cover was assumed by average values of the measurement. This was measured for the sea sides, bottom sides, and mountain sides of the girders. It is shown in Fig. 4.9.

### 2.6.3 Carbonation test

Figure 4.10 shows the carbonation test. Carbonation testing is most commonly carried out by spraying a phenolphthalein solution on freshly exposed surfaces of concrete or on concrete cores. In this study, this carbonation test method was applied to the cut surfaces of the cross-sections cutting-off from the concrete girders. To avoid further carbonation of the cut surfaces, the testing was conducted within 30 minutes of the cross sections being cleaned and prepared for testing. In accordance with Japanese Industrial Standard JIS A 1152, the depth of carbonation is assessed by examining the area of the surface that appears pink or purple after application of the phenolphthalein solution (Fig. 4.11).

The concrete in areas where this coloring appears is alkaline and is considered to be healthy and to have experienced no carbonation. The concrete in areas that remain colorless is not alkaline and is considered to be concrete that has experienced carbonation.

### 4.3.5 Carbonation depth measurement

The carbonation depth of the cross sections cut from the girders was also measured. The carbonation depth is the distance between the concrete cover surface and the boundary between colored and uncolored areas. It can be seen in Fig. 4.12.



Fig. 4.7 Removal girder



Fig. 4.8 Wire saw machine

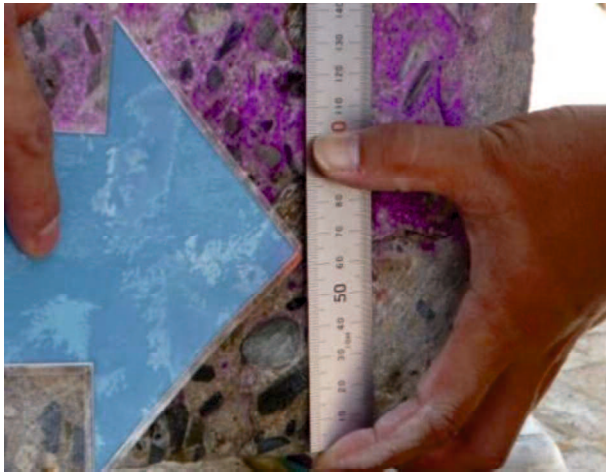


Fig. 4.9 Measurement of the thickness of concrete cover



Fig. 4.10 Carbonation test



Fig. 4.11 Spraying phenolphthalein solution



Fig. 4.12 Carbonation depth measurement

#### 4.4 Results of cross-section cutting-off girder tests

##### 4.4.1 Concrete cover thickness measurement results

Table 4.2 shows the concrete cover thickness measurement results for the cross-section cutting-off girder of Spans 1 and 3. The results shown are the averages of the values obtained by measuring the distances between the concrete cover surface and the outer reinforcing bars. Figs. 4.13 and 4.14 also show the concrete cover thickness measurement results for the cross-section cutting-off girder of Spans 1 and 3 on averages. Figs. 4.15 to 4.17 and Figs. 4.18 to 4.20 show the normal distribution on both Spans 1 and 3, respectively.

In an RC bridge, the most serious deterioration mechanisms are those that lead to corrosion of the reinforcing bars, resulting in a reduction in the effective cross-sectional area of the reinforcing bars and in spalling of the concrete cover [11]. The nature of the deterioration in an RC bridge may be chemical, such as reinforcing bar corrosion due to carbon dioxide and chloride attack on the concrete. Concrete cover serves to protect the reinforcing bars from environmental exposure that leads to corrosion. In the deterioration process caused by carbonation, the thickness of the concrete cover affects the time required for carbon dioxide to reach the reinforcing bars. A thicker cover concrete increases the diffusion time of carbon dioxide in the concrete. Moreover, the thickness of the concrete cover can be used to predict the initiation of corrosion due to carbonation. The initiation of corrosion is frequently identified from the remaining thickness of the concrete cover, or the difference between the thickness of the concrete cover and the carbonation depth. In previous studies, researchers have concluded that the initiation of corrosion occurs when the thickness of remaining concrete cover falls below 10 mm [8]. Thus, the thickness of the concrete cover affects the initiation of corrosion.

Table 4.2 Thicknesses of concrete cover of Spans 1 and 3

No.	Girder	Thickness of concrete cover			Standard deviation		
		Sea side mm	Bottom side mm	Mountain side mm	Sea side Mm	Bottom side mm	Mountain side mm
<b>SPAN 1</b>							
1	G1	56.44	49.06	51.25	20.25	14.41	17.89
2	G2	68.33	55.35	61.05	9.15	6.23	12.22
3	G3	47.17	54.92	50.38	9.60	11.46	13.65
4	G4	52.83	52.58	48.72	7.00	9.24	11.98
5	G5	48.92	63.41	68.00	6.22	5.95	5.05
Average		54.74	55.06	55.88	10.44	9.46	12.16
<b>SPAN 3</b>							
6	G1	49.79	45.59	42.70	9.16	4.79	8.15
7	G2	64.98	45.82	49.06	11.27	10.66	13.85
8	G3	40.38	56.15	76.81	17.47	7.19	10.60
9	G4	82.10	53.28	43.63	14.38	7.28	9.84
10	G5	59.85	51.47	62.96	7.47	10.23	6.81
Average		59.42	50.46	55.03	11.95	8.03	9.85

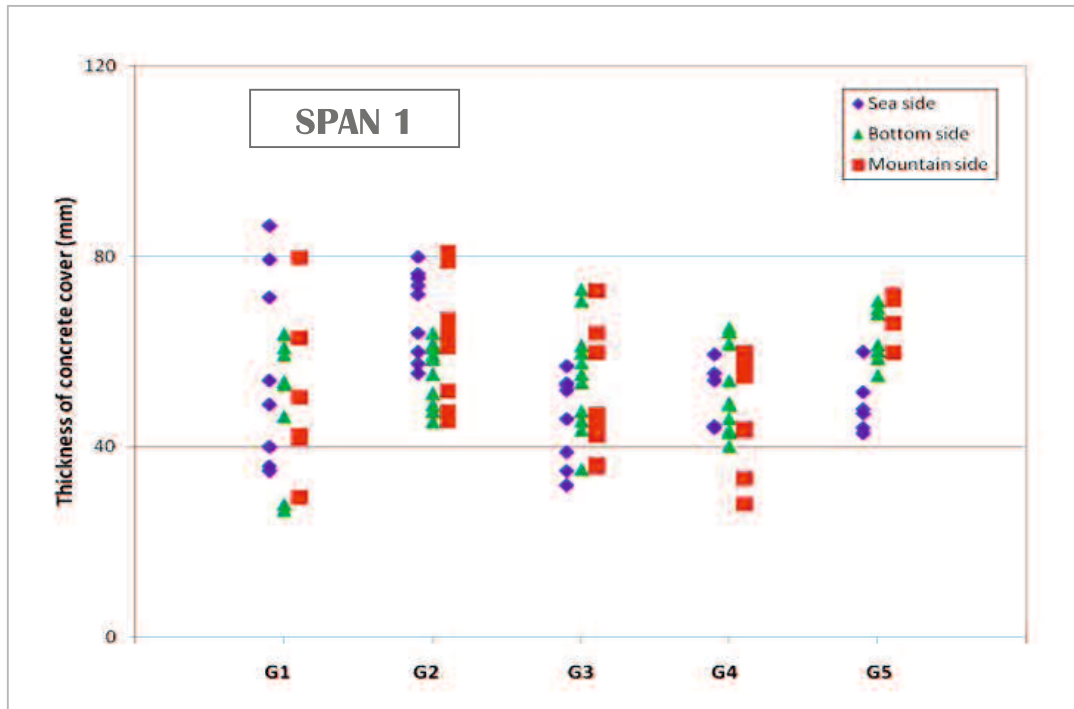


Fig 4.13 Thickness of concrete cover in Span 1

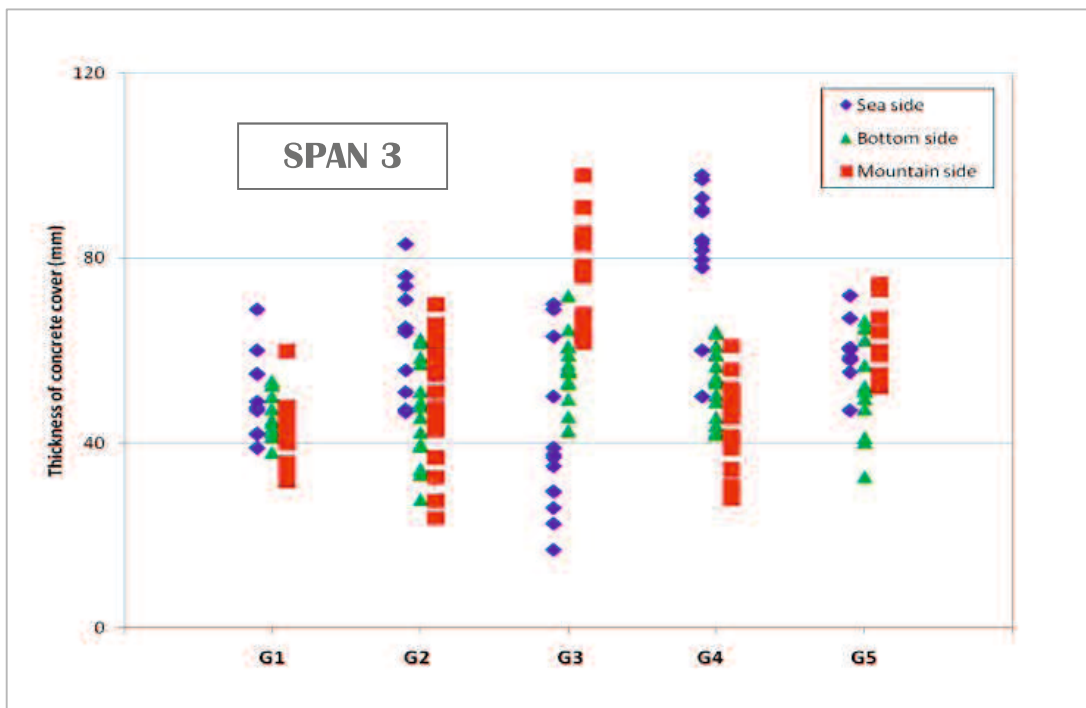


Fig. 4.14 Thickness of concrete cover in Span 3

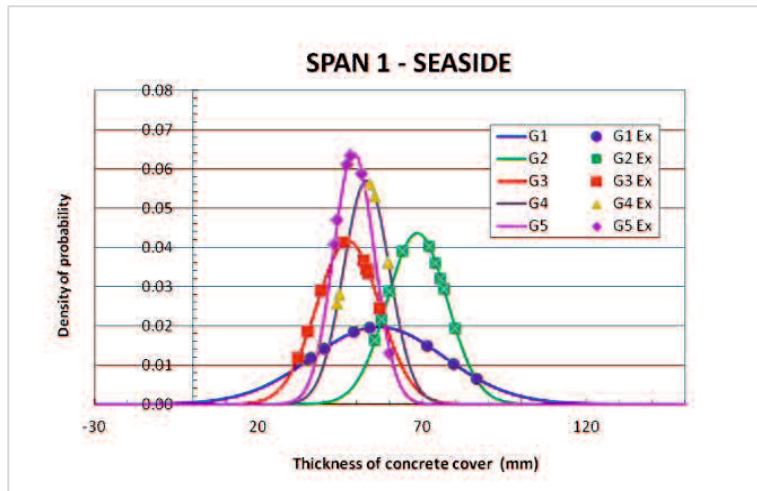


Fig. 4.15 Normal distribution of the thickness of concrete cover in Span 1 sea side

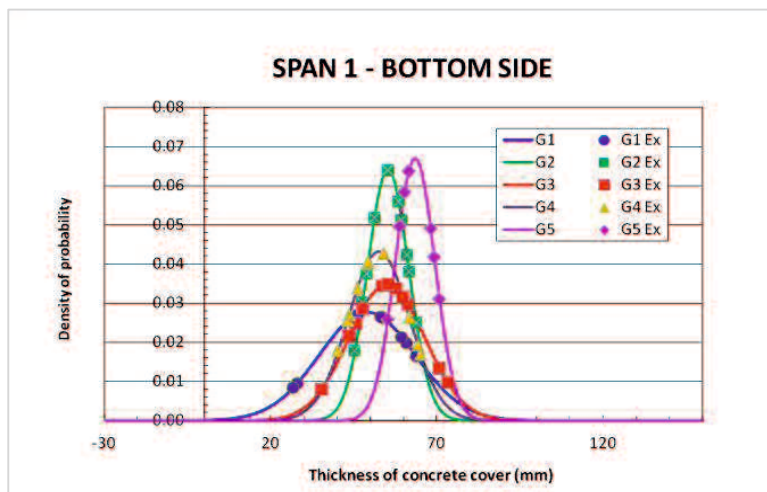


Fig. 4.16 Normal distribution of the thickness of concrete cover in Span 1 bottom side

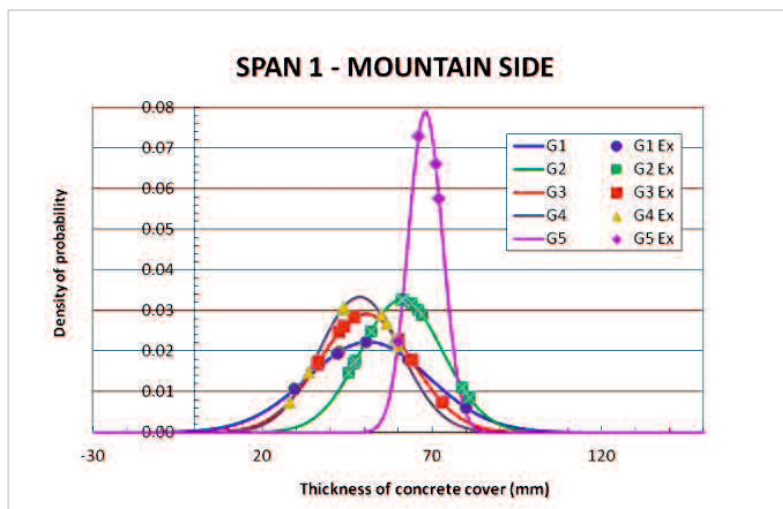


Fig. 4.17 Normal distribution of the thickness of concrete cover in Span 1 mountain side

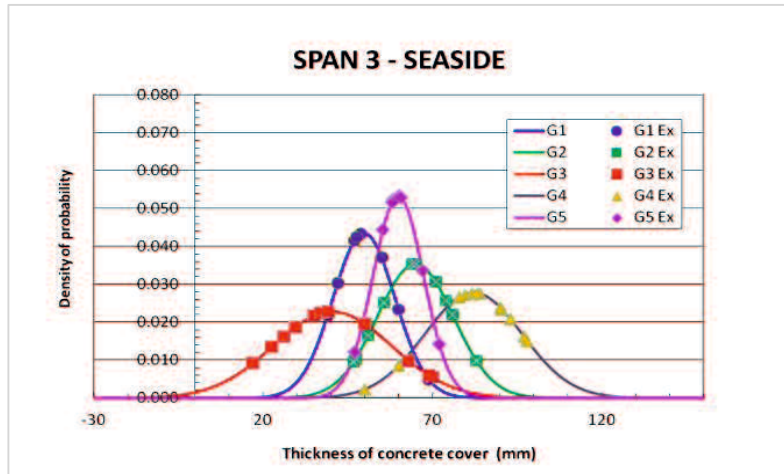


Fig. 4.18 Normal distribution of the thickness of concrete cover in Span 1 sea side

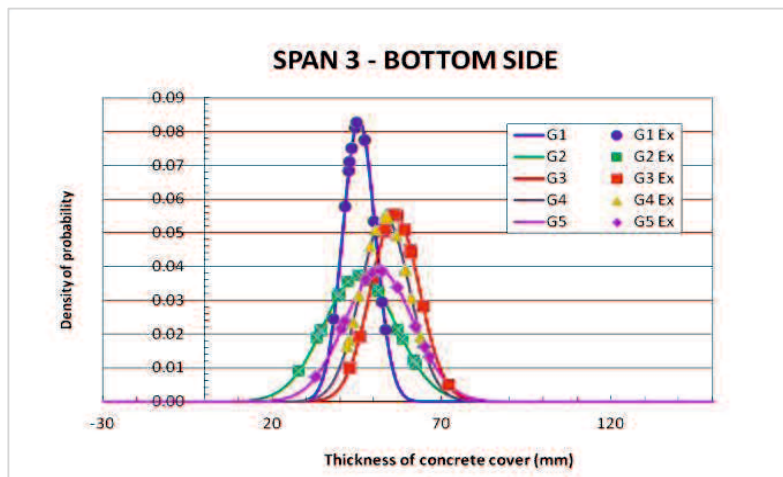


Fig. 4.19 Normal distribution of the thickness of concrete cover in Span 3 bottom side

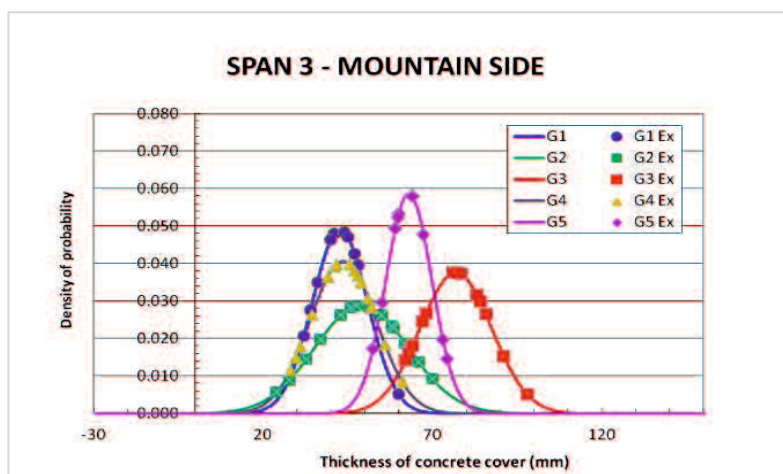


Fig. 4.20 Normal distribution of the thickness of concrete cover in Span 3 mountain side

#### 4.4.2 Carbonation depth measurement results

The results of the carbonation depth measurement were obtained by manual measurement on cross-section cutting-off girders after spraying phenolphthalein solution. It was measured in three parts: seaside, bottom side and mountain side of the girders. The carbonation depth measurement results for the cross-sections cutting-off girders of (Spans 1 and 3) are shown in Figs. 4.21 and 4.22 and in Table 4.3. Figs. 4.23 to 4.25 and Figs. 4.26 to 4.29 show the normal distribution on both Spans 1 and 3, respectively.

The results shown are the averages of the values obtained from five to ten measurement points. The carbonation rate, which can be obtained from the carbonation depth measurements, can be used to predict the carbonation depth in future years.

Table 4.4 Carbonation depths of Spans 1 and 3

No.	Girder	Carbonation depth			Standard deviation		
		Sea side mm	Bottom side mm	Mountain side mm	Sea side mm	Bottom side mm	Mountain side mm
<b>SPAN 1</b>							
1	G1	65.49	27.39	58.76	17.67	13.82	8.29
2	G2	51.57	38.71	49.25	14.19	14.15	15.03
3	G3	61.05	49.68	64.90	13.28	14.47	14.14
4	G4	75.15	63.19	82.13	15.45	15.10	11.20
5	G5	69.84	46.57	72.13	9.15	10.26	10.27
Average		64.62	45.11	65.43	13.95	13.56	11.79
<b>SPAN 3</b>							
6	G1	59.88	22.29	55.83	10.13	16.79	9.85
7	G2	62.43	25.17	57.78	11.31	11.46	10.72
8	G3	58.36	43.33	50.81	16.02	55.09	14.29
9	G4	72.02	50.01	64.71	16.23	14.21	18.31
10	G5	55.72	43.83	56.18	15.49	12.16	9.71
Average		61.68	36.93	57.06	13.84	21.94	12.58

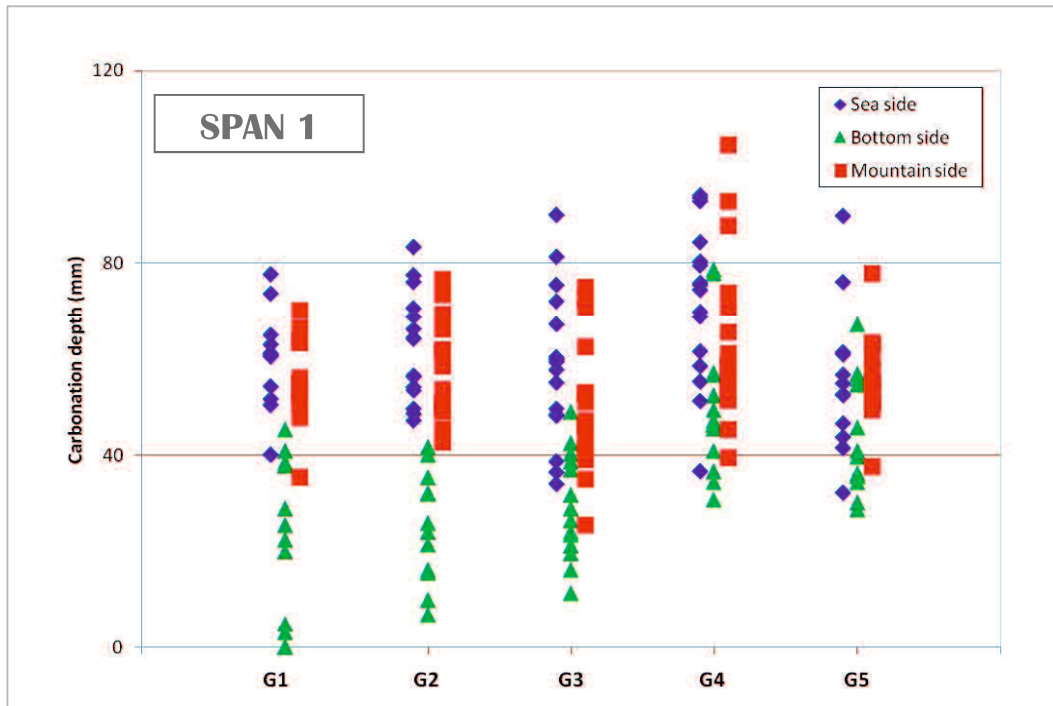


Fig. 4.21 Carbonation depth in Span 1

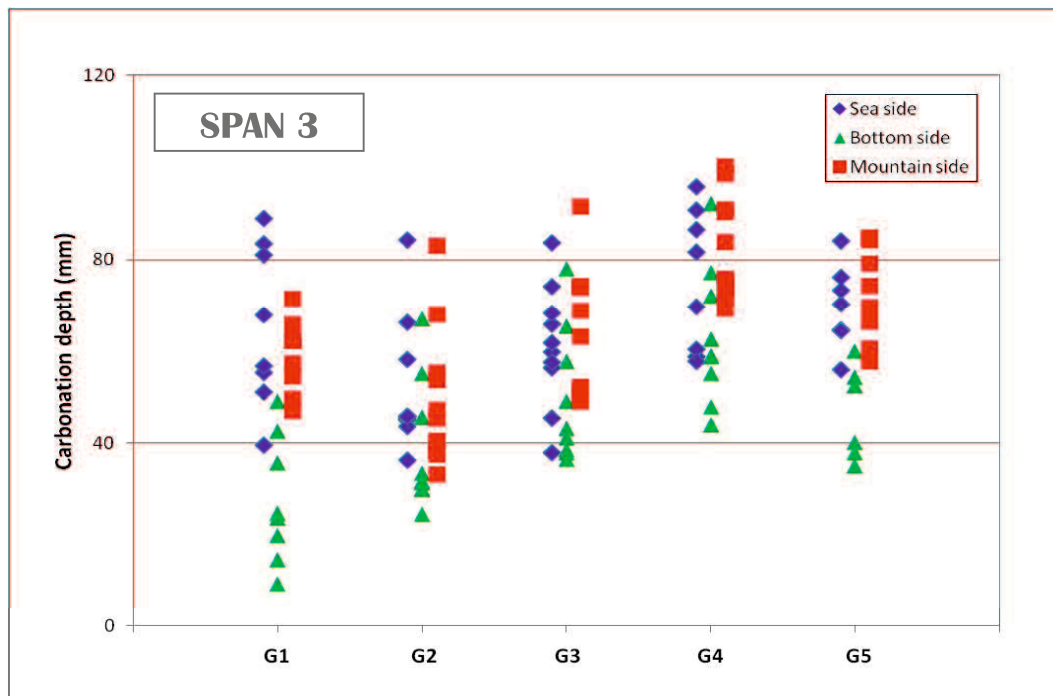


Fig. 4.22 Carbonation depth in Span 3

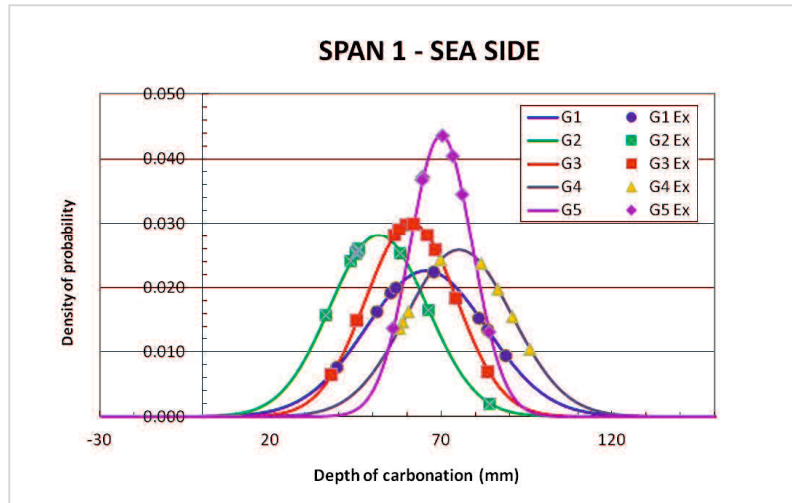


Fig. 4.23 Normal distribution of the carbonation in Span 1 sea side

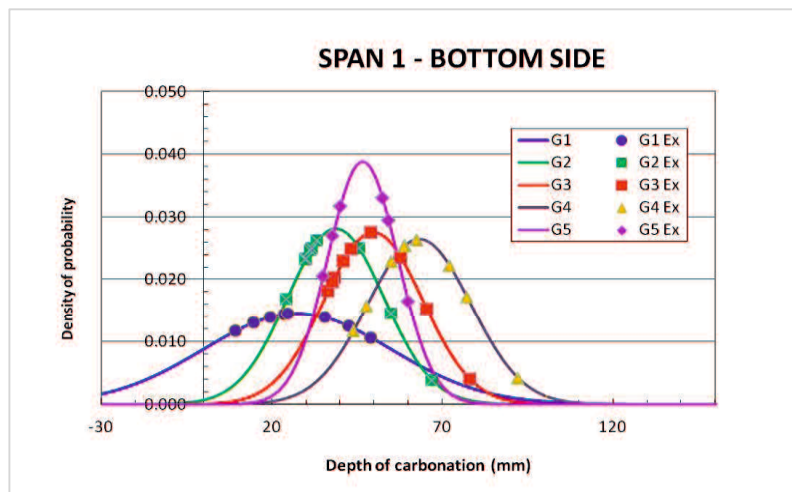


Fig. 4.24 Normal distribution of the carbonation in Span 1 bottom side

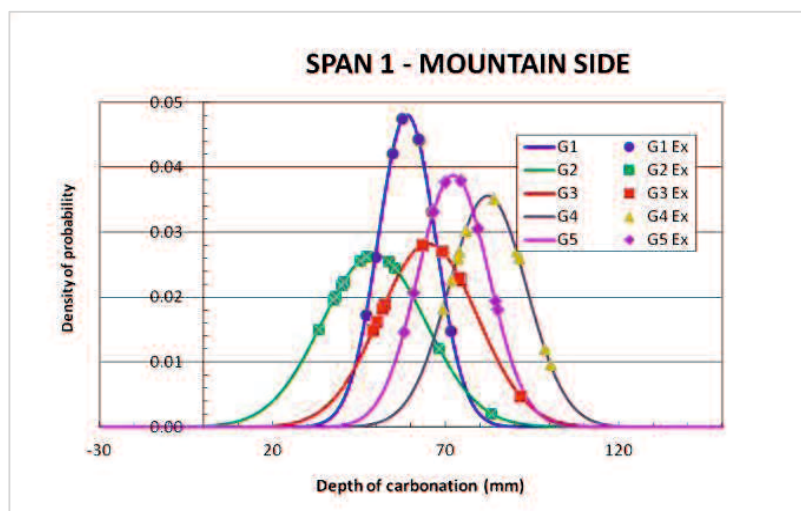


Fig. 4.25 Normal distribution of the carbonation in Span 1 mountain side

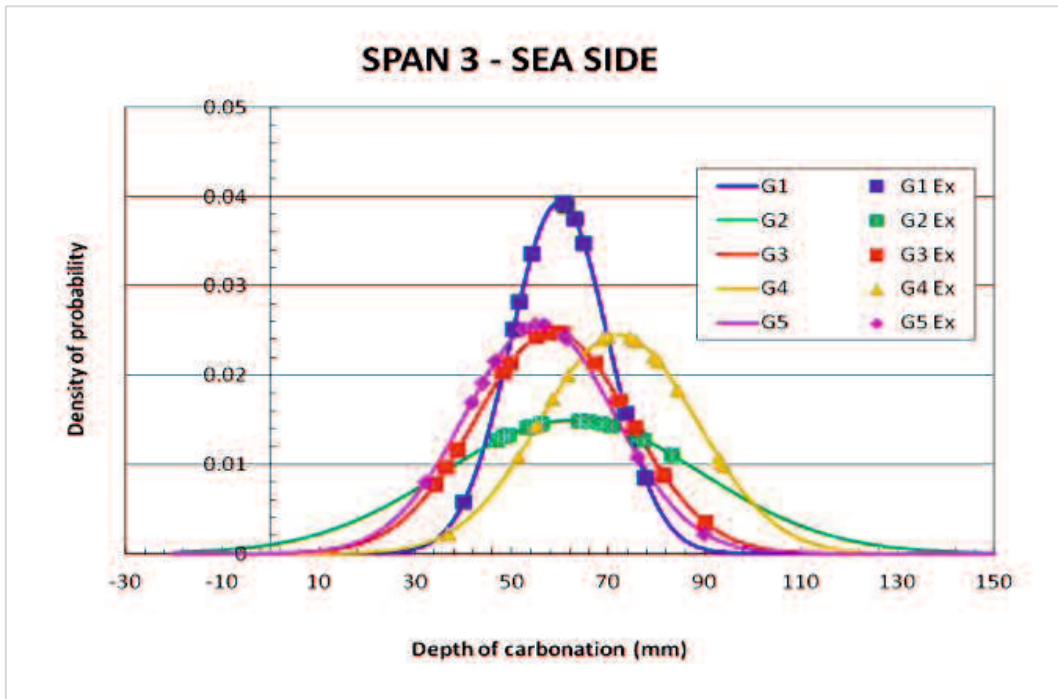


Fig. 4.26 Normal distribution of the carbonation in Span 3 sea side

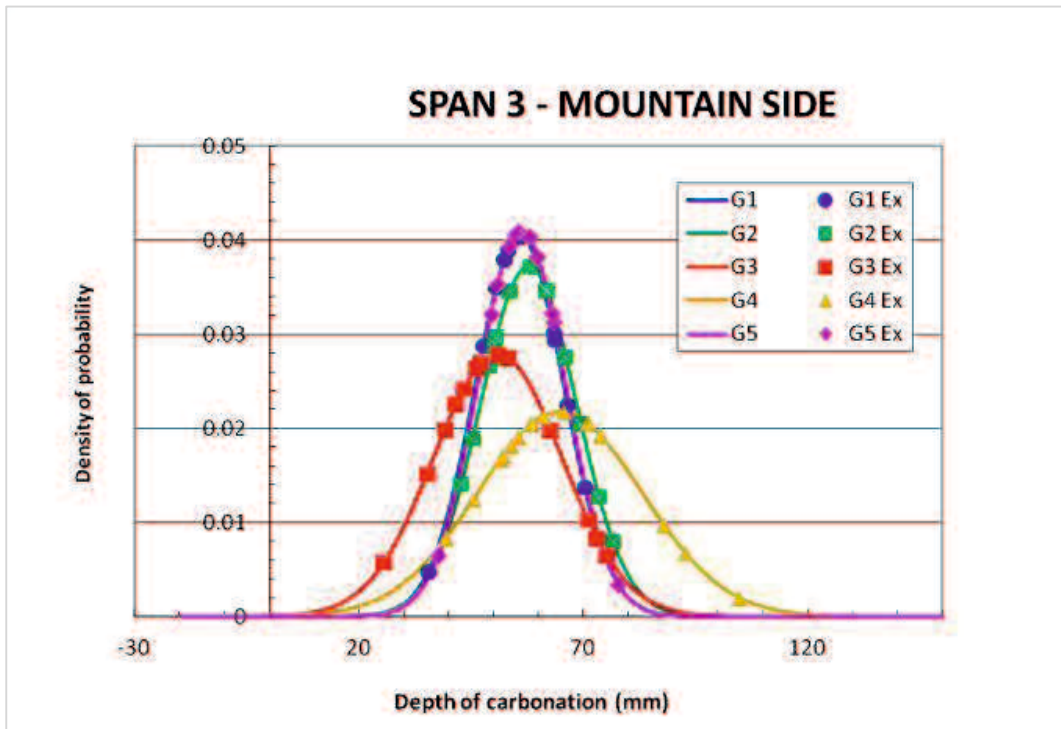


Fig. 4.27 Normal distribution of the carbonation in Span 3 mountain side

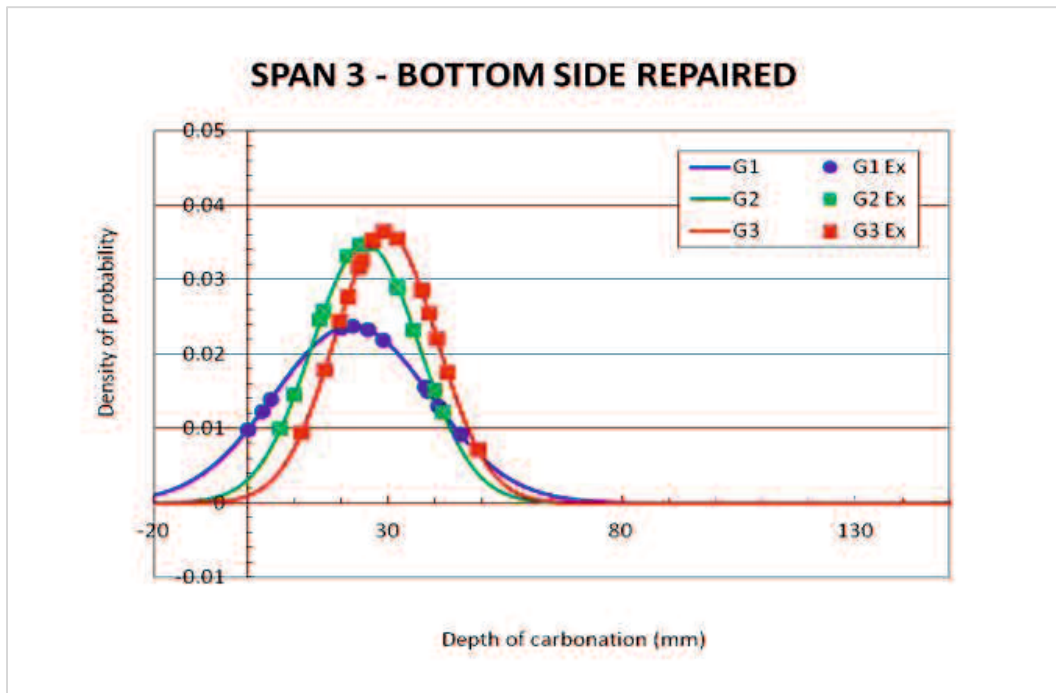


Fig. 4.28 Normal distribution of the carbonation in Span 3 bottom side (repaired)

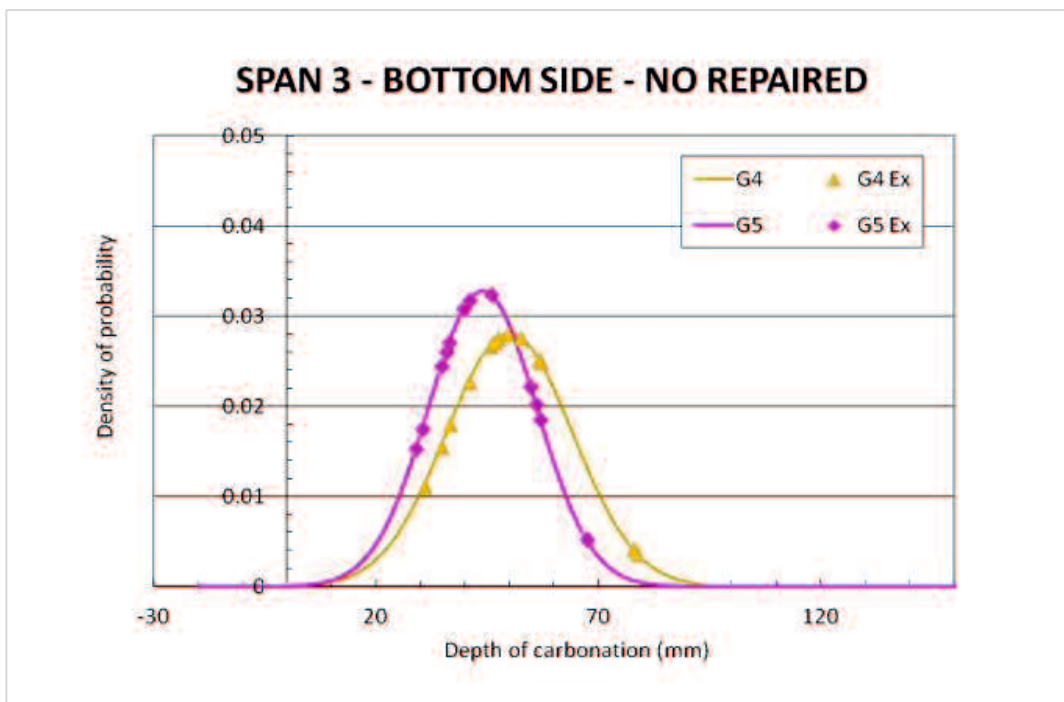


Fig. 4.29 Normal distribution of the carbonation in Span 3 bottom side (no repaired)

### 4.4.3 Remaining concrete cover results

The remaining concrete cover is the most important parameter to assume the carbonation process on the concrete. The remaining concrete cover is calculated using the thickness of concrete cover and the carbonation depth, it can be used to predict the initiation of corrosion due to carbonation. The initiation of corrosion is frequently identified from the remaining concrete cover, i.e., the difference between the thickness of concrete cover and the carbonation depth. In previous studies, researchers have concluded that the initiation of corrosion occurs when the remaining concrete cover falls below 10 mm [8]. Thus, the remaining cover affects the initiation of corrosion. The remaining concrete cover results for Spans 1 and 3 are shown in Figs. 4.30 and 4.31.

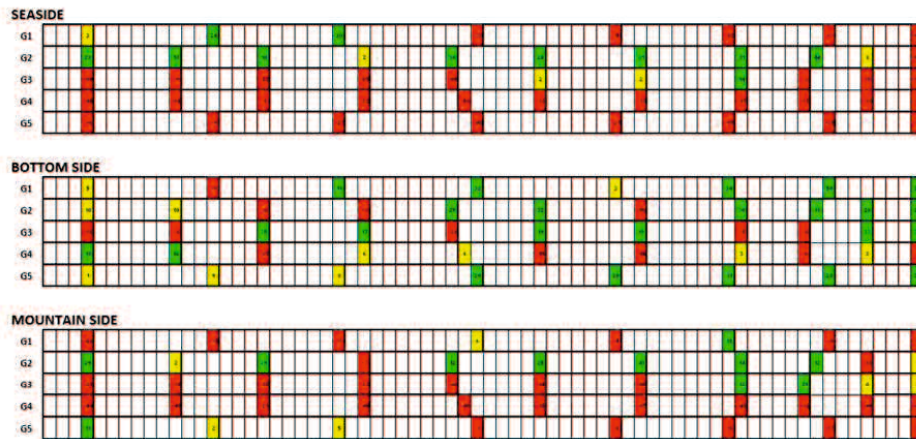


Fig. 4.30 Remaining concrete cover of Span 1

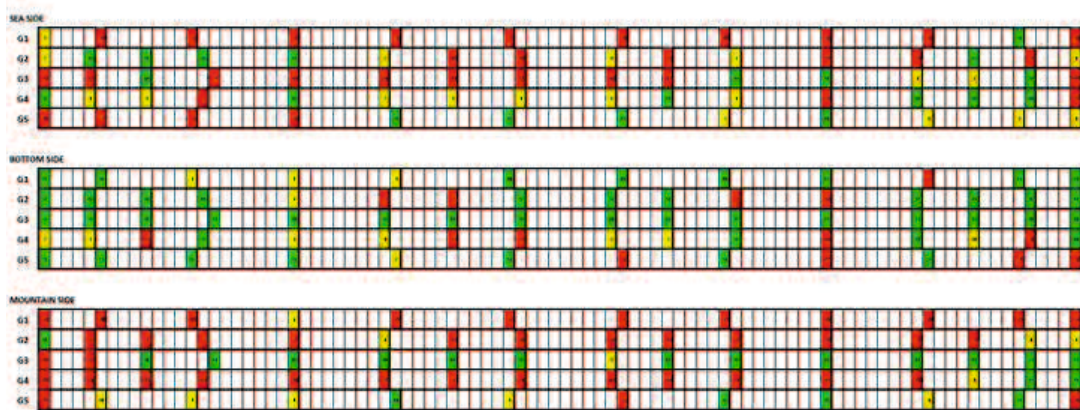
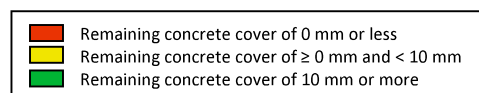


Fig. 4.31 Remaining concrete cover of Span 3



In these figures, differences in the remaining concrete cover are indicated using different colors. The red color indicates remaining concrete cover of 0 mm or less, meaning that the carbonation has reached the reinforcing bars. The yellow color indicates remaining concrete cover greater than 0 mm but less than 10 mm, meaning that the initial corrosion has begun to reach the reinforcing bars. The green color indicates remaining concrete cover of 10 mm or more, meaning that the initial corrosion has not occurred on the reinforcing bars.

#### 4.4.4 Carbonation rate coefficient

The carbonation rate coefficient  $A$  can be obtained from measurements of the carbonation depth  $d(t)$  in mm at time  $(t)$  in years. The change in the carbonation depth over time is calculated according to the  $\sqrt{t}$  rule, as shown in Eq. (4.1).

$$d(t) = A\sqrt{t} \quad (4.1)$$

The carbonation depth results are the averages of the values obtained from eight to sixteen measurements from the cross-sections cutting-off from each girder. Table 4.4 shows the carbonation rate coefficient of Span 1 and 3.

Table 4.4 Carbonation rate coefficient of Spans 1 and 3

No.	Girder	Carbonation rate coefficient			Standard deviation		
		Sea side mm/ $\sqrt{\text{year}}$	Bottom side mm/ $\sqrt{\text{year}}$	Mountain side mm/ $\sqrt{\text{year}}$	Sea side mm/ $\sqrt{\text{year}}$	Bottom side mm/ $\sqrt{\text{year}}$	Mountain side mm/ $\sqrt{\text{year}}$
<b>SPAN 1</b>							
1	G1	7.72	3.23	6.93	2.08	1.63	0.98
2	G2	6.08	4.56	5.80	1.67	1.67	1.77
3	G3	7.19	5.85	7.65	1.56	1.71	1.67
4	G4	8.86	7.45	9.68	1.82	1.78	1.32
5	G5	8.23	5.49	8.50	1.08	1.21	1.21
<b>SPAN 3</b>							
6	G1	7.06	2.63	6.58	1.19	1.98	1.16
7	G2	7.36	2.97	6.81	1.33	1.35	1.26
8	G3	6.88	5.11	5.99	1.89	6.49	1.68
9	G4	8.49	5.89	7.63	1.91	1.67	2.16
10	G5	6.57	5.17	6.62	1.83	1.43	1.14

#### 4.4.5 Chloride ion content

In this study, although the carbonation is the main deterioration factor of SK Bridge based on the location is about 1 km upstream from the mouth of the river it spans, the chloride ion also affects on the deterioration of SK Bridge. Table 4.6 shows the chloride ion data was obtained from the concrete core test on SK Bridge [12,13].

The apparent diffusion coefficient of chloride ions was calculated from the following equation:

$$C(x,t) = C_0 \cdot \left(1 - \operatorname{erf}\left[\frac{x}{2\sqrt{(D_{ap} \cdot t)}}\right]\right) + C_i(x,0) \quad (4.2)$$

where  $C(x,t)$  is the chloride ion content at depth  $x$  at time  $t$ ,  $C_0$  is the chloride ion content at the concrete surface,  $D_{ap}$  is the apparent diffusion coefficient of the chloride ion, and  $C_i(x,0)$  is the initial chloride ion content in the concrete. Table 4.5 summarizes the results of the chloride ion content tests (i.e.,  $C(x,t)$ ,  $C_0$ , and  $C_i(x,0)$ ) of the concrete cores. The apparent diffusion coefficient of the chloride ion content  $D_{ap}$  is an unknown parameter in Eq. (4.2) and is determined from the results of the chloride ion content tests. The results obtained for depths of 30–45 mm in the concrete cores were used as the chloride ion contents at the reinforcement depth  $C(x,t)$ . The values used for concrete cover,  $t_{mp}$  in Eq. (6) and  $W$  in Eq. (5), were 40 mm, 16°C (mean temperature), and 4% [15,16], respectively.

#### 4.4.6 Identification of main deterioration factor

According to the Ref. [8], corrosion due to carbonation typically begins when the thickness of remaining concrete cover falls below 10 mm. This means that remaining concrete cover is an indicator of the degree of influence of carbonation. Tables 4.2 and 4.3 show the results of the concrete cover thickness and carbonation depth measurements. As these tables show, the average values of the carbonation depth in the main girders of both Span 1 and Span 3 are greater than the average thicknesses of concrete cover, except for the bottom side of Span 3, which has received some repair work. The maximum value of the carbonation depth was 60 mm or greater in more than half of the girder cross sections (Figs. 4.21 and 4.22), which is considerably greater than the thickness of the concrete cover (Figs. 4.13 and 4.14).

Table 4.5 Chloride ion content results of Spans 1 and 3

Span No.	Girder No.	Core specimen No.	Surface chloride ion content $C_0$ (kg/m <sup>3</sup> )	Apparent diffusion coefficient $\times 10^{-8}$ $D_{ap}$ (cm <sup>2</sup> /s)	Initial chloride ion content $C_i(x, 0)$ (kg/m <sup>3</sup> )	Chloride ion content at reinforcement location $C(x, t)$ (kg/m <sup>3</sup> )
Span 1	1	C1014	1.10	0.60	0.60	1.00
		C1111	0.60	0.50	0.40	0.60
		C1115	0.80	0.60	0.60	0.90
	2	C2113	2.30	0.90	0.65	1.80
	3	C3011	2.50	1.80	0.90	2.50
		C3015	2.60	1.80	0.50	2.10
		C3114	3.80	1.50	0.80	3.00
	4	C4113	3.10	0.40	0.40	1.30
	5	C5111	3.90	1.80	0.80	3.20
		C5114	1.80	1.80	0.60	1.70
C5115		1.40	1.80	0.30	1.20	
Span 3	1	C1131	0.70	0.40	0.40	0.60
		C1134	0.70	0.08	0.30	0.30
		C1138	0.90	0.40	0.30	0.55
	2	C2031	2.50	0.40	0.50	1.20
		C2136	1.90	0.40	0.65	1.20
	3	C3134	1.00	0.40	0.10	0.40
		C3138	0.70	0.10	0.15	0.18
	4	C4031	0.90	0.08	0.18	0.20
		C4136	1.20	0.05	0.12	0.12
	5	C5031	1.30	0.05	0.20	0.20
		C5134	1.10	0.05	0.12	0.12
		C5038	0.80	0.05	0.30	0.30

The average chloride ion content determined from tests on concrete cores taken from SK Bridge was 1.07 kg/m<sup>3</sup> [12,13] as shown in Table 4.5, this value is lower than the critical chloride ion content for steel corrosion of 1.2 kg/m<sup>3</sup> given in Ref. [14]. This table also shows that only five of the 23 points on the bridge had higher chloride ion contents than the critical content for steel corrosion, and these contents were only slightly higher than the critical content.

Based on these results, it was concluded that the main cause of the deterioration of SK Bridge was carbonation, because the carbonation depth was considerably greater than the concrete cover thickness. The average chloride ion content did not exceed the critical chloride ion content for steel corrosion. However, given that the bridge is located less than 1 km upstream from the mouth of the Sagawa River that it spans, which empties into the Seto Island Sea, chloride ion attack is believed to have also contributed to the deterioration of the bridge.

#### **4.5 Remaining life prediction method through cross-section cutting-off girders**

##### **4.5.1 Concept of remaining life prediction method**

In this study, the end of the service life was defined as the point at which the total amount of steel corrosion due to carbonation and chloride ion attack reached a critical value of  $Q = 75 \text{ mg/cm}^2$ . This value was obtained from the BREX system, which is used in cases in which the main deterioration factor is chloride attack [9] [10].

The remaining life  $R$  as the results of the cross-section cutting-off girders was calculated as the elapsed time  $EL$  (in this case, 72 years) minus the service life  $SL$  in years [7]. The service life  $SL$  in years can therefore be expressed as the sum of the elapsed service life,  $EL$  (in this case, 72 years) and the remaining service life  $R$  in years, as shown in Eq. (4.3).

$$SL = EL + R \quad (4.3)$$

##### **4.5.2 Remaining life prediction for the case in which the deterioration is mainly caused by carbonation and also affected by chloride ion attack**

Figure 4.32 shows a flowchart of the remaining life prediction method for the case in which the deterioration is mainly caused by carbonation but is also affected by chloride ion attack. Initial corrosion due to carbonation is assumed to begin when the remaining concrete cover, i.e., the thickness of the concrete cover minus the carbonation depth, is 10 cm or less [8].

The carbonation depth at 72 years was obtained from the measurements of the cross-section cutting-off girders. The carbonation rate coefficient  $A$  was calculated from the carbonation depth  $d(t)$  at time  $t$  using Eq. (4.1).

Eq. (4.4) is used to calculate the reinforcing bar corrosion rate  $V$  if the remaining concrete cover thickness is 10 mm or less. If the remaining concrete cover at time  $t$  is greater than 10 mm, Eq. (4.5) should be used [17][18].

$$V = 1.32(Cl - 1.2)k \quad (4.4)$$

$$V = (0.840W - 0.145C + 1.32Cl + 0.0293W \cdot C - 0.0917C \cdot Cl + 0.658Cl \cdot W - 2.52)k \quad (4.5)$$

where  $V$  (mg/cm<sup>2</sup>/year) is the steel corrosion rate,  $Cl$  (kg/m<sup>3</sup>) is the chloride ion content at the reinforcement location,  $C$  (mm) is the remaining concrete cover,  $W$  (%) is the surface moisture content of the concrete, and  $k$  is a correction for the temperature  $tmp$  (°C), which can be calculated from Eq. (4.6):

$$k = 1 + 0.0381(tmp - 20) \quad (4.6)$$

The total amount of steel corrosion  $Q(t)$  at time  $t$ , in kg/mm<sup>2</sup>, can be calculated from the steel corrosion rate  $V(t)$  at time  $t$  and the integration time step  $dt$  [12,13] using Eq. (4.7):

$$Q(t) = Q(0) + \sum_{t=\Delta t}^{t=X} \left( \frac{\Delta t}{2} \left( V\left(t - \frac{\Delta t}{2}\right) + V\left(t + \frac{\Delta t}{2}\right) \right) \right) \quad (4.7)$$

where  $Q(0)$  can be calculated using Eq. (4.8):

$$Q(0) = \frac{\Delta t}{4} \left( V(0) + V\left(\frac{\Delta t}{2}\right) \right) \quad (4.8)$$

As in a previous study [12,13] the remaining life  $R$  of SK Bridge as indicated by the results of the tests on the concrete cores was calculated as the life expectancy  $X$  in years minus the period of service  $N$  in years. In this study, the service life  $SL$  was calculated based on the time  $t = t_1$  elapsed before the total amount of steel corrosion, calculated using Eq. (4.7), reaches the critical value  $Q(t_1) = 75$  mg/cm<sup>2</sup>, which was taken to be the indicator of the end of the service life. This is the critical value for the total amount of steel corrosion was used in the prediction method of the BREX system. [9][10]. Then the remaining life prediction can be calculated using Eq. (4.3). The remaining life  $R$  as the results of the cross-section cutting-off girders was calculated as the elapsed time  $EL$  (in this case, 72 years) minus the service life  $SL$  in years [7].

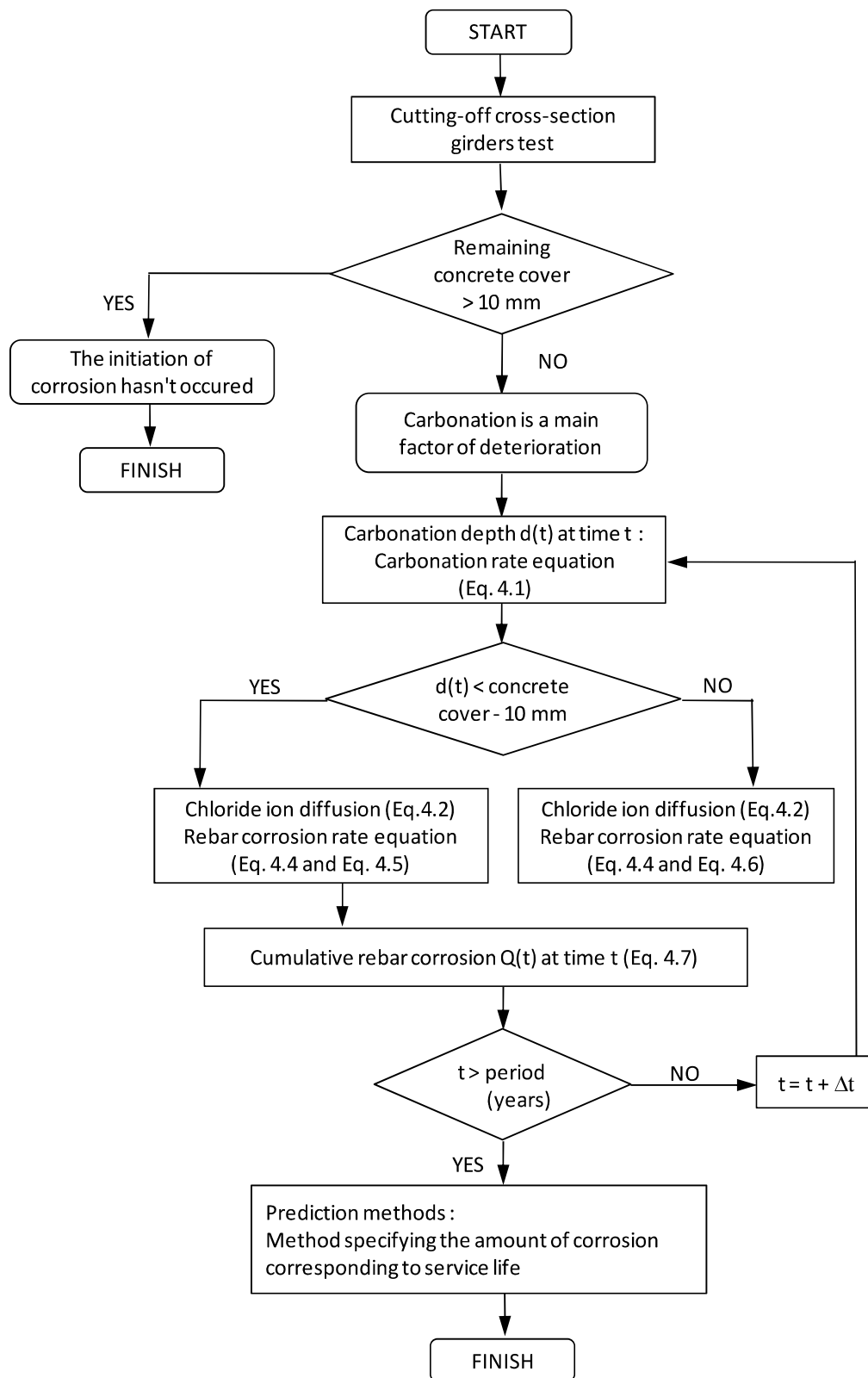


Fig. 4.32 Flowchart of remaining life prediction in this study

Tables 4.6 and 4.7 show the results of the predicted remaining life calculation in Span 1 and Span 3. The results of Span 1 show that the time before reaching the critical amount of corrosion for initial cracking for the sea sides, bottom sides, and mountain sides of the girders were, on average, 46 years, 82 years, and 47 years, respectively. The predicted ends of the service life, which is indicated by the total amount of steel corrosion reaching  $75 \text{ mg/cm}^2$ , were, on average, 63 years, 121 years and 65 years for the sea sides, bottom sides, and mountain sides of the girders, respectively. Then the remaining life prediction can be calculated using Eq. (4.3). The prediction of remaining life were, on average, -9 years, 49 years, and -7 years for the sea sides, bottom sides, and mountain sides of the girders, respectively. As these results show, the predicted remaining life varies from -34 years to 145 years.

The results of Span 3 show that the initial cracking limit for the sea sides, bottom sides, and mountain sides of the girders were, on average, 64 years, 135 years, and 67 years, respectively. The predicted ends of the service life were, on average, 99 years, 175 years, and 98 years for the sea sides, bottom sides, and mountain sides of the girders, respectively. The predicted of remaining life were, on average, 27 years, 103 years, and 26 years for the sea sides, bottom sides, and mountain sides of the girders, respectively. As these results show, the predicted remaining life varies from -16 years to 178 years.

The service life prediction for Span 1 and Span 3 are shown in Figs. 4.33 and 4.34, respectively. In these figures, differences in the service life prediction are indicated using different colors. The red color indicates the service life prediction less than 72 years (72 years is time of investigation), meaning that the bridge's life has ended before the time of investigation. The green color indicates the service life prediction of 72 years or more, meaning that the initial corrosion has not occurred on the reinforcing bars.

Figure 4.33 shows that on Span 1, the red color is dominant on the sea side and mountain side. On the bottom side the green color is dominant. The service life prediction on the sea side and mountain side has 63 and 65 years. On the bottom side, the service life prediction is 121 years. It means that on the sea side and mountain side the bridge's life has ended before the time of investigation (72 years). On the bottom side, it still remains 49 years before reaching the end of the bridge's life.

Table 4.6 Remaining life prediction due to carbonation and chloride in of Span 1

Span	Girder No.	Seaside			Bottom side			Mountain side		
		Q=10mg/cm <sup>2</sup>	Q=75 mg/cm <sup>2</sup>	Q=10mg/cm <sup>2</sup>	Q=10mg/cm <sup>2</sup>	Q=75 mg/cm <sup>2</sup>	Q=10mg/cm <sup>2</sup>	Q=10mg/cm <sup>2</sup>	Q=75 mg/cm <sup>2</sup>	Q=75 mg/cm <sup>2</sup>
		Cracking limit (years)	Service life SL (years)	Remaining life R (years)	Cracking limit (years)	Service life SL (years)	Remaining life R (years)	Cracking limit (years)	Service life SL (years)	Remaining life R (years)
	G1	52	72	0	131	217	145	43	64	-8
	G2	97	116	44	98	135	63	94	112	40
<b>Span 1</b>	G3	28	41	-31	55	88	16	31	47	-25
	G4	28	48	-24	49	68	-4	21	38	-34
	G5	25	39	-33	77	96	24	46	63	-9
<b>Average (years)</b>		46	63	-9	82	121	49	47	65	-7

Table 4.7 Remaining life prediction due to carbonation and chloride ion of Span 3

Span	Girder No.	Seaside			Bottom side			Mountain side		
		Q=10mg/cm <sup>2</sup>	Q=75 mg/cm <sup>2</sup>	Q=10mg/cm <sup>2</sup>	Q=10mg/cm <sup>2</sup>	Q=75 mg/cm <sup>2</sup>	Q=10mg/cm <sup>2</sup>	Q=10mg/cm <sup>2</sup>	Q=75 mg/cm <sup>2</sup>	Q=75 mg/cm <sup>2</sup>
		Cracking limit (years)	Service life SL (years)	Remaining life R (years)	Cracking limit (years)	Service life SL (years)	Remaining life R (years)	Cracking limit (years)	Service life SL (years)	Remaining life R (years)
	G1	42	75	3	136	147	75	30	56	-16
	G2	64	84	12	196	250	178	40	58	-14
<b>Span 3</b>	G3	49	79	7	191	231	159	177	220	148
	G4	78	123	51	71	117	45	34	72	0
	G5	87	133	61	83	130	58	56	83	11
<b>Average (years)</b>		64	99	27	135	175	103	67	98	26

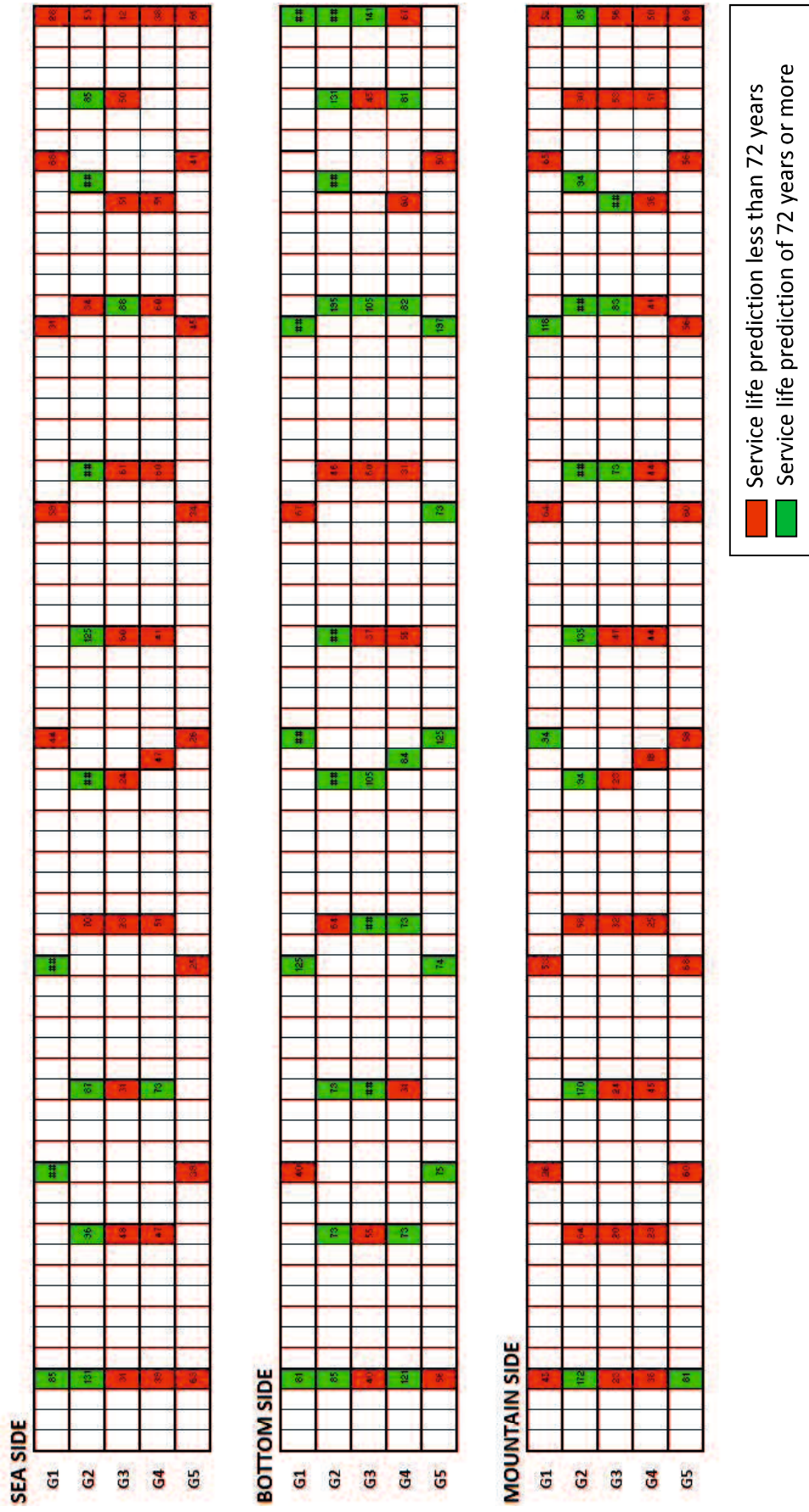


Fig. 4.33 Service life prediction due to carbonation and chloride ion of Span 1

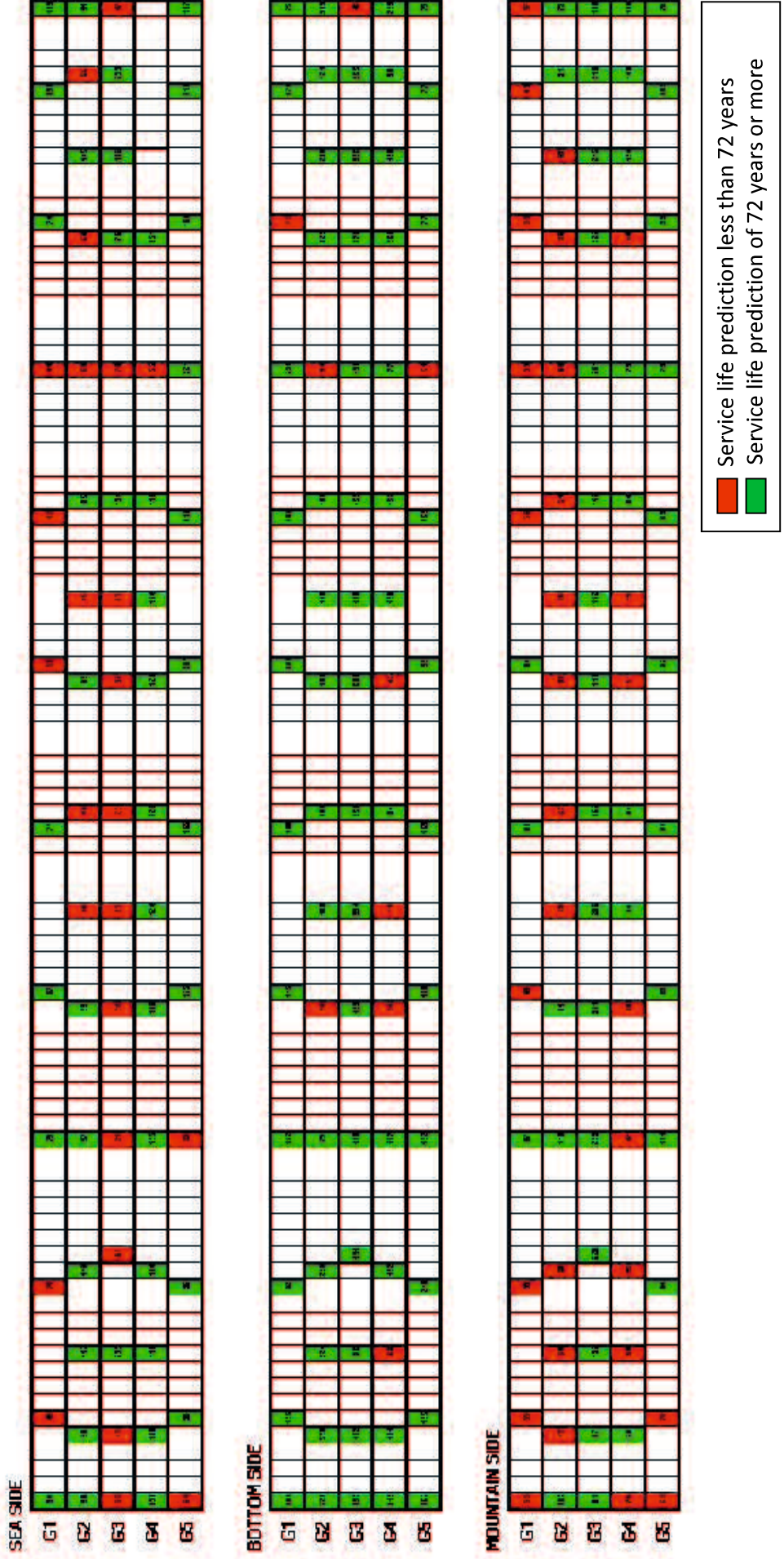


Fig. 4.34 Service life prediction due to carbonation and chloride ion of Span 3

Figure 4.34 shows that on Span 3, the green color is dominant on sea side and mountain side. On the bottom side, the green color is more dominant. The service life prediction on the sea side and mountain side has 99 and 98 years. On the bottom side, the service life prediction is 175 years. It means that on the sea side and mountain side, the end of bridge's life will be reached approximately 27 years later, and on the bottom side it still has more than 100 years (103 years) before reaching the end of the bridge's life.

The comparison of remaining life prediction due to carbonation and chloride ion between Span 1 and Span 3 is shown in Fig. 4.35. Based on this figure, the remaining life prediction on Span 1 has a negative value on the sea side and mountain side, however, the bottom side has a positive value. Span 3 has a positive value on the sea side, mountain side and bottom side. The negative value of remaining life means that the end of bridge's life has already ended before the time of investigation. The positive value of remaining life means that there was a few years before meeting the end of the bridge's life.

Figure 4.36 shows the service life prediction due to carbonation and chloride ion on Span 1 and Span 3. It can simplify the explanation that based on the time of investigation equal with 72 years, the aged of Span 1 is less than 72 years on the sea side and mountain side, however, the bottom side is more than 72 years. The age of Span 3 is more than 72 years on all sides due to the repair work on the bottom side of span 3, which stopped the deterioration process effectively.

Table 4.8 shows the results of the remaining life calculation in both Spans 1 and 3. The results show that the initial cracking limit for the sea sides, bottom sides, and mountain sides of the girders were, on average, 55 years, 108 years, and 57 years, respectively. The predicted ends of the service life were, on average, 81 years, 147 years, and 81 years for the sea sides, bottom sides, and mountain sides of the girders, respectively. The remaining life predictions were, on average, 9 years, 75 years, and 9 years for the sea sides, bottom sides, and mountain sides of the girders, respectively. As these results show that the remaining life prediction varies from -34 years to 178 years. Fig. 4.37 shows the normal distribution of service life prediction due to carbonation and chloride ion in Spans 1 and 3.

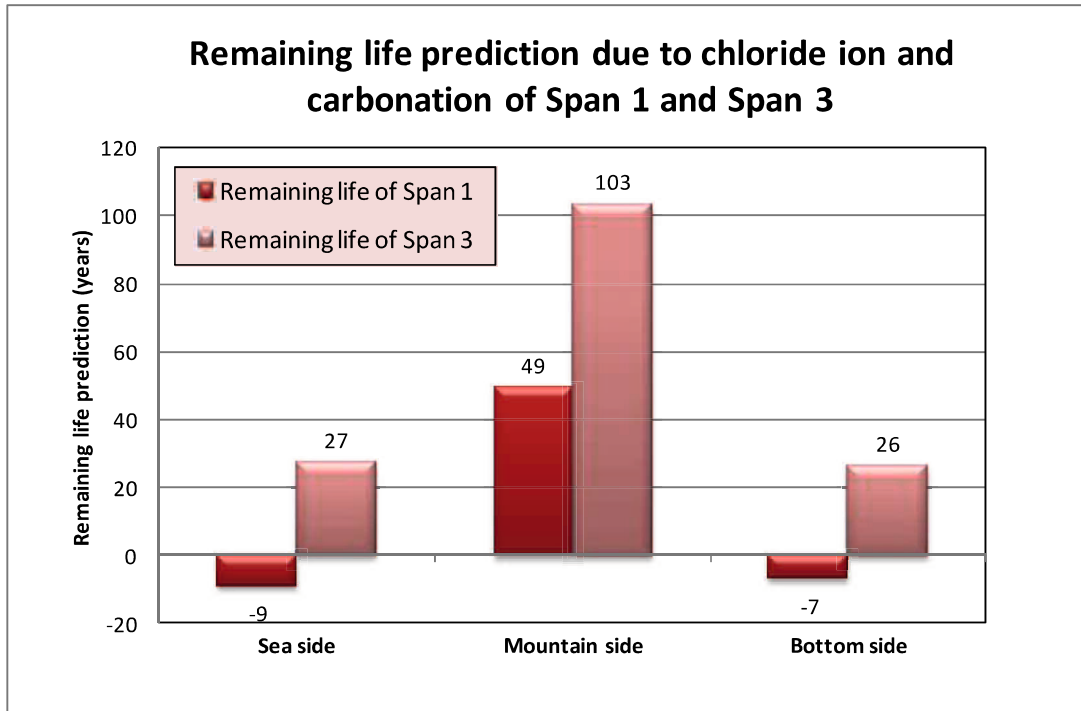


Fig. 4.35 Remaining life prediction due to carbonation and chloride ion of Span 1 and Span 3

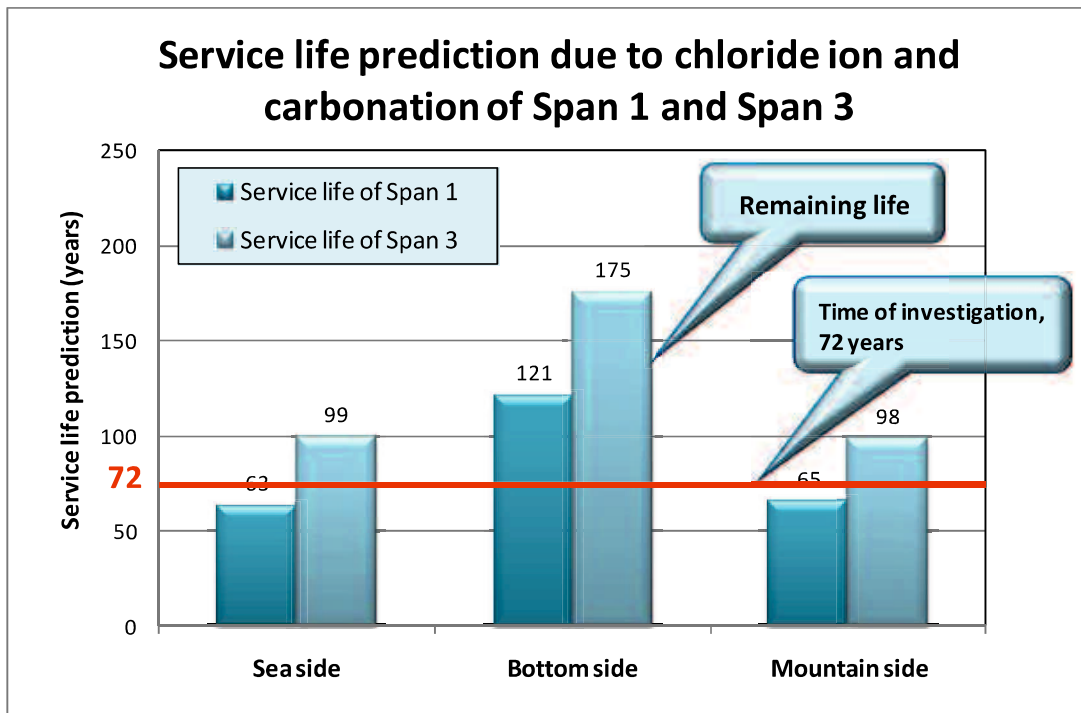


Fig. 4.36 Service life prediction due to carbonation and chloride ion of Span 1 and Span 3

Table 4.8 Remaining life prediction of Spans 1 and 3

Span	No.	Girder No.	Seaside			Bottom side			Mountain side		
			Q=10mg/cm <sup>2</sup>	Q=75 mg/cm <sup>2</sup>	Remaining life	Q=10mg/cm <sup>2</sup>	Q=75 mg/cm <sup>2</sup>	Remaining life	Q=10mg/cm <sup>2</sup>	Q=75 mg/cm <sup>2</sup>	Remaining life
			Cracking limit (years)	Service life SL (years)	R (years)	Cracking limit (years)	Service life SL (years)	R (years)	Cracking limit (years)	Service life SL (years)	R (years)
<b>Span 1</b>	1	G1	52	72	0	131	217	145	43	64	-8
	2	G2	97	116	44	98	135	63	94	112	40
	3	G3	28	41	-31	55	88	16	31	47	-25
	4	G4	28	48	-24	49	68	-4	21	38	-34
	5	G5	25	39	-33	77	96	24	46	63	-9
<b>Span 3</b>	6	G1	42	75	3	136	147	75	30	56	-16
	7	G2	64	84	12	196	250	178	40	58	-14
	8	G3	49	79	7	191	231	159	177	220	148
	9	G4	78	123	51	71	117	45	34	72	0
	10	G5	87	133	61	83	130	58	56	83	11
<b>Average (years)</b>			<b>55.0</b>	<b>81.0</b>	<b>9.0</b>	<b>108.7</b>	<b>147.9</b>	<b>75.9</b>	<b>57.2</b>	<b>81.3</b>	<b>9.3</b>

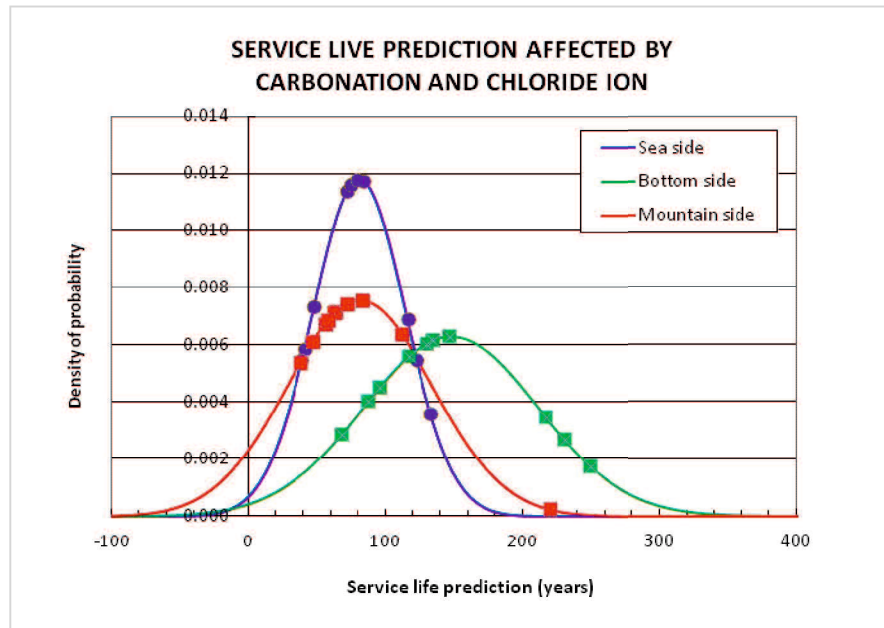


Fig. 4.37 Normal distribution of service life prediction due to carbonation and chloride ion in Spans 1 and 3

#### 4.5.3 Remaining life prediction for the case in which the deterioration is caused only by carbonation

The remaining life prediction for the case in which the deterioration is caused only by carbonation can be seen in Tables 4.9 and 4.10. In Table 4.9, the remaining life prediction was calculated using the method of predicting the remaining life which is established in this study, with the assumption that the chloride ion content has no effect in the result or equal with zero. The comparison between the service life prediction of cross-section cutting-off girders deterioration due to chloride ion and carbonation and carbonation only was examined in order to determine the effect of chloride ion on the deterioration process of the bridge.

Table 4.9 shows the results of the remaining life prediction due to carbonation only in both Spans 1 and 3. The remaining life predictions were, on average, 65 years, 136 years, and 65 years for the sea sides, bottom sides, and mountain sides of the girders, respectively. Fig. 4.38 shows the normal distribution of service life prediction due to carbonation only in Spans 1 and 3.

Table 4.9 Remaining life prediction carbonation only of Spans 1 and 3

Span	No.	Girder No.	Seaside			Bottom side			Mountain side		
			Q=10mg/cm <sup>2</sup>	Q=75 mg/cm <sup>2</sup>	Q=10mg/cm <sup>2</sup>	Q=75 mg/cm <sup>2</sup>	Q=10mg/cm <sup>2</sup>	Q=75 mg/cm <sup>2</sup>	Q=10mg/cm <sup>2</sup>	Q=75 mg/cm <sup>2</sup>	
			Cracking limit (years)	Service life SL (years)	Remaining life R (years)	Cracking limit (years)	Service life SL (years)	Remaining life R (years)	Cracking limit (years)	Service life SL (years)	Remaining life R (years)
Span 1	1	G1	64	126	54	212	213	141	55	119	47
	2	G2	128	205	133	144	225	153	116	193	121
	3	G3	51	113	41	109	184	112	53	111	39
	4	G4	42	97	25	61	124	52	31	81	9
	5	G5	40	97	25	125	205	133	65	126	54
Span 3	6	G1	52	116	44	150	239	167	40	100	28
	7	G2	77	144	72	150	235	163	54	118	46
	8	G3	54	118	46	234	330	258	186	267	195
	9	G4	127	196	124	86	159	87	40	99	27
	10	G5	96	167	95	98	175	103	88	158	86
<b>Average (years)</b>			<b>73.1</b>	<b>137.9</b>	<b>65.9</b>	<b>136.9</b>	<b>208.9</b>	<b>136.9</b>	<b>72.8</b>	<b>137.2</b>	<b>65.2</b>

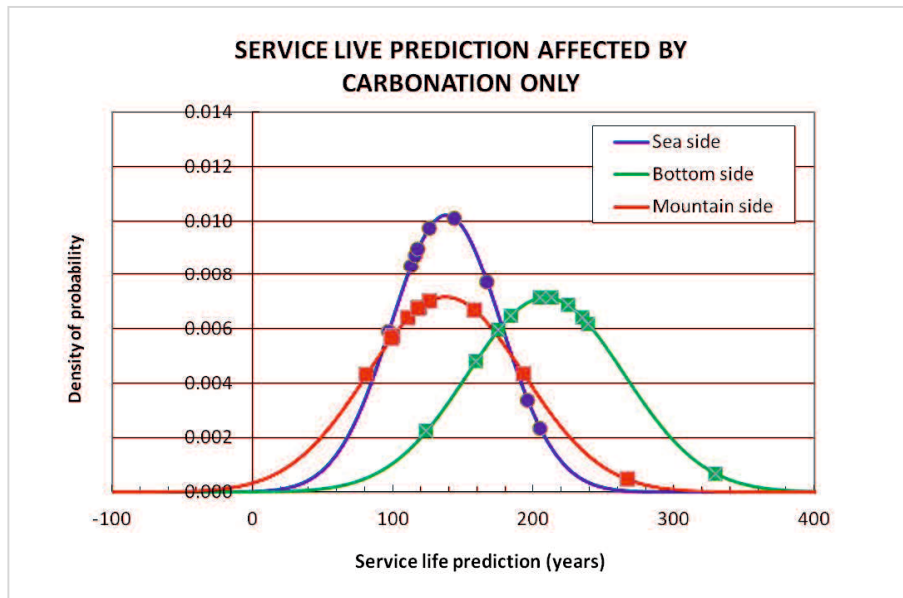


Fig. 4.38 Normal distribution of service life prediction due to carbonation only in Spans 1 and 3

The remaining life prediction for the case in which the deterioration is caused only by carbonation, was calculated using the  $\sqrt{t}$  rule can be seen in Table 4.10. The initial corrosion due to carbonation is assumed to begin when the remaining concrete cover, i.e., the thickness of the concrete cover minus the carbonation depth, is 10 cm or less [8]. The service life as the predicted end of life, was calculated when the carbonation already reached the reinforcing bar (carbonation depth = thickness of concrete cover). The change in the time over carbonation depth was calculated according to the  $\sqrt{t}$  rule, as shown in Eq. (4.1). The predicted remaining life was estimated from the elapsed time  $EL$  (in this case, 72 years) minus the service life  $SL$  in years.

Table 4.10 shows the results of the predicted remaining life calculations. The remaining life predictions were, on average, 8 years, 90 years, and 8 years for the sea sides, bottom sides, and mountain sides of the girders, respectively. Fig. 4.39 shows the normal distribution of service life prediction due to carbonation only in Spans 1 and 3.

Table 4.10 Remaining life prediction carbonation only of Spans 1 and 3 calculated using the  $\sqrt{t}$  rule

Span	No.	Girder No.	Sea side			Bottom side			Mountain side		
			Initial corrosion (years)	Service life (years)	Remaining life (years)	Initial corrosion (years)	Service life (years)	Remaining life (years)	Initial corrosion (years)	Service life (years)	Remaining life (years)
			$SL$ (years)	$SL$ (years)	$R$ (years)	$SL$ (years)	$SL$ (years)	$R$ (years)	$SL$ (years)	$SL$ (years)	$R$ (years)
<b>Span 1</b>	1	G1	36	74	2	89	143	71	36	59	-13
	2	G2	87	151	79	99	188	116	75	139	67
	3	G3	27	55	-17	59	130	58	28	56	-16
	4	G4	24	39	-33	33	66	-6	16	26	-46
	5	G5	23	37	-35	95	152	80	47	67	-5
<b>Span 3</b>	6	G1	32	57	-15	184	207	135	25	45	-27
	7	G2	56	84	12	147	214	142	33	58	-14
	8	G3	20	59	-13	82	296	224	125	220	148
	9	G4	73	122	50	74	103	31	20	41	-31
	10	G5	58	124	52	66	123	51	64	98	26
<b>Average (years)</b>			<b>43.6</b>	<b>80.2</b>	<b>8.2</b>	<b>92.8</b>	<b>162.2</b>	<b>90.2</b>	<b>46.9</b>	<b>80.9</b>	<b>8.9</b>

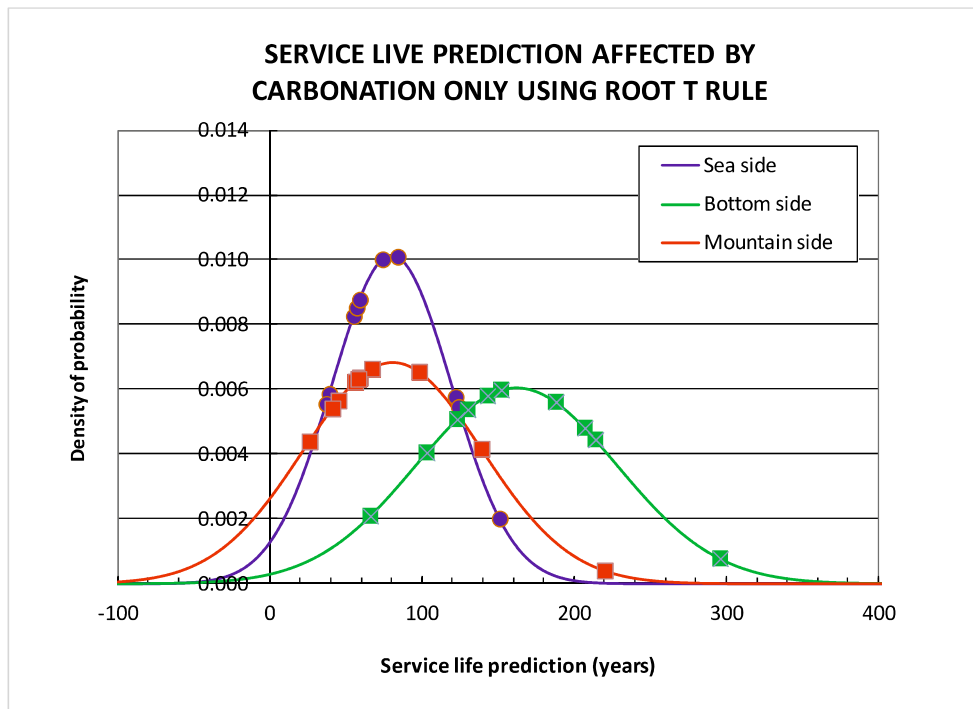


Fig. 4.39 Normal distribution of service life prediction due to carbonation only in Spans 1 and 3 calculated using the  $\sqrt{t}$  rule

#### 4.5.4 Discussion

The remaining life predictions for the case in which the deterioration is mainly caused by carbonation and also affected by chloride ion attack is shown in Table 4.8. Based on a cumulative amount of steel corrosion of  $75 \text{ mg/cm}^2$ , is the same as the criterion used in the BREX system, which is used in cases where the main cause of deterioration is chloride attack [9][10]. The predicted remaining life was almost the same for the sea sides and mountain sides of the girders, 9.0 years and 9.3 years, approximately 9 years. This means that on the sea side and the mountain side, the end of the service life of SK Bridge is approximately 81 years after the construction of the bridge. The predicted remaining life for the bottom side is much longer, at approximately 75 years, because of repair work done on the bottom side. This repair work was proven to work well. It effectively extended the service life by approximately 66 years, compared with that for the sea side and the mountain side.

Figure 4.40 shows the comparison between the service life prediction of cross-section cutting-off girder's deterioration due to chloride ion and carbonation and carbonation only. It was examined using the method of predicting the remaining life which is established in this study in order to determine the effect of chloride ion on the deterioration process of the bridge. In this figure can be seen that the service life due to carbonation only is longer than due to carbonation and chloride ion.

The percentage of influence of chloride ion on the deterioration process was calculated in order to estimate the effect of chloride ion on the deterioration process of the bridge. The results of the influence of chloride ion on the deterioration process are 69 % for the sea side and mountain side and 42 % for the bottom side. From these results, it can be concluded that although chloride ion was not the main deterioration factor, it was however a big influence on the deterioration process. The big influence of chloride ion may have been because the chloride ion content in SK Bridge is fairly high,  $1.07 \text{ kg/m}^3$ , close enough with the requirement of the critical chloride ion content for steel corrosion  $1.2 \text{ kg/m}^3$  [8].

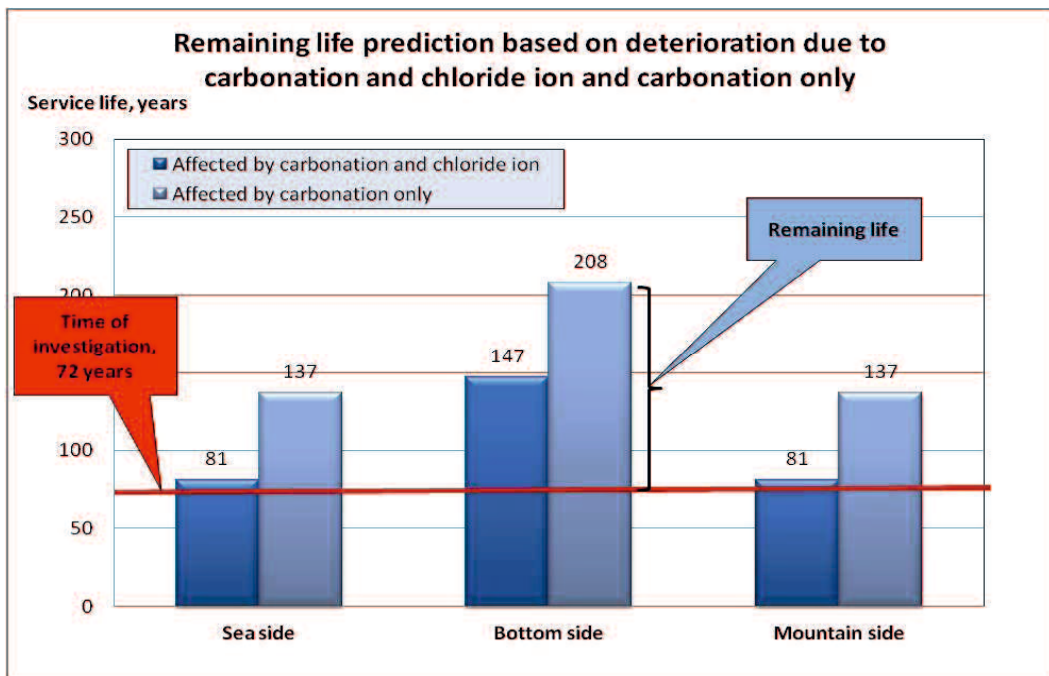


Fig. 4.40 Comparison of remaining life prediction due to carbonation and chloride ion and carbonation only of Span 1 and Span 3

This study also compares between the remaining life prediction for the case in which the deterioration is mainly caused by carbonation and also affected by chloride ion attack and for the case in which the deterioration is caused only by carbonation that was calculated using the  $\sqrt{t}$  rule. The results of the remaining carbonation in the sea side and mountain side of the girders on both cases were almost similar, approximately 9 years and 8 years, respectively. This was not because the chloride ion content had no effect on the remaining life prediction, but rather due to differences in the requirements and thresholds used in determining the end of bridge's life on these cases and the use of different equations. The remaining life prediction for the case in which the deterioration is mainly caused by carbonation and also affected by chloride ion attack used Eq. (4.7) and for the case in which the deterioration is caused only by carbonation used Eq. (4.1).

The predicted remaining life for the bottom side for both cases is quite different. The case in which the deterioration is caused only by carbonation is much longer at approximately 15 years because of repair work done on the bottom side which was proven to stop the carbonation process very well. The chloride ion content already existed on the concrete before repair work was done, because the bridge was located near the sea. Therefore the chloride ion content has a greater effect on the remaining life prediction.

#### **4.6 Conclusions**

This chapter presents the details of carbonation tests of cross-section cutting-off girders of an aged RC bridge and proposes a method to predict the remaining life of an RC bridge based on the extent of deterioration related to corrosion of the reinforcing bars due to carbonation and chloride ion attack. In addition, a flowchart for the proposed remaining life prediction method is presented. The proposed method was used to predict the remaining life of a bridge that had been in service for 72 years.

1. The results of the carbonation tests showed that the main factor in the deterioration of the bridge in question has been carbonation associated with corrosion of the reinforcing bars. However, because the bridge is located less than 1 km upstream from the mouth of the river it spans, which flows into the sea, chloride ion attack should be considered as another factor in the bridge's deterioration.

2. The remaining life prediction due to carbonation and chloride ion of the bridge was defined as the point at which the total amount of steel corrosion reached a critical value of  $Q = 75 \text{ mg/cm}^2$ . The remaining life of SK Bridge was predicted to be approximately 9 years for the sea side and bottom side and approximately 75 years for the bottom side. The predicted remaining life for the bottom side was longer than for the other side because of the repair work that had been completed on the bottom side.
3. The remaining life prediction due to carbonation only was calculated using the method of predicting the remaining life which is established in this study of SK Bridge was predicted to be approximately 65 years for the sea side and bottom side and approximately 136 years for the bottom side.
4. The results of the calculation of the influence of chloride ion on the deterioration process are 69 % for the sea side and mountain side and 42 % for the bottom side. From these results, it can be concluded although chloride ion was not the main deterioration factor however it has a big influence on the deterioration process. The big influence of chloride ion maybe because the chloride ion content in SK Bridge is fairly high,  $1.07 \text{ kg/m}^3$ , close enough with the requirement of the critical chloride ion content for steel corrosion  $1.2 \text{ kg/m}^3$ .
5. The remaining life prediction due to carbonation only was calculated using the  $\sqrt{t}$  rule of SK Bridge was predicted to be approximately 8 years for the sea side and bottom side and approximately 90 years for the bottom side.
6. The results of comparison between remaining life prediction for the case in which the deterioration is mainly caused by carbonation and also affected by chloride ion attack and for the case in which the deterioration is caused only by carbonation was calculated using the  $\sqrt{t}$  rule. In the sea side and mountain side of the girders on both cases were almost similar, approximately 8 years. This caused by the differences in the requirements and thresholds used in determining the end of life on these cases and the use of different equations.

#### 4.7 References

- [1] S, K. Verman, S. S. Bhadauria and S. Akhtar, Estimating residual service life of deteriorated reinforced concrete structures, *American Journal of Civil Engineering and Architecture*, Vol. 1, No. 5, pp. 92-96, 1993.
- [2] M. T. Lian, K. L. Wang and C. H. Liang, Service life prediction of reinforced concrete structure, *Cement and Concrete Research*, 29, pp. 1411-1418, 1999.
- [3] W. Chai, W. Li and H. Ba, Experimental study on predicting service life of concrete in marine environment, *Civil Engineering Journal*, Vol. 5, No. 1, pp. 93-99, 2011.
- [4] D. Vorechovska, B. Tepyly and M. Chroma, Probabilistic assessment of concrete structure durability under reinforcement corrosion, *Journal of Performance of Constructed Facilities*, Vol. 24, No. 6, pp. 571-579, 2010.
- [5] S. J. Kwon, U. J. Na, S. S. Park and S. H. Jung, Service life prediction of concrete wharves with early-aged crack: Probabilistic approach for chloride diffusion, *Structural Safety*, 31, pp. 75-83, 2009.
- [6] S. Ahmad, Reinforcement corrosion in concrete structures, its monitoring and service life prediction – a review, *Cement & Concrete Composites*, 25, pp. 459-471, 2003.
- [7] R. Widyawati, A. Miyamoto, H. Emoto, J. Takahashi, Service life prediction of an aged bridge based on carbonation test of cross-section cutting-off girders, *Journal of The Society of Materials Science, Japan*, Vol., No. 5, 2015.
- [8] Japan Society of Civil Engineers, Standard specifications for concrete structures: Maintenance, JSCE, 2007.
- [9] A. Miyamoto, H. Emoto, J. Takahashi and K. Hiraoka, Remaining life evaluation and its verification of aged bridge based on field inspections, in Japanese, *Concrete Research and Technology*, Vol. 23, No. 3, pp. 119-132, 2012.
- [10] J. Takahashi, A. Miyamoto and H. Emoto, Verification of estimation through concrete core testing of remaining life of bridge during its demolition, in Japanese, *Proceedings of the JSCE Annual Conference*, VI226, 2011.
- [11] V. G. Papadakis, C. G. Vayenas and M. N. Fardis, Physical and chemical characteristics affecting the durability of concrete, *ACI Materials Journal*, Title no. 88-M24, March-April, pp. 186-196, 1991.
- [12] J. Takahashi, R. Widyawati, H. Emoto and A. Miyamoto, Remaining life prediction of an aged bridge based on concrete core test, in Japanese, *Proceedings of the Japan Concrete Institute*, Vol. 36, No. 2, pp. 1339-1344, 2014.

- [13] R. Widyawati, J. Takahashi, H. Emoto, and A. Miyamoto, Remaining life prediction of an aged bridge based on concrete core test, 2<sup>nd</sup> International Conference on Sustainable Civil Engineering Structures and Construction Materials, SCESCM, Yogyakarta, Sept 23-25, pp. 1-10, 2014.
- [14] Japan Society of Civil Engineers, Standard specifications for concrete structures: design, JSCE, 2007.
- [15] H. Koga, H. Aoyama, H. Watanabe and Y. Kimura, Outdoor exposure test on concrete moisture content reducing effect of surface impregnation materials, in Japanese, Proceedings of the Japan Concrete Institute, Vol. 31, No. 1, pp. 1939-1944, 2009.
- [16] H. Koga and H. Watanabe, Results of moisture content monitoring of concrete exposed outdoors, in Japanese, Proceedings of the Japan Concrete Institute, Vol. 28, No. 1, pp. 641-646, 2006.
- [17] R. Iijima, T. Sasaki, M. Yokota and M. Matsushima, A study on corrosion of reinforcement in concrete subjected to combined effect of chloride attack and carbonation, in Japanese, Proceedings of Concrete Structure Scenarios, JSMS, Vol. 4, 2004, pp. 11-16, 2004.
- [18] R. Iijima, T. Kudo, and Y. Tamai, Effect of atmospheric temperature on corrosion rate of reinforcement in concrete, in Japanese, Proceedings of Concrete Structure Scenarios, JSMS, Vol. 8, pp. 299-304, 2009.

# **Chapter 5: COMPARISON OF REMAINING LIFE PREDICTION OF CONCRETE CORES USING CROSS-SECTION CUTTING-OFF GIRDER**

---

## **5.1 Introduction**

This chapter focused on verification of remaining life prediction results of concrete cores using cross-section cutting-off girders of an aged bridge, SK Bridge (approximately 70 years old in service). Under ordinary circumstances, concrete cores are extracted from some parts of the bridge to evaluate the performance of the concrete. The performance of the concrete based on concrete cores represents performance of the locations from which the cores are extracted [1][2]. Carbonation and chloride ion tests were conducted on concrete cores. In this case, remaining life prediction results of concrete cores represent the local evaluation results of the girders. In contrast, remaining life prediction based on cross-sections cutting-off girders represent the entire girders. Many studies of carbonation in RC bridges have been conducted. However, all of them used concrete cores to evaluate the performance of concrete through carbonation test. This study describes the first known application of carbonation testing to cross-section cutting-off girders of SK Bridge [3].

According to the results of investigation on two different specimens, concrete cores and cross-section cutting-off girders, the remaining life predictions were compared. Furthermore, it will make a verification how local evaluation results based on concrete cores tests can be used for the evaluation of the entire span based on cross-section cutting-off girders. The remaining life prediction on both concrete cores using cross-section cutting-off girders were examined from the results of carbonation and chloride ion tests.

Figure 5.1 shows the diagram of the verification of remaining life prediction results of two different specimens, concrete cores and cross-section cutting-off girders. There are four different comparisons in order to examine the relationship between concrete cores and cross-section cutting-off girders on the main girders of the SK Bridge.

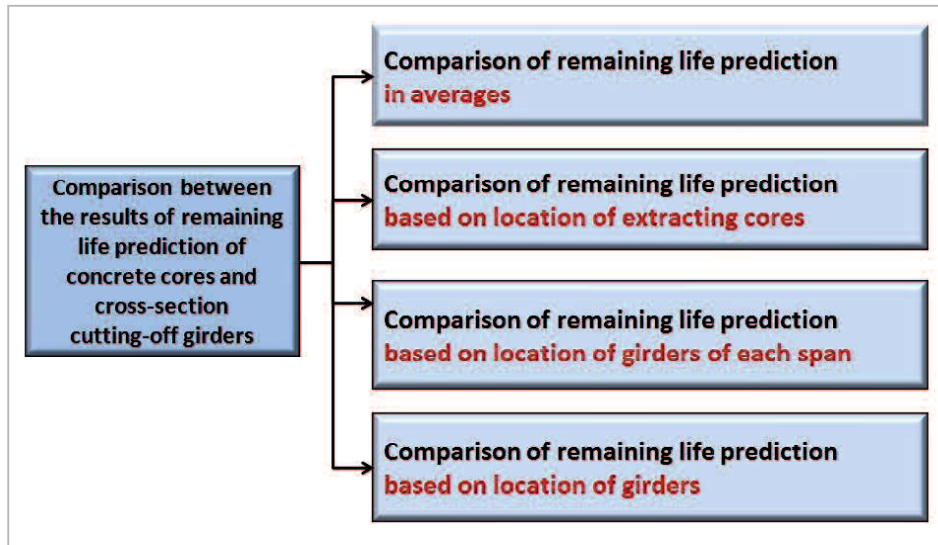


Fig. 5.1 Diagram of the verification of remaining life prediction results

## 5.2 Comparison between the results of remaining life prediction of concrete cores and cross-section cutting-off girders in average

Concrete cores were extracted from all of the girders in Spans 1 and 3 but only from the sea and mountain sides. On the bottom side, it was quite difficult to extract the concrete cores because of the reinforcing bars embedded in the bottoms of the girders.

According to Chapter 3, the concrete cores were extracted from Girder 1 to Girder 5 of Spans 1 and 3 which are the inspected girder spans. Concrete cores were examined for chloride ion content test called C-series that is identified as “C”. The numbers of C-series are 11 specimens for Span 1 and 12 specimens for Span 3. M-series were examined for carbonation test that is identified as “M”. The numbers of M-series are 15 specimens for Span 1 and 20 specimens for Span 3 as shown in Table 3.1 in Chapter 3.

Table 5.1 shows the results of the remaining life prediction due to the carbonation and chloride ion of the concrete cores in Spans 1 and 3. And the service life prediction based on the location of extracted concrete cores of Span 1 and Span 3 are shown in Figs. 5.2 and 5.3, respectively.

Table 5.1 Remaining life prediction due to the carbonation and chloride ion of the concrete cores in Spans 1 and 3

Span Number	Girder Number	Concrete cores	Sea side			Mountain side		
			Q = 10 mg/cm <sup>2</sup>	Q = 75 mg/cm <sup>2</sup>	Q = 10 mg/cm <sup>2</sup>	Q = 75 mg/cm <sup>2</sup>		
			Cracking limit (years)	Service life SL (years)	Remaining life R (years)	Cracking limit (years)	Service life SL (years)	Remaining life R (years)
Span 1	G1	C1014				24	42	-30
		C1111	60	87	15			
		C1115	29	49	-23			
	G2	C2113	42	55	-17			
		C3011				38	50	-22
	G3	C3015				19	30	-42
		C3114	29	38	-34			
	G4	C4113	24	41	-31			
		C5111	32	49	-23			
	G5	C5114	34	48	-24			
C5115		32	49	-23				
<b>Average (years)</b>			<b>35.3</b>	<b>52.0</b>	<b>-20.0</b>	<b>27.0</b>	<b>40.7</b>	<b>-31.3</b>
Span 3	G1	C1131	36	61	-11			
		C1134	38	73	1			
		C1138	61	89	17			
	G2	C2031				51	69	-3
		C2136	34	52	-20			
	G3	C3134	52	85	13			
		C3138	63	110	38			
	G4	C4031	35	74	2			
		C4136	62	114	42			
	G5	C5031				36	75	3
C5134					76	132	60	
		C5038	53	91	19			
<b>Average (years)</b>			<b>48.2</b>	<b>83.2</b>	<b>11.2</b>	<b>54.3</b>	<b>92.0</b>	<b>20.0</b>

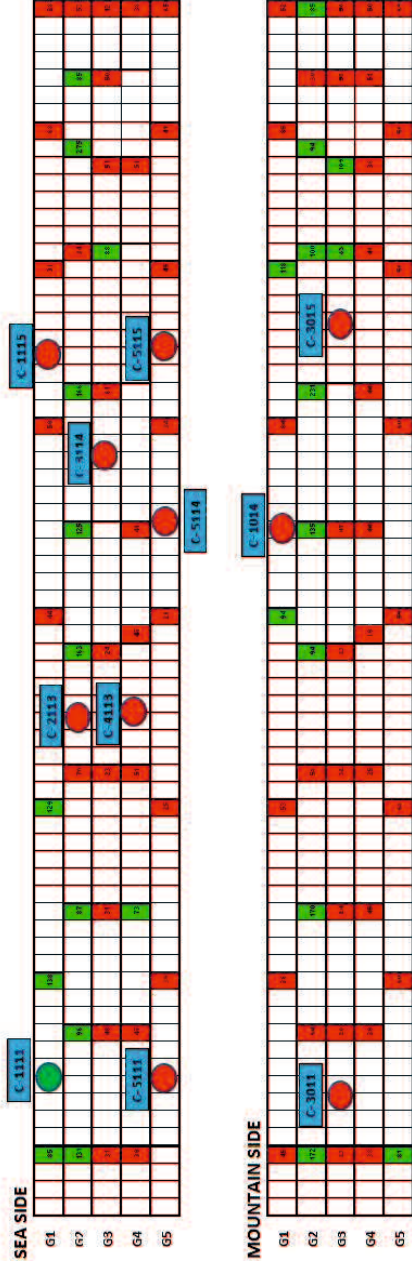


Fig. 5.2 Service life prediction of concrete cores of Span 1

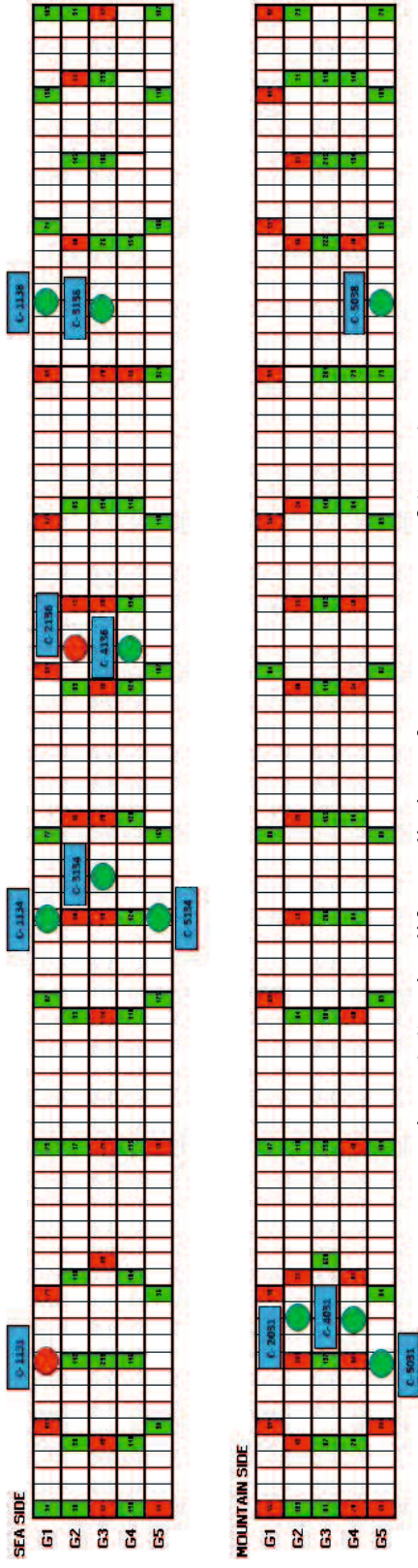


Fig. 5.3 Service life prediction of concrete cores of Span 3

The results of concrete cores in Span 1 show that the remaining life prediction were, on average, -20 years for the sea side and -31 years for the mountain side of the girders. Span 3 show that the remaining life predictions were, on average, 11 years on the sea side and 20 years on the mountain side of the girders.

In Figs. 5.2 and 5.3, differences in the service life prediction are indicated using different colors. The red color indicates the service life prediction less than 72 years (72 years is time of investigation), meaning that the bridge's life has ended before the time of investigation. The green color indicates the service life prediction of 72 years or more, meaning that the initial corrosion has not occurred on the reinforcing bars. Figure 5.2 shows that on Span 1, the red color is dominant on the sea side and mountain side. The service life prediction on the sea side and mountain side has 52 and 40 years. The remaining life has a negative value. Meaning that on the sea side and mountain side the bridge's life has ended before the time of investigation (72 years). On the other hand Fig. 5.3 shows that on Span 3, the green color is dominant on the sea side and mountain side. The service life prediction on the sea side and mountain side has 83 and 92 years. The remaining life has a positive value. Meaning that on the sea side and mountain side the bridge's life still remain several years before reach the end of bridge's life.

The comparison of remaining life prediction between concrete cores and cross-section cutting-off girders (taken from Fig. 4.35 in Chapter 4) is shown in Fig. 5.4. This figure shows that the remaining life prediction of Span 1 both of concrete cores and cross section cutting off girders has a negative value. Meaning the end of bridge's life was ended before the time of investigation (72 years) on both the sea side and mountain side. The remaining life prediction of Span 3 both of concrete cores and cross section cutting off girders has a positive value. Meaning that still remains a few years before meeting the end of bridge's life on both the sea side and mountain side. Fig. 5.5 shows the comparison of service life prediction between concrete cores and cross-section cutting-off girders. It can be explained more clearly that according to the time of investigation is equal with 72 years, the aged of Span 1 is less than 72 years and Span 3 is more than 72 years.

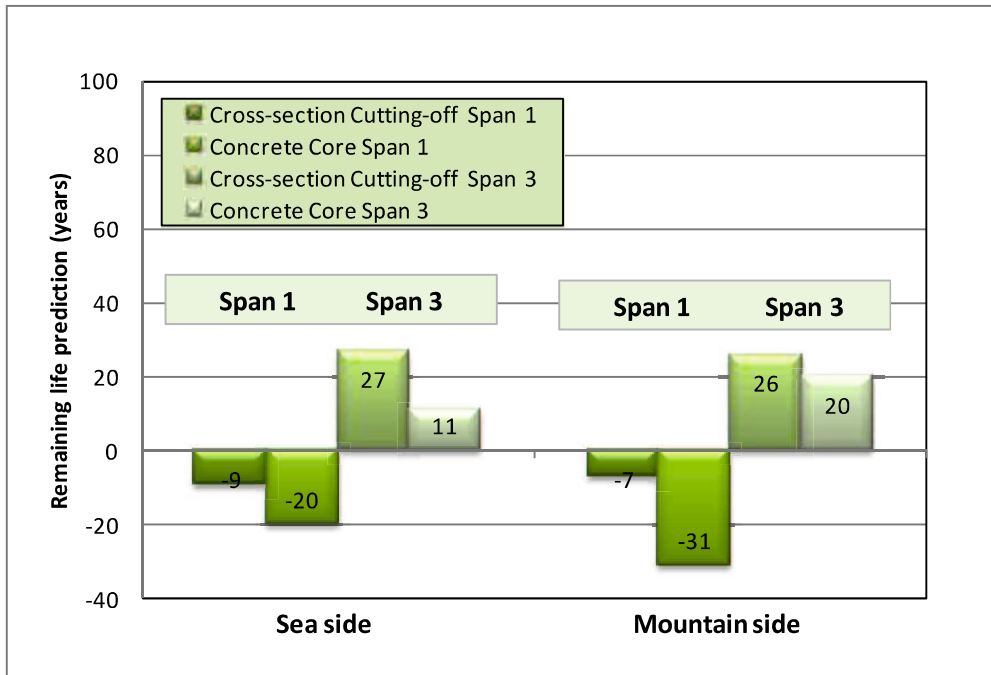


Fig. 5.4 Comparison of remaining life prediction results between concrete cores and cross-section cutting-off girders in both Spans 1 and 3 on average

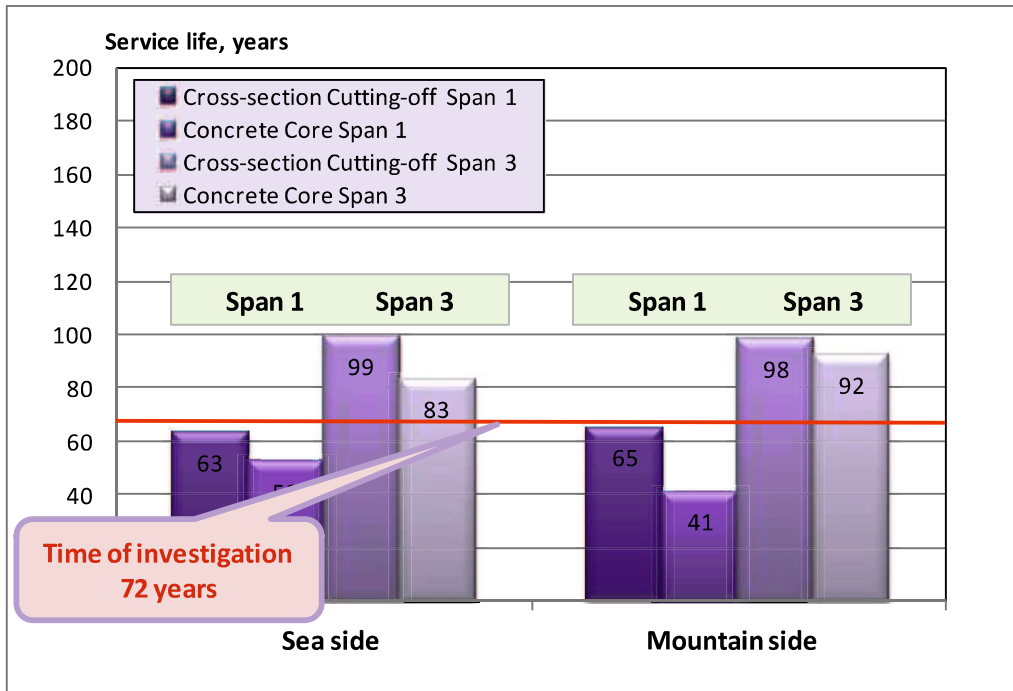


Fig. 5.5 Comparison of service life prediction results between concrete cores and cross-section cutting-off girders in both Spans 1 and 3 on average

### 5.3 Comparison between the results of remaining life prediction of concrete cores and cross-section cutting-off girders based on the location of extracting concrete cores

Concrete cores C-series were extracted from the girders of Spans 1 and 3. The numbers of C-series are 11 specimens for Span 1 and 12 specimens for Span 3. The results of remaining life prediction of concrete cores C-series were compared with the results of cross-section cutting-off girders based on the location of extracted concrete cores.

The remaining life prediction results of concrete cores will be compared to the results of cross-section cutting-off girders in order to verify the similarity between concrete cores and cross-section cutting-off girders. Correlation coefficient ( $r$ ) was used to calculate a relationship between two variables. The mathematical formula for computing  $r$  as follows:

$$r = \frac{\sum_{i=1}^n (x_i - \bar{x})(y_i - \bar{y})}{\sqrt{\sum_{i=1}^n (x_i - \bar{x})^2 \cdot (y_i - \bar{y})^2}} \quad (5.1)$$

The values of  $r$  is such that  $-1 < r < +1$ . The + and – signs are used for positive linear correlation and negative linear correlation, respectively. A correlation coefficient that is greater than 0.8 described as strong correlation, whereas a correlation coefficient that is less than 0.5 described as weak correlation.

Table 5.2 shows the remaining life prediction of concrete cores and cross-section cutting-off girders at 72 years. The correlation coefficient of the remaining life prediction was calculated using Eq. (5.1). According to the location of concrete cores that were extracted in Figs. 3.4 and 4.5, the comparisons of the remaining life prediction were calculated using averages values of remaining life prediction of cross-section cutting-off girders; Yamaguchi (right-side) and Hiroshima (left-side). The two sets of remaining life predictions were compared. The relationship between service life predictions from the concrete cores and those from the girder cross sections had correlation coefficients 0.62 and 0.59 for Spans 1 and 3, respectively, as shown in Tables 5.3 and 5.4. These correlation coefficients indicate a good correlation. The service life prediction based on tests on cores are considered to represent predictions based on local evaluation, whereas those based on tests on cross-section cutting-off girders are considered to represent the service life of the entire span of the bridge. It is also shown in Fig. 5.6.

Table 5.2 Remaining life prediction of concrete cores and cross-section cutting-off girders based on the location of extracted cores

Span Number	Girder Number	Concrete cores	Remaining life at 72 years		Cutting-off number		Location
			Concrete cores (years)	Cutting-off (years)	Hiroshima side	Yamaguchi side	
Span 1	G1	C1014	-30	0	H-16-Y	H-21-Y	Mountain
		C1111	15	39	H-1-Y	H-6-Y	Seaside
		C1115	-23	-27	H-21-Y	H-26-Y	Seaside
	G2	C2113	-17	44	H-18-Y	H-22-Y	Seaside
		C3011	-22	-51	H-3-Y	H-8-Y	Mountain
	G3	C3015	-42	-31	H-32-Y	H-36-Y	Mountain
		C3114	-34	-42	H-28-Y	H-32-Y	Seaside
	G4	C4113	-31	-26	H-20-Y	H-29-Y	Seaside
		C5111	-23	-53	H-5-Y	H-10-Y	Seaside
	G5	C5114	-24	-42	H-17-Y	H-25-Y	Seaside
C5115		-23	-33	H-25-Y	H-30-Y	Seaside	
Span 3	G1	C1131	-11	-12	H-50-Y	H-55-Y	Seaside
		C1134	1	10	H-65-Y	H-70-Y	Seaside
		C1138	17	-14	H-88-Y	H-93-Y	Seaside
	G2	C2031	-3	-21	H-56-Y	H-61-Y	Mountain
		C2136	-20	-5	H-84-Y	H-89-Y	Seaside
	G3	C3134	13	-44	H-77-Y	H-81-Y	Seaside
		C3138	38	1	H-99-Y	H-103-Y	Seaside
	G4	C4031	2	-36	H-58-Y	H-63-Y	Mountain
		C4136	42	55	H-86-Y	H-91-Y	Seaside
	G5	C5031	3	53	H-54-Y	H-59-Y	Mountain
C5038		60	50	H-92-Y	H-97-Y	Mountain	
		C5134	19	98	H-69-Y	H-74-Y	Seaside

Table 5.3 Correlation coefficient calculation of remaining life prediction in Span 1 based on the location of extracted cores

No	x	y	A x- x <sub>mean</sub>	B y-y <sub>mean</sub>	C (x-x <sub>mean</sub> ) <sup>2</sup>	D (y-y <sub>mean</sub> ) <sup>2</sup>	A*B
1	-30	0	-7.00	20.18	49.00	407.31	-141.27
2	15	39	38.00	59.18	1444.00	3502.49	2248.91
3	-23	-27	0.00	-6.82	0.00	46.49	0.00
4	-17	44	6.00	64.18	36.00	4119.31	385.09
5	-21	-51	2.00	-30.82	4.00	949.76	-61.64
6	-34	-31	-11.00	-10.82	121.00	117.03	119.00
7	-42	-42	-19.00	-21.82	361.00	476.03	414.55
8	-31	-26	-8.00	-5.82	64.00	33.85	46.55
9	-23	-53	0.00	-32.82	0.00	1077.03	0.00
10	-24	-42	-1.00	-21.82	1.00	476.03	21.82
11	-23	-33	0.00	-12.82	0.00	164.31	0.00
	<b>-23.00</b>	<b>-20.18</b>			<b>2080.00</b>	<b>11369.64</b>	<b>3033.00</b>

$$r = \frac{3033.00}{4863.007674}$$

$$r = 0.62$$

Table 5.4 Correlation coefficient calculation of remaining life prediction in Span 3 based on the location of extracted cores

No	x	y	A x- x <sub>mean</sub>	B y-y <sub>mean</sub>	C (x-x <sub>mean</sub> ) <sup>2</sup>	D (y-y <sub>mean</sub> ) <sup>2</sup>	A*B
1	-11	-12	-23.91	-15.36	571.64	236.04	367.33
2	1	10	-11.91	6.64	141.83	44.04	-79.03
3	17	-14	4.09	-17.36	16.74	301.50	-71.03
4	-3	-21	-15.91	-24.36	253.10	593.59	387.60
5	-20	-5	-32.91	-8.36	1083.01	69.95	275.24
6	13	-44	0.09	-47.36	0.01	2243.31	-4.31
7	38	1	25.09	-2.36	629.55	5.59	-59.31
8	2	-36	-10.91	-39.36	119.01	1549.50	429.42
9	42	55	29.09	51.64	846.28	2666.31	1502.15
10	3	53	-9.91	49.64	98.19	2463.77	-491.85
11	60	50	47.09	46.64	2217.55	2174.95	2196.15
12			-12.91	-3.36	166.64	11.31	43.42
	<b>12.91</b>	<b>3.36</b>			<b>6143.55</b>	<b>12359.86</b>	<b>4495.79</b>

$$r = \frac{4495.79}{8713.980768}$$

$$r = 0.59$$

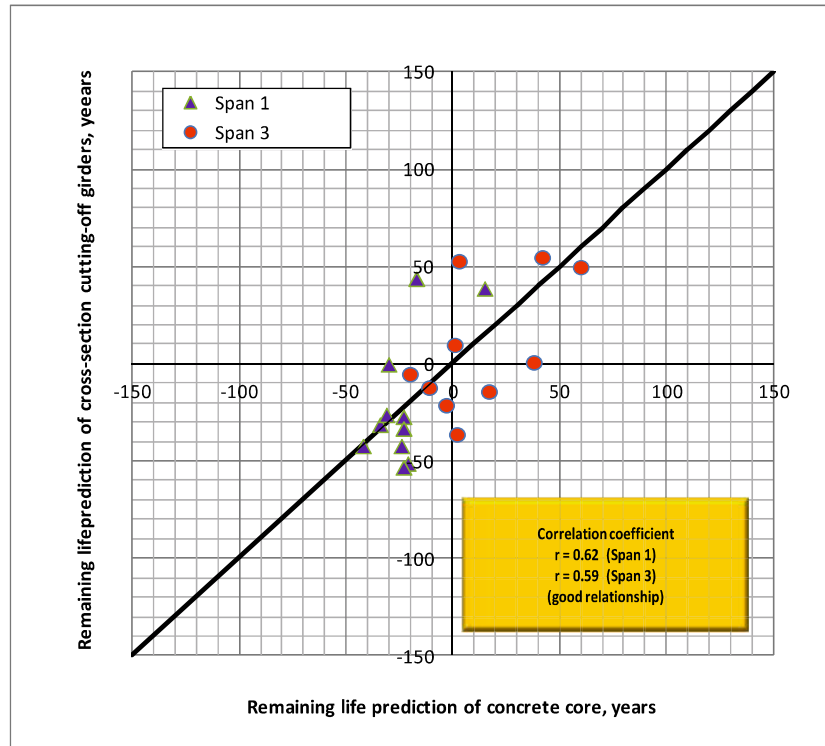


Fig 5.6 Relationship between remaining life prediction of concrete cores and cross-section cutting-off girders in Spans 1 and 3 based on the location of extracted cores

#### 5.4 Comparison between the results of remaining life prediction of concrete cores and cross-section cutting-off girders based on the location of girders of each span

The comparison of remaining life prediction of concrete cores and cross-section cutting-off girders based on the location of girders of each span was assumed that the numbers of cross-section cutting-off girders in one girder as an unified girder, as shown in Fig. 5.7. The calculation of remaining life prediction of concrete cores and cross-section cutting-of girders is shown in Table 5.5.

Figure 5.8 shows the relationship between service life predictions from the concrete cores and those from the girder cross sections had correlation coefficients 0.78 and 0.65 for Spans 1 and 3, respectively, as shown in Tables 5.6 and 5.7. These correlation coefficients indicate a good correlation. The service life prediction based on tests on cores are considered to represent predictions based on local evaluation, whereas those based on tests on cross-section cutting-off girders are considered to represent the service life of the entire span of the bridge.

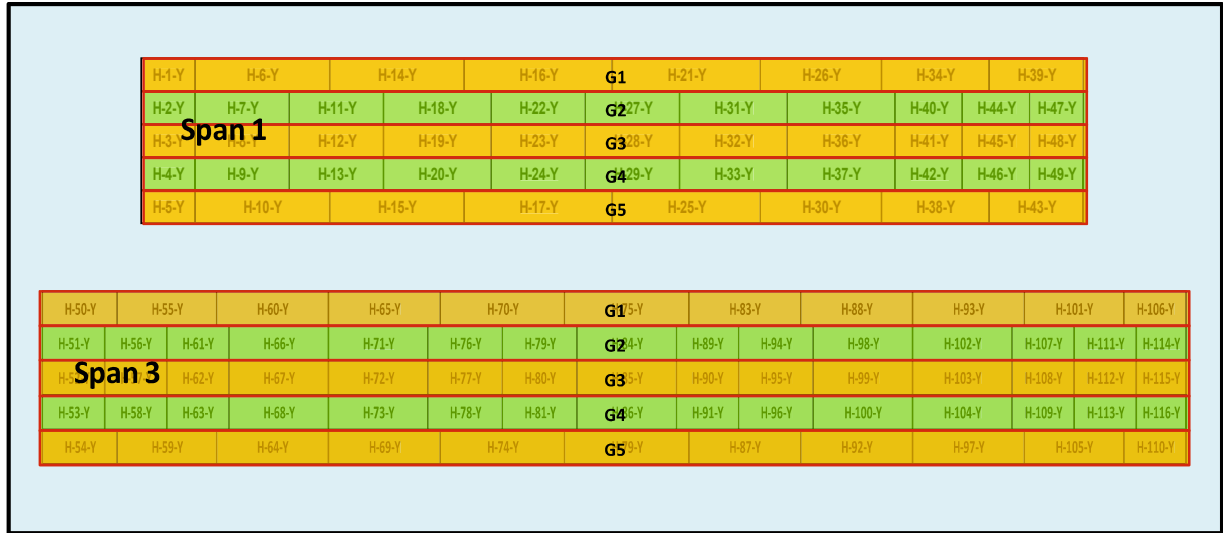


Figure 5.7 Cross-section cutting-off girders based on the location of girders of each span

Table 5.5 Remaining life prediction of concrete cores and cross-section cutting-off girders based on the location of girders of each span

Span Number	Girder Number	Sea side		Bottom side		Mountain side	
		Remaining life (years)		Remaining life (years)		Remaining life (years)	
		Concrete cores	Cross-section cutting-off girders	Concrete cores	Cross-section cutting-off girders	Concrete cores	Cross-section cutting-off girders
<b>Span 1</b>	G1	-4	0	-	145	-30	-8
	G2	-17	44	-	63	-	40
	G3	-34	-31	-	16	-32	-25
	G4	-31	-24	-	-4	-	-34
	G5	-23	-33	-	24	-	-9
<b>Span 3</b>	G1	3	3	-	75	-	-16
	G2	-20	12	-	178	-3	-14
	G3	25	71	-	159	-	148
	G4	22	51	-	45	-	0
	G5	19	61	-	58	20	11

Table 5.6 Correlation coefficient calculation of remaining life prediction in Span 1 based on the location of girders of each span

No	x	y	A x- x <sub>mean</sub>	B y-y <sub>mean</sub>	C (x-x <sub>mean</sub> ) <sup>2</sup>	D (y-y <sub>mean</sub> ) <sup>2</sup>	A*B
1	-4	0	20.43	11.00	417.33	121.00	224.71
2	-17	44	7.43	55.00	55.18	3025.00	408.57
3	-34	-31	-9.57	-20.00	91.61	400.00	191.43
4	-31	-24	-6.57	-13.00	43.18	169.00	85.43
5	-23	-33	1.43	-22.00	2.04	484.00	-31.43
6	-30	-8	-5.57	3.00	31.04	9.00	-16.71
7	-32	-25	-7.57	-14.00	57.33	196.00	106.00
	<b>-24.43</b>	<b>-11.00</b>			<b>697.71</b>	<b>4404.00</b>	<b>968.00</b>

$$r = \frac{968.00}{1752.92148}$$

$$r = 0.78$$

Table 5.7 Correlation coefficient calculation of remaining life prediction in Span 3 based on the location of girders of each span

No	x	y	A x- x <sub>mean</sub>	B y-y <sub>mean</sub>	C (x-x <sub>mean</sub> ) <sup>2</sup>	D (y-y <sub>mean</sub> ) <sup>2</sup>	A*B
1	3	3	-6.43	-15.71	41.33	246.94	101.02
2	-20	12	-29.43	-6.71	866.04	45.08	197.59
3	25	7	15.57	-11.71	242.47	137.22	-182.41
4	22	51	12.57	32.29	158.04	1042.37	405.88
5	19	61	9.57	42.29	91.61	1788.08	404.73
6	-3	-14	-12.43	-32.71	154.47	1070.22	406.59
7	20	11	10.57	-7.71	111.76	59.51	-81.55
	<b>9.43</b>	<b>18.71</b>			<b>1665.71</b>	<b>4389.43</b>	<b>1251.86</b>

$$r = \frac{1251.86}{2703.984815}$$

$$r = 0.65$$

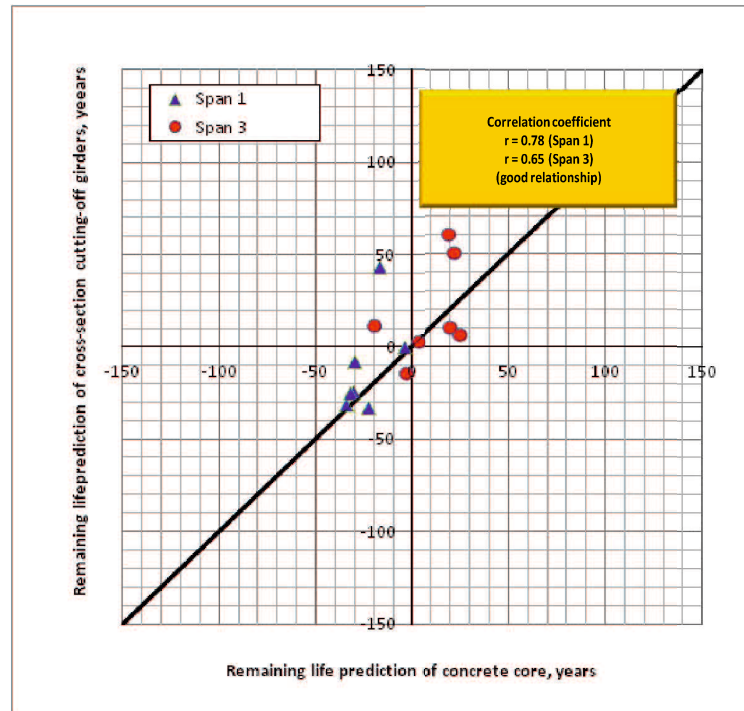


Fig. 5.8 Relationship between remaining life prediction of concrete cores and cross-section cutting-off girders in Spans 1 and 3 based on the location of girders of each span

In the target bridge, each span has five girders. Based on the position of the girders, G1 and G5 were the outer girders, G2, G3 and G4 were the inner girders. Carbonation and chloride ion attack tend to affect the outer girders more severe than the inner girders. The outer girders faced the environmental attack directly, whereas the inner girders were sheltered because it was located in the middle of the span.

Figure 5.9 shows a comparison between distribution of service life prediction of G1 to G5 in Span 1 and Span 3. It will be more obvious when referred to the normal distribution of service life prediction of Span 1 and Span 3 as shown in Figs. 5.10 to 5.15. From these figures, it can be found that the service life prediction of each location of each girder in both Span 1 and Span 3 varies greatly. However, these figures could not make a clear description of the influence of the location of girders on the end of life of the bridge.

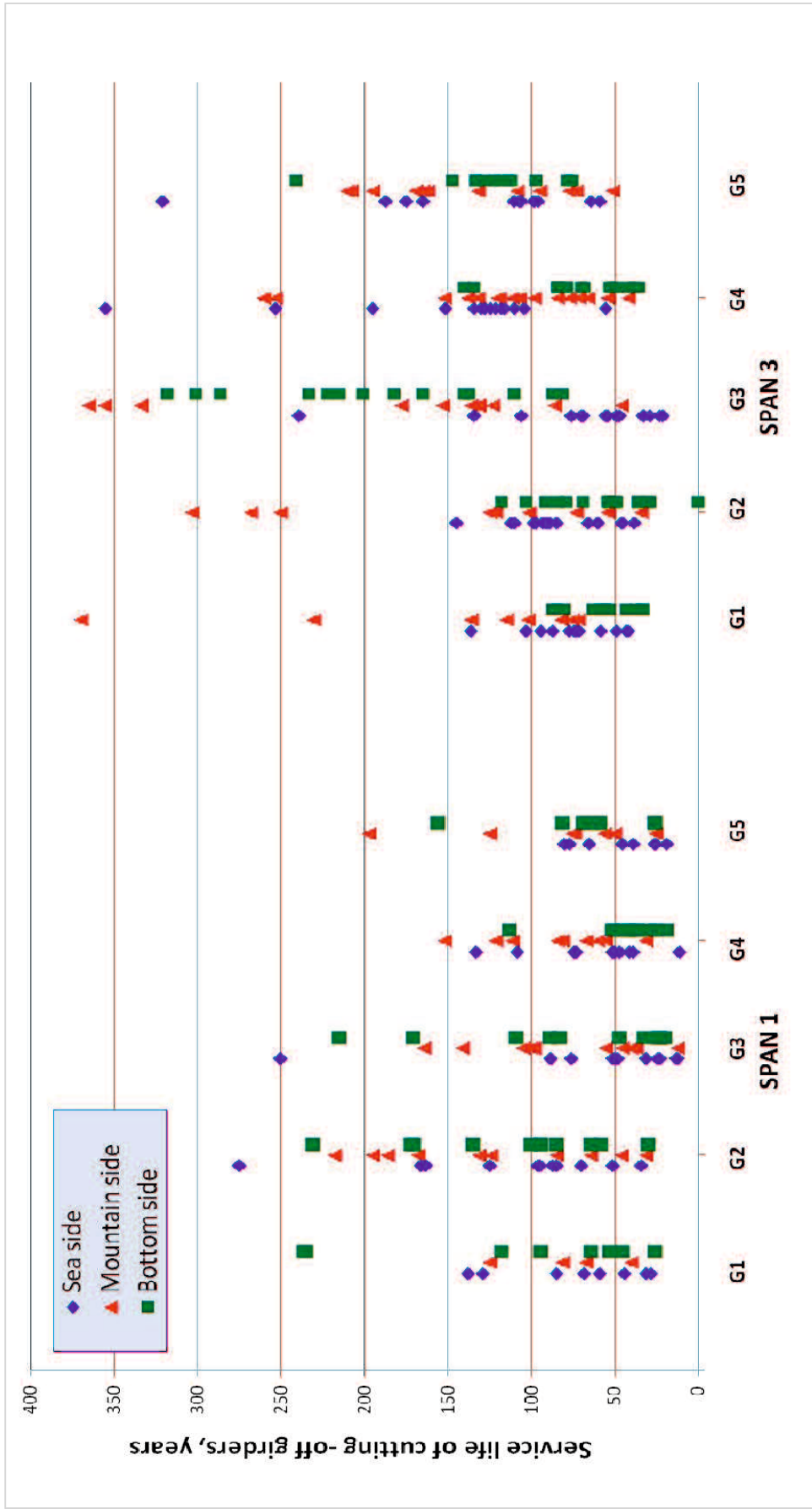


Figure 5.9 Comparison between distribution of service life prediction of cross-section cutting-off girders in Span 1 and Span 3 based on the location of girders of each span

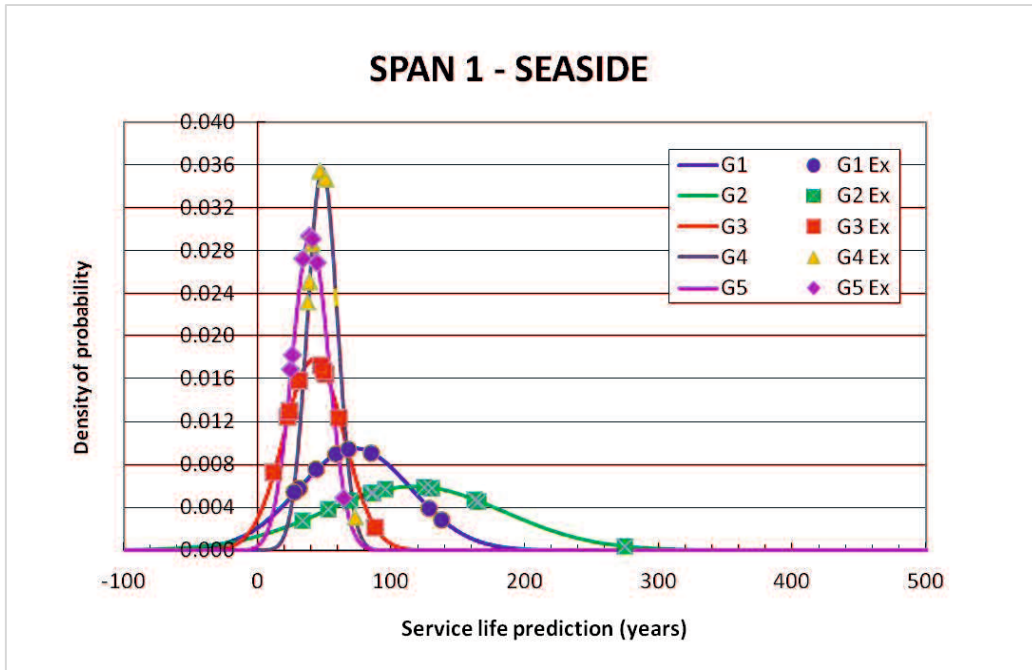


Figure 5.10 Normal distribution of service life prediction in Span 1 sea side

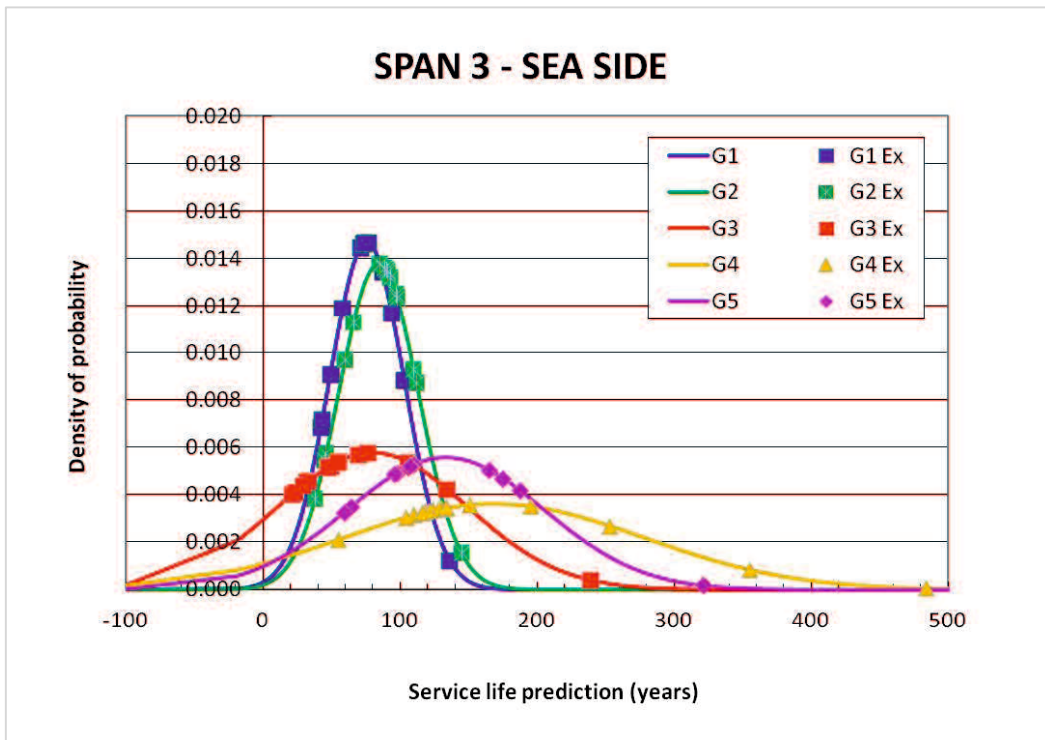


Figure 5.11 Normal distribution of service life prediction in Span 3 sea side

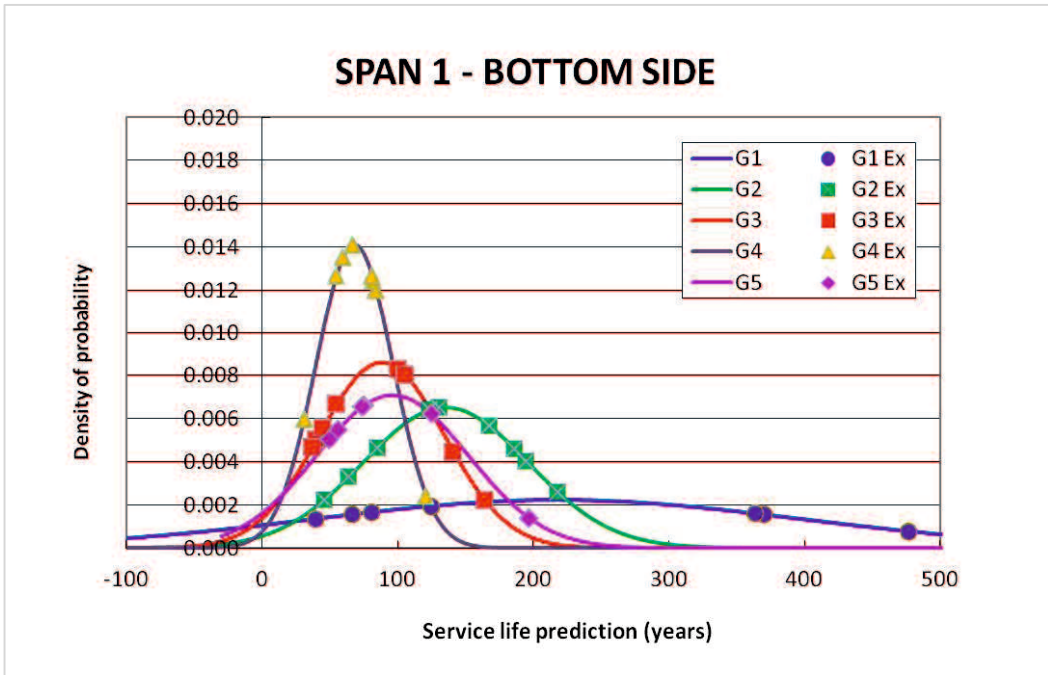


Figure 5.12 Normal distribution of service life prediction in Span 1 bottom side

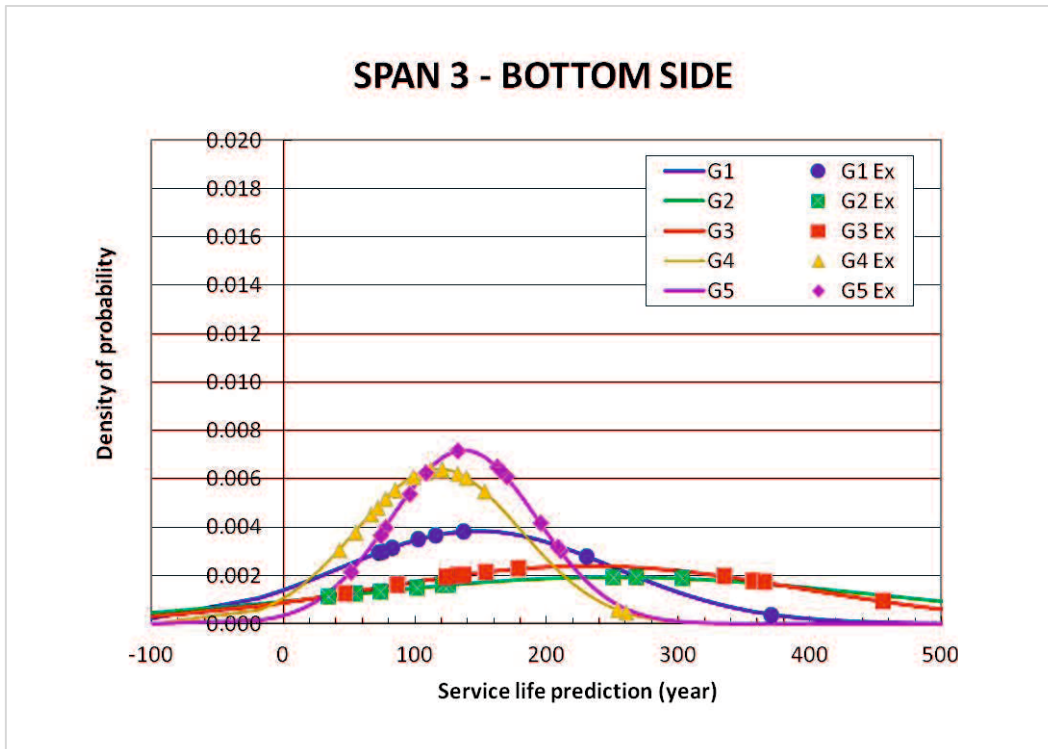


Figure 5.13 Normal distribution of service life prediction in Span 3 bottom side

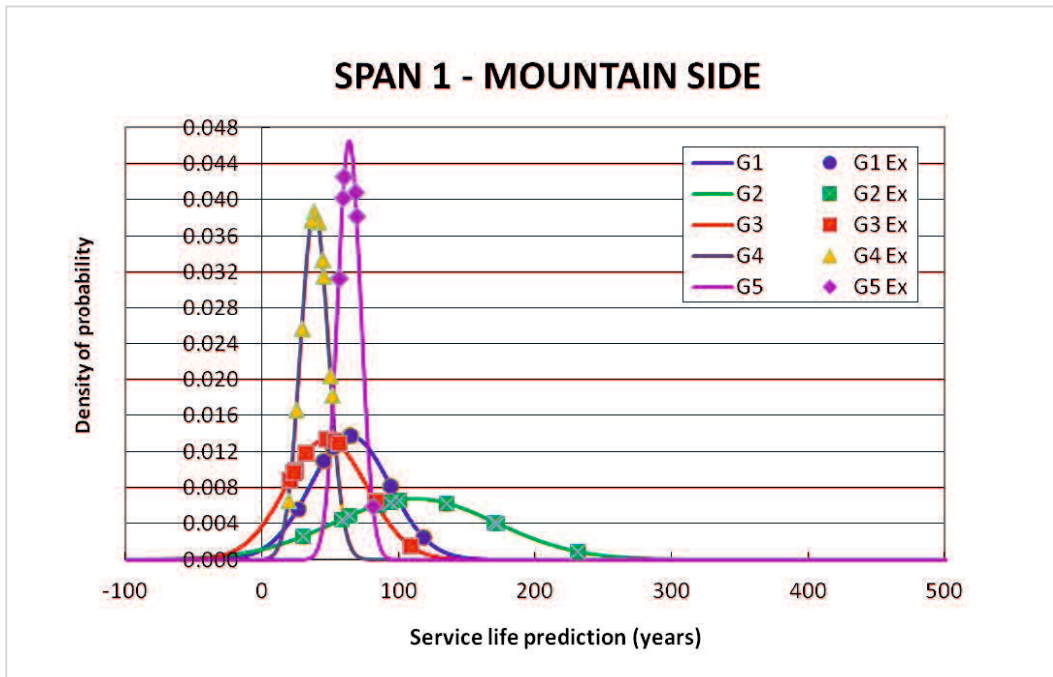


Figure 5.14 Normal distribution of service life prediction in Span 1 mountain side

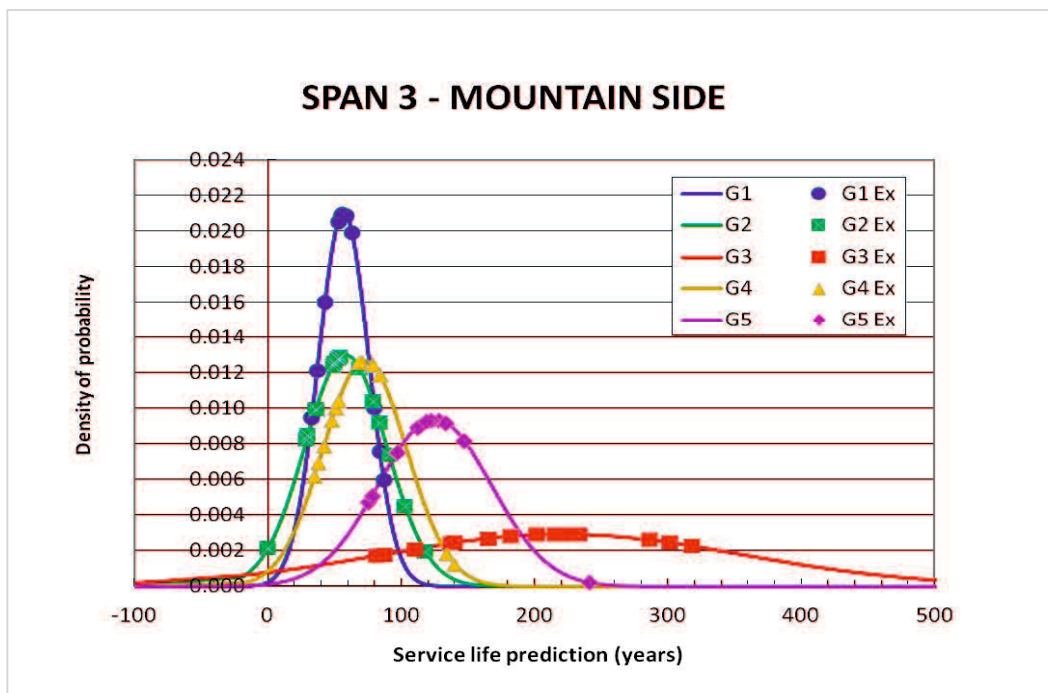


Figure 5.15 Normal distribution of service life prediction in Span 3 mountain side

Figure 5.16 shows the comparison of remaining life prediction of the unified girders both on Span 1 and Span 3. From the Fig. 5.16, it can be noticed that the environmental condition such as carbonation and chloride ion attack tend to affect the outer girders more severe than the inner girders. The outer girders faced the environmental attack directly, whereas the inner girders were sheltered because it was located in the middle of the span.

From the results of remaining life prediction it can be concluded that in the SK Bridge the outer girders had a shorten age compared the inner girders because the outer girders faced the environmental attack directly.

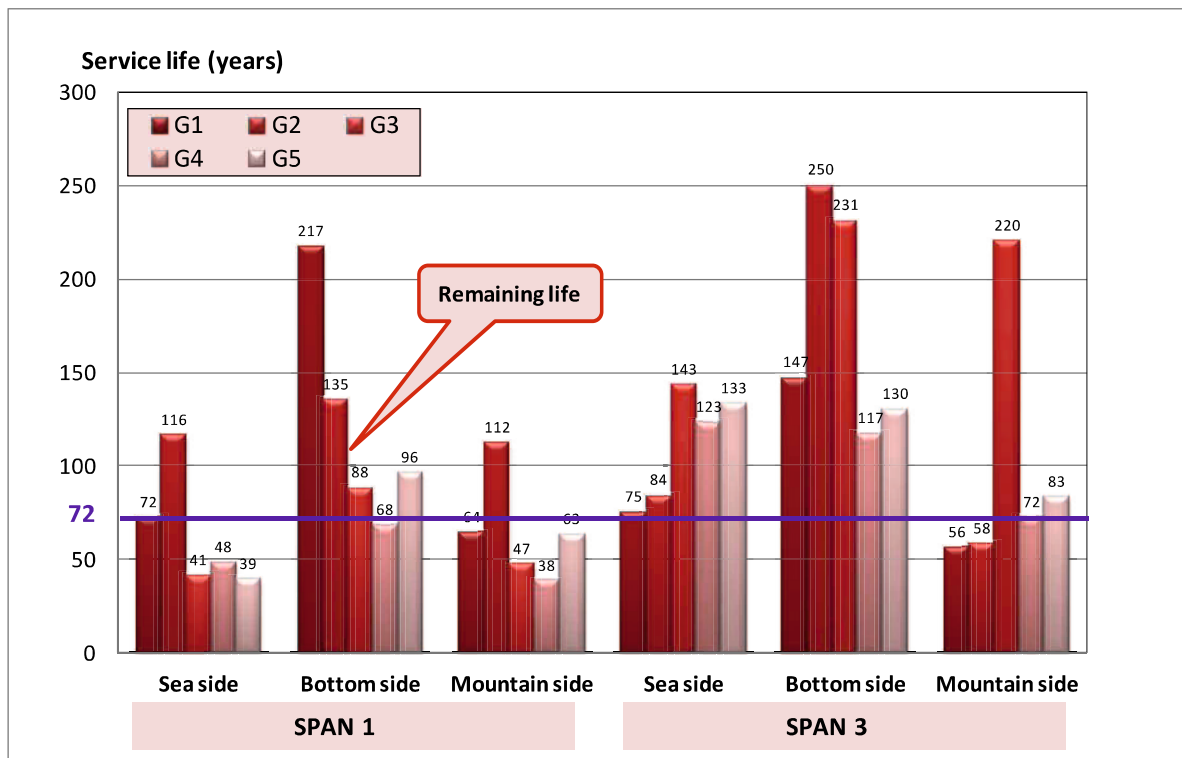


Figure 5.16 Comparison of remaining life prediction of cross-section cutting-off girders in Span 1 and Span 3 based on the location of girders of each span

### 5.5 Comparison between the results of remaining life prediction of concrete cores and cross-section cutting-off girders based on the location of girders

The remaining life prediction of cross-section cutting-off girders based on the location of girders was assumed that each girder (G1 to G5) of Span 1 and Span 3 will be considered as full girders as shown in Fig. 5.17. The calculation of remaining life prediction of cross-section cutting-off girders is shown in Table 5.8.

Figure 5.18 shows distribution of service life prediction of G1 to G5 in the full girders. It will be more obvious when referred to the normal distribution of service life prediction of Span 1 and Span 3 as shown in Figs. 5.19 to 5.21. From these figures, it can be found that the service life prediction of each location of each girder varies greatly.

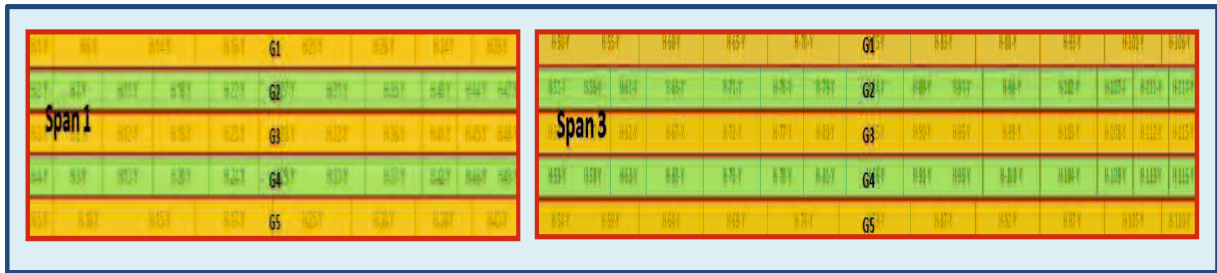


Figure 5.17 Merged girders of spans 1 and 3 based on the location of girders

Table 5.8 Remaining life prediction of the merged girders of spans 1 and 3 based on the location of girders

Girder Number	Span Number	Sea side		Bottom side		Mountain side	
		Remaining life (years)		Remaining life (years)		Remaining life (years)	
		Cross-section cutting-off girders	Average	Cross-section cutting-off girders	Average	Cross-section cutting-off girders	Average
G1	Span 1	0	2	217	182	-8	-12
	Span 3	3		147		-16	
G2	Span 1	44	28	135	193	40	13
	Span 3	12		250		-14	
G3	Span 1	-31	-12	88	160	-25	62
	Span 3	7		231		148	
G4	Span 1	-24	14	68	93	-34	-17
	Span 3	51		117		0	
G5	Span 1	-33	14	96	113	-9	1
	Span 3	61		130		11	

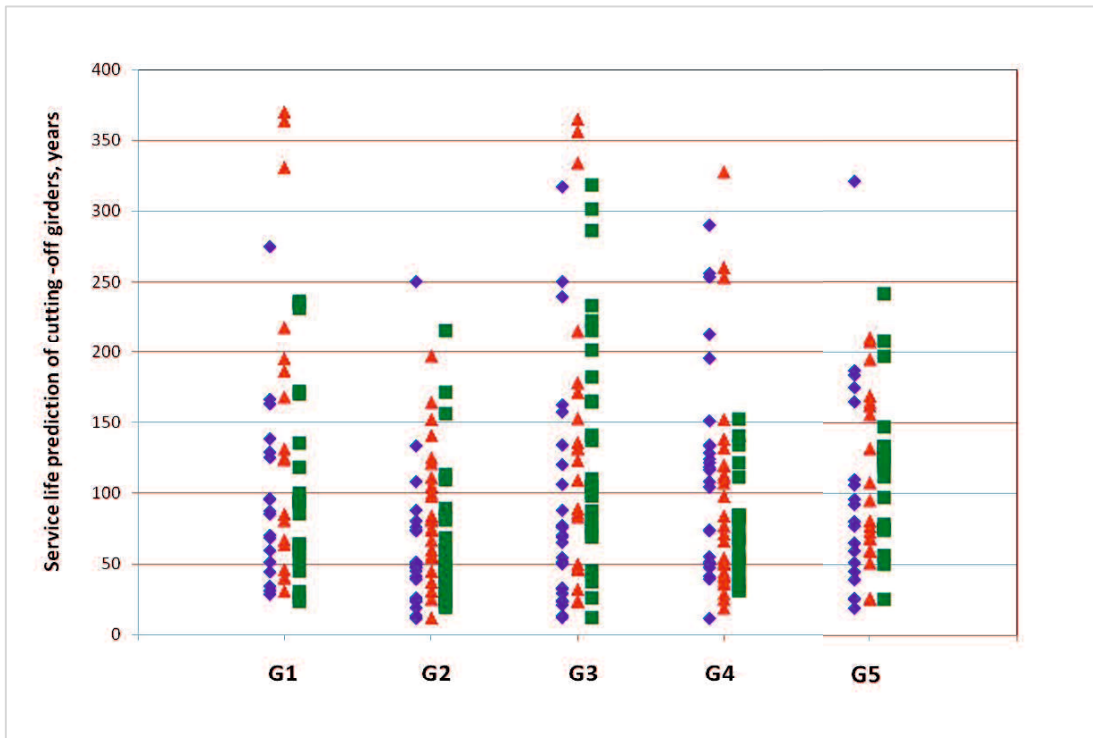


Figure 5.18 Service life distributions of the merged girders of spans 1 and 3

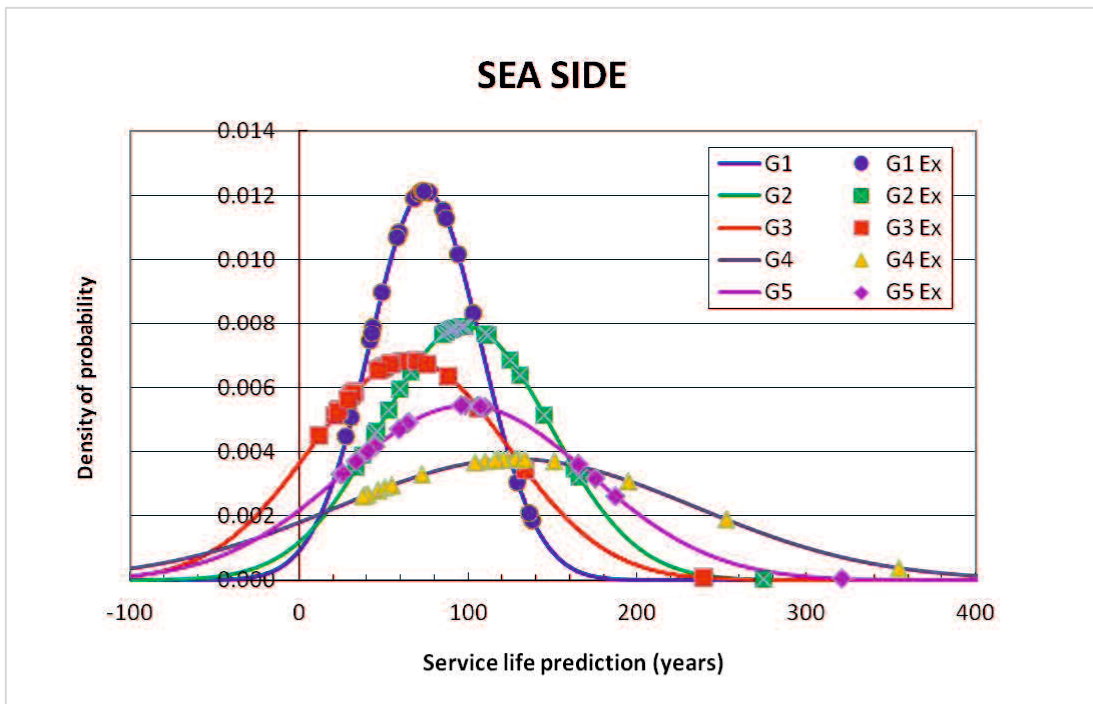


Figure 5.19 Normal distribution of service life prediction of spans 1 and 3 sea side

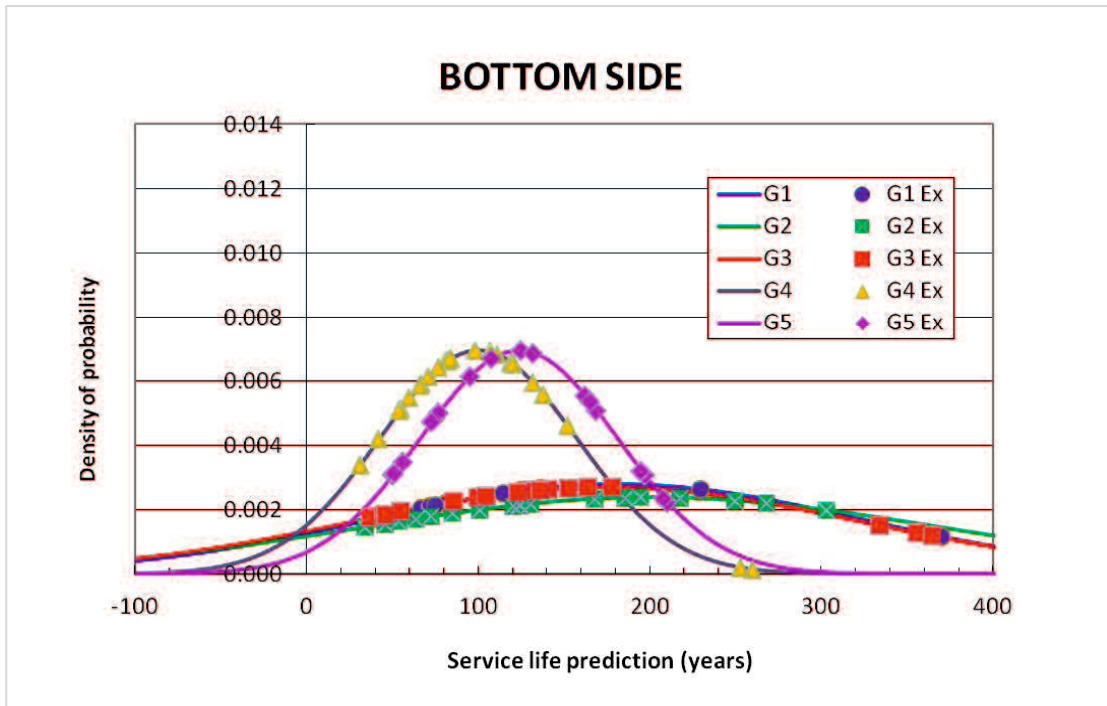


Figure 5.20 Normal distribution of service life prediction of Spans 1 and 3 bottom side

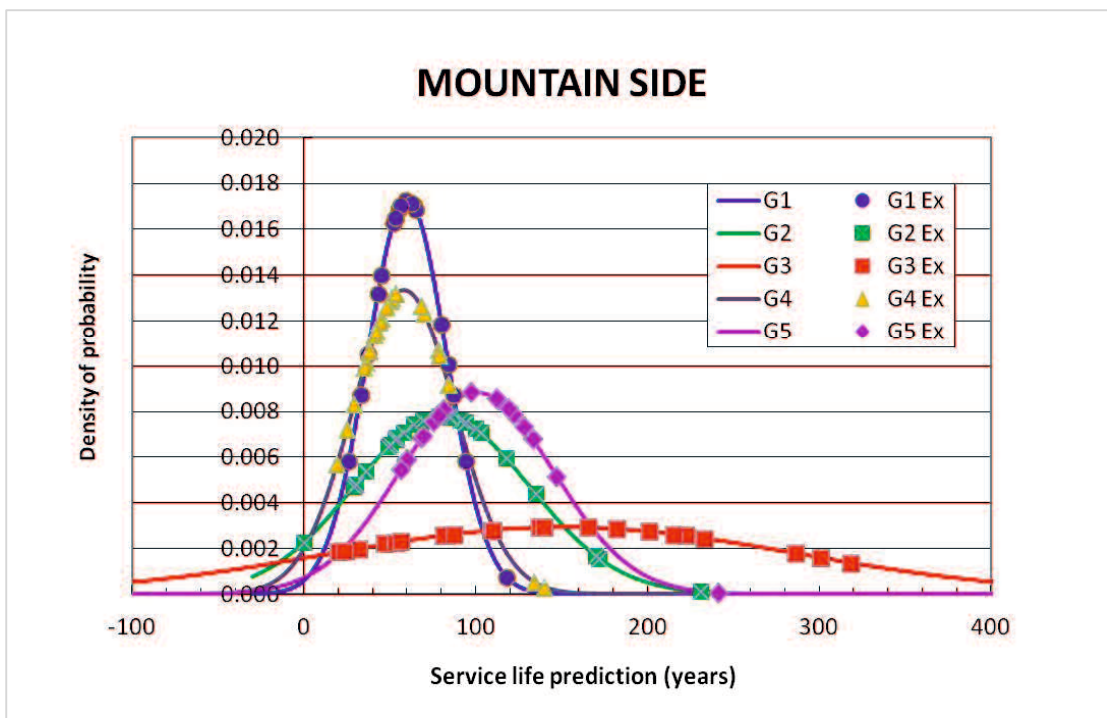


Figure 5.21 Normal distribution of service life prediction of Spans 1 and 3 mountain side

Figure 5.22 shows the comparison of remaining life prediction of the merged girders of Spans 1 and 3. In this figure, the remaining life prediction on the bottom side, especially in G1, G2 and G3 reminds quite a long time before it reached the end of the bridge's life. It is due to the repair work on the bottom side of Span 3. On the other hand, the remaining life of G1 and G4 on the mountain side, have already reached the end of life before the investigation time. Meaning the aged of G1 and G4 are less than 72 years.

Unfortunately the influences of environmental conditions, such as carbonation and chloride ion attack tend to affect the outer girders more severe than the inner girders, however, this could not be confirmed clearly.

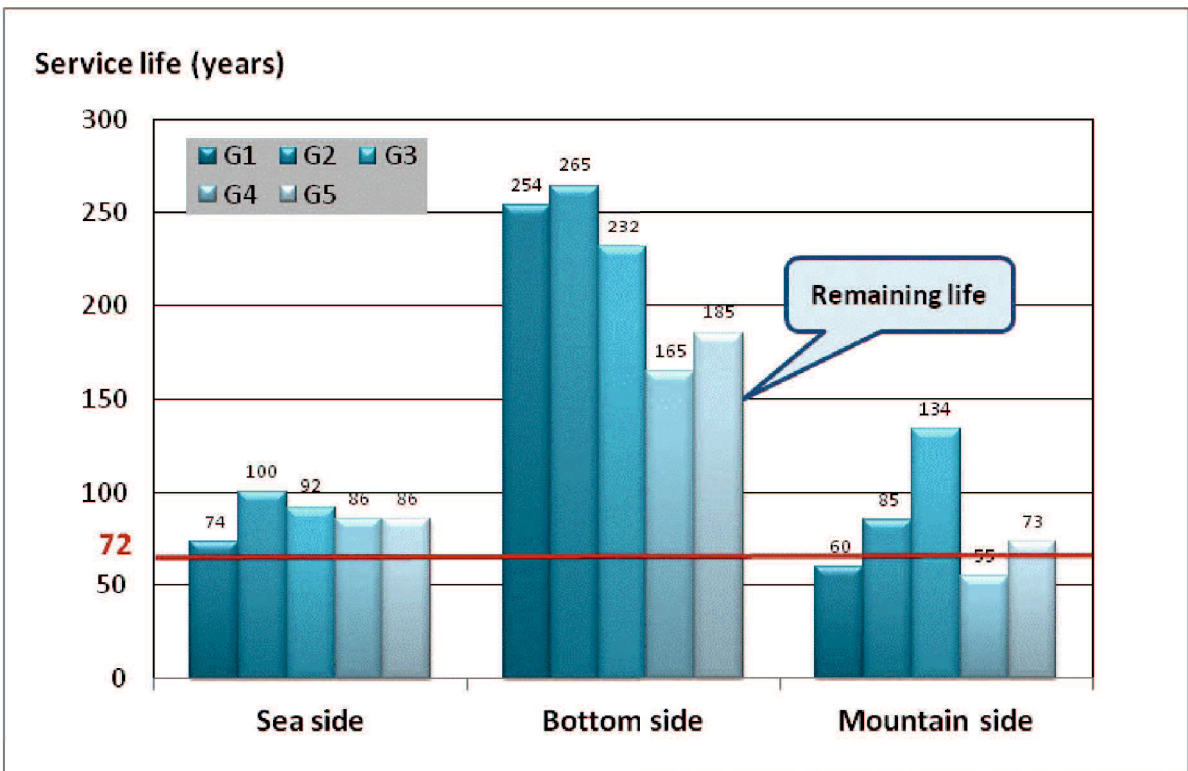


Figure 5.22 Comparison of remaining life prediction of merged girders of Span 1 and Span 3 based on the location of girders

## 5.6 Conclusions

This chapter presents the comparison of remaining life and service life prediction as the results of carbonation tests of concrete cores and cross-section cutting-off girders of an aged RC bridge. Also, in addition the influence of the girders position is elaborated.

1. The remaining life prediction which was obtained based on the concrete cores were similar to those obtained based on the cross-section cutting-off girders, which represent the entire span of the bridge. The relationship between the thickness of concrete cover and service life prediction tends to have a good correlation.
2. Carbonation and chloride ion attack tend to affect the outer girders more severe than the inner girders. The outer girders faced the environmental attack directly, whereas the inner girders were sheltered because it was located in the middle of the span. From the results of service life prediction it can be concluded that in the SK Bridge the outer girders had a shorten service life prediction more so than the inner girders because the outer girders faced the environmental attack directly.

## 5.7 References

- [1] J. Takahashi, R. Widyawati, H. Emoto and A. Miyamoto, Remaining life prediction of an aged bridge based on concrete core test, in Japanese, Proceedings of the Japan Concrete Institute, Vol. 36, No. 2, pp. 1339-1344, 2014.
- [2] R. Widyawati, J. Takahashi, H. Emoto, and A. Miyamoto, Remaining life prediction of an aged bridge based on concrete core test, 2<sup>nd</sup> International Conference on Sustainable Civil Engineering Structures and Construction Materials, SCESCM, Yogyakarta, Sept 23-25, pp. 1-10, 2014.
- [3] R. Widyawati, A. Miyamoto, H. Emoto, and J. Takahashi, Service life prediction of an aged bridge based on carbonation test of cross-section cutting-off girders, Journal of The Society of Materials Science, Japan, Vol., No. 5, 2015.

# Chapter 6: CONCLUSIONS

---

## 6.1 Conclusions

The main objectives of this thesis as outlined in Chapter 1 are satisfied as follows:

1. Develop a method for estimating the remaining life prediction of an aged bridge through the chloride ion and carbonation tests on concrete cores and cross-section cutting-off girders.
2. Determine the main deterioration factor of an aged bridge, whether due to chloride attack or carbonation, through the chloride ion and carbonation tests on concrete cores and cross-section cutting-off girders.
3. Estimate the remaining life and service life prediction from concrete cores and cross-section cutting-off girder. The service life prediction is restricted by a criterion value i.e. cumulative amount of steel corrosion  $Q = 75 \text{ mg/cm}^2$ , which is obtain by the BREX system.
4. Verify the remaining life prediction results of the concrete cores together with cross-section cutting-off girders.

The main conclusions obtained in this thesis can be summarized as follows:

1. This thesis introduces the details of how to predict the remaining life of an aged RC-T girder bridge based on carbonation test which is one of the field tests required to determine the performance of concrete which is affected by an environmental condition, i.e. carbon dioxide. Also, to try to establish the method to predict the remaining life based on the chloride ion and carbonation tests results of concrete core and cross-section cutting-off girders.
2. The results of the carbonation tests showed that the main factor in the deterioration of the bridge has been carbonation associated with corrosion of the reinforcing bars. However, because the bridge is located less than 1 km upstream from the mouth of the river it spans, which flows into the sea, chloride ion attack should be considered as another factor in the bridge's deterioration.

3. The remaining life is affected by the cumulative amount of steel corrosion (Q), which is used as an end of life indicator. The remaining life prediction is restricted by a cumulative amount of steel corrosion of  $Q = 75 \text{ mg/cm}^2$  (based on the BREX system) as an end of life indicator showed that the remaining life results of the bridge are predicted as follows:

- The remaining life of concrete cores approximately 7 years (service life = 7 years + 72 years = 79 years).
- The remaining life of cross-section cutting-off girders approximately 9 years (service life = 8 years + 72 years = 81 years) for sea side and mountain side.
- The remaining life of cross-section cutting-off girders approximately 75 years (service life = 75 years + 72 years = 147 years) for bottom side.

The predicted remaining life for the bottom side was longer than for the other side because of repair work that has been done on the bottom side.

4. The extent of carbonation is typically assessed by examining concrete cores. In this study, however, it was possible to conduct carbonation test on cross-section cutting-off girders of an existing bridge. The carbonation tests yielded a considerable amount of information, but the results exhibited vary greatly. Therefore, the results of the remaining life prediction of concrete cores were verified by the results of cross-section cutting-off girders. The remaining life prediction obtained based on of concrete cores was similar to those obtained based on cross-section cutting-off girders, which represent the entire span of the bridge.

## 6.2 Future work

This thesis introduces the details of how to predict the remaining life of an aged RC-T girder bridge based on carbonation test, and try to establish the method to predict the remaining life based on the chloride ion and carbonation tests results from the concrete cores and cross-section cutting-off girders by using the averages results. There are still several problems that should be considered. A few suggestions as to the future work can be given as follows:

1. The results of carbonation depth measurement in an actual bridge exhibited vary greatly. To estimate the remaining life prediction in this thesis using averages results of carbonation depth. Further consideration on using the statistical approaches to examine the results of carbonation depth in order to estimate the remaining life.
2. The correlation of remaining life prediction between concrete cores which represent the local evaluation and cross-sections cutting-off girders which represent the entire span of the bridge were not clearly define. In future work, using statistical evaluations in the correlation between concrete cores and cross-section cutting-off girders are expected to derive more accurate results.
3. This research is the part of SK Bridge research, and in this dissertation, the discussion only concentrated to establish the method to estimate the remaining life prediction from the material point of view, such as chloride ion and carbonation investigation. However there is also a data on axial compressive strength which was obtained from the concrete cores. Further consideration to discuss the remaining life prediction from the mechanical/structural point of view.

# **APPENDIX: TEST MANUAL**

## **CARBONATION TEST FOR CROSS SECTION CUTTING-OFF GIRDERS**

**How to prepare, measure, collect and  
analysis**

**July 2014**

**By RATNA WIDYAWATI**

# CONTENTS

---

## ABSTRACT

1. INTRODUCTION .....	A1
2. CARBONATION IN CONCRETE .....	A2
3. TARGET BRIDGE .....	A5
4. CUTTING-OFF GIRDERS, CUT-OFF AND EXAMINATIONS .....	A6
4.1 Cross-section cutting-off girders .....	A6
4.2 The process of cutting-off the girders .....	A8
4.3 Cross-section cutting-off girder examination .....	A9
4.3.1 Carbonation test.....	A9
4.3.2 Measurement of the thickness of concrete covers .....	A9
4.3.3 Measurement of carbonation depth .....	A10
4.3.4 Measurement of the remaining concrete covers .....	A11
4.3.5 Phenolphthalein solution .....	A12
4.3.6 Carbonation test equipment.....	A13
4.3.7 Safety equipment .....	A13
4.3.8 Flow of experiment .....	A14
5. DATA COLLECTION AND ANALYSIS DATA .....	A18
5.1 Data collection .....	A18
5.1.1 The thickness of concrete cover data .....	A18
5.1.2 The carbonation depth data .....	A18
5.1.3 Inputting data.....	A19
5.2 Plotting data .....	A21
5.3 Analysis data .....	A23
5.3.1 Calculating the average and maximum value of carbonation depth.....	A23
5.3.2 Calculating the coefficient of carbonation rate .....	A24
5.3.3 Calculating the average and maximum value of concrete covers .....	A24
5.3.4 Calculating the remaining of concrete covers .....	A25
6. CONCLUSION REMARKS .....	A27
REFERENCES .....	A28

# ABSTRACT

---

In Japan, a large number of bridges have become aged which results in a necessity for maintenance as well as the decision on whether or not to demolish the bridges. The existing bridge is generally exposed to various environmental conditions such as the influence of carbon dioxide, chloride, acid, alkali, and so on during their period of service life. Therefore, the deterioration possibility occurs and it will have a significant effect on the remaining life of the bridge. In RC concrete bridge, the most serious deterioration mechanisms are due to corrosion. Corrosion is influenced by various factor, however, the most common corrosion is a result of carbonation or chloride attack or combination of both factors. There was a good opportunity to conduct an investigation in an actual bridge. An aged RC bridge was demolished and used to acquire the useful information from the cross-section cutting-off girders. This manual aims to investigate the carbonation depth of cutting-off girders of an actual bridge. The carbonation depth results will be used to predict the remaining life of the target bridge.

**Keywords:** Carbonation, remaining life, an aged RC bridge, cross-section cutting-off girder

# 1. INTRODUCTION

---

Nowadays, a large number of bridges in Japan have become aged which results in a necessity for maintenance as well as the decision on whether or not to demolish the bridges. Therefore, there is a need to predict the remaining life of the bridge in order to assist in determining the decision. In ordinary circumstances, the concrete core is extracted from some parts of the bridge in order to evaluate the performance of the bridge (Takahashi et al. 2014) . However, in this research, there was a good opportunity to conduct an investigation in an actual bridge. An aged RC bridge was demolished and used to acquire the useful information from the cross-section cutting-off girders.

The existing bridge is generally exposed to various environmental conditions such as the influence of carbon dioxide, chloride, acid, alkali, and so on during their period of service life. Therefore, the deterioration possibility occurs and it will have a significant effect on the remaining life of the bridge. In RC concrete bridge, the most serious deterioration mechanisms are due to corrosion. Corrosion is influenced by various factor, however, the most common corrosion is a result of carbonation or chloride attack or combination of both factors.

In this investigation, the target bridge (see Figure A1) had been constructed on the main route of the National Highway. The high volume of traffic that passed in this route leads a high level of carbon dioxide on the environment. Therefore, the carbonation is expected as the main deterioration factor in the target bridge.

This manual aims to investigate the carbonation depth of cutting-off girders of an actual bridge. The details of carbonation test are explained in this manual, including removal and cutting girders activities, preparing the cutting-off girders for carbonation test, collecting data and data analysis of the carbonation depth result. The carbonation depth results will be used to predict the remaining life of the target bridge.



Figure A1. General view of the SK Bridge

## 2. CARBONATION IN CONCRETE

---

Carbonation in structures means the carbonation reaction of carbon dioxide and cement hydrate as result of the penetration of the carbon dioxide of the air into concrete, as shown in Figure A2.

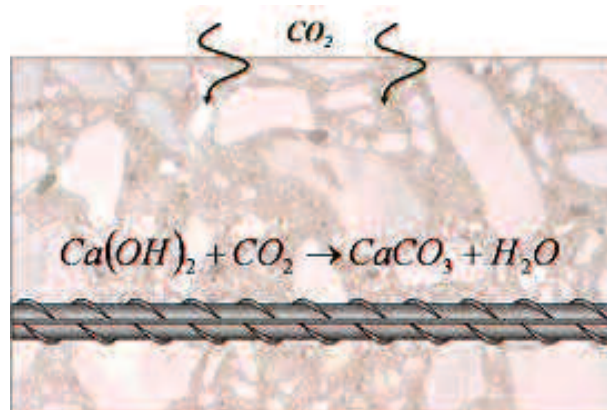
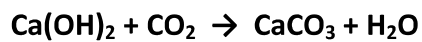


Figure A2. Chemical reaction of carbonation

The reaction of carbon dioxide and cement hydrate as follows:



The water void in the concrete has the pH value in the range of 12.5-13.5. The highly pH makes the steel reinforcement is passive and protected of corrosion.

Figure A3 shows the carbonation process, reaction between carbon dioxide and calcium hydroxide (cement hydrate) generate calcium carbonate (acid). Carbonation causes the water void is more acidic, thus lowering pH. It destroys the passivation film on the steel reinforcement surface and leads the corrosion progress with supplies of oxygen and water. The corrosion of steel reinforcement induces cracking and then peeling of concrete cover. It causes reduction of the load bearing capacity.

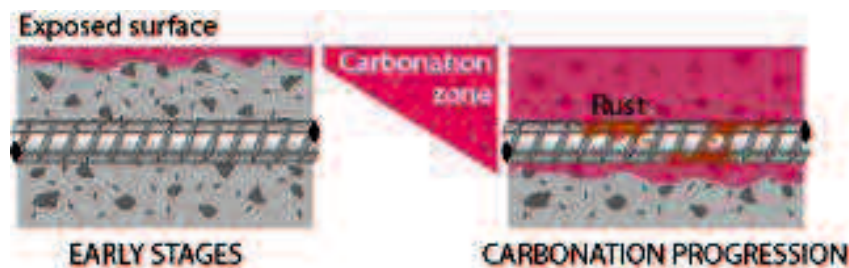


Figure A3. The carbonation process

Figure A4 describes the stages of the carbonation process; there are five stages of the carbonation process as seen in Table A1.

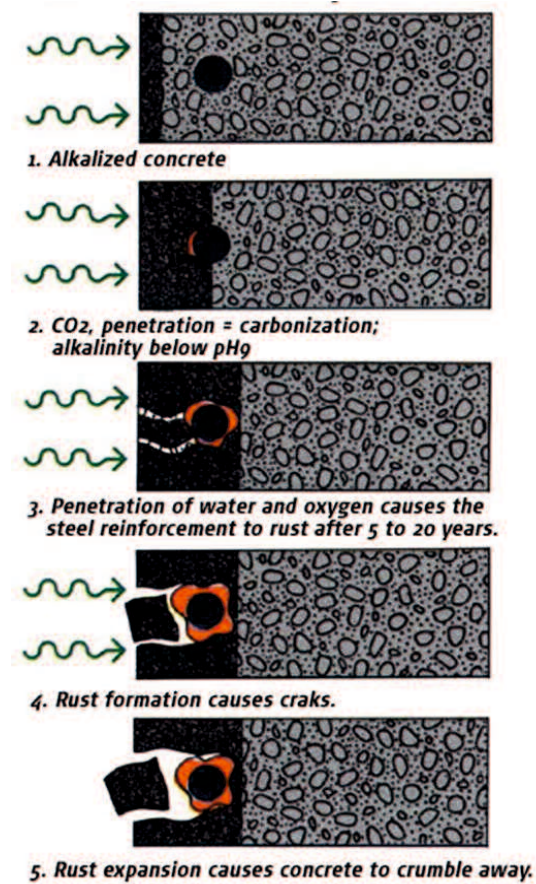
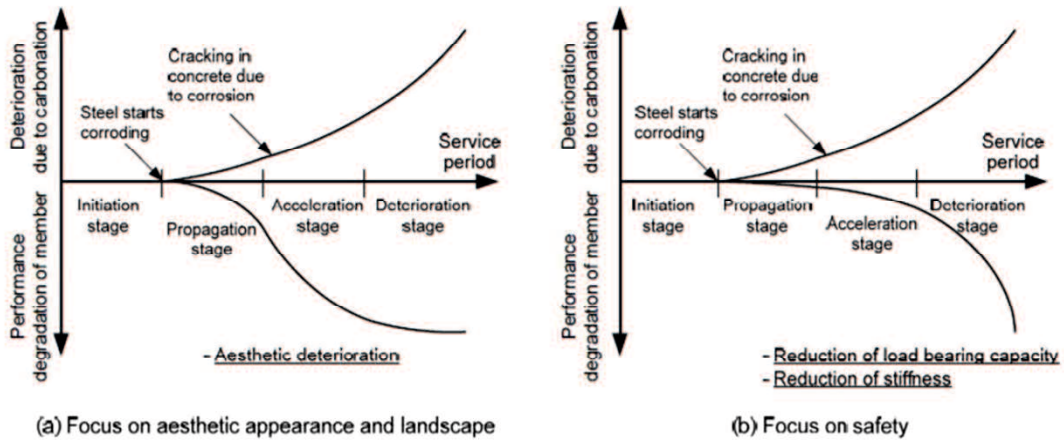


Figure A4. Stage of carbonation process

Table A1. Stage of carbonation process

Stage of carbonation process	Activity	Factor determining the stage
Stage 1	Alkalinity of the concrete	pH value in the range of 12.5-13.5
Stage 2	CO <sub>2</sub> penetrated the concrete cover causes carbonation	pH value is below 9
Stage 3	Penetration of water and oxygen causes corrosion process	Rust of steel reinforcement
Stage 4	Rust formation causes cracks	Cracks of concrete cover
Stage 5	Rust expansion causes spalling	Spalling of each part of concrete cover

Deterioration due to carbonation and steel corrosion during the incubation stage, propagation stage, acceleration stage and deterioration stage is shown in Figure A5 and Table A2 as follow:



**Figure A5. Conceptual view of deterioration progress due to carbonation**

**Table A2. Definition of deterioration stages**

Stage of deterioration	Definition	Factor determining the stage
Incubation stage	Until the depth of carbonation reaches the limit state for the occurrence of corrosion	Rate of carbonation
Propagation stage	From the initiation of corrosion steel until cracking due to corrosion	Rate of steel corrosion
Acceleration stage	Stage in which steel corrodes at a high rate due to cracking due to corrosion	Rate of corrosion of steel with cracks
Deterioration stage	Stage in which load bearing capacity is reduced considerably due to increased steel corrosion	

In each stage, deterioration has varying influences on the structure. The degree of performance degradation with the progress of deterioration also varies according to the performance attribute. The methods of assessment (investigation, deterioration prediction, evaluation or determination), remedial measures implementation and recording vary in respective deterioration stage (JSCE, 2007).

### 3. TARGET BRIDGE

The investigation was carried out on the cross-section cutting-off girders of an aged bridge (SK Bridge) are shown in Figure A1. The SK Bridge is T-girder concrete bridge. It has eight spans, and each span consists of five girders. The bridge has a total length of 168 m and a width of 11 m. The SK Bridge had been completed in 1942. After approximately 70 years of service, the bridge had been demolished in 2013.

The SK Bridge had been constructed on the main route of the National Highway No. 2 which connected Waki-city in Yamaguchi Prefecture and Otake-city in Hiroshima Prefecture, the location is shown in Figure A6. The SK Bridge has a high level of carbon dioxide because of the high traffic volume based on its location in the main route. The main deterioration factor is expected caused by carbonation. Figure A7 shows the specification of SK Bridge.

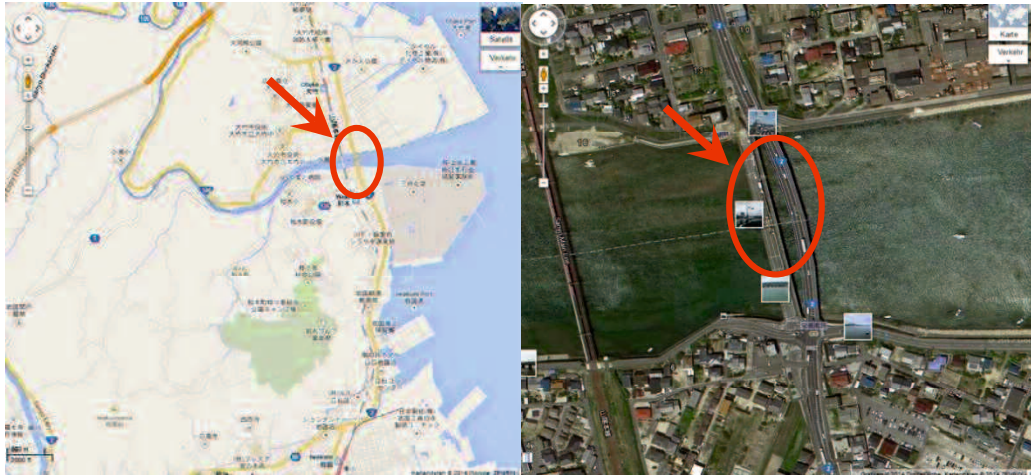


Figure A6. Geographical location of the SK Bridge



Name	Sakaebashi-Bridge
Size	L = 168.29 m W = 11.0 m (2 lines + sidewalk) W = 2.5 m (sidewalk)
Superstructure	Girder Beam
Substructure	Abutment : 2 (two) Pier : 7 (seven)
Abutment	Wood pile Caisson pier
Built	1937-1939
Traffic Volume	32,100 vehicles/day
Heavy Traffic Volume (%)	2.37 %

Figure A7. Specification of the SK Bridge

# CUTTING-OFF GIRDERS, CUT-OFF AND EXAMINATIONS

## 4.1 Cross-section cutting-off girders

There is a good opportunity to get many kinds of useful information from the real bridge which was demolished after 70 years of service. From the SK Bridge, there were two inspected span, Span 1 and Span 3 are show in Figure A8 and Figure A9. Each span consisted of five girders, Girder 1 (G1) to Girder 5 (G5). The total number of cross-section cutting-off girders of Span 1 and Span 3 were 49 and 67, respectively, are shown in Table A3. The cross-section cutting-off girders locations are shown in Figure A10 (a) for Span 1 and Figure A10 (b) for Span 3.

**TableA3. Number of cutting-off cross-section (specimens)**

No	Girder symbol	Number of cutting-off cross-section(specimens)	
		Span 1	Span 3
1.	G1	8	11
2.	G2	11	15
3.	G3	11	15
4.	G4	11	15
5.	G5	8	11
	<b>Total</b>	49	67

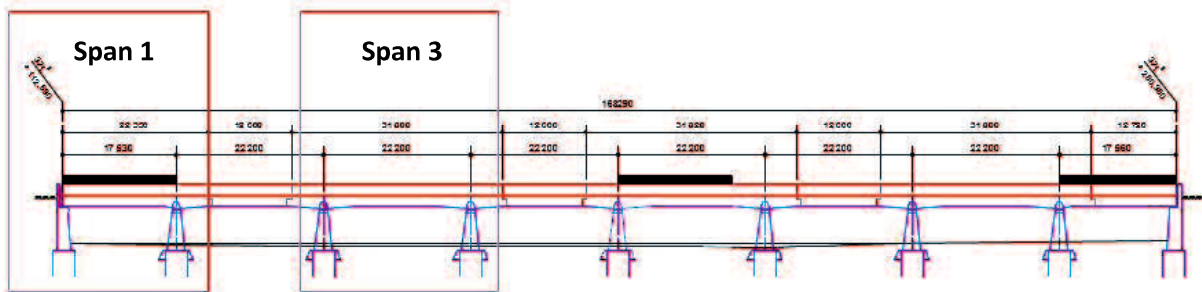


**Figure A8. Span 1 and span 3 of SK Bridge**

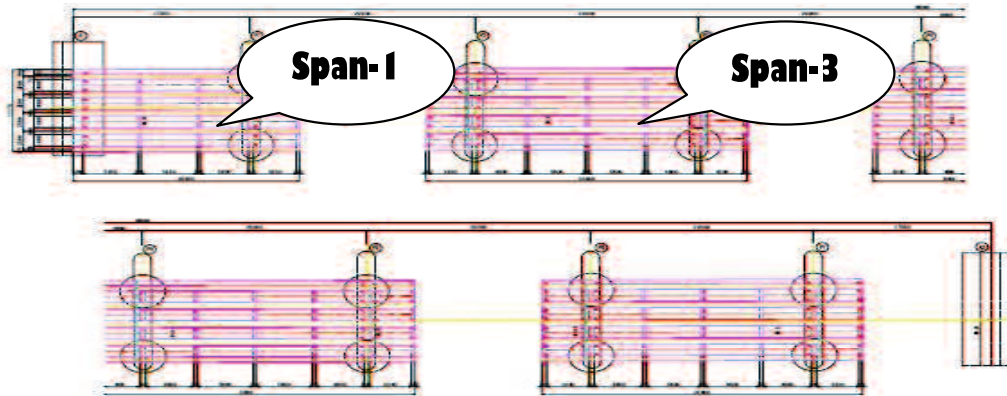


**Figure A9. Object of research Span 1 and Span 3**



## 4.2 The process of cutting-off the girders

The demolition of SK Bridge was started by removing the main girders of each span from the bridge. It was started from outer girder in the mountain side G5, then another outer girder in the seaside G1. After that, inner girders were removing; G4, G2, and G3, respectively. It can be seen in Figure A11. After removing from the bridge, the removal girders were placed in the temporary bridge.

In the temporary bridge the removal full girders were cut into several parts as shown in Table A3. It used the equipment called Wire Saw Machine with the diamond wire. Figure A12 shows the Wire Saw machine and the cutting process. The cutting-off girder has a maximum weight approximately 10 tons, the maximum weight could be moved by the truck to another place to be demolished.



Figure A11. Cross-section cutting-off girders locations



Figure A12. Wire saw machine using diamond wire

### 4.3 Cross-section cutting-off girder examination

#### 4.3.1 Carbonation test

Figure A13 shows the carbonation test. The carbonation test is most commonly carried out by spraying the Phenolphthalein solution on freshly exposed surfaces of concrete or on concrete cores. In our research, we carried out the carbonation test on the cross section surface of concrete girder. Carbonation depth is assessed using the Phenolphthalein solution, the indicator that appears pink (or purple) in contact with alkaline concrete. Colored area is detected as alkaline areas. It is defined as the healthy concrete area (no carbonation). Colorless area is defined as the carbonation area.



Figure A13. Carbonation test

#### 4.3.2 Measurement of the thickness of concrete covers

The cross-section cutting-off girders were measured for the thickness of concrete cover. The thickness of concrete cover is the distance between the concrete cover surface and the outer steel reinforcement. It was measured in three parts: seaside, bottom side and mountain side of the girders. It shows in Figure A14.

Steel corrosion due to carbonation accelerates the performance degradation of the reinforced concrete structures. Corrosion due to carbonation generally starts before carbonation reaches the steel.



**Figure A14. Measurement of the thickness of concrete covers**

#### **4.3.3 Measurement of carbonation depth**

Figure A15 shows that the cross-section cutting-off girders were also measured for carbonation depth, in accordance with JIS A 1152. Carbonation test was applied on the concrete cutting-off surface. To avoid further carbonation on the concrete surface, the carbonation test was carried out immediately within 30 minutes after cleaning. A phenolphthalein indicator 1% was sprayed on the concrete cutting-off surface. The carbonation area not changes in color but the healthy concrete area turned pink (or purple) in contact with the indicator. The carbonation depth is the distance between the concrete cover surface and the boundary between colored and uncolored areas.

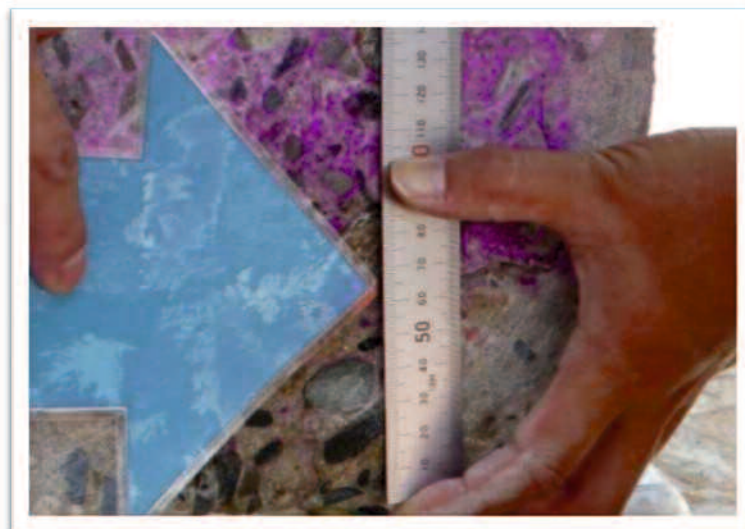


**Figure A15. Measurement of carbonation depth**

#### 4.3.4 Measurement of the remaining concrete covers

Steel corrosion due to carbonation accelerates the performance degradation of the reinforced concrete structures. Corrosion due to carbonation generally starts before carbonation reaches the steel (JSCE, 2007). The initiation of corrosion is frequently identified using the thickness of remaining concrete cover, or the variance between the thickness of concrete cover and the carbonation depth. The carbonation can be assumed started when remaining concrete cover reaches 10 mm. Corrosion occurs as the thickness of remaining concrete cover falls below 10 mm. If the thickness of remaining concrete cover is 10 mm or less, it can be recognized that the main deterioration factor is carbonation. The remaining of concrete cover can be seen in Figure A16.

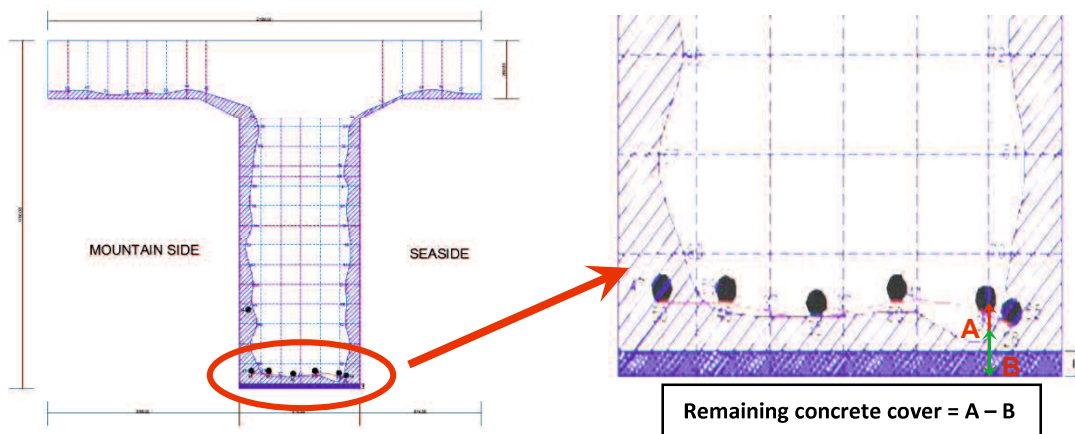


Figure A16. The remaining of concrete cover

The carbonation depth  $x(t)$  at time  $t$  is calculated by using the carbonation rate coefficient  $K$  by Equation (1). The changes in the carbonation depth over time are predicted in accordance with the law, and the carbonation rate coefficient  $A$  is calculated from the carbonation depth  $x(t)$  at time  $t$  by using the following equation:

$$K = \frac{x(t)}{\sqrt{t}} \quad (1)$$

where  $x(t)$  is the carbonation depth in mm at time  $t$ ,  $t$  is period of carbonation in years, and  $K$  is the carbonation rate coefficient in  $\text{mm} / \sqrt{\text{year}}$ . From structure investigations with a low sample scope, the mean value of the carbonation depth  $x$  at the respective concrete surface can be measure. With the knowledge of structure age and the exposure time, the equation can be solved for  $K$  (Sarja, 2006).

#### 4.3.5 Phenolphthalein solution

Figure A17 shows the Phenolphthalein solution which is used in this experiment. Phenolphthalein is used as an acid or alkali indicator where in contact or presence of acid it will turn colorless and with alkali; it will turn into a pink or purple color. It is also a component in universal indicator, a solution consisting of a mixture of pH indicators.

The acid-alkali indication abilities of phenolphthalein also make it useful for testing for signs of carbonation reactions in concrete. Concrete has naturally high pH due to the calcium hydroxide formed when Portland cement reacts with water. The pH of the ionic water solution present in the pores of fresh concrete may be over 14. Normal carbonation of concrete occurs as the cement hydration products in concrete react with carbon dioxide in the atmosphere, and can reduce the pH to 8.5 to 9, although that reaction usually is restricted to a thin layer at the surface. When a 1% phenolphthalein solution is applied to normal concrete it will turn bright pink. If the concrete has undergone carbonation, no color change will be observed.

In the case of Phenolphthalein solution used in this experiment, as seen in Figure A18 the visual transition interval as the pH requirement, if the pH of the concrete is 7.8 or lower the concrete will be colorless. The colorless phenomena define that the carbonation was occurred. The pH of the concrete is over than 10.0, the concrete will turn pink on purple.



Figure A17. Phenolphthalein solution

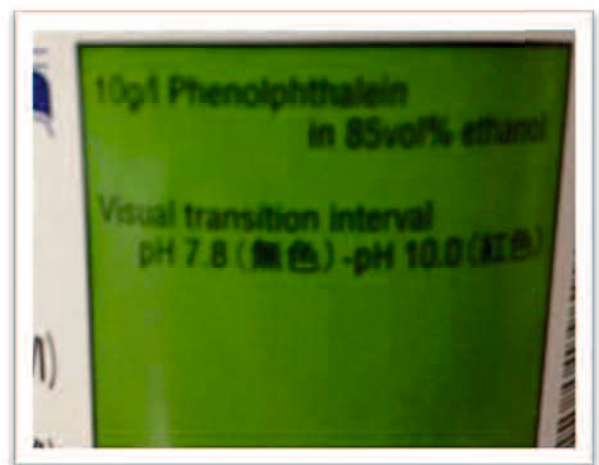


Figure A18. pH requirement

#### 4.3.6 Carbonation test equipment

Table A4 shows the list of equipment which are used in the carbonation test as follows:

**Table A4. The list of carbonation test equipment**

<b>No.</b>	<b>Carbonation test equipment</b>	<b>Amount</b>
1.	Scrub (big)	1
2.	Scrub (small)	1
3.	Grinder	2
4.	Dryer	1
5.	Brush	4
6.	Bucket	5
7.	Cloth	5
8.	Sprayer	2
9.	Ruler	4
10.	Roll ruler	2
11.	Marker pen	5
12.	Camera	1

#### 4.3.7 Safety equipment

Table A5 shows the list of equipment which are used for safety work during the carbonation test in the field, as follows:

**Table A5. The list of safety equipment**

<b>No.</b>	<b>Safety equipment</b>
1.	Helmet
2.	Mask
3.	Glasses
4.	Gloves
5.	Tent
6.	Boots

#### 4.3.8 The flow of experiment

No.	Picture	Activity
1.	 A photograph showing a large, T-shaped concrete girder lying on a construction site. The girder has a wide top flange and a narrower vertical web. It appears to be made of light-colored concrete with some rebar protrusions.	Original concrete cutting-off girder.
2.	 A worker in a white shirt and dark pants is using a scrubbing machine on the vertical surface of a concrete girder. The machine is creating a textured, dark grey surface on the concrete.	Scrubbing the concrete cutting-off surface with scrub equipment.
3.	 A worker in a grey uniform and white hard hat is using a hand-held grinder on the vertical surface of a concrete girder. The grinder is creating a smooth, light-colored surface on the concrete.	Smoothing the concrete cutting-off surface with grinder, to omit the outermost layer.
4.	 A worker in a grey uniform and white hard hat is using a blue bucket to clean the vertical surface of a concrete girder. The worker is kneeling and using a brush or sponge to clean the surface.	Cleaning the concrete cutting-off surface to clean the dust used water.

No.	Picture	Activity
5.		<p>Drying the concrete cutting-off surface used dryer equipment.</p>
6.		<p>Concrete cutting-off girder after cleaning and drying</p>
7.		<p>Add the identification of the cutting-off girder.</p>
8.		<p>Making a sign, each 10 cm to plot the measurement of carbonation depth.</p>

No.	Picture	Activity
9.		<p>Measuring dimension of cutting-off girder; including width, height and length</p>
10.		<p>Measuring the location of reinforcing bar to define the thickness of concrete cover</p>
11.		<p>Phenolphthalein solution</p>
12.		<p>Spraying the Phenolphthalein solution into concrete cutting surface to detect the carbonation area</p>

No.	Picture	Activity
13.		Concrete cutting-off girder after spraying with Phenolphthalein solution.
14.		Measuring the carbonation depth.
15.		Collecting data from the measurement of carbonation depth.
16.		Taking picture after finished measurement.

# 5. DATA COLLECTION AND ANALYSIS DATA

## 5.1 Data collection

### 5.1.1 Thickness of concrete cover data

Figure A19 shows the original data of the location of steel reinforcement. The thickness of concrete cover can be defined from these data by measure the distance between the concrete cover surface and the outer steel reinforcement. The thickness of concrete cover was measured in three parts: seaside, bottom side and mountain side of the girders.

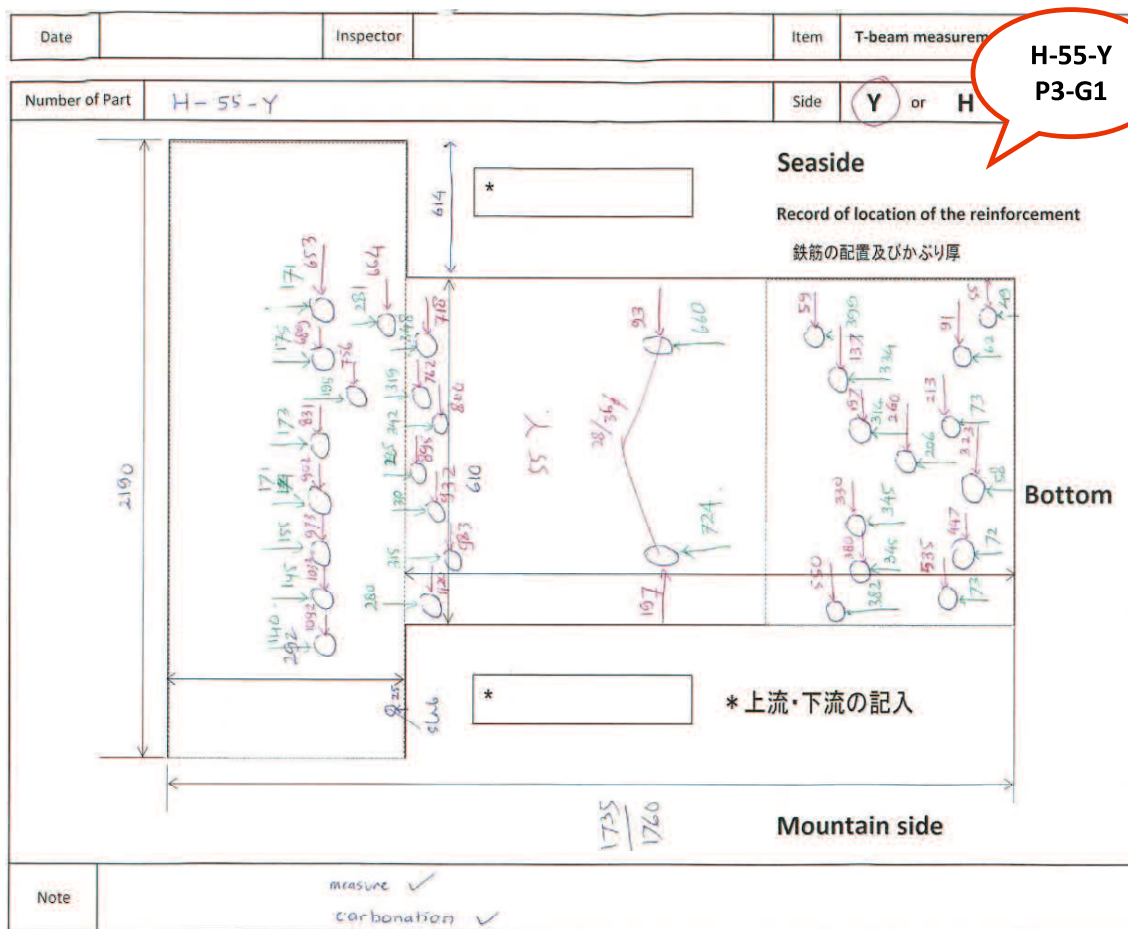


Figure A19. Original data of the location of steel reinforcement

### 5.1.2 The carbonation depth data

The first step to prepare carbonation tests is making a mark or dots each 10 cm in three parts: seaside, bottom side and mountain side of the cutting-off surface of the girders, to plot the measurement of carbonation depth. After that, the cutting-off surface was

sprayed with Phenolphthalein solution as an indicator. The healthy concrete area turned pink (or purple) in contact with an indicator and the carbonation area not change in color. The carbonation depth was measured by the distance between the concrete cover surface and the boundary between colored and uncolored areas. The measurement of carbonation depth was performed on the mark which was prepared. Based on the size of cutting-off surface girders, there were 5 – 6 dots on the bottom side, and approximately 10 – 18 dots on the seaside and mountainside. Also measure the maximum value of carbonation depth. For attention, the cutting-off girders which near the pier are bigger than those are located in the middle of the girder. Figure A20 shows the original data of the carbonation depth measurement.

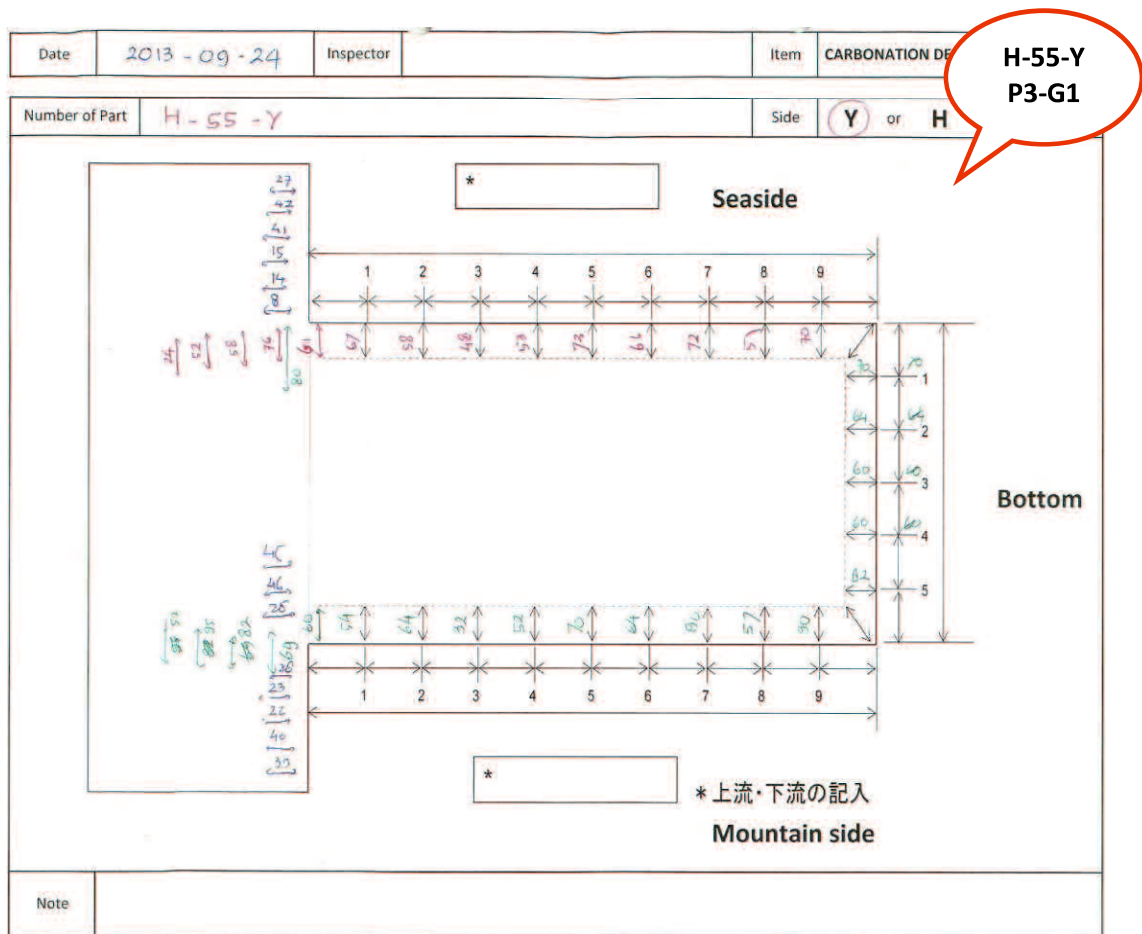


Figure A20. Original data of the carbonation depth measurement

### 5.1.3 Inputting data

Inputting data were obtained from measurement of the thickness of concrete cover and the carbonation depth to the special form is shown in Figure A21.

Date	2013-09-24		Inspector			
No	Part	Beam			Slab	
		Seaside	Bottom	Mountain side	Seaside	Mountain side
<b>55 - Y</b>	1	70	15	90	27	39
	2	51	41	57	42	40
	3	72	37	90	41	22
	4	66	37	64	15	23
	5	73	59	70	14	28
	6	53		52	8	28
	7	48		32		46
	8	58		64		45
	9	67		54		
	10	61		60		
	11	76		69		
	12	58		82		
	13	52		95		
	14	24		52		
	Max	80				
<b>Average</b>		<b>60.6</b>	<b>37.8</b>	<b>66.5</b>	<b>24.5</b>	<b>33.9</b>
<b>Maximum value</b>		<b>80</b>	<b>59</b>	<b>95</b>	<b>42</b>	<b>46</b>

<b>Note</b>	Repairing layer on the bottom of the beam G1 The higher carbonation depth on beam : Mountain side The higher carbonation depth on slab : Mountain side
-------------	--

**The thickness of concrete cover**

No	Part	Beam			Slab	
		Seaside	Bottom	Mountain side	Seaside	Mountain side
<b>55 - Y</b>	1	55	26	32		
	2		39			
	3		50			
	4		35			
	5		49			
	6		50			
<b>Average</b>		<b>55.0</b>	<b>41.5</b>	<b>32.0</b>		
<b>Minimum value</b>		<b>55</b>	<b>26</b>	<b>32</b>		

<b>Note</b>	Repairing in the bottom of the beam Repairing in the seaside was broken
-------------	--

**Figure A21. Data of carbonation depth and the thickness of concrete cover**

## 5.2 Plotting Data

The results of measurement will be plotted by using AutoCAD software. For example, Figure A22 shows the original cutting-off surface girder H-55-Y. The result of the thickness of concrete cover measurement after plotting is shown in Figure A23.



Figure A22. Cutting-off surface girder

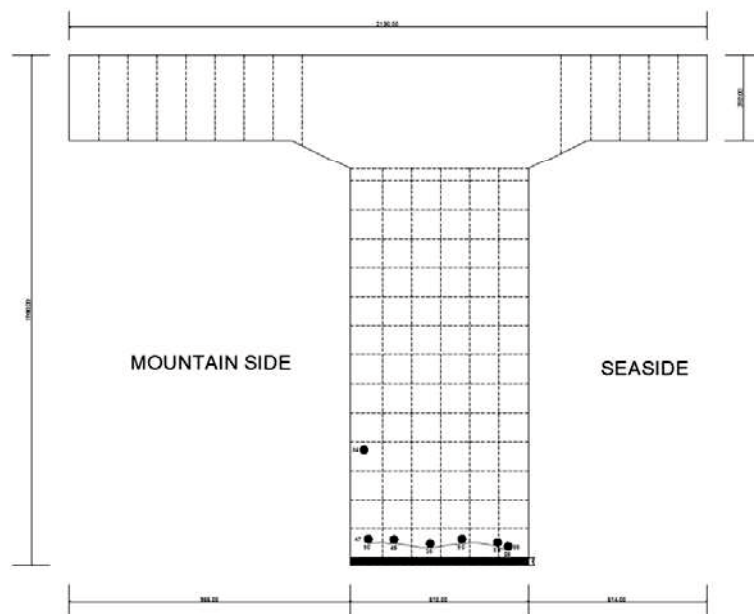


Figure A23. Plotting figure of the thickness of concrete covers

Figure A24 shows the cutting-off surface girder H-55-Y after sprayed by Phenolphthalein solution. The result of the carbonation depth measurement after plotting is shown in Figure A25.



Figure A24. Cutting-off girder after spraying Phenolphthalein solution

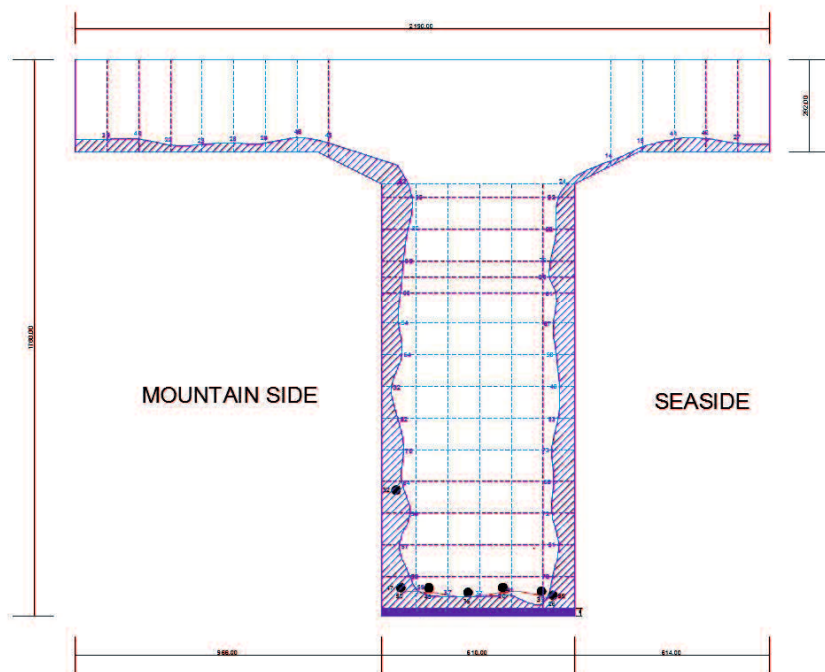


Figure A25. Plotting figure of the carbonation depth

### 5.3 Analysis Data

#### 5.3.1 Calculating the average value and maximum value of the carbonation depth

Average value and the maximum value of the carbonation depth are calculated from the data were taken from the measurement of carbonation depth. The result is shown in Table A6.

**Table A6. Average value and the maximum value of the carbonation depth**

Date	<b>2013-09-24</b>		Inspector			
No	Part	Beam			Slab	
		Seaside	Bottom	Mountain side	Seaside	Mountain side
<b>55 - Y</b>	1	70	15	90	27	39
	2	51	41	57	42	40
	3	72	37	90	41	22
	4	66	37	64	15	23
	5	73	59	70	14	28
	6	53		52	8	28
	7	48		32		46
	8	58		64		45
	9	67		54		
	10	61		60		
	11	76		69		
	12	58		82		
	13	52		95		
	14	24		52		
	Max	80				
<b>Average</b>		<b>60.6</b>	<b>37.8</b>	<b>66.5</b>	<b>24.5</b>	<b>33.9</b>
<b>Maximum value</b>		<b>80</b>	<b>59</b>	<b>95</b>	<b>42</b>	<b>46</b>

### 5.3.2 Calculating the coefficient of the carbonation rate

The carbonation rate coefficient  $K$  can be obtained from the measurement of the carbonation depth  $x(t)$  in mm at time  $t$  in years using Equation (1). The changes in the carbonation depth over the time are predicted in accordance the  $\sqrt{t}$  rule, as follows:

$$x(t) = K\sqrt{t} \quad (1)$$

where  $x(t)$  is the carbonation depth at  $t$  time in mm,  $t$  is period of carbonation in years, and  $K$  is the carbonation rate coefficient in mm /  $\sqrt{\text{year}}$ . The result is shown in Table A7.

**Table A7. Carbonation rate coefficient,  $K$  (mm /  $\sqrt{\text{year}}$ )**

H-55-Y	Beam			Slab	
	Seaside	Bottom	Mountain side	Seaside	Mountain side
Average (mm)	60.6	37.8	66.5	24.5	33.9
Maximum value (mm)	80	59	95	42	46
$K$ at 72 years (Ave)	7.14	4.45	7.84	2.89	3.99
$K$ at 72 years (Max)	9.43	6.95	11.20	4.95	5.42

### 5.3.3 Calculating the average value and maximum value of the thickness of concrete covers

Average value and the maximum value of the thickness of concrete cover are calculated from the data were taken from the measurement of the thickness of concrete cover. The result is shown in Table A8.

**Table A8. Average value and maximum value of the thickness of concrete covers (mm)**

No	Part	Beam		
		Seaside	Bottom	Mountain side
<b>55 - Y</b>	1	55	26	32
	2		39	
	3		50	
	4		35	
	5		49	
	6		50	
Average (mm)		<b>55.0</b>	<b>41.5</b>	<b>32.0</b>
Minimum value (mm)		<b>55</b>	<b>26</b>	<b>32</b>

### 5.3.4 Calculating the remaining concrete covers

The initiation of corrosion is frequently identified using the thickness of remaining concrete cover, or the variance between the thickness of concrete cover and the depth of carbonation. The carbonation can be assumed started when the thickness of remaining concrete cover reaches 10 mm. Corrosion occurs as the thickness of remaining concrete cover falls below 10 mm.

From the results of measurement of the carbonation depth (section 4.3.1) and the thickness of concrete cover (section 4.3.3), the remaining of concrete cover can be determined as the thickness of concrete cover subtracted by the carbonation depth, or the remaining concrete cover (A-B) is the variance between the thickness of concrete cover (A) and the depth of carbonation (B).

In the case when the result is over than 10 mm, it indicates the corrosion has not occurred, below 10 mm indicates the initiation of corrosion already occurred, 0 mm or minus value indicates the carbonation already reached and exceeded the reinforcing bar. The results are represented by three colors; green, yellow and blue. Green indicates the corrosion has not occurred, yellow indicates the initiation of corrosion already occurred, and red indicates the carbonation already reached and exceeded the reinforcing bar. Table A9 shows the result of the remaining concrete cover.

**Table A9. Result of the remaining concrete covers (mm)**

Time		The thickness of concrete cover (A)			The depth of carbonation (B)			The thickness of remaining concrete cover (A-B)		
Year	Elapsed Year	Seaside	Bottom side	Mountain side	Seaside (A=55mm)	Bottom side (A=41.5mm)	Mountain side (A=32mm)	Seaside	Bottom side	Mountain side
1941	0	55	41.5	32	0.00	0.00	0.00	55.00	41.50	32.00
1942	1	55	41.5	32	7.14	4.45	7.84	47.86	37.05	24.16
1943	2	55	41.5	32	10.10	6.30	11.08	44.90	35.20	20.92
1944	3	55	41.5	32	12.37	7.72	13.57	42.63	33.78	18.43
1945	4	55	41.5	32	14.28	8.91	15.67	40.72	32.59	16.33
1946	5	55	41.5	32	15.97	9.96	17.52	39.03	31.54	14.48
1947	6	55	41.5	32	17.49	10.91	19.20	37.51	30.59	12.80
1948	7	55	41.5	32	18.90	11.79	20.74	36.10	29.71	11.26
1949	8	55	41.5	32	20.20	12.60	22.17	34.80	28.90	9.83
1950	9	55	41.5	32	21.43	13.36	23.51	33.57	28.14	8.49
1951	10	55	41.5	32	22.58	14.09	24.78	32.42	27.41	7.22
1952	11	55	41.5	32	23.69	14.77	25.99	31.31	26.73	6.01
1953	12	55	41.5	32	24.74	15.43	27.15	30.26	26.07	4.85
1954	13	55	41.5	32	25.75	16.06	28.26	29.25	25.44	3.74
1955	14	55	41.5	32	26.72	16.67	29.32	28.28	24.83	2.68
1956	15	55	41.5	32	27.66	17.25	30.35	27.34	24.25	1.65
1957	16	55	41.5	32	28.57	17.82	31.35	26.43	23.68	0.65
1958	17	55	41.5	32	29.45	18.37	32.31	25.55	23.13	-0.31
1959	18	55	41.5	32	30.30	18.90	33.25	24.70	22.60	-1.25
1960	19	55	41.5	32	31.13	19.42	34.16	23.87	22.08	-2.16

Time		The thickness of concrete cover (A)			The depth of carbonation (B)			The thickness of remaining concrete cover (A-B)		
Year	Elapsed Year	Seaside	Bottom side	Mountain side	Seaside (A=55mm)	Bottom side (A=41.5mm)	Mountain side (A=32mm)	Seaside	Bottom side	Mountain side
1961	20	55	41.5	32	31.94	19.92	35.05	23.06	21.58	-3.05
1962	21	55	41.5	32	32.73	20.41	35.91	22.27	21.09	-3.91
1963	22	55	41.5	32	33.50	20.89	36.76	21.50	20.61	-4.76
1964	23	55	41.5	32	34.25	21.36	37.59	20.75	20.14	-5.59
1965	24	55	41.5	32	34.99	21.82	38.39	20.01	19.68	-6.39
1966	25	55	41.5	32	35.71	22.27	39.19	19.29	19.23	-7.19
1967	26	55	41.5	32	36.42	22.71	39.96	18.58	18.79	-7.96
1968	27	55	41.5	32	37.11	23.15	40.72	17.89	18.35	-8.72
1969	28	55	41.5	32	37.79	23.57	41.47	17.21	17.93	-9.47
1970	29	55	41.5	32	38.46	23.99	42.20	16.54	17.51	-10.20
1971	30	55	41.5	32	39.12	24.40	42.93	15.88	17.10	-10.93
1972	31	55	41.5	32	39.76	24.80	43.64	15.24	16.70	-11.64
1973	32	55	41.5	32	40.40	25.20	44.33	14.60	16.30	-12.33
1974	33	55	41.5	32	41.03	25.59	45.02	13.97	15.91	-13.02
1975	34	55	41.5	32	41.64	25.98	45.70	13.36	15.52	-13.70
1976	35	55	41.5	32	42.25	26.35	46.36	12.75	15.15	-14.36
1977	36	55	41.5	32	42.85	26.73	47.02	12.15	14.77	-15.02
1978	37	55	41.5	32	43.44	27.10	47.67	11.56	14.40	-15.67
1979	38	55	41.5	32	44.02	27.46	48.31	10.98	14.04	-16.31
1980	39	55	41.5	32	44.60	27.82	48.94	10.40	13.68	-16.94
1981	40	55	41.5	32	45.17	28.17	49.57	9.83	13.33	-17.57
1982	41	55	41.5	32	45.73	28.52	50.18	9.27	12.98	-18.18
1983	42	55	41.5	32	46.28	28.87	50.79	8.72	12.63	-18.79
1984	43	55	41.5	32	46.83	29.21	51.39	8.17	12.29	-19.39
1985	44	55	41.5	32	47.37	29.55	51.99	7.63	11.95	-19.99
1986	45	55	41.5	32	47.91	29.88	52.57	7.09	11.62	-20.57
1987	46	55	41.5	32	48.44	30.21	53.15	6.56	11.29	-21.15
1988	47	55	41.5	32	48.96	30.54	53.73	6.04	10.96	-21.73
1989	48	55	41.5	32	49.48	30.86	54.30	5.52	10.64	-22.30
1990	49	55	41.5	32	49.99	31.18	54.86	5.01	10.32	-22.86
1991	50	55	41.5	32	50.50	31.50	55.42	4.50	10.00	-23.42
1992	51	55	41.5	32	51.00	31.81	55.97	4.00	9.69	-23.97
1993	52	55	41.5	32	51.50	32.12	56.51	3.50	9.38	-24.51
1994	53	55	41.5	32	51.99	32.43	57.05	3.01	9.07	-25.05
1995	54	55	41.5	32	52.48	32.74	57.59	2.52	8.76	-25.59
1996	55	55	41.5	32	52.96	33.04	58.12	2.04	8.46	-26.12
1997	56	55	41.5	32	53.44	33.34	58.65	1.56	8.16	-26.65
1998	57	55	41.5	32	53.92	33.63	59.17	1.08	7.87	-27.17
1999	58	55	41.5	32	54.39	33.93	59.69	0.61	7.57	-27.69
2000	59	55	41.5	32	54.86	34.22	60.20	0.14	7.28	-28.20
2001	60	55	41.5	32	55.32	34.51	60.71	-0.32	6.99	-28.71
2002	61	55	41.5	32	55.78	34.79	61.21	-0.78	6.71	-29.21
2003	62	55	41.5	32	56.23	35.08	61.71	-1.23	6.42	-29.71
2004	63	55	41.5	32	56.69	35.36	62.21	-1.69	6.14	-30.21
2005	64	55	41.5	32	57.13	35.64	62.70	-2.13	5.86	-30.70
2006	65	55	41.5	32	57.58	35.92	63.18	-2.58	5.58	-31.18
2007	66	55	41.5	32	58.02	36.19	63.67	-3.02	5.31	-31.67
2008	67	55	41.5	32	58.46	36.46	64.15	-3.46	5.04	-32.15
2009	68	55	41.5	32	58.89	36.73	64.63	-3.89	4.77	-32.63
2010	69	55	41.5	32	59.32	37.00	65.10	-4.32	4.50	-33.10
2011	70	55	41.5	32	59.75	37.27	65.57	-4.75	4.23	-33.57
2012	71	55	41.5	32	60.18	37.54	66.04	-5.18	3.96	-34.04
2013	72	55	41.5	32	60.60	37.80	66.50	-5.60	3.70	-34.50

Figure A26 shows the graphic of the carbonation rate distribution of cutting off girder H-55-Y. Based on this figure, it can be seen that the carbonation depth values increase in line with the increased time. The lowest carbonation rate value is on the bottom side location due to the repairing work in the bottom of the girder.

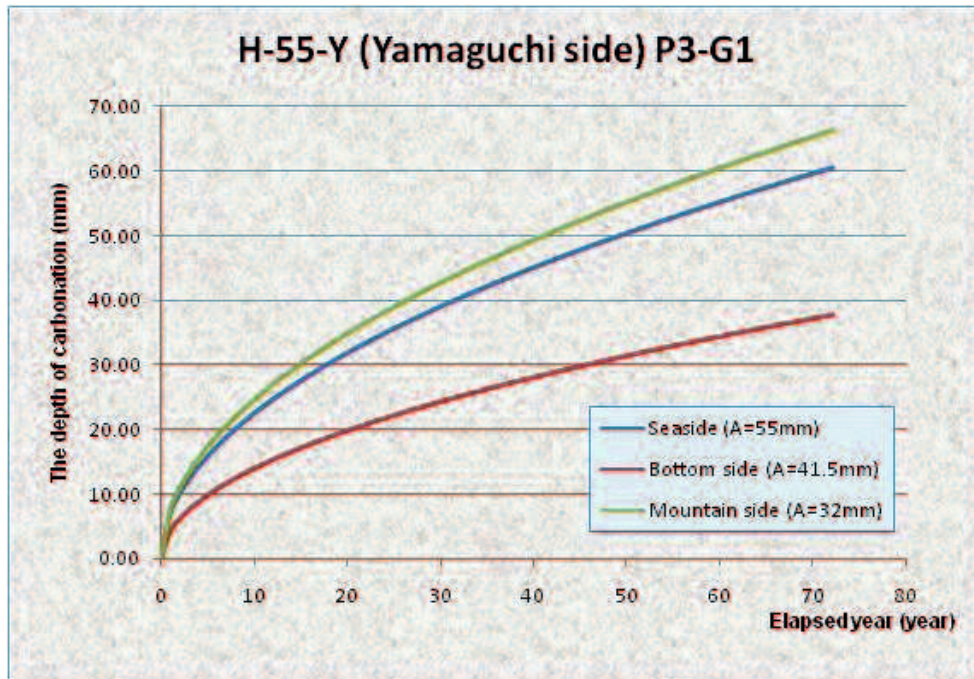


Figure A26. The carbonation rate distribution

## 6. CONCLUSION REMARKS

In ordinary circumstances, the concrete core is extracted from some parts of the RC bridge in order to evaluate the performance of the bridge. However, only a few number of the concrete core specimens usually use due to of the high cost of the test specimen extraction processes. Thus, the results of the concrete core need to be verified so that it can be considered how local evaluation results based on the concrete core test can be used for the evaluation of the entire span. In this research, there was a good opportunity to conduct an investigation in a real bridge. An aged RC bridge was demolished and used to acquire the useful information from the cross-section cutting-off girders, such as the carbonation process. The results of this research can be used to verify the results of the concrete core test. If the results have an equal tendency, it can be considered that the concrete core test results can be used for entire span evaluation.

# REFERENCES

---

Japan Society of Civil Engineers, Standard specifications for concrete structures: maintenance, JSCE, 2007.

J. Takahashi, R. Widyawati, H. Emoto, and A. Miyamoto, Remaining life prediction of an aged bridge based on concrete core test, in Japanese, Proceedings of the Japan Concrete Institute, Vol. 36, No. 2, pp. 1339-1344, 2014.

Sarja, Predictive and optimized life cycle management, Building and Infrastructure, Taylor & Francis, 2006.